



Peptides derived from *Yersinia pestis* V-
antigen as novel therapeutic interventions
for sepsis

Jack Hales

Degree award title: PhD in Medicine

Year of submission: 2021

Word count: 42,038

Abstract:

Yersinia pestis V-antigen has long been known to modulate the inflammatory response and multiple previous studies have highlighted the importance of V-antigen as a virulence factor for *Yersinia spp in vivo*. Evidence of a rapid IL-10-mediated immunomodulatory response has been debated due to discrepancies between and within *in vivo* and *in vitro* studies and the short-lived nature of the response, however evidence has also emerged of a potent secondary round of immunomodulation that begins after internalisation. This second immunomodulatory effect has never been studied in detail. In this study, using both immortalised and primary human monocytes/monocyte-derived macrophages, the development of V-antigen's immunomodulation over 16hr was investigated in detail to examine its potential as a therapeutic intervention in highly inflammatory conditions. The analysis revealed a reduction in the secretion in numerous pro- and anti-inflammatory cytokines although a potential increase in IFN γ in response to LPS. The reduction also included IL-10 which did not appear to be responsible for the initial immunomodulation that occurred in primary cells. Investigation into the IL-1 β pathway revealed inhibition within the TLR pathway and qPCR gene arrays looking at the expression of genes within the TLR pathway and those related to the inflammasome uncovered peculiarities in expression that suggested an inhibition specific to the MyD88 pathway and evidence of elevated TGF β signalling. Upon further investigation of secreted cytokines using a TGF β ELISA, it was shown that V-antigen induced TGF β secretion to significantly higher levels than control stimulations at 16hr post-introduction. Genes expressing V-antigen fragments derived from a conserved central epitope of V-antigen (aa135-275) were then expressed and tested for their immunomodulatory capabilities through similar stimulations and were found to be capable, to varying degrees, to inhibit cytokine secretion in a similar fashion to the WT, alter gene expression in a similar way, and also induce TGF β expression.

I would like to give thanks to my supervisors; Dr Martha Triantafilou and Prof Kathy Triantafilou for supporting me throughout the last few years and giving me the skills that I needed to make it in the field of science.

I would like to thank my family for their unending support throughout my PhD and every step prior to it.

Table of Contents

Abstract:	ii
Abbreviations:	xviii
1: Chapter 1: Introduction	1
1.1: Inflammation	1
1.1.1: Overview of inflammation in healthy individuals.....	1
1.1.2: The instigation of inflammation.....	1
1.1.2.1: Detection of inflammatory stimuli.....	1
1.1.2.2: TLR pathway	3
1.1.2.3: Lipopolysaccharide, TLR4, and the innate immune response.....	7
1.1.3: A dysregulated innate immune response: sepsis.....	10
1.1.4: Resolving inflammation	14
1.1.4.1: Natural resolution	14
1.1.4.2: Attempts to modulate dysregulated immune responses	15
1.2: <i>Yersinia pestis</i> and V-antigen.....	18
1.2.1: <i>Yersinia pestis</i>	18
1.2.2: V-antigen.....	20
1.2.2.1: V-antigen within <i>Yersinia pestis</i> lifecycle	20
1.2.2.2: Immunomodulatory activity of V-antigen.....	23
1.2.2.3: V-antigen and the IL-10 response	24
1.2.2.4: The prospect of long-term anti-inflammatory properties.....	26
1.3: Thesis aims.....	26
2: Chapter 2: Methodology:	28
2.1: Cell culture:	28
2.1.1: Mono Mac-6 culture:.....	28
2.1.2: Primary peripheral blood monocyte isolation/culture/differentiation:	28

2.1.3: Trypan blue assay:.....	29
2.1.4: Monocyte stimulation:.....	29
2.2: DNA/RNA techniques:.....	29
2.2.1: Plasmid isolation:	29
2.2.2: Restriction enzyme (RE) digest:	30
2.2.3: DNA electrophoresis:	30
2.2.4: qPCR gene arrays:.....	31
2.3: Protein techniques:	31
2.3.1: Cell lysis (for western blot):	31
2.3.2: Western blotting (HRP):	32
2.3.3: Western blotting (fluorescent):.....	32
2.3.4: Protein purification	33
2.3.4.1: V-antigen expression.....	33
2.3.4.2: Protein isolation by GST-columns:	33
2.3.4.3: Endotoxin removal:.....	34
2.3.4.4: Thiobarbituric acid assay for LPS detection:.....	34
2.3.5: Coomassie blue protein staining:	34
2.3.6: Fluorescent labelling of V-antigen:	35
2.3.7: Fluorescent cell imaging:.....	35
2.3.8: Cytokine detection:.....	36
2.3.9: TGF β ELISA:.....	36
2.4: Bioinformatic analysis:.....	37
2.4.1: Qiagen Geneglobe Analysis software:.....	37
2.4.2: STRING:	37
2.4.3: Statistical analysis.....	37
2.5: Antibody information:	39

3: Chapter 3: Isolation and cytokine analysis of recombinant V-antigen	42
3.1 Introduction	42
3.1.1: Monocytes.....	42
3.1.2: The protective epitope of V-antigen.....	43
3.1.3: Chapter aims.....	43
3.2: Results.....	45
3.2.1: Plasmid construction/details	45
3.2.2: Plasmid testing.....	46
3.2.3: Purification of WT V-antigen and V-antigen fragments	47
3.2.4: Imaging of V-antigen internalising	51
3.2.5: Changes in cytokine response in the presence of V-antigen	52
3.2.5.1: MM6 cells.....	52
3.2.5.2: PBMDMs.....	56
3.3: Discussion.....	64
3.3.1: V-antigen internalises in the absence of <i>Y.pestis</i> within 4hr	64
3.3.2: V-antigen triggers a minor inflammatory response in monocytes.....	64
3.3.3: V-antigen alters ongoing inflammation in response to LPS, but does not entirely inhibit it.....	65
4: Chapter 4: V-antigen and the inflammasome.....	67
4.1: Introduction	67
4.1.1: Chapter introduction.....	67
4.1.2: IL-1 β secretion	67
4.1.3: The inflammasome.....	69
4.1.4: Chapter aims.....	72
4.2: Results.....	73
4.2.1: Intracellular IL-1B processing	73

4.2.2: Inflammasome qPCR gene array	76
4.2.2.1: Gene cluster analysis	76
4.2.2.2: Expression analysis of key identified genes	89
4.3: Discussion:.....	98
4.3.1: Inhibition of IL-1 β by V-antigen does not appear to affect secretion or maturation.....	98
4.3.2: V-antigen has a wide effect on the transcriptomic profile of inflammasome-related genes under LPS stimulation	98
5: Chapter 5: V-antigen and the TLR pathway	101
5.1: Introduction	101
5.1.1: Chapter introduction	101
5.1.2: TLR4 signalling pathway	101
5.1.3: Transcription of TLR4-response genes	102
5.1.4: Chapter aims:.....	104
5.2: Results.....	105
5.2.1: V-antigen's effects on NF κ B activation	105
5.2.2: TLR pathway qPCR gene array.....	108
5.2.2.1: Gene cluster analysis	108
5.2.2.2: Expression analysis of key identified genes	128
5.2.3: Comparison between Inflammasome and TLR qPCR gene arrays common genes.	136
5.2.4: TGF β	137
5.2.4.1: TGF β 1.....	137
5.2.4.2: Evidence of TGF β involvement	139
5.3: Discussion.....	144
5.3.1: V-antigen inhibits the transcription of pro-IL-1 β by inhibiting the TLR pathway:	144
5.3.2: V-antigen promotes a TRIF-dominant response to LPS	144

5.3.3: V-antigen utilises TGF β to suppress TLR signalling, cytokine signalling, and subsequent inflammation	146
6: Chapter 6: Fragments of V-antigen	149
6.1: Introduction	149
6.1.1: Chapter introduction	149
6.1.2: Defined regions of V-antigen	149
6.1.3: V-antigen fragments in this study	151
6.1.4: Chapter aims	153
6.2: Results	154
6.2.1: Purification of fragments	154
6.2.2: Cytokine analysis	154
6.2.3: TLR-related gene analysis	161
6.2.4: TGFB induction	178
6.3: Discussion	182
6.3.1: The central protective epitope of V-antigen is responsible for V-antigen's immunomodulatory effects on cytokine secretion	182
6.3.2: pV1 and pV2 induce similar gene expression changes to WT V-antigen	183
6.3.2.1: pV1:	183
6.3.2.2: pV2:	185
6.3.3: The central epitope of V-antigen is responsible for inducing TGF β 1 secretion	187
6.3.4: Considerations	188
7: Chapter 7: Discussion	189
7.1: Study summary	189
7.2: Considerations about the use of MM6 cells and PBMDMs	190
7.3: V-antigen's mechanism of action	191
7.3.1: V-antigen has a complex effect on inflammation	191

7.3.2: V-antigen’s immunomodulation and the wider literature	193
7.4: The therapeutic potential of V-antigen.....	196
7.4.1: The suppression of MyD88 and the effects within the TLR signalling pathway	196
7.4.2: Endogenous TGF β and its therapeutic potential.....	197
7.4.3: V-antigen and its fragments as anti-inflammatory therapeutics.....	200
7.5: Future experiments:	202
8: Appendix	205
8.1: Appendix A - recipes	205
8.2: Appendix B – Supplementary figures and tables	212
8.2.1: Supplementary figures	212
8.2.2: Supplementary tables.....	229
9: References	237

Table of figures

Figure 1 - TLR localisation and morphology	4
Figure 2 - TLR signalling pathway	5
Figure 3 – The effect of LPS stimulation <i>in vivo</i>	9
Figure 4 - The effects of the septic immunopathology on the blood, vasculature, and tissues/organs.....	13
Figure 5 - Localisation of V-antigen throughout the <i>Yersinia pestis</i> lifecycle.....	22
Figure 6 - Plasmid maps for recombinant V-antigen and its fragments.....	45
Figure 7 - Plasmid DNA isolated from transformed <i>E.coli</i>	46
Figure 8 - EcoRI digest of isolated V-antigen fragment plasmid DNA.....	47
Figure 9 - The principle of GST column purification.....	48
Figure 10 - Coomassie blue gel of recombinant V-antigen fragments	49
Figure 11 - Western blot on purified recombinant V-antigen.....	50
Figure 12 - Fluorescent imaging of V-antigen internalisation	52
Figure 13 - MM6 secreted level of IL-6 in response to LPS/V-antigen stimulation	54
Figure 14 - MM6 secreted level of IL-6 in response to 12hr LPS/V-antigen stimulation	55
Figure 15 - Experimental design of PBMDM-V-antigen stimulations.....	56
Figure 16 - IL-1 β secretion in PBMDMs in response to V-antigen stimulation (+/-) over 16hr	58
Figure 17 - IL-6 secretion in PBMDMs in response to V-antigen stimulation (+/-) over 16hr	59
Figure 18 - IL-8 secretion in PBMDMs in response to V-antigen stimulation (+/-) over 16hr	60
Figure 19 - IFN γ secretion in PBMDMs in response to V-antigen stimulation (+/-) over 16hr	61
Figure 20 - TNF α secretion in PBMDMs in response to V-antigen stimulation (+/-) over 16hr	62

Figure 21 - IL-10 secretion in PBMDMs in response to V-antigen stimulation (+/-) over 16hr	63
Figure 22 - Summary of IL-1B secretory pathways.....	69
Figure 23 - Caspase 1 cleavage/inflammasome activity.....	71
Figure 24 - IL-1β western blots on LPS/V-antigen-stimulated MM6 cells.....	74
Figure 25 - Caspase 1 western blots on LPS/V-antigen-stimulated MM6 cells.....	76
Figure 26 - Clustergram of Qiagen RT ² qPCR – Human Inflammasome gene array results for WT V-antigen (+/- LPS).....	79
Figure 27 - Volcano plot of ‘LPS only’ gene expression compared to ‘unstimulated’ control expression – Inflammasome gene array.....	80
Figure 28 - STRING analysis of LPS-upregulated in PBMDMs – Inflammasome gene array	83
Figure 29 - STRING analysis of LPS-downregulated genes in PBMDMs – Inflammasome gene array.....	84
Figure 30 - Volcano plot of ‘V+LPS’ gene expression compared to ‘LPS only’ expression ..	85
Figure 31 - STRING analysis of V-antigen-upregulated genes in LPS-stimulated PBMDMs – Inflammasome gene array	88
Figure 32 - STRING analysis of V-antigen-downregulated genes in LPS-stimulated PBMDMs – Inflammasome gene array.....	89
Figure 33 - IFN γ , IFN β , and IL-12B gene expression under stimulation with combinations of LPS and V-antigen.....	91
Figure 34 - IL-1 β , IL-6, and IL-18 gene expression under stimulation with combinations of LPS and V-antigen	92
Figure 35 - TNF α gene expression under stimulation with combinations of LPS and V- antigen.....	93
Figure 36 - AIM2 and NLRC4 gene expression under stimulation with combinations of LPS and V-antigen	94
Figure 37 - IRF1 gene expression under stimulation with combinations of LPS and V-antigen	95

Figure 38 - MAPK11, MAPK12, and MAPK13 gene expression under stimulation with combinations of LPS and V-antigen	96
Figure 39 - TLR4-LPS binding process	102
Figure 40 - IκBα western blots on LPS/V-antigen-stimulated MM6 cells	106
Figure 41 - TLR/TNFα/IFNγ pathways.....	109
Figure 42 - Clustergram of Qiagen RT ² qPCR – Human TLR Pathway gene array results	112
Figure 43 - Volcano plot of ‘LPS only’ gene expression compared to ‘unstimulated’ control expression	113
Figure 44 - Differentially expressed genes in LPS-stimulated PBMDMs.....	116
Figure 45 - STRING analysis of LPS-upregulated genes in PBMDMs – TLR pathway gene array	119
Figure 46 - STRING analysis of LPS-downregulated genes in PBMDMs – TLR pathway gene array	120
Figure 47 - Volcano plot of V+LPS gene expression compared to LPS only expression ...	121
Figure 48 - Differentially expressed genes in LPS-stimulated PBMDMs co-stimulated with V-antigen	124
Figure 49 - STRING analysis of V-antigen-upregulated genes in LPS-stimulated PBMDMs	127
Figure 50 - STRING analysis of V-antigen-downregulated genes in LPS-stimulated PBMDMs	128
Figure 51 - TLR3, IRF1 and PELI1 gene expression under stimulation with combinations of LPS and V-antigen.....	130
Figure 52 - IFNγ and CXCL10 gene expression under stimulation with combinations of LPS and V-antigen	132
Figure 53 - CD14 and HSPD1 gene expression under stimulation with combinations of LPS and V-antigen	133
Figure 54 - SARM1 gene expression under stimulation with combinations of LPS and V-antigen	135

Figure 55 – MAP3K7 gene expression under stimulated with combinations of LPS and V-antigen	139
Figure 56 - CD14 western blot on LPS/V-antigen-stimulated MM6 cells.....	140
Figure 57 - TGFβ1 western blot on LPS/V-antigen-stimulated MM6 cells.....	141
Figure 58 - Secreted mature TGFβ1 ELISA on the growth media of LPS/V-antigen-stimulated PBMDMs.....	142
Figure 59 - The tertiary structure of V-antigen and key functional regions	151
Figure 60 - Location of V-antigen fragments (pV1-pV6) within the WT V-antigen structure	152
Figure 61 - IL-1β secretion in PBMDMs in response to V-antigen fragment stimulation (+/- LPS).....	155
Figure 62 - IL-6 secretion in PBMDMs in response to V-antigen fragment stimulation (+/- LPS).....	156
Figure 63 - IL-8 secretion in PBMDMs in response to V-antigen fragment stimulation (+/- LPS).....	157
Figure 64 - IFNγ secretion in PBMDMs in response to V-antigen fragment stimulation (+/- LPS).....	158
Figure 65 - TNFα secretion in PBMDMs in response to V-antigen fragment stimulation (+/- LPS).....	159
Figure 66 - IL-10 secretion in PBMDMs in response to V-antigen fragment stimulation (+/- LPS).....	160
Figure 67 - Clustergram of Qiagen RT ² qPCR – Human TLR Pathway gene array results for pV1/pV2 (+LPS).....	162
Figure 68 - Clustergram of Qiagen RT ² qPCR – Human TLR Pathway gene array results for pV3/pV6 (+LPS).....	163
Figure 69 - Volcano plot of ‘LPS only’ gene expression compared to ‘unstimulated’ control expression (pV3/pV6 plate) – TLR pathway gene array	164
Figure 70 - Volcano plot of ‘LPS only’ gene expression compared to ‘unstimulated’ control expression (pV1/pV2 plate) – TLR pathway gene array	165

Figure 71 - STRING analysis of LPS-upregulated genes in PBMDMs - TLR pathway gene array	168
Figure 72 - Volcano plot of 'pV1+LPS' gene expression compared to 'LPS only' control expression (pV1/pV2) – TLR pathway gene array	169
Figure 73 - Volcano plot of 'pV2+LPS' gene expression compared to 'LPS' only expression (pV1/pV2 plate) – TLR pathway gene array	172
Figure 74 - STRING analysis of pV1-upregulated genes in LPS-stimulated PBMDMs – TLR pathway gene array	175
Figure 75 - STRING analysis of pV1-downregulated genes in LPS-stimulated PBMDMs – TLR pathway gene array	176
Figure 76 - STRING analysis of pV2-upregulated genes in LPS-stimulated PBMDMs – TLR pathway gene array	177
Figure 77 - STRING analysis of pV2-downregulated genes in LPS-stimulated PBMDMs – TLR pathway gene array	178
Figure 78 - Secreted mature TGFβ1 ELISA on the growth media of LPS/V-antigen-stimulated PBMDMs.....	179
Supplementary Figure 1 - MM6 secreted level of IL-1β in response to LPS/V-antigen stimulation.....	212
Supplementary Figure 2 - MM6 secreted level of IL-8 in response to LPS/V-antigen stimulation.....	213
Supplementary Figure 3 - MM6 secreted level of IFNγ in response to LPS/V-antigen stimulation.....	214
Supplementary Figure 4 - MM6 secreted level of IL-12p40 in response to LPS/V-antigen stimulation.....	215
Supplementary Figure 5 - MM6 secreted level of TNFα in response to LPS/V-antigen stimulation.....	216
Supplementary Figure 6 - MM6 secreted level of IL-10 in response to LPS/V-antigen stimulation.....	217

Supplementary Figure 7 - MM6 secreted level of IL-1 β in response to 12hr LPS/V-antigen stimulation.....	218
Supplementary Figure 8 - MM6 secreted level of TNF α in response to 12hr LPS/V-antigen stimulation.....	219
Supplementary Figure 9 - NLRP12, NLRP5, and NLRP9 gene expression under stimulation with combinations of LPS and V-antigen.....	220
Supplementary Figure 10 - NF κ B1, NF κ BIA, NF κ BIB, and RELA gene expression under stimulation with combinations of LPS and V-antigen	221
Supplementary Figure 11 - MAPK1 and MAPK3 gene expression under stimulation with combinations of LPS and V-antigen	222
Supplementary Figure 12 - MAPK8, MAPK9, and MAP3K7 gene expression under stimulation with combinations of LPS and V-antigen	223
Supplementary Figure 13 - BCL2L1 and BIRC3 gene expression under stimulation with combinations of LPS and V-antigen	224
Supplementary Figure 14 - NF κ B1, NF κ B2, NF κ BIA gene expression under stimulation with combinations of LPS and V-antigen	225
Supplementary Figure 15 - MyD88, IRAK4, and TBK1 gene expression under stimulation with combinations of LPS and V-antigen.....	226
Supplementary Figure 16 - CD180 and LY86 gene expression under stimulation with combinations of LPS and V-antigen	227
Supplementary Figure 17 - SIGIRR and TOLLIP gene expression under stimulation with combinations of LPS and V-antigen	228

Table of tables

Table 1 - Examples of human PRRs and their stimuli.....	3
Table 2 - TLR pathway inhibitors.....	6
Table 3 - RE mastermix.....	30
Table 4 - Antibody information.....	39
Table 5 - Gene list for the Human Inflammasome Qiagen RT ² profiler gene array.....	77
Table 6 - Upregulated genes within LPS-stimulated PBMDMs – Inflammasome gene array.....	80
Table 7 - Downregulated genes within LPS-stimulated PBMDMs – Inflammasome gene array.....	81
Table 8 - Upregulated genes within LPS-stimulated PBMDMs co-stimulated with V-antigen.....	86
Table 9 - Downregulated genes within LPS-stimulated PBMDMs co-stimulated with V-antigen.....	86
Table 10 - Densitometry of western blots probed for pIKBa/IKBa/GAPDH after 6hr and 12hr LPS+V-antigen stimulation.....	107
Table 11 - Gene list for the Human TLR Pathway Qiagen RT ² Profiler gene array.....	108
Table 12 - Upregulated genes within LPS-stimulated PBMDMs – TLR pathway gene array.....	114
Table 13 - Downregulated genes with LPS-stimulated PBMDMs - TLR pathway gene array.....	115
Table 14 - Upregulated genes within LPS-stimulated PBMDMs co-stimulated with V-antigen – TLR pathway gene array.....	121
Table 15 - Downregulated genes within LPS-stimulated PBMDMs co-stimulated with V-antigen – TLR pathway gene array.....	122
Table 16 - Fold regulation and significance of common genes between the Qiagen RT ² ‘TLR pathway’ and ‘Inflammasome’ gene arrays.....	136
Table 17 - Recombinant V-antigen fragment details.....	151
Table 18 - Upregulated genes within LPS-stimulated PBMDMs (pV1/pV2 plate).....	165

Table 19 - Downregulated genes within LPS-stimulated PBMDMs (pV1/pV2 plate)	167
Table 20 - Upregulated genes within LPS-stimulated PBMDMs co-stimulated with pV1	170
Table 21 - Downregulated genes within LPS-stimulated PBMDMs co-stimulated with pV1	170
Table 22 - Upregulated genes within LPS-stimulated PBMDMs co-stimulated with pV2	173
Table 23 - Downregulated genes within LPS-stimulated PBMDMs co-stimulated with pV2	173
Table 24 - Two-way ANOVA (with repeated measures) results for PBMDM TGFβ1 secretion in response to V-antigen fragments	180
Table 25 - SDS-PAGE gel recipes.....	208
Supplementary Table 1 - Qiagen RT ² qPCR - Inflammasome gene array full results – WT V-antigen.....	229
Supplementary Table 2 - Qiagen RT ² qPCR – TLR pathway gene array full results – WT V-antigen.....	231
Supplementary Table 3 - Qiagen RT ² qPCR – TLR pathway gene array full results – pV1/pV2	233
Supplementary Table 4 - Qiagen RT ² qPCR – TLR pathway gene array full results – pV3/pV6	235

Abbreviations:

A20 – TNF α -induced protein 3

aa – Amino acid

AAM – Alternatively-activated macrophages

ABCA1 – ATP-binding cassette transporter A1

AChR – α 7 nicotinic acetylcholine receptor

ACTB – β -actin

AFT3 – Activating transcription factor 3

AhR – Aryl hydrocarbon receptor

AIM2 – Absent in melanoma 2

Akt – Protein kinase B

ALR – AIM2-like receptor

AMP – Adenosine monophosphate

AP1 – Activating protein-1

APC – Antigen presenting cell

ASC – Apoptosis-associated speck-like protein containing a CARD

ATP – Adenosine triphosphate

β 2M – β -2 microglobulin

Bcl-3 – B-cell lymphoma 3 protein

Blimp1 – B-lymphocyte-induced maturation protein 1

BMP-2 – Bone morphogenic protein 2

BSA – Bovine serum albumin

Caf1 – Capsule-like antigen, fraction 1

CAM – Classically-activated macrophages

CARD – Caspase-recruitment domain

Cbl-b – Cbl proto-oncogene B

CCL(2/5/7) – C-C motif ligand (2/5/7)

CCR(1/2/5) – C-C motif chemokine receptor (1/2/5)

CDC – Centre for Disease Control

cDC – Conventional dendritic cell

CD – Cluster of differentiation

CFU – Colony forming units

cGAS – Cyclic GMP-AMP synthase

ChemR23 – Chemerin receptor 23

CLEC(4E/10A) – C-type lectin domain containing (4E/10A)

CLR – C-type lectin receptor

CNS – Central nervous system

COX1/2 – Cyclooxygenase 1/2

CSF2/3 – Colony stimulating factor 2/3

CT – Cycle threshold

CV – Column volume

CXCL(8/10/13) – C-X-C ligand motif (8/10/13)

CYLD – Ubiquitin carboxy-terminal hydrolase CYLD

D6 – Chemokine-binding protein D6

DAMP – Damage-associated molecular pattern

DARC – Duffy antigen chemokine receptor

DC – Dendritic cell

ddH₂O – Double-distilled H₂O

DEAF1 – Deformed epithelial autoregulatory factor-1

DMSO – Dimethyl sulphoxide

DUBA – Deubiquitinating enzyme A

ECL – Enhanced chemiluminescence

ECM – Extracellular matrix

ECSIT – Evolutionarily conserved signalling intermediate in Toll pathway, mitochondrial

EDHF – Endothelial-derived hyperpolarising factor

EDTA – Ethylenediaminetetraacetic acid

EEA1 – Early endosome antigen 1

EIF2AK2 – See PKR

ELISA – Enzyme-linked Immunosorbent Assay

ELK1 – ETS-like protein 1

eNOS – Endothelial nitric oxide synthase

ER – Endoplasmic reticulum

ERK1/2 – Extracellular signal-regulated kinase 1/2

FADD – Fas-associated death domain protein

FCS – Foetal calf serum

FDR – False discovery rate

GAPDH – Glyceraldehyde 3-phosphate dehydrogenase

GLUT1 – Glucose Transporter 1

GM-CSF – Granulocyte-macrophage colony-stimulating factor

GMP – Guanosine monophosphate

GOLD – Golgi dynamics

Gr1 – Granulocyte marker 1

GSDMD – Gasdermin D

GST – Glutathione-S-transferase

GTPase - Guanosine Triphosphatase

HIF-1 α – Hypoxia-induced factor-1 α

HLA-DR – Human leukocyte antigen-DR

HMGB1 – High mobility group box 1 protein

HPeV – Human parechovirus

HRAS – HRas proto-oncogene, GTPase

HRP – Horseradish peroxidase

HSPA1A – Heat shock protein 70

HSPD1 – Heat shock protein 60

HSV – Herpes simplex virus

ICAM-1/2 – Intracellular adhesion molecule 1/2

IF – Immunofluorescence

IFA – Immunofluorescent assay

IFN ($\alpha/\beta/\gamma$) – Interferon ($\alpha/\beta/\gamma$)

IFN γ R – Interferon γ receptor

I κ B/ α – Inhibitor of nuclear factor kappa-light-chain-enhancer of activated B cells / α

I κ BNS – Inhibitory of nuclear factor kappa-light-chain-enhancer of activated B cells, delta

I κ K($\alpha/\beta/i$) – Inhibitor of kappa kinase ($\alpha/\beta/i$)

IL – Interleukin

IL-1R – IL-1 receptor

IL-1RA – Interleukin-1 receptor antagonist

iNOS – Inducible nitric oxide synthase

IPTG - Isopropyl β -d-1-thiogalactopyranoside

IRAK1/4 – IL-1 receptor-associated kinase 1/4

IRF(1/3/5/7/9)– interferon regulatory factor (1/3/5/7/9)

JAK – Janus kinase

JMJD – Jumonji C domain-containing demethylase

JNK – c-Jun N-terminal kinase

KDO – Keto-3-Deoxy-octonate

LAP – Latency associated peptide

LB – Luria broth

LBP – Lipopolysaccharide binding protein

LCR – Low calcium response

LD50 – 50% lethal dose

LDL – Low-density lipoprotein

LFA-1 – Lymphocyte function-associated antigen-1

LPS – Lipopolysaccharide

LRR – Leucine rich repeat

LRS – Leukocyte reduction system

LY86 – Lymphocyte antigen 86

Mac-1 – Macrophage-antigen 1

MAM – Mitochondrial-associated membrane

MAPK – Mitogen activated protein kinase

MAPK8IP3 – MAPK8 interacting protein 3

MAPKK/MKK/MEK – Mitogen activated protein kinase kinase

MAPKKK – Mitogen activated protein kinase kinase kinase

MCP-1 – Monocyte chemoattractant protein-1

MCS – Multiple cloning site

MD-1/2 – Myeloid differentiation protein 1/2

MDA5 – Melanoma differentiation-associated protein 5

MDSC – Myeloid-derived suppressor cell

MES – 2-(N-morpholino)ethanesulphonic acid

MHC – Major histocompatibility complex

MMP – Matrix metalloproteinase

MM6 – Mono-mac-6

MyD88 – Myeloid differentiation primary response protein 88

NACHT – Nucleotide-binding oligomerization domain (synonymous with NOD)

NAD⁺ - Nicotinamide adenine dinucleotide

NADPH – Reduced Nicotinamide Adenine Dinucleotide Phosphate

NAIP – NLR family apoptosis inhibitory protein

NEB – New England Biolabs

NEMO – Nuclear factor κB essential modulator

NET – Neutrophil extracellular trap

NFκB (1/2) – Nuclear factor kappa-light-chain-enhancer of activated B cells (1/2)

NIK – NFκB-inducing kinase

NK – Natural Killer

NLR – NOD-like receptor

NLRC4 – NLR family CARD domain-containing protein 4

NLRP (1/3) – NACHT, LRR, and PYD domains-containing protein (1/3)

NO – Nitric oxide

NOD1/2 – Nucleotide-binding oligomerization domain 1/2

NOX – NADPH oxidase complex

NR2C2 – Nuclear receptor subfamily 2 group C member 2

NRDP-1 – Ring finger protein 41

NS1 – Non-structural protein 1

NSAIDs – Non-steroidal anti-inflammatory drugs

Nurr1 – Nuclear receptor related-1 protein

OG-V – Oregon Green-V-antigen

OPI – Oxaloacetate pyruvate insulin

P2X7 – P2X purinoceptor 7

p38/SAPK – Stress-activated protein kinase

PACT – Protein activator of interferon protein kinase EIF2AK2

PAR1 – Protease-activated receptor 1

PAF – Platelet activating factor

PAGE – Polyacrylamide gel electrophoresis

PAMP – Pathogen-associated molecular patterns

PBMDMs – Primary blood monocyte-derived macrophages

PBS – Phosphate-buffered saline

PBST – Phosphate-buffered saline (0.1% tween 20)

PcrV – Pseudomonas V-antigen

PD1 – Programmed cell death protein 1

pDC – Plasmacytoid dendritic cell

PDL1 – Programmed cell death protein ligand 1

PDLIM2 – PDZ and LIM domain protein 2

PECAM-1 – Platelet endothelial cell adhesion molecule-1

PELI1 – Pellino E3 ubiquitin protein ligase 1

PFA – Paraformaldehyde

PGC1 β – Peroxisome proliferator-activated receptor γ co-activator 1 β

PGD2 – Prostaglandin D2

PGE2 – Prostaglandin E2

PGI2 – Prostacyclin 2

PGK – Phosphoglyceratekinase

PI3K – Phosphoinositide-3-kinase

plkB α - Inhibitor of nuclear factor kappa-light-chain-enhancer of activated B cells α
(phosphorylated)

Pin1 – Peptidyl-prolyl cis-trans isomerase

PKR – Protein kinase R

PPAR(γ/δ) – Peroxisome proliferator-activated receptor (γ/δ)

PRR – Pattern recognition receptor

PSGL-1 – P-selectin glycoprotein ligand-1

PTGS2 – Prostaglandin-endoperoxidase synthase 2

PYD – Pyrin domain

RA – Rheumatoid arthritis

RACK1 – Receptor for activated C kinase 1

RAUL – Ubiquitin E3 ligase RAUL

RE – Restriction enzyme

RELA – Transcription factor p65

RIG-I – Retinoic acid inducible gene I

RIP1/2 – Receptor-interacting serine/threonine-protein kinase 1/2

RLR – RIG-I-like receptor

RLT – RNA lysis buffer

RNS – Reactive nitrogen species

ROS – Reactive oxygen species

RPE – RNA wash plus ethanol

RPMI – Roswell Park Memorial Institute

RT – Room temperature

RW1 – RNA wash 1

SARM1 – Sterile alpha and TIR motif containing 1

SDS – Sodium dodecyl sulphate

SDS-PAGE – Sodium dodecyl sulphate-polyacrylamide gel electrophoresis

SHP1 – Src homology region 2 domain-containing phosphatase 1

SIGIRR - Single Ig IL-1-Related Receptor

SIRT1/6 – Sirtuin 1/6

SLE – Systemic lupus erythematosus

SOCS1/3 – Suppressor of cytokine signalling 1/3

Sp1 – Specificity protein 1

STAT(1/2/3/4/5/6) – Signal transducer and activator of transcription (1/2/3/4/5/6)

STET – Saline/Tris/EDTA/Triton

T3SS – Type 3 secretion system

TAB1/2/3 – TGF β -activated kinase 1 binding protein 1/2/3

TAG – TRAM adaptor with GOLD domain

TAK1 – TGF β -activated kinase 1

TANK – TRAF family member associated NF κ B activator

TBE – Tris/Borate/EDTA buffer

TBK1 – TANK binding kinase 1

TF – Transcription factor

TGF β (1/2/3) – Transforming growth factor β (1/2/3)

TIMP – Tissue inhibitor of metalloproteinases

TIR – Toll/IL-1 Receptor

TIRAP – TIR-domain-containing adaptor protein

TLR – Toll-like receptor

TMD – Transmembrane domain

TOLLIP - Toll-interacting Protein

TNF(α) – Tumour necrosis factor (α)

TNFR1/2 – Tumour necrosis factor receptor 1/2

TPL2 – Tumour progression locus 2

TRADD – Tumour necrosis factor receptor type 1-associated DEATH domain protein

TRAF3/6 – Tumour necrosis factor receptor-associated factor 3/6

TRAM – Translocating chain-associated membrane protein

TRIF – TIR-domain-containing adaptor-inducing interferon- β

TRIM30/38 – Tripartite motif-containing protein 30A/38

Ubc13 – Ubiquitin-conjugating enzyme E2 N

UCHL1 – Circulating monocyte antigen

USP4 – Ubiquitin specific peptidase 4

UTP – Uridine triphosphate

VCAM-1 – Vascular cell adhesion molecule-1

VEGF – Vascular endothelial growth factor

VEGFR2 – VEGF receptor 2

VLA-4 – Very late antigen 4

VLDL – Very low density lipoprotein

VSMC – Vascular smooth muscle cell

WB – Western blot

WHO – World Health Organisation

WPB – Weibel-Palade body

WT – Wild type

Yop(B/D/E/J/H/M/P) – Yersinia outer protein (B/D/E/J/H/M/P)

Ysc – Yersinia secretion complex

1: Chapter 1: Introduction

1.1: Inflammation

1.1.1: Overview of inflammation in healthy individuals

Inflammation is a rapid, protective response generated by the body when faced with infection, injury, or the presence of foreign bodies. The goal of inflammation is to assist in returning the body to homeostasis by clearing offensive non-self-entities and promoting wound healing. Four cardinal signs of inflammation were described as early as the 1st century: redness, swelling, heat, and pain, with a fifth cardinal sign, loss of tissue function, being added in the 19th century. These cardinal signs are an overview of what defines inflammation on a macro, clinical scale but the explanation for these five cardinal signs and how inflammation assists in the return to homeostasis is found at the cellular and molecular level.

At this level, inflammation is an orchestration by leukocytes and local tissue to focus an immune response appropriately, as well as increase leukocyte infiltration into the affected tissue, prime the vasculature and circulating bodies for blood clotting, and encourage healing. A rapid and effective response is key for limiting damage/infection and this requires quick recruitment of circulating leukocytes into the afflicted tissue and appropriate priming of those cells to respond to the type of stimuli present. This is achieved through the use of inflammatory signalling molecules like cytokines, prostaglandins, chemokines, and leukotrienes which are secreted by activated leukocytes to alert other leukocytes and tissues to the presence of damage or foreign bodies. This then orchestrates both local and body-wide changes that promote infiltration, effective clearance, and repair. Inflammation is, however, damaging in nature and alters local and systemic metabolism, cellular function, behaviour, and the extracellular environment. Therefore, it must be a transient condition in healthy patients, lasting only until the inflammatory stimuli has been removed before being resolved. Failure to resolve the inflammation; chronic inflammation, can be highly detrimental to patient health and can lead to tissue damage and fibrosis as well as increased risk of arthritis, asthma, cancer, cardiovascular disease, and periodontal disease.

1.1.2: The instigation of inflammation

1.1.2.1: Detection of inflammatory stimuli

In 1989, Charles Janeway developed the theory of Pathogen-associated Molecular Patterns (PAMPs) and Pattern Recognition Receptors (PRRs) which speculated that the

innate immune system contained germline-encoded receptors that detected common structures and molecules associated with 'non-self' pathogens(2) - structures like bacterial lipoproteins, dsRNA, and flagellin which are not endogenous to humans. Each receptor was theorised to only bind specific structures and have a specific downstream signalling pathway which led to an inflammatory response tuned towards the type of stimuli that triggered that receptor such as a virus being recognised by a viral PRR and triggering an antiviral response. In 1994, Polly Matzinger added to the theory with Danger-associated Molecular Patterns (DAMPs)(3). These were 'self' molecules, often cytoplasmic and nuclear proteins/molecules like Adenosine Triphosphate (ATP) and High-mobility Group Box 1 Protein (HMGB1) that interacted with the same PRRs. As these were not naturally found extracellularly, their interaction with their PRR would denote cellular rupturing and so alert the body of necrosis and tissue damage. This addition to the theory helped to explain how sterile inflammation could arise as this is inflammation in the absence of 'non self' molecules.

Nowadays, the PAMP/DAMP/PRR theory is the proven basis for how inflammation is initialised and a considerable number of PRR families have been identified along with many of the 'self' and 'non-self' stimuli that they detect. These PRR families include Toll-like Receptors (TLRs), NOD-like Receptors (NLRs), RIG-I-like Receptors (RLRs), Absent in Melanoma 2(AIM2)-like Receptors (ALRs), C-type Lectin Receptors (CLRs), and cytoplasmic DNA sensors like Cyclic Guanosine Monophosphate(GMP)-Adenosine Monophosphate(AMP) Synthase (cGAS)(4). Each family utilises a signalling pathway downstream of the receptor to instigate cellular changes like alterations in gene expression and metabolic changes, though some of these PRRs do share some common signalling molecules. For example, TLRs utilise both Myeloid Differentiation Primary Response Protein 88 (MyD88) and TIR-domain-containing Adaptor-inducing Interferon- β (TRIF) to trigger downstream activation of a number of key transcription factors (TFs) that include Nuclear Factor Kappa-light-chain-enhancer of Activated B cells (NF κ B), Interferon Regulatory Factor 3 (IRF3), and IRF7. RLR stimulation also leads to the activation of NF κ B, IRF3, and IRF7 though this is achieved by activating proteins within the TLR signalling pathway downstream of MyD88 and TRIF but not MyD88 or TRIF itself(5, 6). This can give rise to common features between different inflammatory responses. Between and within each PRR family however, each receptor has a different specificity for which PAMPs and DAMPs they detect. Retinoic Acid Inducible Gene I (RIG-I) and Melanoma Differentiation-associated Protein 5 (MDA5), both members of the RLR family, detect dsRNA however RIG-I detects dsRNA up to 1kb and MDA5 detects dsRNA in excess of 2kb(7). Examples of known PAMP and DAMP stimuli for PRRs are shown in Table 1.

Table 1 - Examples of human PRRs and their stimuli

PRR	Examples of known ligands
TLR1	Triacyl lipopeptides
TLR2	Lipoteichoic acid, glycolipids, HSPA1A, Zymosan A
TLR3	dsRNA, poly I:C
TLR4	LPS, heat shock family proteins, fibrinogen, nickel, heparin sulphate fragments
TLR5	Flagellin, profilin
TLR6	Diacyl lipopeptides
TLR7	ssRNA, imidazoquinoline
TLR8	ssRNA, bacterial RNA
TLR9	Unmethylated CpG oligodeoxynucleotide DNA
TLR10	Triacyl lipopeptides
RIG-I	dsRNA (up to 1kb)
MDA5	dsRNA (over 2kb)
NOD1	D-glutamyl-meso-diaminopimelic acid (component of bacterial peptidoglycan)
NOD2	Muramyl dipeptide
Dectin-1	β -1,3-linked glucans, β -1,6-linked glucans
Dectin-2	β -glucans, α -mannans

TLR, Toll-like receptor; RIG-I, Retinoic acid-inducible gene I; MDA5, Melanoma differentiation-associated protein 5; NOD, Nucleotide-binding oligomerization domain 1; HSPA1A, Heat shock protein 70; LPS, Lipopolysaccharide

1.1.2.2: TLR pathway

TLRs are a highly studied family of transmembrane PRRs, named for their relation to the *Drosophila* anti-microbial protein; Toll(8). In total, there have been 10 human TLRs (TLR1-TLR10) and 12 murine TLRs (TLR1-TLR9 and TLR11-13) identified - the murine TLR10 gene is not included as endogenous retrovirus insertion has rendered it a pseudogene(9). With the exception of TLR3, TLR7, TLR8, and TLR9, which are found in endosomes, TLRs are found at the cell surface (Figure 1). A full array of TLRs are found on macrophages, dendritic cells (DCs), B-cells, mast cells, natural killer (NK) cells, monocytes, neutrophils, basophils, T-reg cells, platelets, and respiratory and intestinal epithelial and endothelial cells(10). TLR2, TLR3, TLR4, and TLR6 are also expressed by cardiomyocytes and TLR1 and TLR6 are expressed in the smooth muscle and endothelial cells within blood vessels(11).

Figure 1:

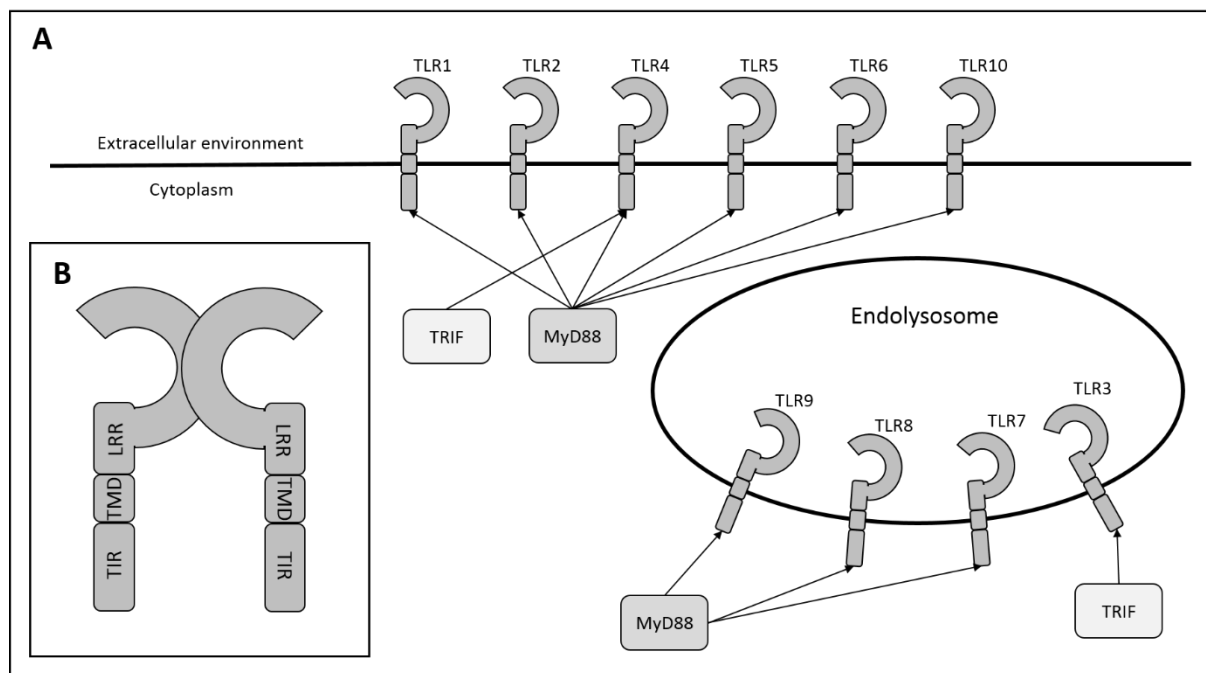


Figure 1 – TLR localisation and morphology – A; the localisation of TLRs within the cellular environment as well as the major downstream signalling pathway they utilise is shown – MyD88 or TRIF. B; a representation of the orientation taken by monomers when TLR dimers are formed and the location of key domains within the TLR monomer structure

TLR, Toll-like receptor; TIR, Toll/IL-1 receptor; TMD, Transmembrane domain; LRR, Leucine rich repeat; MyD88, Myeloid differentiation primary response protein 88; TRIF, TIR-domain-containing adaptor-inducing interferon β

TLRs function as dimers. These are typically homodimers however TLR2 instead forms heterodimers with TLR1 and TLR6. Structurally, each TLR consists of a horseshoe-shaped ectodomain which contains a Leucine Rich Repeat (LRR) domain that is involved in ligand interaction, a Transmembrane Domain (TMD), and a cytoplasmic Toll/IL-1 Receptor (TIR) domain(12). Upon stimulation, the TIR domain recruits TIR domain-containing adaptor molecules; TRIF, or TIR-domain-containing Adaptor Protein (TIRAP) which acts as an adaptor molecule for the recruitment of MyD88. As shown in Figure 1, all TLRs except for TLR3 recruit MyD88. TLR3 however recruits TRIF and TLR4 recruits both TRIF and TIRAP/MyD88. Both MyD88 and TRIF have subsequent downstream signalling pathways – shown in Figure 2 – and both pathways end with the activation of the TFs that regulate response genes such as cytokines, chemokines, and other signalling molecules that drive inflammation and orientate the immune response.

proliferation, differentiation, apoptosis, inflammation, and cell cycle regulation(13-15). Their inclusion within a pathway allows for rapid upscaling of initial responses so that substantial cellular changes can occur in a short time frame after the detection of an inflammatory stimulus.

Regulation of the TLR signalling pathway is highly important due to the inherently damaging nature of inflammation and a number of natural inhibitory proteins exist that are capable of restricting TLR signalling to prevent cases of chronic inflammation, inhibit excessively strong inflammation, and prevent errant pathway activation. Table 2 shows a few key proteins within the TLR signalling pathway and examples of their endogenous inhibitors/regulators.

Table 2 - TLR pathway inhibitors

TLR signalling pathway protein	Inhibitors
MyD88	NRDP-1, SOCS1, Cbl-b
TRIF	SARM1, TAG
TRAF3	SOCS3, DUBA
TRAF6	A20, USP4, CYLD, TANK, TRIM38, SHP1
NFκB	Bcl-3, IκBNS, Nurr1, ATF3, PDLIM2, IκB
IRF3	Pin1, RAUL

Examples of key TLR signalling pathway proteins and their corresponding regulatory proteins(16)

MyD88, myeloid differentiation primary response protein 88; TRIF, TIR-domain-containing adaptor-associated membrane protein; TRAF3/6, tumour necrosis factor receptor-associated factor 3/6; NFκB, nuclear factor kappa-light-chain-enhancer of activated B cells; IRF3, interferon regulatory factor 3; NRDP-1, ring finger protein 41; SOCS1/3, suppressor of cytokine signalling 1/3; Cbl-b, Cbl proto-oncogene B; SARM1, sterile alpha and TIR motif containing 1; TAG, translocating chain-associated membrane protein adaptor with golgi dynamics domain; DUBA, Deubiquitinating Enzyme A; A20, TNFα-induced protein 3; USP4, ubiquitin specific peptidase 4; CYLD, Ubiquitin carboxy-terminal hydrolase CYLD; TANK, TRAF family member associated NFκB activator; TRIM38, tripartite motif containing 38; SHP1, Src homology region 2 domain-containing phosphatase 1; Bcl-3, B-cell lymphoma 3 protein; IκBNS, inhibitor of nuclear factor kappa-light-chain-enhancer of activated B-cells, delta; Nurr1, nuclear receptor related-1 protein; ATF3, activating transcription factor 3; PDLIM2, PDZ and LIM domain protein 2; IκB, inhibitor of nuclear factor kappa-light-chain-enhancer of activated B cells; Pin1, peptidyl-prolyl cis/trans isomerase; RAUL, ubiquitin E3 ligase RAUL

Failure to restrain and inhibit TLR signalling has been shown in multiple studies to be highly detrimental. TLR7(17) and TLR9(18) have been implicated in the production of autoantibodies and autoreactive DCs and B cells within mouse models(19) and humans(20). The detection of 'self' nucleic acids leads to a systemic lupus erythematosus (SLE)-like disease in mice and this mechanism has been supported by the discovery of a mutation in DNase I within human patients of SLE which prevents the effective degradation of 'self' nucleic acids from apoptotic cells(21). This in turn leads to excessive TLR7/9 stimulation and autoinflammation. TLR stimulants are also regularly used within mice to generate organ-specific autoimmunity for animal models of conditions like rheumatoid arthritis (RA)(22) and autoimmune encephalitis(23) showing the dangers of excessive TLR activation. Further

mouse studies have also shown that the loss of the regulatory molecule SHP1 gives rise to inflammatory lesions(24), the loss of TRAF family member associated NFκB activator (TANK) gives rise to autoimmune glomerular nephritis(25), and the loss of A20 causes multi-organ inflammatory disorders that cause premature death(26). These inhibitory proteins are shown in Table 2 as TRAF6-regulatory proteins.

Outside of general inflammation, TLRs also play a role in platelet priming with TLR4 being shown to interact with Adenosine Diphosphate (ADP), arachidonic acid, and epinephrine to increase the capability of platelets to aggregate(27). This role has implicated it in the development of thrombosis and the responsiveness it shows to oxidised low-density lipoprotein (LDL) also shows a likely role for TLR4 in propagating atherosclerosis in humans. This was further evidenced in hyperlipidaemic mice where TLR2 and TLR4 were shown to be required for the production of atherosclerotic lesions. Additionally, the presence of some TLRs on cardiac tissue highlights their role in cardiac function and studies have shown that mice lacking TLR2, TLR4, or MyD88 have a reduced infarction rate in response to cardiac injury or cerebral ischemic-reperfusion injury(28).

1.1.2.3: Lipopolysaccharide, TLR4, and the innate immune response

Not long after the 1989 proposal of the PAMP/PRR theory, the question arose as to the identity of the specific PRR for LPS. The outer membrane component of gram-negative bacteria had long since been known to be a major trigger of inflammation and was already understood to trigger the activation of both innate and adaptive immune cells, however the receptor responsible for its detection had never been identified. In 1998 the question was finally answered by Bruce Beutler and his group who identified genetic mutations within the TLR4 gene in two lab strains of mice that were documented as being non-responders to LPS (C3H/HeJ and C57BL/10ScCr mice)(29). This was further confirmed weeks later by an independent group led by Shizuo Akira who showed experimentally that macrophages and B-cells from TLR4^{-/-} mice were hyporesponsive to LPS(30).

LPS itself is a glycolipid consisting of three main components: a hydrophobic lipid A base, a core oligosaccharide, and an outer glycan polymer termed the O antigen. Of these three components, the majority of the immune stimulation is attributed to lipid A as this is the component of LPS that is bound by TLR4 – however there is evidence that the core oligosaccharide and O antigen components do also play a role in promoting inflammation, albeit less significantly(31). The full binding process of LPS with TLR4 takes place via a series of co-factors and co-receptors including Lipopolysaccharide Binding Protein (LBP),

Cluster of Differentiation 14 (CD14), and Myeloid Differentiation protein 2 (MD-2), to shuttle LPS (and most importantly lipid A) from serum to the TLR4 structure and bind it efficiently. A full description of this process is presented in detail in 5.1.2.

The LPS/TLR4 model for inflammation became a staple within inflammatory research, in particular to reveal new mechanisms around TLR-directed inflammation but also to study the physiology of general inflammation *in vivo*. Simultaneous MyD88 and TRIF pathway activation during TLR4 stimulation is a unique property within the TLR family and it results in the activation of substantial amounts of both NF κ B and IRF3 simultaneously. In combination these TFs give rise to the expression of both classical bacterial cytokines like Interleukin-1 β (IL-1 β), IL-6, and Tumour Necrosis Factor α (TNF α), as well as more viral-associated cytokines like type 1 interferons (Figure 3), and this results in a potent inflammatory response that triggers cellular activation(32), the oxidative burst in phagocytes(33), the induction of the glycolytic flux(34), and in *in vivo* mouse studies, causes the mice to exhibit the classical signs of sickness behaviour including anhedonia, reduced motor activity, and impaired cognitive abilities(35). LPS/TLR4 therefore became an effective model for studying the mechanisms and effects of inflammation, an overview of which is shown in Figure 3.

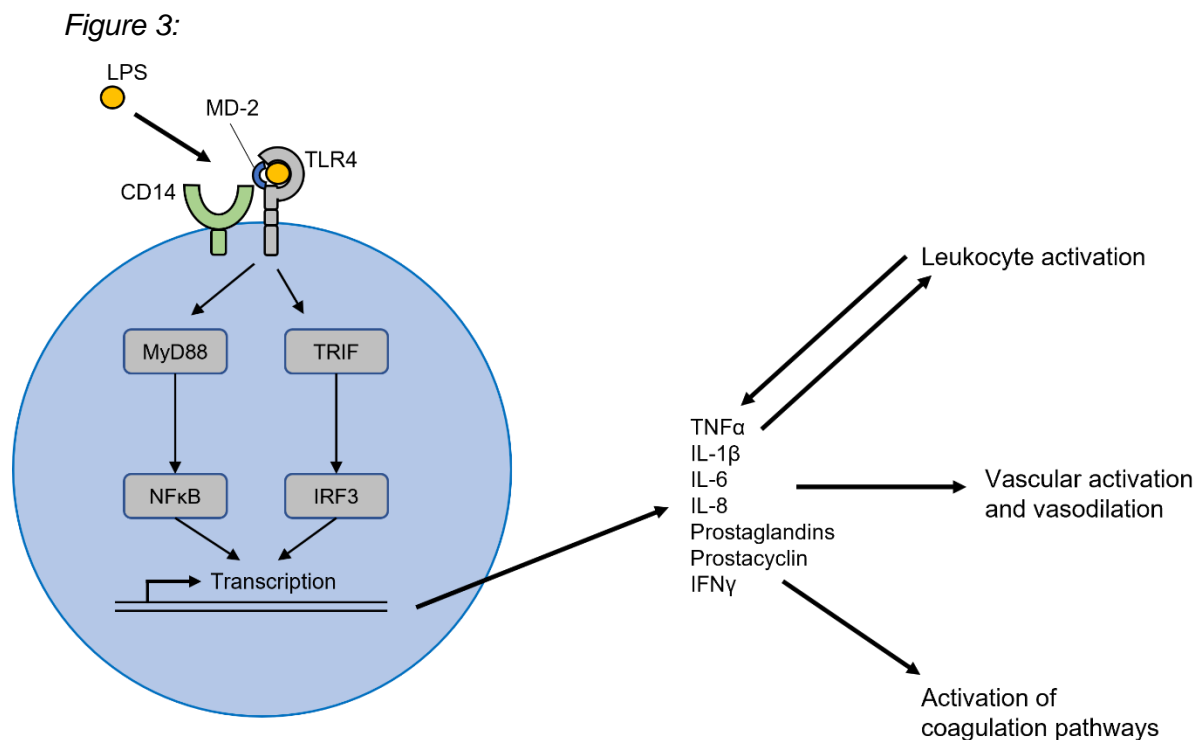


Figure 3 – The effect of LPS stimulation in vivo – The detection of LPS and subsequent instigation of the MyD88 and TRIF pathways triggers the transcription of inflammatory genes such as cytokines and chemokines. The secretion of these leads to local/systemic inflammation which activates surrounding leukocytes, triggers the activation and dilation of the local vasculature, and instigates the priming of the coagulation pathways within the blood

LPS, lipopolysaccharide; MD-2, myeloid differentiation protein 2; CD14, cluster of differentiation 14; TLR4, toll-like receptor 4; MyD88, myeloid differentiation primary response protein 88; TRIF, TIR-domain-containing adaptor-inducing interferon- β ; NF κ B, nuclear factor kappa-light-chain-enhancer of activated B cells; IRF3, interferon regulatory factor 3; TNF α , tumour necrosis factor α ; IL-1 β /6/8, interleukin 1 β /6/8; IFN γ , interferon γ

Models of LPS-induced inflammation were not just used to explore normal, healthy levels of inflammation though. Studies also tested the extremes of inflammation, analysing the effects of excessive immune activation at both the cellular and physiological level. Studies into what was termed; endotoxemia, and endotoxic shock had by this point already shown that a high enough dose of LPS in LPS-responsive models is lethal and that this lethality is caused by a dysregulation of the innate immune response. Further studies showed that this was largely driven by TNF α - as shown by the similarities between endotoxic shock and inoculation with high levels of TNF α alone(36) - however, other major inflammatory factors such as IL-6, IL-1 β , and Nitric Oxide (NO) were all shown to also contribute to the lethality of LPS-induced shock(37-39). Within healthy inflammation, proinflammatory cytokines like these promote cellular activation and vasodilation to increase the recruitment potential of the local vasculature. NO, for example, is a well-known vasodilator within healthy inflammation but during endotoxemia, a higher than normal level of NO production leads to excessive vasodilation which causes hypotension and haemoconcentration(39). Hypoxic tissue damage as a result of altered tissue perfusion can then occur and in extreme enough cases,

so can hypotensive shock. In this way, protective mechanisms of the inflammatory pathway can become deleterious when excessively stimulated. Another example is the local priming and activation of coagulation pathways that occurs during healthy inflammation. This occurs as a preparatory measure for clotting damaged vasculature and wounds, but studies have shown that endotoxemia causes systemic priming which can cause disseminated intravascular coagulation – a condition that can also cause organ dysfunction via altered tissue perfusion(40). These pathologies do not arise in TLR4^{-/-} mice(30), and both anti-inflammatory therapeutics and inoculation with the anti-inflammatory cytokine IL-10 reduce morbidity and the lethality of LPS *in vivo*(41) - evidencing that the pathophysiology that arises in endotoxemia is caused solely by TLR4-LPS interactions driving a dysregulated inflammatory response.

In human studies, doses as low as 2ng/kg of LPS cause rapid fever, tachycardia, reduced heart rate variability, and mild-moderate hypotension(42). This is accompanied by up to 95% of all circulating monocytes from all monocyte subsets rapidly disappearing from circulation(43) – a phenomenon that is theorised to arise from the systemic activation of circulating monocytes and therefore vascular binding and rolling as they attempt to extravasate. These monocyte populations are then repopulated from the bone marrow within 8-24hr - results which correlate to mouse studies which showed that circulating TLR stimuli like LPS could induce the emigration of bone marrow monocytes within 24hr of inoculation(44). This highlights not only the activating abilities of LPS but also the ability it has to trigger further inflammation through the recruitment of more active innate immune cells, which can, therefore, promote further dysregulation in excessively inflammatory conditions.

1.1.3: A dysregulated innate immune response: sepsis

LPS-TLR4 inflammation studies have largely focused on understanding the core mechanisms of inflammation and cellular responses to inflammatory stimuli, however endotoxemia also became an early model for understanding some of the key pathophysiological symptoms within sepsis. Although it is now understood to be an inadequate model of the condition, the presence of endotoxemia in up to 82% of cases of sepsis(45) and the presence of a dysregulated innate immune response in both conditions allowed these initial studies to identify similarities and understand some of the mechanisms that drive the sepsis pathology.

Sepsis is defined by the European Society of Intensive Care Medicine/Society of Critical Care(46) as a 'life-threatening condition caused by a dysregulated host response to infection'. Most commonly, it arises through pneumonia, intra-abdominal infection, or urinary tract infection but it can occur through any route of infection(47). During the course of this infection, the causal pathogen or its products infiltrate the bloodstream and generate a dysregulated systemic inflammatory response which creates a unique, deleterious pathology that is entirely separate from the pathology generated by the causal pathogen itself(46). More than 80% of the transcriptional response seen within leukocytes during sepsis is common between cases, regardless of the route of infection or the type of causal pathogen(48) and these transcriptional changes were found to be highly similar to the transcriptional changes seen in trauma, burn injuries, and non-infectious respiratory distress patients(49). Therefore, the immunopathology seen in sepsis would appear to be a unique state of the immune system that arises when dealing with extreme insult.

Unlike other inflammatory diseases which are often underlined by genetic defects, inappropriate responsiveness, or autoimmunity, the immunopathology of sepsis can arise in healthy immune systems as a result of extreme insult. It is not currently understood how this transition into the unhealthy, dysregulated state occurs, however it is known that after this switch, the immunopathology of sepsis is driven by the dysregulation of both the proinflammatory and anti-inflammatory sides of the immune response. Instead of following the path of healthy inflammation (Figure 3), sepsis is a condition where inflammation fails to sustain and resolve appropriately giving rise to a critical, acute immunopathology that poses a danger to the life of the patient (Figure 4) particularly due to the systemic nature of the inflammation.

Septic patients often present with excessively high levels of circulating proinflammatory cytokines like IL-6, TNF α , IL-1, IL-8, IL-18, and IL-3(50) which are capable of activating resting innate immune cells, triggering vasodilation, and promoting coagulation, as in Figure 3. Strong correlations between the levels of these proinflammatory cytokines and mortality rates have already been well characterized(51). While this is similar to endotoxemia, unlike endotoxemia, studies have also shown a correlation between increased levels of anti-inflammatory cytokines and increased mortality suggesting that stronger inflammatory signalling; pro- or anti-, is negatively linked to survival in sepsis patients(50). TNF α , widely regarded as one of the most important cytokines in driving the excessive proinflammatory state within both endotoxemia and sepsis, promotes endothelial cell apoptosis when present at high enough concentrations and within both conditions this has been recognised as a source of additional inflammation due to the increase in circulating DAMPs(52, 53). The increased recognition of DAMPs further promotes activation of immune cells and the

endothelium and this in turn exacerbates the dysregulation of the inflammatory response. The exposure of underlying Extracellular Matrix (ECM) components after endothelial cell apoptosis also increases local clotting potential.

Cellular activation is also affected in the dysregulated response of sepsis. Described in 1.1.2.3, endotoxemia results in large scale systemic activation of circulating cells. Similarly, in sepsis, an increased migration of both mature and immature neutrophils into the peripheral blood is often seen(54) and the excessive stimulation can trigger the release of Neutrophil Extracellular Traps within the vasculature(55), adding to the clotting potential within local blood vessels and also adding to a depletion of mature neutrophils as they undergo NETosis. Both features are also seen within endotoxemia studies(55, 56).

Complement, a cascade of serum proteins involved in inflammation and immunity, also becomes activated to a higher degree within sepsis and endotoxemia and uncontrolled activation of C3a and C5a – two effector proteins of the complement system – leads to tissue damage and organ failure by promoting further inflammation and vasodilation, vascular damage, leukocyte invasion of tissues, and cardiac dysfunction.

The sepsis pathology therefore acts as a real-world example of the dangers of dysregulation of host innate immune responses. Mechanisms that are naturally protective at healthy levels are unable to maintain their regulation and become damaging and potentially life-threatening. Of particular note, the septic immunopathology forms a self-promoting cycle as inflammation-led tissue damage and cellular apoptosis triggers subsequent leukocyte activation and increased cytokine signalling which then feeds back into greater inflammation (Figure 4). The result, as in endotoxemia, can be hypoxic tissue damage through poor tissue reperfusion and lactic acidosis, haemoconcentration, hypotension, and in some cases hypovolemic shock.

Figure 4:

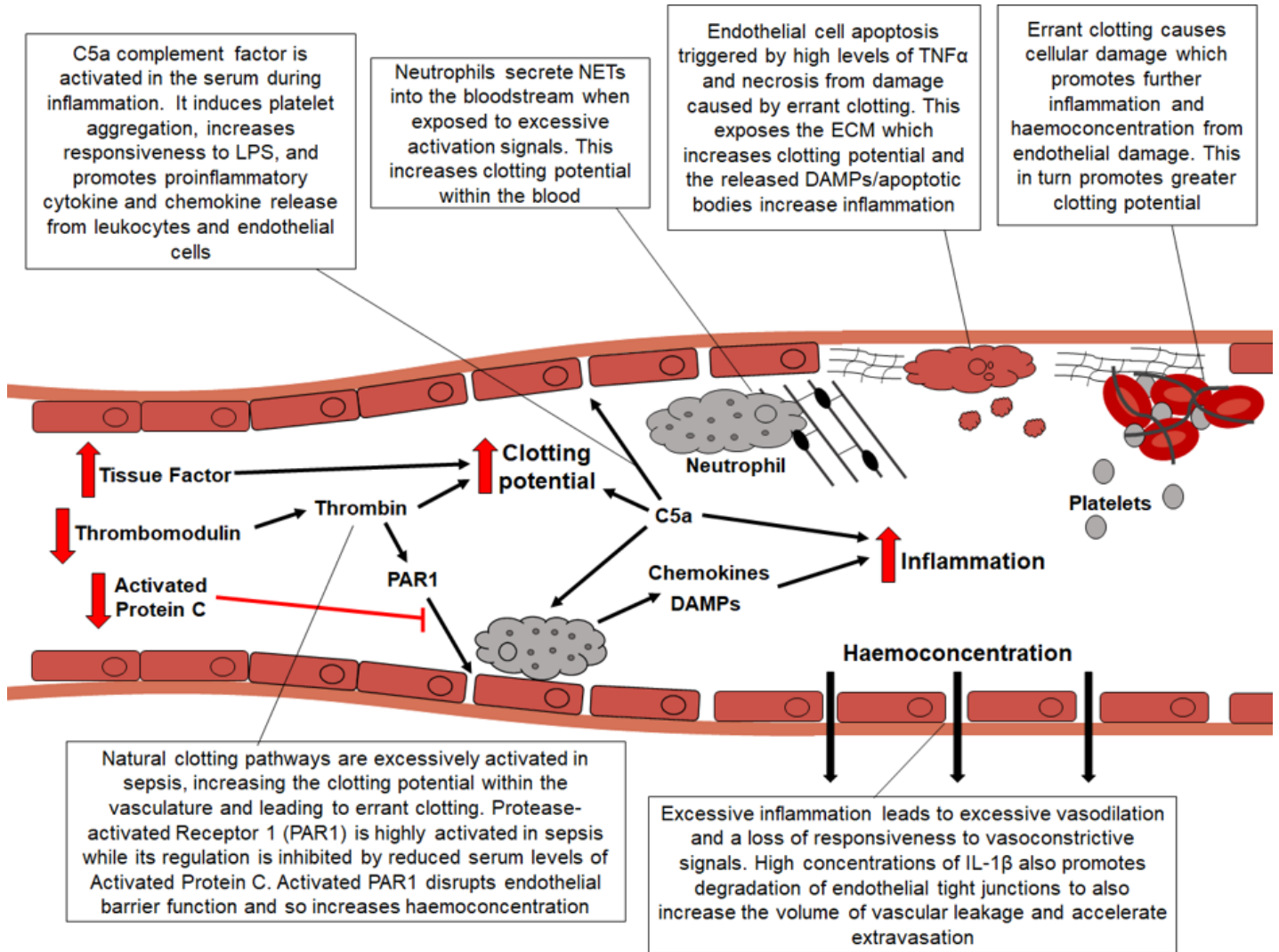


Figure 4 – The effects of the septic immunopathology on the blood, vasculature, and tissues/organs – The effects of sepsis on the vasculature and through tissues occur through exposure to high levels of inflammatory cytokines and errant clotting within the blood vessels. This leads to haemoconcentration, epithelial cell death, increased inflammation, and promotion of further clotting

PAR1, protease-activated receptor 1; LPS, lipopolysaccharide; NET, neutrophil extracellular trap; DAMP, damage-associated molecular pattern; ECM, extracellular matrix

1.1.4: Resolving inflammation

1.1.4.1: Natural resolution

Inflammation is, at its fundamental core, an attempt by the body to return afflicted tissues to homeostasis and inflammation is, by its nature, destructive. Therefore, resolving inflammation effectively is critical to prevent excessive tissue damage and to allow the tissue to return to its natural, healthy state. The majority of this process is controlled through anti-inflammatory and pro-reparative cytokines like IL-10, Transforming Growth Factor β (TGF β), IL-4, IL-1 Receptor Antagonist (IL-1RA), and Vascular Endothelial Growth Factor (VEGF).

Early in resolution, macrophages undergo a phenotypic change into an anti-inflammatory phenotype(57). These are termed 'resolution-phase macrophages' and they arise through TGF β signalling(58) or after the phagocytosis of apoptotic neutrophils. Once they have begun differentiating, resolution-phase macrophages become hyporesponsive to proinflammatory stimuli like TLR stimulation(59). They cease production of proinflammatory cytokines and lipid mediators, and begin to secrete the anti-inflammatory cytokines IL-10 and TGF β (60). Additionally, they also develop a higher efficacy for phagocytosing apoptotic neutrophils, upregulate the expression of proteins involved in antigen processing and presentation, and secrete higher levels of B- and T-cell chemoattractants like C-C Motif Ligand 5 (CCL5) and C-X-C Motif Ligand 13 (CXCL13). As they infiltrate the tissue, the recruited T-cells are exposed to anti-inflammatory cytokines like TGF β , triggering their differentiation into Treg cells and promoting immune tolerance within the tissue(61).

While reducing the inflammatory potential of the environment, these macrophages also reduce tissue infiltration from circulating leukocytes by sequestering chemokines through the secretion of Matrix Metalloproteinases (MMPs)(62-65) - a process that is also assisted by apoptotic neutrophils which sequester local chemokines by expressing a high level of surface C-C Motif Chemokine Receptor 5 (CCR5) to ensure that their apoptotic bodies bind and neutralise chemokines in the local environment(66). Downstream signalling of some chemokine receptors such as CCR1, CCR2, and CCR5 are directly inhibited by increased IL-10 however only downstream signalling is inhibited and not receptor expression, converting the receptors into sequestering receptors(67). These factors combine with the anti-inflammatory properties of upregulated cytokines like IL-4, IL-10, and TGF β to reduce the inflammatory state of the local environment and so also reduce tissue infiltration by circulating leukocytes.

Finally, once the inflammation and infiltration has been controlled, the final step of resolving inflammation is tissue repair. There are a number of tissue-specific steps that

depend on which tissue was inflamed however the common factors of tissue repair involve resolution-phase macrophages, stem cells, and progenitor cells(68) orchestrated again by anti-inflammatory and pro-reparative mediators like IL-1RA and IL-10 but with particular emphasis on TGF β (69, 70). Secreted TGF β promotes fibroblast to myofibroblast differentiation, the synthesis of interstitial fibrillar collagen from myofibroblasts, and upregulates the expression of Tissue Inhibitors of Metalloproteinases (TIMPs) which combine to regulate ECM components and remodel the local ECM to support the effective migration of cells involved in tissue repair(71, 72). During this stage, VEGF and TGF β also regulate angiogenesis to promote vascular restructuring within the repairing tissue(73).

1.1.4.2: Attempts to modulate dysregulated immune responses

In cases of dysregulated innate immune responses such as in sepsis, natural pathways of resolution fail to initially control the inflammation due to the extreme inflammatory environment in which the innate immune cells are situated and the systemic nature of the inflammation. Despite the elevated levels of anti-inflammatory cytokines often seen in sepsis patients, natural resolution is unable to occur due to the excessive proinflammatory stimulation. Attempts to improve patient prognosis has therefore often been targeted at reducing stimulation or proinflammatory signalling to allow natural resolution mechanism to regain regulatory control of the immune response.

Early attempts at this utilised general anti-inflammatory therapies like glucocorticoids. These showed promise in endotoxic models but mixed results in human disease and have failed to provide any real conclusive evidence of benefiting sepsis patients since the initial studies. This is likely due to the inadequacies of the endotoxic model as a model for sepsis disease. Despite this though, low dose glucocorticoids are still occasionally used(74). Higher doses of steroids were also trialled however these were shown to increase mortality in septic patients(75). Vasopressors, like norepinephrine, epinephrine, and dopamine are occasionally used in high-risk patients to try and counteract the vasodilation and hypotension caused by excessive inflammation(103). While it has been recorded to reverse septic shock in some instances, the efficacy has been questioned by some studies as mortality at 28-days is not significantly improved in larger studies(104). Another method of combatting the vascular pathology is use of activated Protein C. Protein C is inhibited from being converted into activated Protein C in septic patients, and as shown in Figure 4, activated Protein C is an important anticoagulant factor that inhibits thrombin function and prevents overactivation of Protease Activated Receptor 1 (PAR1) – a regulator of vascular integrity, inflammation and coagulation. Recombinant activated Protein C was cleared for therapeutic use in human

septic patients in 2001(105). However, in 2011, the failure to replicate the initial study's significance in 28-day mortality combined with the side effect of encephalitic haemorrhage in roughly 2.5% of patients treated with recombinant activated Protein C, led to the withdrawal of it as a treatment(106).

Novel and more focused attempts to modulate inflammation, particularly in response to LPS, have targeted a wide range of proteins and effectors from the TLR pathway (Figure 2) and general inflammatory mechanisms (Figure 3). TLR4 antagonists; TAK-242 and Eritoran, were both developed as potential sepsis therapeutics to restrict LPS-TLR4-mediated inflammation, however despite promising results at early-stage clinical trials, neither showed any benefits at stage III and so did not progress further(76, 77). Alternative attempts to inhibit the interaction of LPS and TLR4 focused on sequestering LPS within the bloodstream. Examples such as Polymyxin B(78), which showed high efficacy but was not well tolerated in humans, and Geniposide(79), which shows promising results at inhibiting LPS-triggered inflammation in *in vivo* mouse models and cell culture systems but has not advanced to human studies, show that this method has the potential to reduce inflammation to LPS however there are still many challenges to overcome with it to create a credible therapeutic for human sepsis disease. The use of synthetic triglyceride-rich lipids to mimic the LPS sequestering capabilities of natural triglyceride-rich lipids like LDLs and Very Low Density Lipoproteins (VLDLs) may provide a better route for this method as these are likely to be better tolerated than non-endogenous substances(80). Other attempts to inhibit the LPS-TLR4 route of inflammation have centred around the inhibition of C5a(81) – a complement effector protein which promotes platelet aggregation, leukocyte tissue invasion, cardiac dysfunction, and increasing inflammation (Figure 4). Part of its mechanism to promote inflammation is by increasing cellular sensitivity to LPS, leading to higher proinflammatory cytokine secretion. However, although C5a inhibitors showed promise modulating the inflammatory response in mice, they have not advanced to human studies. Direct restriction of the NF κ B pathway has also been evaluated and once again these attempts showed promise at inhibiting the inflammatory response and the emergence of chronic lung injury in mice studies but did not advance further(82).

The inhibition of key proinflammatory mediators and their signalling has also been highly studied in attempts to regain regulatory control in inflammation. IL-1 β , a major vasodilatory and proinflammatory cytokine, was targeted through intravenous delivery of recombinant IL-1RA however these attempts showed no statistically significant benefit to survival(83-85). Attempts to inhibit TNF α activity with blocking antibodies(86-92) and soluble TNF α receptors(93) also failed to show any survival benefits, despite the strong correlations between TNF α signalling and poor prognosis. A meta-analysis of 17 anti-TNF α trials did

reveal a slight significant increase in the survival of septic shock patients when using monoclonal anti-TNF α antibodies (38.6% survival vs 36% survival $p=0.04$) however it was also shown that this benefit did not extend to polyclonal antibodies or receptor blockers(94). Despite this significance though, anti-TNF α monoclonal antibodies are not used clinically due to the relatively small benefit seen as well as the cost for providing the treatment. More recently, attempts at a combined approach targeting both TNF α and IL-1 β simultaneously with TNF soluble receptor I and IL-1RA have shown promising results(95).

The sepsis immunopathology can also display an excessive anti-inflammatory presentation though and recent studies have also shown that mediating the immunosuppressive side of sepsis could be beneficial in patients who are experiencing particularly strong immunodepression. This has been evidenced in mice with the administration of IFN γ (96). Other studies have also shown that replenishing DCs(97), inhibiting T-cell apoptosis(98), and reversing the Th2-style response(99) all improve survival in septic animal models though these have not advanced to human studies currently. Some of the greatest promise so far, however, has been achieved through the personalisation of the treatment for septic patients depending on their immunopathology. For example, the use of intravenous IFN γ to reverse monocyte deactivation(100) has shown benefits to survival in both mice and humans. *Ex vivo* studies in human immunodepressed monocytes found that IFN γ increases HLA-DR expression as well as cytokine production(101) which may also be why IFN γ treatments have shown benefits in immunodepressed septic patients(96). A recent study which used serum IFN γ :IL-10 ratio as a means to determine the level of bloodstream infection within septic mice, used low-dose hydrocortisone as a treatment for mice that presented with lower levels of bloodstream infection and was able to show significant survival benefits from this approach(102). This benefit was further corroborated by re-analysis of data from previous studies which examined hydrocortisone use and patient survival in humans, suggesting that human patients may also benefit from a similar personalisation of their treatment.

The difficulties in developing these therapeutic interventions outline the importance in identifying novel molecules that are able to modulate the innate immune responses not only in sepsis but also in other inflammatory conditions, in both the aim to develop new therapeutics directly and to further understand the pathways that could potentially be targeted. In this stead, a wide variety of virulence factors derived from bacteria have been shown to be able to modulate innate immune responses and the focus of this thesis is to characterise one such virulence factor from *Yersinia pestis*.

1.2: *Yersinia pestis* and V-antigen

1.2.1: *Yersinia pestis*

Yersinia pestis is the causative agent of the plague and is a gram-negative coccobacillus that is both a facultative anaerobe and a facultative intracellular pathogen. *Y.pestis* diverged from *Y.pseudotuberculosis* 5700-6000 years ago after the acquisition of two virulence plasmids – pMT1 and pPCP1 – by lateral transfer which allowed *Y.pestis* to colonise fleas and cause systemic infections(107). *Y.pseudotuberculosis* is well documented as being capable of surviving long periods in soil or water outside of a host however a large number of genes involved in this survival have been lost in *Y.pestis* in favour of genes relating to vector-borne transmission. Despite this, *Y.pestis* has still been seen to survive considerable periods of time within the environment(108). Historically, *Y.pestis* has caused some of the largest and most impactful epidemics in recorded human history however, with the advancements of human understanding of disease transmission and modern medicines, *Y.pestis* is considerably less of a global threat in the modern world. According to the World Health Organisation (WHO) and Centre for Disease Control (CDC), there are only roughly 500-1000 confirmed cases per annum worldwide. There are occasionally outbreaks such as the 2017 Madagascan outbreak which recorded 2414 clinically suspected cases of the plague with 202 deaths(109). However, the 8.3% mortality of this outbreak was dramatically lower than the 60-100% mortality rate of untreated plague, showing that modern medical practices and antibiotic treatments have long since reduced the threat of another large-scale *Y.pestis* epidemic.

Despite the human disease, *Y.pestis* is primarily a vector-borne rodent disease and they act as an animal reservoir for the human disease. Transmission via fleas requires the blood meal to contain $\sim 10^2 - 10^3$ bacteria to sufficiently infect and colonise the flea(110). Considering the average flea can only ingest $\sim 0.1\mu\text{l}$ of blood in a single meal, *Y.pestis* must reach a concentration of at least 10^7 Colony Forming Units (CFU)/ml within the blood without killing the host prematurely. It achieves this by being remarkably adept at avoiding, and inhibiting the function of, the immune system. The 50% Lethal Dose (LD50) of *Yersinia pestis* is cited as just 1-10 CFU(111). Although it also survives in the lymph nodes, *Yersinia pestis* primarily resides in necrotic foci in the liver and spleen that eventually join together after a few days of growth and rupture into the bloodstream in high concentrations where it can be ingested by feeding fleas. Fleas though, being a parasite, do not usually change hosts without reason and so transmission of *Y.pestis* also relies on the lethality of the infection to force fleas to change host to a living counterpart. This is achieved with a mix of

organ damage, sepsis, and *Yersinia* murine toxin. Unlike most pathogenic species therefore, lethality is an important evolved trait of *Y.pestis*.

Within humans, transmission can occur via vector-borne routes from infected fleas, or aerosol inhalation. Symptoms of *Yersinia pestis* infection occur within 1-3 days of incubation and usually only arise once *Y.pestis* has established a significant and dangerous infection. This is largely due to the immunosuppressive nature of *Y.pestis* and so the prevention of normal inflammatory symptoms like fever, lethargy, and malaise. Mouse studies have shown that mice also have very minor inflammatory responses until the necrotic foci rupture(107). Macrophages and DCs are the primary targets of *Y.pestis* which is why the spleen and liver, as well as lymph nodes, are the predominant primary target organs of the infection. Although *Y.pestis* is predominantly extracellular, it is capable of surviving intracellularly which is key in early infection before immunosuppression occurs. Infected phagocytes cannot acidify their phagolysosomes, leading to a failure to kill the bacteria(112). In neutrophils, this triggers apoptosis which promotes an anti-inflammatory response from subsequent macrophages/monocytes and, in macrophages, monocytes, and DCs, this allows *Y.pestis* survival and transfer to the local lymph nodes.

Human patients infected with *Y.pestis* have low levels of TNF α , IFN γ , IL-1 β , and IL-18 and so have low levels of activation and innate immune cell function(107, 113, 114). To create this immunosuppression, *Yersinia pestis* utilises virulence factors to inhibit and disrupt inflammatory pathways within hosts. A key group of virulence proteins are the Yersinia Outer Proteins (Yop), and these are secreted via a Type 3 Secretion System (T3SS) that is encoded by the pCD1 plasmid. YopB and YopD form pores that the T3SS attaches to and then other Yop factors are secreted directly into target host cells from the bacterial cytoplasm. YopB and YopD are also secreted into the cell for reasons currently unknown but their secretion can trigger inflammasome activation and caspase 1 cleavage. YopK however regulates the secretion of YopB and YopD to prevent the initiation of pro-cytokine cleavage(115).

Studies have shown that YopM causes a global depletion of NK cells as well as a decrease of IFN γ production at day 2 post-infection which inhibits any further activation of macrophages and inhibits the development of the Th1 subclass of T-helper cells(116). It is also anti-pyrototic and anti-inflammatory as it directly blocks caspase 1 proteolysis and its recruitment to pre-inflammasome complexes. This inhibition is considered essential in the *Y.pestis* lifecycle as pyroptosis is a largely inflammatory process and is limiting to *Y.pestis* infection(117).

YopH suppresses ROS formation by inhibiting the production of ROS pathway intermediates in macrophages and polymorphonuclear leukocytes (PMNs)(118). Within T-cells, it also encourages mitochondria-driven apoptosis which depletes the population(119). It also has a role as a focal adhesion complex inhibitor and, along with two other *Yersinia* factors – Rho Guanosine Triphosphatase (GTPase) inhibitor and TopE (Rho-GAP inhibitor), it is capable of inhibiting intracellular actin dynamics to prevent phagocytosis from phagocytic innate cells and DC migration(120).

YopP inhibits the release of TNF α by macrophages(121) and suppresses CD8 T-cell response development(122). It also inhibits IL-8 secretion by epithelial and endothelial cells and, in combination with YopJ, reduces the expression of ICAM-1 and E-selectin in endothelial cells to inhibit leukocyte recruitment(123). YopJ also acetylates MAPKs to inhibit proinflammatory signalling and trigger apoptosis in naïve macrophages(124, 125). It can also trigger apoptosis in other cell types, preventing pyroptosis which, as mentioned previously, limits *Yersinia* infection. YopE inhibits caspase 1 as well, as studies have shown both YopJ and YopE have to be knocked out to see IL-1 β release from infected cells(126).

Furthermore, *Yersinia pestis* changes its LPS to contain tetra-acylated-lipid A at 37°C so that it becomes antagonistic for TLR4(127). It also has serum resistance to complement factors via its Ail protein(128). The surface protein Capsule-like Antigen, Fraction 1 (Caf1) also renders the bacteria difficult to phagocytose and also induces long term inhibition in phagocytes that have been exposed to it(129).

1.2.2: V-antigen

1.2.2.1: V-antigen within *Yersinia pestis* lifecycle

V-antigen is a *Yersinia* virulence protein encoded within the Low Calcium Response (LCR) element on the ~70kb pCD1 plasmid. It is a highly conserved protein showing a 96% sequence homology across all pathogenic *Yersinia* species(130) with a tertiary structure that has been described as ‘dumbbell-like’ (Figure 59)(131). Monomeric V-antigen is ~37kDa (327 residues) but is often found in higher multimers like homodimers and homotetramers. Though it is believed to function as a pentamer at the bacterial surface, the biological relevance of higher multimers and their interactions within *in vitro* experiments has been questioned(132). It’s surface localisation, along with its importance in *Yersinia* pathogenesis and high level of conservation, make it an appealing target for vaccination and protective epitopes within it are being used in conjunction with the *Yersinia* F1 surface antigen as a basis for vaccine design(133). Mice inoculated with V-antigen or treated with anti-V-antigen

antibodies are protected from *Yersinia* infection to at least a minimum of 1000x lethal dose of fully pathogenic *Yersinia pestis*(134).

Despite being encoded within the LCR element, V-antigen has a basal expression within *Yersinia* and is found both free within the cytoplasm and at the cell surface as the needle tip of a T3SS – Figure 5. Upon cell-cell contact or in the presence of low calcium concentrations, expression of V-antigen is upregulated and cytoplasmic V-antigen becomes secreted into the environment by a mechanism that doesn't involve the *Yersinia* secretion complex (Ysc) T3SS(135).

Figure 5:

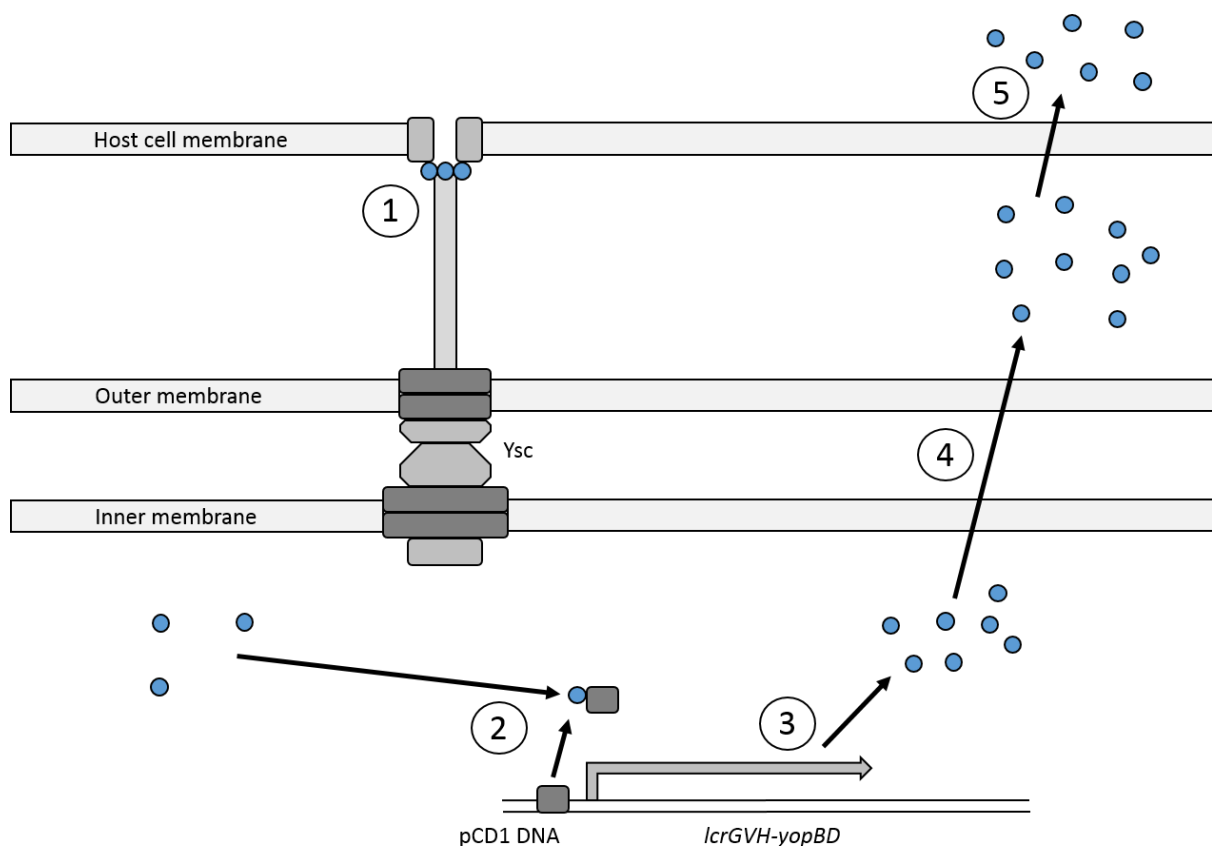


Figure 5 - Localisation of V-antigen throughout the *Yersinia pestis* lifecycle

- 1) V-antigen is found localised to the tip of the *Yersinia* Secretion Complex (Ysc) T3SS
- 2) V-antigen is also found intracellularly within the cytoplasm of pCD1⁺ *Yersinia*. Upon cell-cell contact or in low calcium conditions, cytoplasmic V-antigen binds to LcrG; a transcriptional repressor of the lcrGVH-yopBD operon, causing it to dissociate from the operon promoter region.
- 3) With repression lifted, transcription of the lcrGVH-yopBD operon takes place which, amongst other genes, upregulates the expression of V-antigen
- 4) Through an unknown mechanism, V-antigen is secreted from the cytoplasm of *Yersinia* into the extracellular environment. This process is known to not take place through the Ysc T3SS and does not include V-antigen that is present at the tip of the Ysc T3SS either
- 5) V-antigen binds and internalises into host cells where it has been shown to have specific internal host interactors and act as a virulence protein modifying host cell behaviour

Regulation of the LCR element is controlled by V-antigen and LcrG. LcrG acts as a transcriptional repressor to the operon which encodes the LCR element genes – the lcrGVH-yopBD operon. Upon cell-cell contact or in conditions of low calcium concentration, repression is lifted, and expression is heavily upregulated. Studies showed that knocking out V-antigen prevented the expression of LCR element genes in response to low calcium or cell-cell contact(136) and also that there was direct interaction between V-antigen and LcrG(137) revealing that V-antigen alleviates the repression by directly binding LcrG.

V-antigen is also found at the needle tip of the Ysc T3SS (Figure 5) and, as such, V-antigen is involved in the translocation of virulence proteins into host cells(135, 138). As the

needle tip protein, V-antigen interacts with YopB and YopD – pore-forming proteins – to attach the T3SS to the pore. V-antigen also acts as a scaffold for the interaction between YopH and host Receptor For Activated C Kinase 1 (RACK1) which prevents bacterial phagocytosis(139). Studies have shown that rapid interaction of YopH and RACK1 is key for preventing phagocytosis and that loss of V-antigen delays the interaction substantially. There is evidence from *Pseudomonas aeruginosa* and *Shigella* that suggests that T3SS tip proteins also play a role in sensing cell-cell contact as well so V-antigen may also play a direct role in this which may also explain why it regulates LCR element expression(140, 141).

1.2.2.2: Immunomodulatory activity of V-antigen

Secreted V-antigen has been described as having numerous immunomodulatory effects such as the inhibition of neutrophil chemotaxis both *in vitro* and *in vivo*(142) as well as the downregulation of proinflammatory cytokines like IFN γ and TNF α . These changes have been associated with transcription and are prevented in pathogenic *Yersinia pestis* by treatment with anti-V-antigen antibodies(130). Treatment with intravenous V-antigen can also extend the time before mouse skin allograft rejection occurs; a process which is directed by IL-2 and IFN γ (143). Discussion of the mechanisms behind these features is presented in 1.2.2.2-1.2.2.4. V-antigen has also been recently shown to trigger apoptosis in T-cells by interacting with human IFN γ receptor when IFN γ is bound(144). Previous studies had shown that a rapid induction of decreased TNF α expression (4hr) occurred in splenic macrophages and monocytes only in the presence of T-cells(130).

Secreted V-antigen internalises within 4hr of secretion(135). All internalised V-antigen is sourced from the secreted molecules and is not sourced from V-antigen found within the T3SS and is not directly secreted from the bacterial cytosol into host cells via the T3SS. This internalisation was declared dependent on the presence of *Yersinia* bacteria due to the failure of V-antigen to internalise within 4hr in the absence of *Yersinia*. However, currently unpublished data from Prof K.Triantafilou and Dr M.Triantafilou has shown internalisation of V-antigen in monocytes within 6hr without *Yersinia* present. The internalisation of V-antigen has not been widely studied and numerous studies about the effects of V-antigen have failed to include considerations about this aspect of V-antigen's mechanisms, making long-term studies on V-antigen less reliable. This is despite previous research showing that V-antigen has specific internal interactors like host ribosomal protein S3 which it uses to delay apoptosis in macrophages(145).

1.2.2.3: V-antigen and the IL-10 response

IL-10 is an anti-inflammatory cytokine that can be secreted by innate immune cells, most lymphocytes, keratinocytes, epithelial cells, and tumour cells. Although not all of the mechanisms by which it functions are understood, it is known to bind to its heterodimeric receptor and trigger dimerization and activation of STAT3. Through STAT3 it induces the activation of SOCS3 which inhibits Janus Kinase (JAK)/STAT signalling (except for IL-10 receptor/STAT3) and particularly inhibits IFN γ signalling through STAT1(146). STAT3 is also a TF and promotes increased expression of genes linked to subduing inflammation including IL-10 and SOCS3. There is evidence to suggest that IL-10 leads to diminished NF κ B activation too, potentially through inhibited Inhibitor of Kappa Kinase (IKK) activity and the prevention of p65 NF κ B nuclear translocation. The overall effect of IL-10 stimulation is a reduced expression and secretion of proinflammatory cytokines, particularly TNF α , IFN γ , IL-1 β , IL-6, and IL-12, as well as inhibited DC maturation, inhibited monocyte to DC differentiation, reduced expression of antigen presentation proteins leading to reduced APC function, suppression of Th1/Th2 development via loss of cytokines, and reduced expression and secretion of CC and CXC chemokines.

Multiple studies have linked IL-10 and V-antigen. One early mouse study revealed that the initial resistance to LPS-mediated endotoxic shock granted by V-antigen correlated to a raised anti-inflammatory IL-10 response(147). Studies since then have corroborated that IL-10 induction can occur rapidly after V-antigen introduction *in vivo*(148-152). Mouse studies have shown the importance of IL-10 in V-antigen's immunomodulation as IL-10 deficient mice were fully protected from *Yersinia pestis* infection(151). This response was not also due to increased Th1 responses as IL-4 deficient mice were not protected. An early study investigating *in vitro* stimulations of V-antigen on primary and Mono-mac-6 (MM6) monocytes saw suppression of TNF α after 3hr V-antigen pre-incubation followed by Zymosan A – a TLR2 stimulant; an effect that was prevented by co-incubation with anti-IL-10 antibodies(149). The IL-10 levels were also tested at 2hr into the pre-incubation and were significantly higher in V-antigen samples than in control or in that incubated with the related protein; *Pseudomonas' Pseudomonas* V-antigen (PcrV). Since these studies have been published, the investigation into V-antigen's immunomodulatory capabilities have been focused on the initial, surface-receptor binding which triggers IL-10 induction up until V-antigen internalises.

However, V-antigen is capable of more than just inducing IL-10. Studies showed that it was also capable of driving the phenotypic change of DCs into tolerogenic DCs(151). These

anti-inflammatory DCs cannot arise via IL-10 alone but can if TLR2/6 binding occurs also. V-antigen co-localises with human TLR2 in *in vitro* stimulations however cells without CD14 saw no NF κ B response suggesting that CD14 acts as an essential coreceptor(149). TLR2 and CD14 deficient mice macrophages failed to generate an IL-10 response from V-antigen incubation unlike control cells or TLR4 deficient cells. A follow-up study also showed that TLR6 was also involved in this process as mice deficient in CD14 or TLR6 saw a partial survival advantage to *Yersinia* infection though interestingly, TLR2 deficient mice did not and instead only saw a reduced IL-10 expression, greater IFN γ expression, and a similar bacterial load and mortality as control mice(151). Finally, human IFN γ bound in its receptor has been identified as a fourth receptor responsible for V-antigen binding and IL-10 upregulation(152).

There is however a great deal of controversy in this area with different studies being unable to replicate data or draw the same conclusions. CD14, for example, was reported in subsequent studies to enhance binding of V-antigen to TLR2 however was not essential for it(132, 151). One study also reported that TLR2 $^{-/-}$ mice revealed no significant differences in IL-10 levels or inflammation during *Yersinia* infection when treated with V-antigen(132). The TLR-binding region was reported as amino acid (aa)31-37; a region with no homologous sequence in PcrV which contained a highly conserved sequence, however mutation studies found no altered binding kinetics when mutating amino acids at this site and saw no IL-10 induction from either the mutant or the Wild Type (WT) protein(153). The mutant did however induce a higher level of TNF α .

Part of the reason for these controversies has been linked to the use of V-antigen from *Yersinia enterocolitica* by some studies which, although at least 96% homologous in sequence, may still have differences to that of *Yersinia pestis*. This also highlights another problem, the lack of standardization. The length of time for pre-incubations, incubations, concentrations of proteins and stimuli used, source species of V-antigen, and cell type, make direct comparisons difficult.

There is controversy around the importance of the initial IL-10 response also. Numerous studies have reported not seeing an IL-10 response, especially in *in vitro* studies, and even when present it can be fairly weak, comparable to that induced by 1ng/ml LPS at 3hr post-introduction in one study. Even the *in vivo* study(147) that highlighted the resistance to endotoxic shock that it gave showed that the IL-10 response only lasted around 6-8hr and faded steadily from induction until then. IL-10 is clearly essential in V-antigen immunomodulation as shown by IL-10 $^{-/-}$ mouse infection studies but, due to the reasons

above, the IL-10 induced by surface receptor binding before internalisation does not pose a convincing argument as being responsible for this.

1.2.2.4: The prospect of long-term anti-inflammatory properties

Continuing from the evidence presented in 1.2.2.2 and 1.2.2.3, the controversies and evidence around the immunomodulatory capabilities of V-antigen have given rise to an additional possibility; that V-antigen has an undiscovered longer-term interaction with the immune response that occurs after its internalisation. The initial IL-10 response has been the focus of all V-antigen immunomodulation experiments so far published and, while IL-10^{-/-} mice are consistently reported as completely protected from the immunomodulatory effects of V-antigen(148, 151, 153), TLR2^{-/-}, TLR6^{-/-}, and CD14^{-/-} mice are not(132, 153). This suggests that although IL-10 is essential for V-antigen's virulence, the initial IL-10 response may not be the main source of this. Currently, no long term, detailed cytokine studies exist *in vivo* or *in vitro* that uses multiple time points to sample how the expression/secretion of cytokines change under V-antigen stimulation. The only long term study into V-antigen's effects was by *Y.Nedialkov et al, 1997*(147) which investigated how different lengths of time from initial V-antigen exposure affected the lethal dose of LPS in mice. After the initial 10hr, the group stopped measuring cytokine profile. Around this time, a second wave of resistance began to develop and peaked at 48hr with the LD50 value of LPS increased ~9-fold compared to control mice. Even when readings stopped at 72hr, there remained a ~4-fold increase in LD50 value compared to the control baseline. Due to recent developments that show that V-antigen internalises and has specific internal interactors(145), there remains the unexplored possibility that V-antigen has intracellular effects that causes an inhibited inflammatory response and that these explain the discrepancies seen in the studies presented here and in 1.2.2.3.

1.3: Thesis aims

In this project, I therefore intend to investigate the longer-term effects of V-antigen incubation on the inflammatory response in both primary cells and immortalised cell lines. This will be studied with the goal of detailing the immunomodulatory effects of V-antigen on endotoxin-stimulated inflammation in greater detail than previously studied. To achieve this understanding, I will:

- Analyse the cytokine profiles of longer-term stimulated monocytes over time to identify how the inflammatory response evolves in the presence of V-antigen

- Use large data techniques such as gene arrays to identify key inflammatory pathways that are influenced by V-antigen once internalised and compare them to control cells to see how these pathways function differently during LPS stimulation
- Identify the mechanism by which V-antigen functions to shed light on how these changes occur as well as why the secondary immunomodulatory response arises and why it is dependent on IL-10
- Investigate whether the region within V-antigen which correlates to the central protective epitope is responsible for the protein's immunomodulatory capabilities and whether it can be isolated while still retaining this effect
- Evaluate whether there is potential therapeutic use for V-antigen or its fragments within inflammatory conditions based on the results seen in this project

2: Chapter 2: Methodology:

2.1: Cell culture:

2.1.1: Mono Mac-6 culture:

MM6 cells were cultured at 37°C/5% CO₂ in 24-well plates using growth media that consisted of: 'Roswell Park Memorial Institute (RPMI) 1640 + Glutamax™' media (Thermo Fisher Scientific, Massachusetts, United States), 10% (v/v) Foetal Calf Serum (FCS), 0.02% (v/v) supplementary non-essential amino acids, and 1 vial of Oxaloacetate Pyruvate Insulin (OPI) Hybri-Max™ (Sigma Aldrich, Missouri, United States) per litre of media for a final concentration of 1mM oxaloacetate, 0.45mM pyruvate, and 0.2U/ml insulin.

2.1.2: Primary peripheral blood monocyte

isolation/culture/differentiation:

Primary peripheral blood monocytes were isolated from primary blood donors and arrived in Leukocyte Reduction System (LRS) cones. The cones were drained into a 50ml falcon tube containing 15ml Ficoll buffer (GE Healthcare, Illinois, United States) and flushed through with 10ml sterile 1x Phosphate-Buffered Saline (PBS) (Appendix A) before the tube was topped to 40ml using sterile 1x PBS and mixed thoroughly. The contents were then split into 2x 50ml Accuspin columns and centrifuged at 20min/1000 x *g*/room temperature (RT). The supernatant above the buffy coat layer was removed and the buffy coat layer from both columns was added to a single tube and the volume was made up to 50ml with sterile 1x PBS and mixed gently. The cells were pelleted by centrifugation – 10min/1000 x *g*/RT and the supernatant was removed. The pellet was resuspended in 1ml ice cold Miltenyi buffer (Appendix A) and 100µl of MACS® CD14 beads (Miltenyi Biotec, Bergisch Gladbach, Germany) was added before incubation at 4°C for 15min. The volume was adjusted to 50ml with Miltenyi buffer before centrifugation at 5min/1000 x *g*/RT and removal of the supernatant. The pellet was resuspended in 1ml Miltenyi buffer and the solution was dripped through Miltenyi columns (Miltenyi Biotec) held by a magnet tube holder and pre-washed with 3ml Miltenyi buffer. The columns were washed 3x with 3ml Miltenyi buffer. Cells were eluted by removing the tubes from the magnetic tube holder and flushing the tubes forcibly with 5ml Miltenyi buffer in a syringe. The final solution was centrifuged for 5min/1000 x *g*/RT and the supernatant was removed. The pellet of CD14+ mononuclear cells was resuspended in 10ml RPMI media and counted using a Vicell cell counter (Beckman Coulter, California, US) and then diluted to a final concentration of 1x10⁶ cells/ml using RPMI media. GM-CSF was added to a final concentration of 5ng/ml and then 1ml per well of the cell

solution was plated in 24 well plates for 7 days until differentiation into peripheral blood monocyte-derived macrophages (PBMDMs) was observed.

The human biological samples were produced and handled according to the following policies to comply with both the Human Tissue Act and GSK Human Biological Sample Management policy:

POL-GSKF-410 – ‘Standards for collecting, obtaining, or using human biological samples in research’

SOP_56365 – ‘Use of human biological samples in research and development’

2.1.3: Trypan blue assay:

A 0.4% (w/v) solution of Trypan blue was produced using Trypan blue powder (Sigma Aldrich) and sterile 1x PBS. 100µl of 0.4% Trypan blue was mixed with 100µl of suspended cells and incubated for 2min/RT before being loaded into a haemocytometer and counted. The percentage of unstained cells to stained cells was then calculated based off an average over 4 separate counts.

2.1.4: Monocyte stimulation:

Monocyte growth media (as described in 2.1.1) was replaced with serum-free growth media before stimulations to prevent serum TGFβ from affecting the inflammatory response. This serum-free growth media consisted of the same components as 2.1.1 omitting the 10% FCS. Monocytes that were stimulated with V-antigen received a 30-minute preincubation before LPS addition (if it was to be added) to allow V-antigen to disperse and interact with cells (but not internalise) before LPS addition. The recording of stimulation times then began after the 30-minute preincubation (Figure 15). The concentration of LPS used in all stimulations was 100ng/ml.

2.2: DNA/RNA techniques:

2.2.1: Plasmid isolation:

To ensure that the *E.coli* still contained the plasmids correlating to the V-antigen protein fragments, the plasmid DNA was isolated from samples of the *E.coli* bacteria using phenol:chloroform:isoamyl alcohol extraction as this gives greater yields than plasmid extraction kits. Each sample was grown in 6x 20ml Luria Broth (LB) (ampicillin(100µg/ml)) at

37°C/70rpm/overnight before being centrifuged at 4000rpm/10min and their supernatant discarded. The pellet was resuspended in 400µl Saline/Tris/Ethylenediaminetetraacetic acid (EDTA)/Triton (STET) buffer (Appendix A) and vortexed thoroughly. 1mg of lysozyme was added and immediately the sample was boiled for 1min and then incubated on ice for a further 5min. The cellular debris was removed by toothpick after centrifuging for 30min at 12,000 x g. 0.1mg of RNase A was added and then samples were incubated for 30min at 37°C. 400µl of phenol/chloroform/isoamyl alcohol was added and the mixture was vortexed and then centrifuged at 12,000 x g for 15min. The upper aqueous layer was removed and kept while the lower layer was discarded. 400µl of chloroform:isoamyl alcohol was added and the samples were vortexed and centrifuged at 12,000 x g for 15min with the upper, aqueous layer once again being removed and kept and the rest was discarded. 20µl of 2M sodium acetate and 1ml of ethanol was added before a 1hr incubation at -80°C. After a 20min centrifugation at 12,000 x g, all liquid was removed from the samples and a second 1min/12,000 x g centrifugation was performed with any residual liquid being removed once more. The samples were then resuspended in 50µl sterile water and stored at -20°C.

2.2.2: Restriction enzyme (RE) digest:

A mastermix was created according to the measurements given in Table 4. This was then incubated for 15min at 37°C. As the New England Biolabs REs used in this experiment required no heat inactivation, there was no inactivation step undertaken. Samples were run immediately on an electrophoretic gel for analysis.

Table 3 - RE Mastermix

Reagent	Volume (µl)	
DNA	0.5µg	1µg
10x New England Biolabs (NEB) buffer	2.5	5
RE	0.5	1
Double-distilled H ₂ O(ddH ₂ O)	Up to 25	Up to 50
Total	25	50

2.2.3: DNA electrophoresis:

1g of agarose powder was dissolved under heat in 100ml 1x Tris/Borate/EDTA buffer (TBE) (Appendix A) and when sufficiently cooled, 5µl ethidium bromide was added and mixed into the solution. It was then poured into a gel cast and allowed to set and once solid, was placed within a horizontal gel electrophoresis chamber and covered with 1x TBE. DNA samples were mixed at a 5:1 volumetric ratio of DNA sample:6x DNA loading buffer (New

England Biolabs, Massachusetts, United States) before being loaded and run at 100V for ~40min. The resulting gel was then imaged using a UV spectrometer.

2.2.4: qPCR gene arrays:

Stimulated PBMDMs were stimulated with 50µg WT V-antigen for 30min before LPS was added to a final concentration of 100ng/ml. After 16hr, cells were lysed with vigorous pipetting in RNA Lysis (RLT) buffer (Qiagen, Hilden, Germany) (+1% β-Mercaptoethanol) and passed through QIAshredder (Qiagen) columns using centrifugation for 2min/8000 x g. A 1:1 ratio of sample:70% ethanol added to the RNeasy column (Qiagen) followed by 700µl RNA Wash 1 (RW1) buffer (Qiagen) and two washes of 500µl RNA Wash Plus Ethanol (RPE) buffer (Qiagen) with 2min/8000 x g centrifugation steps between each. The RNA was eluted from the column using 30µl RNase-free water. Following the RT² First Strand (Qiagen) protocol, 1µg of RNA was mixed with genomic DNA elimination mix (Qiagen) and incubated at 42°C for 5min before being placed on ice for 5min. 10µl of reverse-transcription mix (Qiagen) was added and the sample was incubated at 42°C for 15min before the reaction was stopped with 5min at 95°C. 91µl of RNase-free water was then added and mixed with pipetting. A further 548µl of RNase-free water and 650µl of the 2x RT2 SYBR Green Mastermix (Qiagen) was added to the cDNA sample, mixed with pipetting, and then loaded onto a 384-well RT2 Gene Profiler Array (Qiagen). The plate was sealed with optical adhesive film, centrifuged for 1min/1000 x g and then placed in a QuantStudio7Flex qPCR thermocycler (Applied Biosciences, Life Technologies) to run a programme of 1 cycle: 10min/95°C followed by 40 cycles: 15s/95°C → 1min/60°C.

2.3: Protein techniques:

2.3.1: Cell lysis (for western blot):

Cells intended to be lysed for western blotting were first pelleted by centrifugation, either 5min at 1200 x g for 15ml/50ml falcon tubes or 2000rpm/5min in a benchtop microcentrifuge, and the supernatant removed and discarded. The remaining pellet was then lysed in an appropriate volume of a denaturing 2x sample buffer (Appendix A) which contained bromomethyl blue and 5% β-mercaptoethanol by thorough pipetting.

2.3.2: Western blotting (HRP):

Samples prepared as specified above were boiled at 100°C for 10min before being loaded into a denaturing, reducing Sodium dodecyl sulphate (SDS)-Polyacrylamide Gel Electrophoresis (PAGE) (SDS-PAGE) gel and run at 180V for ~1hr in 1x running buffer (Appendix A) or 2-(N-morpholino)ethanesulphonic acid (MES) buffer (Thermo Fisher Scientific) if appropriate. The proteins within the gel were then wet transferred into a nitrocellulose membrane (Amersham, GE Healthcare) at a constant voltage of 210mA for 1hr in 1x transfer buffer (Appendix A). The membrane was blocked in 5% skim milk powder (1x PBS (0.1% tween 20) (PBST)) for 3hr and then incubated in an appropriate concentration of primary antibody in 5% skim milk powder (PBST) for 1hr before being washed in PBST. The secondary antibody was made to an appropriate concentration in PBST and then incubated with the membrane for 1hr before being washed again thoroughly with PBST. The membrane was then coated in equal volume Enhanced Chemiluminescence (ECL) reagents (Amersham, GE Healthcare) and a cassette was used to expose x-ray film (Amersham, GE Healthcare) to the membrane which was then developed by hand.

2.3.3: Western blotting (fluorescent):

Samples prepared as specified above were boiled at 100°C for 10min before being loaded into a denaturing, reducing SDS-PAGE gel and run at 180V for ~1hr in 1x running buffer (Appendix A) or MES buffer (Thermo Fisher Scientific) if appropriate. The proteins within the gel were then wet transferred into a low-fluorescent background nitrocellulose membrane (Amersham, GE healthcare) at a constant voltage of 210mA for 1hr in 1x transfer buffer (Appendix A). The membrane was blocked in 5% skim milk powder (PBST) for 3hr and then incubated in an appropriate concentration of primary antibodies in 5% skim milk powder (PBST) for 1hr before being washed in PBST. The advantage of fluorescent western blotting is the potential to use two primary antibodies on one membrane if they are sourced from different species as secondary antibodies with different fluorescent wavelengths can be used to distinguish between them. The secondary fluorescent antibodies were made to appropriate concentrations in PBST and then incubated with the membrane for 1hr before being washed again thoroughly with PBST. The membrane was then placed in the Odyssey Infrared Imaging System (Licor Biosciences, Nebraska, United States) and imaged using the Odyssey Imaging computer program (Licor) which allowed for the isolation of both 680nm and 800nm wavelengths during imaging and alteration of the fluorescence intensity to give a higher quality image.

2.3.4: Protein purification

2.3.4.1: V-antigen expression

Transformed *E.coli* was grown on a LB agar (Appendix A) plate (ampicillin(100µg/ml)) at 37°C for 24hr before six colonies were picked and expanded in 6x 20ml LB-containing universal containers (ampicillin(100µg/ml)) overnight at 37°C/70rpm. Each 20ml culture was added to 500ml LB (ampicillin(100µg/ml) + Isopropyl β-d-1-thiogalacopyranoside (IPTG) (12µg/ml)) to stimulate gene expression on the previously introduced plasmid. Each sample was incubated for 6hr at 37°C/70rpm before being centrifuged at 4°C/7000rpm/30min. The supernatant was removed and the pellet was resuspended in 1ml 1x PBS and removed with an additional wash of 1ml 1x PBS ensuring all of the *E.coli* pellet was recovered. The sample was then frozen at -20°C before being thawed, thoroughly vortexed, and then refrozen six times to lyse the *E.coli* before being centrifuged at 4°C/3500rpm/30min and the pellet discarded. The centrifugation and pellet disposal were repeated until no new pellet formed.

2.3.4.2: Protein isolation by GST-columns:

The GSTrap FF column (GE Healthcare) is designed to isolate GST-tagged proteins and so was used to purify WT V-antigen and V-antigen fragments from *E.coli* lysate. The column was first washed through with 5x column volume (CV) 1% Triton X-100 (sterile 1x PBS) before 4x CV sample was passed through slowly using a syringe. The column was capped and left to incubate for 1hr/RT. The column was then washed with 6x CV sterile 1x PBS before 1x CV cleavage buffer (Appendix A) and then 1x CV cleavage buffer(+50µl PreScission™ protease (GE Healthcare) per ml of cleavage buffer) was added. The column was capped and left to incubate for 3hr/RT. The protein was then eluted using 5x CV cleavage buffer into a sterile container.

The samples were concentrated using Vivaspin 15R protein concentrators (Sartorius Stedim Biotech, Göttingen, Germany). The protein sample was loaded into the top section of the concentrator and placed in the correct orientation before being centrifuged at 2500rpm/4°C until the sample had been concentrated to 5ml. A buffer exchange was then performed, filling the concentrator with sterile 1x PBS to the fill line and centrifuging at 2500rpm/4°C until it had again concentrated to 5ml. This was repeated a further two times to replace the cleavage buffer with sterile 1x PBS.

2.3.4.3: Endotoxin removal:

A sterile column was loaded with 10ml Pierce™ Endotoxin Removal Resin (Thermo Fisher Scientific) and the storage buffer was removed via centrifugation at 500 x *g*/4°C/5min. All subsequent passing of liquid through the column was performed using centrifugation at 500 x *g*/4°C/5min. Sterile 1x PBS was washed through the column 3x to ensure no storage buffer remained. 2M NaCl was added to the column until near the lip of the column before being passed through, followed by ddH₂O and then sterile 1x PBS. The sample was then passed through the column a total of three times to ensure maximum removal of endotoxin. Regeneration of the resin was achieved through incubation with 0.2N NaOH for 24hr/RT.

2.3.4.4: Thiobarbituric acid assay for LPS detection:

10-fold serial dilutions of 1mg/ml LPS down to 1ng/ml LPS were created to act as standards for the assay alongside a blank standard. 100µl of each sample and standard was added to 250µl 10mM H₂SO₄ and incubated at 100°C for 15min to undergo mild acid hydrolysis. 125µl of 40mM H₅IO₆ (in 60mM H₂SO₄) was added and left to incubate in the dark for 30min/RT. 125µl 0.2M NaAsO₂ (in 0.5M HCl) was then added and, once the brown colouration faded, 250µl 0.6% (w/v) aqueous thiobarbituric acid was also added and incubated at 100°C/15min. Finally, 500µl Dimethyl Sulphoxide (DMSO) was added to each Eppendorf and the solution was mixed and allowed to cool. The absorbance of each sample and standard at 549nm was measured and the blank reading was subtracted to give a relative absorbance value that correlated to LPS content of each sample.

2.3.5: Coomassie blue protein staining:

Samples in sample buffer (Appendix A) were boiled at 100°C for 10min before being loaded into a denaturing, reducing SDS-PAGE gel and run at 180V for ~1hr in 1x running buffer (Appendix A). The gel was then placed in fixing solution (Appendix A) for 30min/RT before being transferred to Coomassie blue stain (Appendix A) for 1hr/RT. The gel was then destained in Coomassie blue destain (Appendix A) overnight/RT with rocking. Finally, once bands were visible, the gel was removed from the destain solution and placed in ddH₂O for 10min to allow the gel to expand once more for the results to be photographed and analysed.

2.3.6: Fluorescent labelling of V-antigen:

For fluorescent imaging, V-antigen was labelled with Oregon Green 488 dye (Thermo Fisher Scientific). 1mg of V-antigen was buffer exchanged with 1M sodium bicarbonate buffer (Appendix A) using Vivaspin 15R protein concentrators (Sartorius Stedim Biotech) at 2500rpm/4°C to concentrate the sample and then re-dilute it in 1M sodium bicarbonate buffer three times. The sample was then concentrated to ~1mg/ml using the same equipment and centrifugation settings. 1ml of V-antigen was then mixed with 500µl 10mg/ml Oregon Green (DMSO) and then covered with tinfoil to protect the fluorescent dye from bleaching. The sample was inverted a few times to mix the sample and then was left to incubate at RT/3hr. The conjugation was terminated by adding 150µl 1.5M hydroxylamine (Appendix A), mixing by inversion, and then incubating at RT/15min. Removal of unconjugated Oregon Green was achieved by using a Sephadex PD-10 column (GE Healthcare) to separate the mixed sample by size. The column was equilibrated with 1x PBS and then the mixture of Oregon Green-V-antigen (OG-V) and unbound Oregon Green was added to the column and allowed to pass through under gravity. 1x PBS was used to elute the sample from the column. The heavier portion – bound Oregon Green – travelled fastest and eluted from the column first. It was then wrapped in tinfoil once more and stored at 4°C until use.

2.3.7: Fluorescent cell imaging:

Primary peripheral blood monocytes were isolated from donor blood (described in 2.1.2) and seeded into Nunc Lab-Tek II CC² Chamber slides (Thermo Fisher Scientific) at a density of 1×10^4 cells per well. These were then differentiated over the course of 7 days into monocyte-derived macrophages using the techniques also described in 2.1.2, as these cells are highly adherent and so ideal for use in imaging experiments. If V-antigen stimulations were performed, then they were performed at this stage. The cells were washed twice with 1x PBS and then incubated at RT/10min with 300µl 4% paraformaldehyde (PFA) (Appendix A) to fix them. Each well was washed with 1x PBS again and then blocked in 150µl Immunofluorescent Assay (IFA) blocking solution (1x PBS (0.02% Bovine Serum Albumin (BSA)/0.02%NaN₃/0.02% saponin) (Appendix A) for 30min/RT. 5µl of primary antibody was then added to the IFA blocking solution and the samples were incubated for a further 3hr/RT. The antibody solution was removed, and the wells were washed twice more with IFA blocking solution before another 150µl of IFA blocking solution and 5µl secondary antibody was added for 45min/RT/in the dark. The antibody solution was removed, and the wells were washed another two times with IFA blocking solution before another 150µl of IFA blocking solution was added along with 5µl To-Pro™-3 nuclear stain (Invitrogen) for 10min/RT/in the

dark. The solution was removed, and the wells were washed twice more in IFA blocking solution before all liquid was removed and the gasket and cover chambers were removed along with any residual glue. A drop of Vectashield (Vectorlabs, Maravai LifeSciences, California, United States) was added per pair of wells and a coverslip was laid over the samples. Air bubbles were removed using a yellow pipette tip and then the coverslips were sealed with nail varnish with completed slides then stored in the dark until use. These were then viewed with fluorescent confocal microscopy.

2.3.8: Cytokine detection:

Cytokine detection was performed using the 7-plex™ MSD Multi-spot Assay System (Meso Scale Diagnostics, Maryland, United States). As the 7-plex kit detects IFN γ , an initial 1hr/RT blocking step using 150 μ l Blocker B solution (Meso Scale Diagnostics) per well and vigorous plate shaking was required. The plate was then washed 3x with 150 μ l 1x PBS (0.05% Tween 20) per well. 25 μ l of each test sample and standard curve sample was added to each well before it was sealed and shaken vigorously for 1hr/RT. 25 μ l of 1x detection antibody solution (Meso Scale Diagnostics) was added to each well, the plate was resealed, and the plate was once again shaken vigorously for 1hr/RT. The plate was then washed a further 3x with 150 μ l of 1x PBS (0.05% Tween 20) per well and 150 μ l of 2x Read Buffer (Meso Scale Diagnostics) was then added to each well. The results were then analysed using the MESO Quickplex SQ 120 Multi-Array Reader (Meso Scale Diagnostics).

2.3.9: TGF β ELISA:

The Human/Mouse TGF-beta 1 Enzyme-linked Immunosorbent Assay (ELISA) Ready-SET-Go kit (eBioscience, California, United States) was used for detecting mature TGF β 1 from the growth media of stimulated cells. An ELISA plate was washed with the capture antibody diluted in Coating Buffer (eBioscience), sealed, and incubated at 4°C overnight. The wells were then washed 5x with Wash Buffer (eBioscience) before being blocked with 1x Assay Diluent (eBioscience) for 1hr/RT. 20 μ l of 1N HCl was added per 100 μ l for 10min/RT to acid activate latent TGF β 1 in the samples before being neutralised with 10 μ l 1N NaOH. 100 μ l of standards and samples were loaded into the plate before it was sealed and left to incubate for 2hr/RT. The plate was washed again before 100 μ l/well of detection antibody (in 1x Assay Diluent) was incubated with the samples for 1hr/RT. This was repeated with the Avidin-Horseradish Peroxidase(HRP) (1x Assay Diluent); 1hr/RT. After another wash, 100 μ l/well of Substrate Solution (eBioscience) was added and incubated for

15min/RT before the reaction was stopped with 50µl Stop Solution (eBioscience). The plate was then read at 450nm and 570nm and the final reading was presented as: OD450nm-OD570nm.

2.4: Bioinformatic analysis:

2.4.1: Qiagen Geneglobe Analysis software:

Data collected from the Qiagen RT² Profiler Arrays are exported to Microsoft Excel and uploaded to the online resource; the Qiagen Geneglobe analysis software. Designed specifically to take data from Qiagen kits and make analysis easy, the Geneglobe analysis software uses identification from the product to determine which wells in the 384-well plate correspond to which gene. Sorting the samples into 'control' and then 'sample groups', the online data software is capable of using any combination of the five housekeeping genes on the plate, as well as arithmetic or geometric means of these, to normalise the datasets and display the differences in gene regulation between different sample sets. It also contains the capability to run statistical analysis if enough replicates are present and generate an array of plots and graphs that can be directly downloaded.

2.4.2: STRING:

STRING is an online database that accepts large protein lists as an input to develop protein interaction networks as well as clustering/enrichment analysis based on publicly available protein-protein interaction information, KEGG pathway information, and Gene Ontologies. The pathway enrichment data was particularly of interest as it also provides false discovery rates (FDR) to add statistical value to enriched categories. In addition, it also provides strength values – $\log_{10}(\text{observed}/\text{expected})$ – and 'count in network' values which show how many proteins within the data provided are in a particular functional cluster list as well as the total number of members of that functional cluster. It's also possible to highlight these within generated figures to create clear visual representatives of what genes are present within the enriched pathways.

2.4.3: Statistical analysis

Statistical analysis was carried out in IBM Statistics SPSS 27 with the exception of the transcriptomic data presented in Chapters 4 (4.2.2), 5 (5.2.2), and 6 (6.2.3) where the t-tests were carried out by the Qiagen Geneglobe Analysis software (2.4.1). The comparisons between multiple conditions in 4.2.2.2 and 5.2.2.2 were then further adjusted using a manual

Benjamini-Hochberg post-hoc adjustment to account for multiple comparisons. This was performed using an online resource developed for Benjamini-Hochberg post-hoc adjustments (<https://tools.carbocation.com/FDR>).

2.5: Antibody information:

Table 4 - Antibody information

Primary/ Secondary?	Target	Polyclonal/ Monoclonal?	Species	Supplier	ID	Applications	Concentrations	Source
Primary	Caspase 1 p20	Monoclonal	Mouse	R&D	MAB6215	WB	WB: 1:1000	Mouse immunised with synthetic, recombinant peptide corresponding to human p20 and isolated from <i>E.coli</i> . Recovered using protein A purification
Primary	TGFβ	Monoclonal	Rabbit	Cell Sig. Tech.	#3709	WB	WB: 1:1000	Rabbit immunized with synthetic peptide with peptide near carboxy terminus of human TGFβ1
Primary	β2M	Monoclonal	Mouse	MyBioSource	MBS246617	WB	WB: 1:1000	Mouse immunised with full length β2M-GST and isolated via GST purification
Primary	CD14	Monoclonal	Mouse	MyBioSource	MBS178874	WB	WB: 1:1000	Mouse immunized with human CD14 then monoclonal ab purified by protein A purification
Primary	IL-1β	Polyclonal	Goat	R&D	AF-401-NA	WB	WB: 1:1000	~150aa peptide of mouse IL-1β used to generate IgG in goats and purified by antigen affinity
Primary	pIκBα (S32)	Monoclonal	Rabbit	Invitrogen	701271	WB	WB: 1:1000	<i>In vitro</i> generation of IgG using a phosphopeptide corresponding to aa27-32 of human IκBα (pS32)
Primary	pIκBα (S32/36)	Monoclonal	Mouse	Cell Signalling	92465	WB	WB: 1:1000	Phosphopeptide correlating to the Ser32/36 region of human IκBα is used to immunise mice
Primary	GAPDH	Monoclonal	Mouse	Abcam	ab8245	WB	WB: 1:10,000	Raised from mice immunised with rabbit muscle GAPDH and purified by Protein A
Primary	Histone H3	Polyclonal	Rabbit	Abcam	ab1791	WB	WB: 1:10,000	A C-terminal 100aa peptide corresponding to human Histone H3 conjugated to keyhole limpet haemocyanin that is used to immunise

								rabbits. It is purified using immunogen affinity purification
Primary	EEA1	Monoclonal	Mouse	BD Biosciences	AB_397830	IF	IF:1:500	Mouse IgG1 raised against recombinant human EEA1 (aa3-281)
Primary	V-antigen	Monoclonal	Mouse	Abcam	Ab20024	WB	WB: 1:1000	Mouse IgG1 raised against recombinant full-length <i>Yersinia pestis</i> V-antigen and purified by Protein G Sepharose chromatography
Secondary - HRP	Rabbit ab	Polyclonal	Goat	Dako	P044801-2	WB	WB:1:3000	Goat Igs isolated and specific abs isolated using affinity chromatography purification using rabbit Igs. HRP was then conjugated using Dako's own two-step glucoaldehyde HRP-conjugation method
Secondary - HRP	Mouse ab	Polyclonal	Rabbit	Dako	P0260	WB	WB: 1:3000	Rabbit Igs isolated and specific abs isolated using affinity chromatography purification using mouse Igs. HRP was then conjugated using Dako's own two-step glucoaldehyde HRP-conjugation method
Secondary - 800	Goat ab	Polyclonal	Donkey	LiCor	926-32214	WB	WB: 1:5000	Raised against full goat IgG (both heavy and light chains) and isolated via immunoaffinity chromatography
Secondary - 800	Mouse ab	Polyclonal	Donkey	LiCor	926-32212	WB	WB: 1:5000	Raised against full goat IgG (both heavy and light chains) and isolated via immunoaffinity chromatography
Secondary - 800	Rabbit ab	Polyclonal	Donkey	LiCor	926-32213	WB	WB: 1:5000	Raised against full rabbit IgG (both heavy and light chains) and isolated via immunoaffinity chromatography
Secondary - 680	Mouse ab	Polyclonal	Goat	LiCor	926-68070	WB	WB: 1:5000	Raised against full mouse IgG (both heavy and light chains) and isolated via immunoaffinity chromatography
Secondary - 680	Mouse ab	Polyclonal	Donkey	LiCor	926-68022	WB	WB: 1:5000	Raised against full mouse IgG (both heavy and light chains) and isolated via immunoaffinity chromatography

Secondary - 680	Rabbit ab	Polyclonal	Donkey	LiCor	926-68073	WB	WB: 1:5000	Raised against full rabbit IgG (both heavy and light chains) and isolated via immunoaffinity chromatography
Secondary - HRP	Rabbit ab	Monoclonal	Mouse	Santa Cruz	sc2357	WB	WB: 1:10,000	Mouse monoclonal abs raised against rabbit IgG and then affinity purified before HRP conjugation
Secondary - 680	Mouse ab	Polyclonal	Donkey	Invitrogen	AB_2534014	IF	IF: 1:30	Donkey polyclonal abs raised against mouse heavy and light chain IgGs, affinity-purified, and then conjugated with Alexa Fluor 680 dye

IF, immunofluorescence; WB, western blot; TGF β , transforming growth factor β ; β 2M, β -2 microglobulin; CD14, cluster of differentiation 14; IL-1 β , interleukin-1 β ; plkB α , inhibitor of nuclear factor kappa-light-chain-enhancer of activated B cells α (phosphorylated); GAPDH, glyceraldehyde 3-phosphate dehydrogenase; EEA1, early endosome antigen 1; GST, glutathione-S-transferase; HRP, horse radish peroxidase; aa, amino acid; ab, antibody

3: Chapter 3: Isolation and cytokine analysis of recombinant V-antigen

3.1 Introduction

3.1.1: Monocytes

This study aimed to highlight and understand the immunomodulatory effects of V-antigen on cellular inflammatory responses as a way of assessing not only the mechanism of action for V-antigen's effects, but also the potential for V-antigen to be utilised as a therapeutic intervention in inflammatory conditions. This aspect was central to our choice of cell type for use in this study.

The investigation into inflammatory responses meant that the use of innate immune cells was more appropriate. The innate immune response is responsible for the initiation and largely the propagation of an inflammatory response *in vivo* and as such the cells within it are particularly responsive to PAMPs and DAMPs and are particularly potent secretors of a full range of cytokines. This makes them the most biologically valid group of cells to draw conclusions about inflammatory conditions from. The group includes macrophages, monocytes, neutrophils, basophils, eosinophils, and DCs and of these, eosinophils and basophils were not suitable candidates as their primary roles involve parasitic and allergic responses. DCs are also more difficult to work with and form a branch between the innate and adaptive immune responses so were also considered less suitable.

Of those that remained in consideration, monocytes were selected as the most viable candidate for two main reasons. Firstly, while monocytes make up only around 2-8% of circulating white blood cells within humans - a significantly smaller percentage than neutrophils which make up 50-75% of all circulating leukocytes - monocytes and monocyte-derived macrophages, have a considerably longer average lifespan than neutrophils. They also contain a constitutively active basal level of NFκB that protects monocytes from TNFα-mediated apoptosis(154). Previous studies on V-antigen had highlighted that the secondary immunomodulatory effects of the protein occurred from 6-8hr onwards and, due to the need to stimulate cells with inflammatory stimuli for at least this long, the resistance to both routes of apoptosis, by age and by inflammation, was an appealing characteristic. Secondly, monocytes and monocyte-derived macrophages have been highlighted for their role in inflammatory conditions like sepsis, RA, psoriasis, and atopic dermatitis. Monocytes secrete particularly high levels of key proinflammatory and anti-inflammatory cytokines that drive the immunopathology of inflammatory disease and so they are highly relevant to studying the potential therapeutic capabilities of V-antigen as an anti-inflammatory.

An immortalised cell line was initially chosen to provide greater standardization and reliability than primary donors where there is far greater variability in responses. Of the common monocytic cell lines, three were briefly considered; MM6, THP-1 and U937 cells. U937 cells represent a more immature stage of development in primary cells and so were quickly ruled out due to a lower relevancy to mature monocytes. Both MM6 and THP-1 cells represent a more developed primary phenotype however MM6 cells have been shown to express a number of key mature monocyte markers that THP-1 cells do not, such as; M42, LeuM3, 63D3, Mo2, and Circulating Monocyte Antigen (UCHMI). They have also been reported to display consistent phenotypic and physiological attributes with primary monocytes(155) and so were selected as the most appropriate for this project.

It is, however, well established that immortalised cell lines are not entirely representative of primary cell types and, in particular, monocytic cell lines have been shown to compare more closely with more immature and under-developed primary monocytes(156) due to low expression of key surface markers like CD14. MM6 cells themselves do not effectively express IFN α (157) and so cannot be a perfect representation of all monocyte characteristics. Therefore, these experiments also utilised primary blood monocytes where possible (see 2.1.2 for ethics details) though these were differentiated to monocyte-derived macrophages to make them more adhesive to plates and therefore easier to use reliably.

3.1.2: The protective epitope of V-antigen

Chapter 6 of this study investigates the possibility that a central protective epitope of V-antigen is responsible for the immunomodulatory effects and whether that effect can be isolated from the full protein. The details of this work are presented in Chapter 6 however the isolation of the six V-antigen fragments (pV1-pV6) was performed alongside the isolation of WT V-antigen and so they are presented in the isolation section of Chapter 3 (3.2.1-3.2.3).

These V-antigen fragments were expressed using a plasmid expression system that was the same as the WT and were created by Dr Claire Vernazza (Ministry of Defence, Porton Down, UK) during their study on the protective capabilities of antibodies raised to these fragments(158). These were then provided to Prof Kathy Triantafilou and Dr Martha Triantafilou.

3.1.3: Chapter aims

The aims of this chapter are:

- To successfully purify a sample of WT V-antigen and the V-antigen fragments for use in further experimentation
- To validate the internalisation of V-antigen into monocytes in the absence of *Yersinia spp*
- To explore the changes in cytokine secretion as the immunomodulation caused by V-antigen progresses over time
- To compare the alterations V-antigen triggers in the cytokine profile of MM6 cells and primary PBMDMs

3.2: Results

3.2.1: Plasmid construction/details

WT V-antigen and the six V-antigen fragments (pV1-pV6) used in this project were isolated from transformed populations of BL21 *E.coli* that have been described in previous studies(158-160). These were acquired from Prof. Richard Titball (Chemical and Biological Defence Establishment, Porton Down, UK) and Dr Claire Vernazza (Ministry of Defence, Porton Down, UK) respectively. As shown in Figure 6, the expression plasmids are based on a pGEX-6P backbone (Merck, Sigma Aldrich) which contain a Glutathione-S-Transferase (GST) gene upstream of the multiple cloning site (MCS) to create a GST-tagged recombinant protein with a cleavable protease sequence for tag removal. This gene is controlled by Laclq repression. Both sets of plasmids also contain an ampicillin resistance gene that is not under Laclq repression to allow for bacterial selection.

Figure 6:

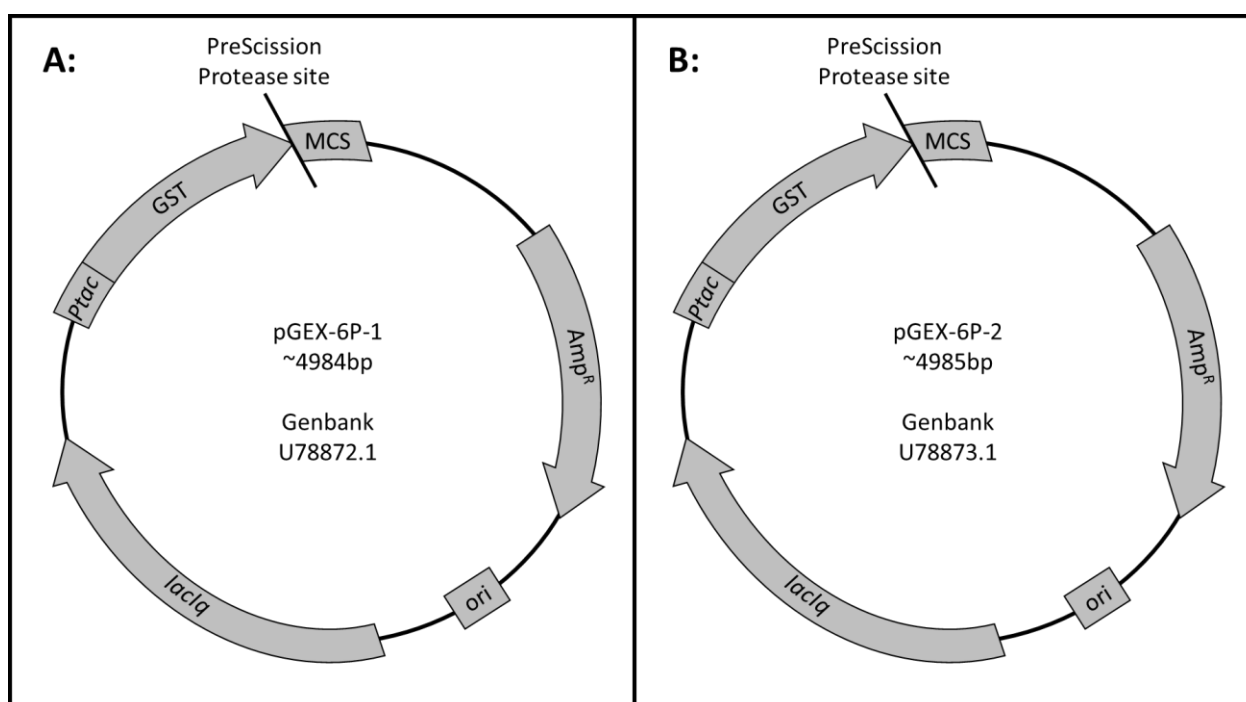


Figure 6 - Plasmid map for recombinant V-antigen and its fragments – A map of the plasmids used for V-antigen expression A; WT V-antigen, and B; V-antigen fragments. Both plasmids had their multiple cloning site (MCS) attached to a glutathione-S-transferase (GST) tag gene and both MCS sites were regulated through Lacl repression. The promoter used for GST-MCS expression was Ptac; a combination promoter of trp and lac promoters that is ideal for *E.coli* expression. Both plasmids also contained an ampicillin resistance gene (Amp^R) to allow for clone selection

Ori, bacterial origin of replication; lacIq, lac operon inhibitor IA

3.2.2: Plasmid testing

The transformed *E.coli* samples had been stored at -80°C in 50% glycerol until use in this study. However, to ensure that each still contained the transformed plasmids, cultures of each population were grown in ampicillin-containing LB (2.2.1) before plasmid DNA was isolated using phenol:chloroform extraction. The results were examined by electrophoretic gel, shown in Figure 7.

Figure 7:

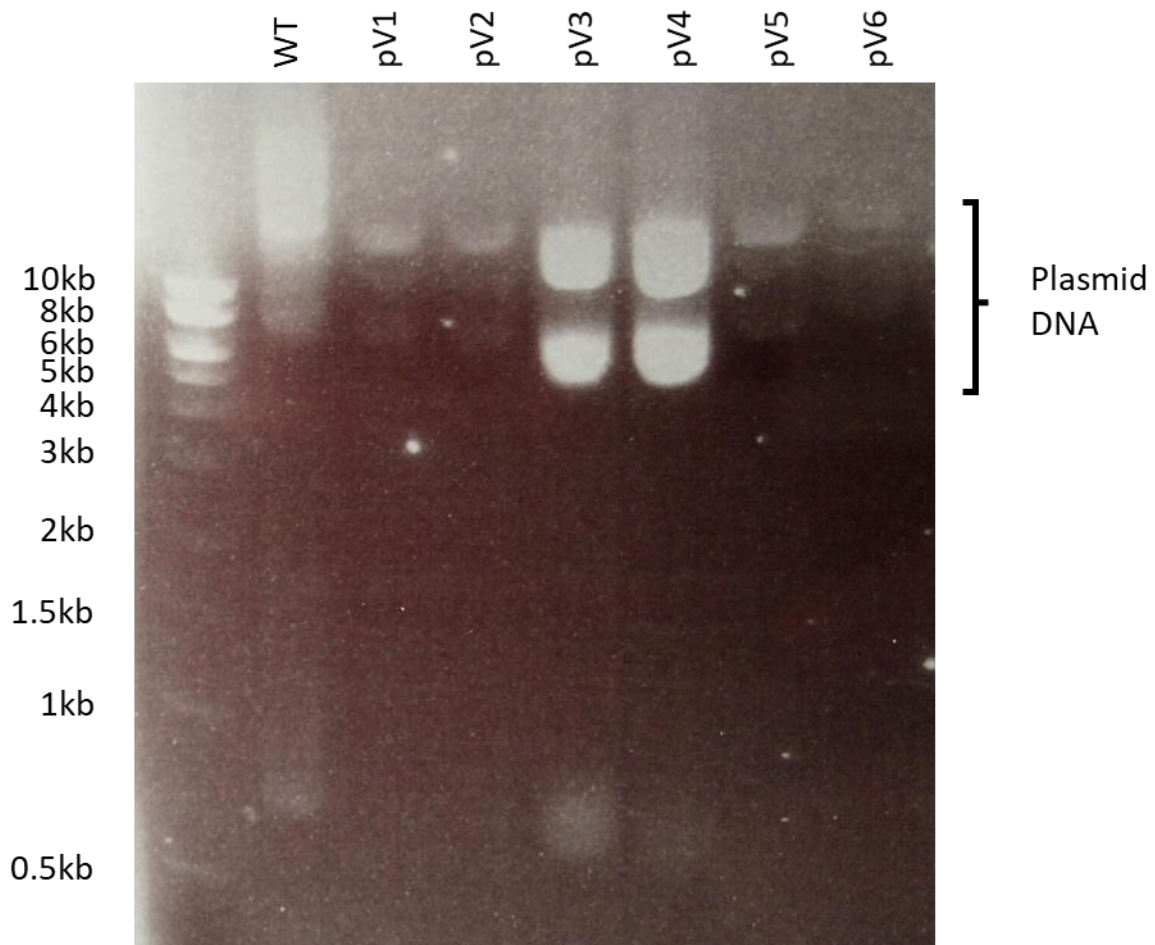


Figure 7 - Plasmid DNA isolated from transformed *E.coli* – Cultures of transformed *E.coli* from stocks containing the pGEX-6P plasmids for recombinant WT V-antigen (WT) and six V-antigen fragment (pV1-pV6) genes were grown overnight in luria broth (100µg/ml ampicillin) to select for plasmid⁺*E.coli* before plasmid DNA from each population was isolated by phenol:chloroform extraction. The isolated plasmid DNA was then visualised on an electrophoretic gel which showed that all stocks contained plasmid DNA of the expected size to contain the V-antigen/V-antigen fragment genes

An EcoRI digest on the isolated plasmid DNA from the V-antigen fragment samples revealed prominent bands at ~5,500-6,000bp – the expected size of lineated pGEX-6P-1 plasmid with a V-fragment gene insert (Figure 8). This confirmed that the majority, if not all,

of the DNA seen in Figure 7 came from a single plasmid population that was the same size as our expected plasmid and that also contained a single EcoRI site as the original plasmids had. It was therefore deemed reasonable to conclude that the *E.coli* transformed with plasmids for the V-antigen fragments had retained their plasmids and were suitable to use.

Figure 8:

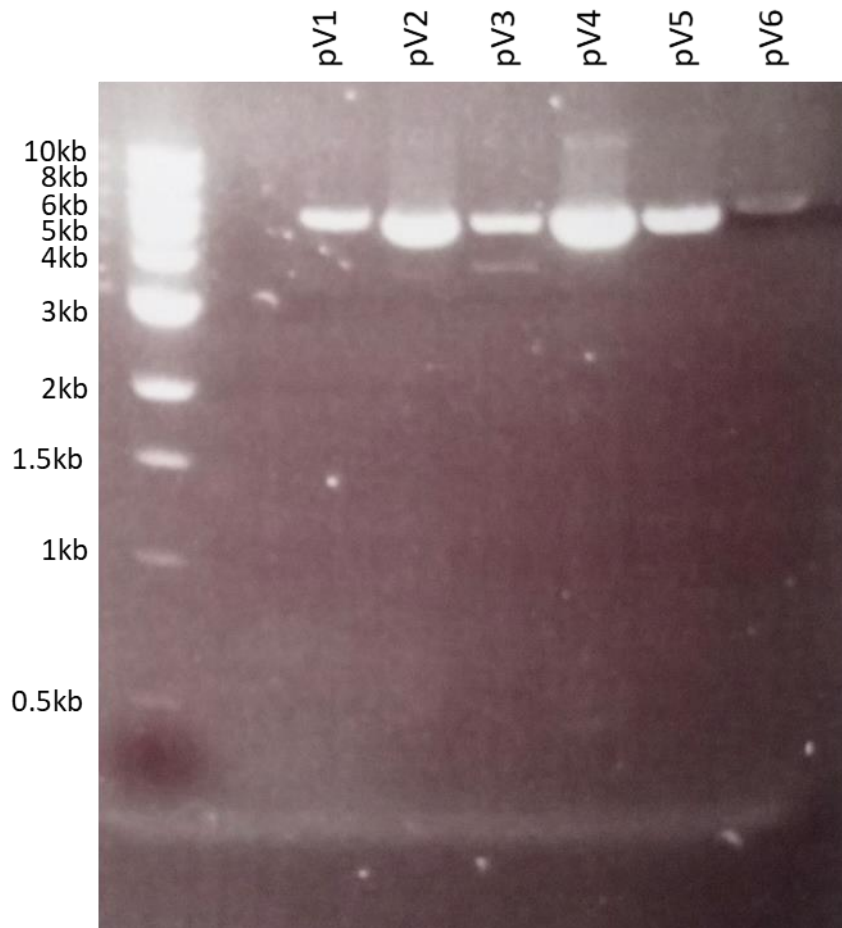


Figure 8 - EcoRI digest of isolated V-antigen fragment plasmid DNA – Cultures of transformed *E.coli* from stocks containing the pGEX-6P plasmids for six recombinant V-antigen fragment (pV1-pV6) genes were grown overnight in luria broth (100µg/ml ampicillin) to select for plasmid+*E.coli* before plasmid DNA from each population was isolated by phenol:chloroform extraction. The isolated plasmid DNA was then subjected to an EcoRI restriction enzyme digestion and visualised on an electrophoretic gel where linearized plasmid of the expected size to include the V-antigen fragment genes was seen

3.2.3: Purification of WT V-antigen and V-antigen fragments

To purify adequate quantities of V-antigen to use in stimulations, substantial volumes of the transformed *E.coli* had to be grown. To do this, 4L batches of *E.coli* were grown in LB containing ampicillin and IPTG to allow for the selection of plasmid-containing *E.coli* and the expression of the V-antigen and V-antigen fragment protein (2.3.4.1/3.2.1). To generate enough final yield of protein, 2-4 batches per population were grown and processed. As

described in 2.3.4.1, the *E.coli* were lysed by freeze-thaw cycles and the cellular debris was removed to prevent clogging of the GSTrap FF columns used in V-antigen-GST isolation.

The GSTrap columns are lined with glutathione which binds to GST and therefore retains the recombinant tagged protein within the column. The protein can then be eluted after washing steps to give pure samples of recombinant protein (described in 2.3.4.2). As shown in Figure 9, the elution step is achieved by using the PreScission Protease site that is encoded in the pGEX-6 series of expression plasmids(3.2.1).

Figure 9:

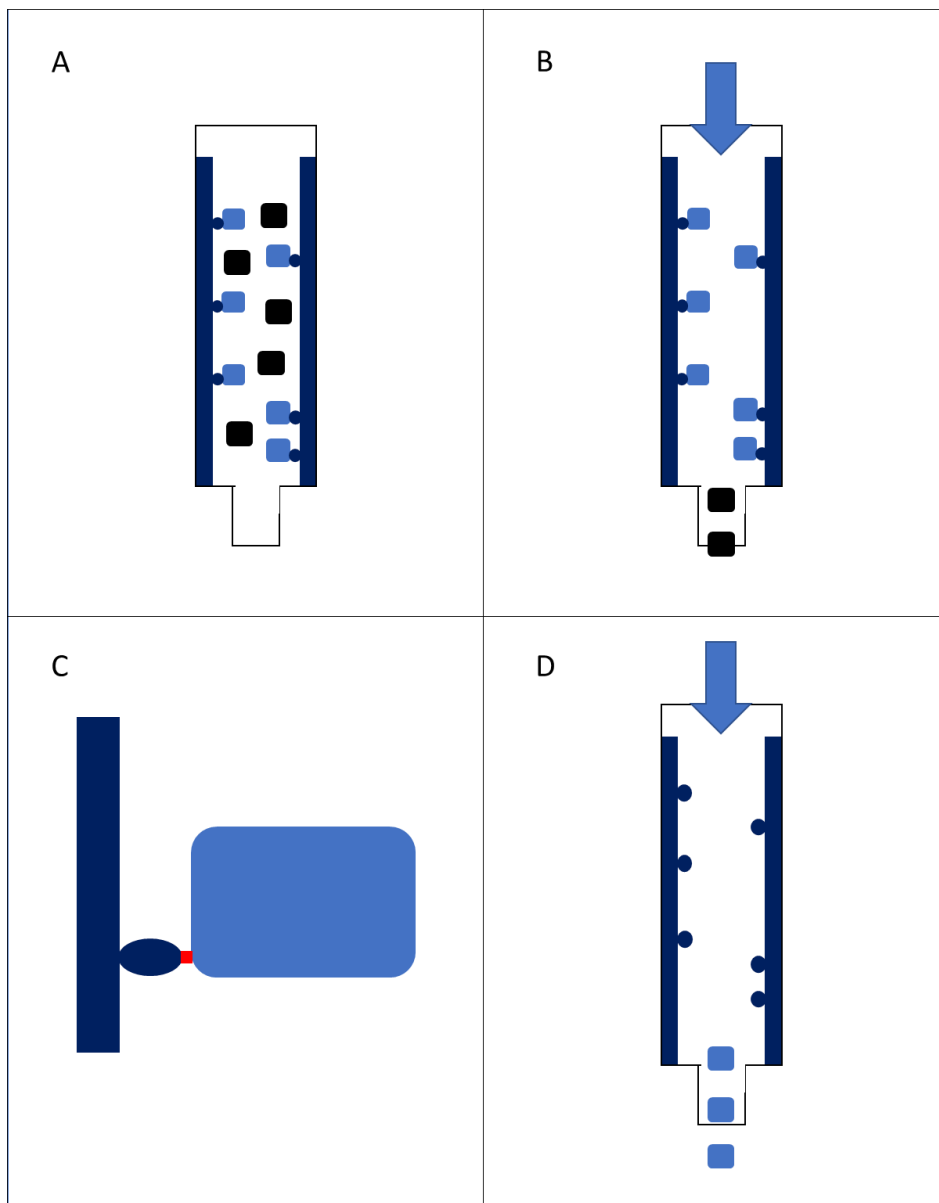


Figure 9 - The principle of GST column purification – A; sample to be purified is passed into the GSTrap column and incubated for a few minutes to allow GST-Glutathione binding between the protein's GST tag and the glutathione coating the inside of the column. B; washing steps flush unbound proteins out of the column leaving behind only bound GST-tagged protein. C; The PreScission Protease is added which cleaves at the PreScission protease cleavage site (red) between the GST tag and the native protein. D; the final elution step washes out native, untagged protein from the column to be collected

The elution buffer was buffer exchanged for 1x PBS and the sample was concentrated. To confirm the success of the purification, 100ng of each fragment sample was loaded into SDS-PAGE gels in reducing, denaturing conditions Coomassie blue staining (2.3.5). Figure 10 shows the Coomassie blue gels which reveal the presence of bands only at the expected sizes of the V-antigen fragments and their multimers.

Figure 10:

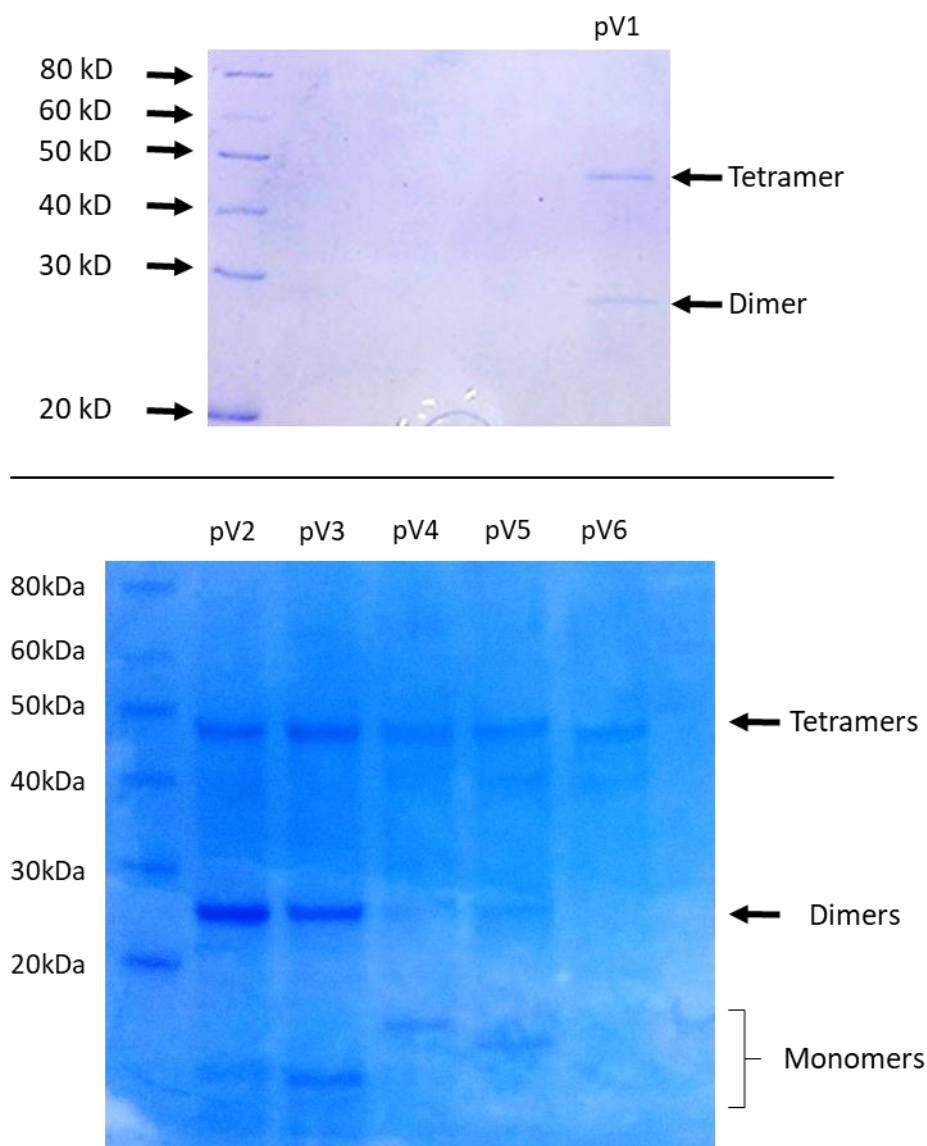


Figure 10 - Coomassie blue gel of recombinant V-antigen fragments – *E.coli* cultures containing expression plasmids for V-antigen fragments (pV1-pV6) (Figure 6) were grown for 6hr in the presence of isopropylthio- β -galactoside (IPTG) to induce expression, before the bacteria were pelleted and lysed. Using GSTrap columns, the fragments were isolated from the lysate and then 100ng of each sample was run on an SDS-PAGE gel in reducing, denaturing conditions. The gel was stained with Coomassie blue stain and revealed successful isolation of all fragments

As Coomassie blue staining stains all proteins, a specific western blot was used for WT V-antigen as this would show more assuredly that the protein isolated was V-antigen. Again, 100ng was loaded onto a reducing, denaturing SDS-PAGE gel and the resulting blot was stained with a commercially available antibody for V-antigen (2.3.2). The resulting blot is presented in Figure 11 where monomers and higher multimers of V-antigen are clearly visible. As no commercial antibodies existed for the V-antigen fragments, it was not possible to confirm their presence using the same technique, however the Coomassie blue stain coupled with the confirmation of the plasmids' presence and the success of the purification protocol (Figure 11) provided enough evidence to continue the protein preparation.

Figure 11:

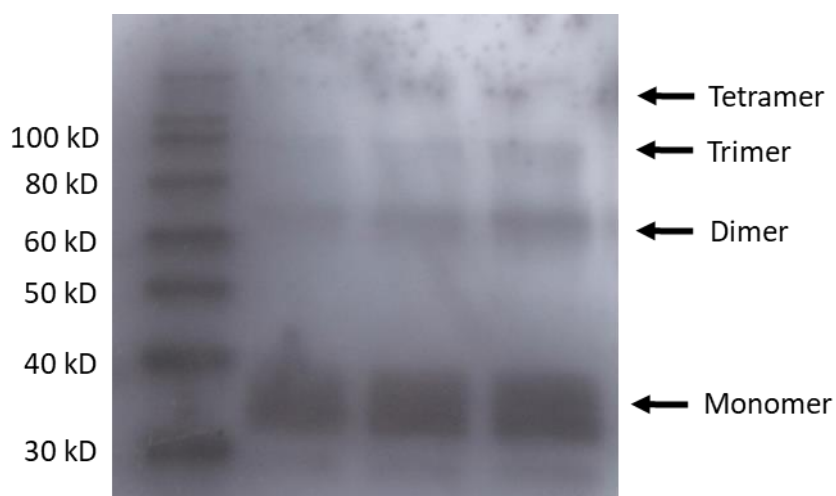


Figure 11 - Western blot on purified recombinant V-antigen – An *E.coli* culture containing an expression plasmid for WT V-antigen (Figure 6) was grown for 6hr in the presence of isopropylthio- β -galactoside (IPTG) to induce expression, before the bacteria were pelleted and lysed. Using GSTrap columns, V-antigen was isolated from the lysate and then 100ng the sample was run in technical triplicate on an SDS-PAGE gel in reducing, denaturing conditions. The protein from the gel was transferred to a nitrocellulose membrane and probed with anti-V-antigen antibody (Abcam ab20024) and then anti-mouse-HRP antibody (Dako P0260) before the blot was developed using ECL reagents and x-ray film. The results show that V-antigen was successfully isolated from the *E.coli* culture using the GSTrap columns

Cell stimulation experiments with the purified V-antigen samples were to be performed in the presence and absence of LPS and so to ensure the reliability of our results, LPS had to be removed from our V-antigen samples as it may not have been removed by washing steps in the GSTrap FF columns. Samples were therefore passed three times through sterile columns packed with Pierce™ Endotoxin Removal Resin (2.3.4.3) before the resulting elute was concentrated once more to a final concentration of ~0.10-0.25mg/ml. An aliquot of each sample was then tested for the presence of LPS via a thiobarbituric acid assay which detects the presence of Keto-3-Deoxy-octonate (KDO), an essential component of LPS. This process is detailed in 2.3.4.4. Standards of LPS ranged from 1.0mg/ml to 10ng/ml and none

of the isolated V-antigen samples showed any detectable levels of KDO and so were concluded to be sufficiently low in LPS for use in stimulations.

The rest of this chapter focuses purely on WT V-antigen with the V-antigen fragments investigated in 6.2.

3.2.4: Imaging of V-antigen internalising

It was previously reported that the internalisation of V-antigen was dependent on the presence of *Y.pestis*(135). However, this hypothesis was based upon a single assay at the 4hr timepoint using HeLa cells rather than innate immune cells like macrophages or monocytes which are primary target cells for *Y.pestis*. More recent data from Prof. Kathy Triantafilou and Dr Martha Triantafilou (unpublished) instead showed that V-antigen was capable of internalisation within monocytes in the absence of *Y.pestis*, and so to confirm this was the case, a fluorescent imaging experiment was performed.

To achieve this, V-antigen was conjugated to Oregon Green (OG) 488 dye, a green, fluorescent dye, to create OG-V that could be visualised via confocal microscopy (2.3.6). Peripheral blood monocytes were isolated from donor blood, seeded at 1×10^4 cells per well onto a Nunc Lab-Tek II CC² Chamber slide, and grown in accordance with 2.1.2 to induce differentiation into PBMDMs. These were then stimulated with 50µg OG-V for 4hr before being washed with 1x PBS fixed in 4% PFA. The fixed cells were blocked with IFA blocking solution (Appendix A) then fluorescently labelled for Early Endosome Antigen 1 (EEA1) using the protocol described in 2.3.7. The resulting slide was then analysed by confocal microscopy with the images for OG-V and EEA1 overlayed to show colocalization. Figure 12 shows that there was a clear colocalization of V-antigen and EEA1 at 4hr suggesting that V-antigen has begun internalising at this point.

Figure 12:

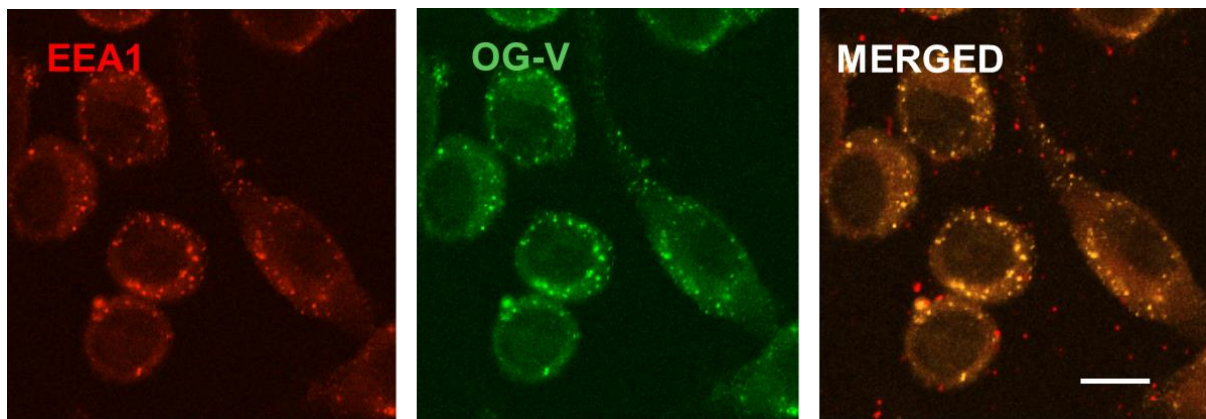


Figure 12 – Fluorescent imaging of V-antigen internalisation – Peripheral blood monocyte were isolated from human donor blood and seeded at a density of 1×10^4 into Nunc Lab-Tek II CC² chamber slides with 5ng/ml granulocyte macrophage-colony stimulating factor (GM-CSF) to differentiated them into peripheral blood monocyte derived macrophages (PBMDMs) within 7 days. These cells were then incubated with 50 μ g V-antigen that had previously been conjugated to the fluorescent dye; Oregon green (OG-V), for 4hr before being fixed in 4% paraformaldehyde and subsequently labelled with anti-early endosome antigen 1 (EEA1) antibody (BD Biosciences AB_397830) and then anti-mouse-680 antibody (Invitrogen AB_2534014). Images were obtained using a Zeiss 780 Confocal microscope. The data shown is a representative image of three biological replicates and nine technical replicates. A merged image was produced showing colocalization of V-antigen and EEA1. Scale bar 10 μ m.

3.2.5: Changes in cytokine response in the presence of V-antigen

3.2.5.1: MM6 cells

Once it was confirmed that V-antigen internalises in the absence of *Yersinia spp*, it was necessary to confirm that the recombinant V-antigen could inhibit inflammation as previous studies had shown. Initially this was attempted on MM6 cells as immortalised cell lines were expected to provide more consistency than primary cells. This data however remained preliminary at $n=2$ due to a poor responsiveness from the MM6 cells to LPS alone and so a decision to move onto primary cells. It has, however, been included here to show the reason for its abandonment for cytokine analysis.

MM6 cells were seeded at a confluency of 5×10^4 cells per well on a 24-well plate and left overnight to attach and grow to confluency. The cells were then stimulated with a range of concentrations of V-antigen (0 μ g, 1 μ g, 5 μ g, 10 μ g, 50 μ g) for 30min before half were stimulated with 100ng/ml LPS and half were not. These plates were then incubated at 37°C/5% CO₂ for 1hr, 4hr, 6hr, or 12hr before the growth media as removed for cytokine analysis, and the cells were lysed in 2x sample buffer (Appendix A) for future use. Each combination of time, V-antigen concentration, and presence/absence of LPS was performed in technical triplicate. An additional set of stimulations consisting of combinations of 0 μ g and 50 μ g V-antigen, and 0ng/ml and 100ng/ml LPS was also performed, and after 12hr, the cells

were stained with Trypan Blue to ensure that cell viability was not affected by the long stimulations with V-antigen and/or LPS. No evidence of decreased cell viability was seen compared with control cells. The 7-plex™ MSD Multi-spot assay was used to detect the concentration of secreted cytokines in the growth media by way of ELISA (2.3.8). These included the proinflammatory cytokines; IL-1 β , IL-6, IL-12p70, IL-8, IFN γ and TNF α , and the anti-inflammatory cytokine; IL-10.

The initial preliminary dataset showed higher variability than expected and the LPS-stimulated control, even at 12hr, was not particularly responsive. Figure 13 shows a representation of this lack of response with low levels of IL-6 being induced by LPS alone despite it being well characterized that LPS induces substantial secretion of IL-6 from human monocytes. Supplementary Figures S1-S6 (Appendix B) show the remaining six cytokines determined in this initial stimulation.

Figure 13:

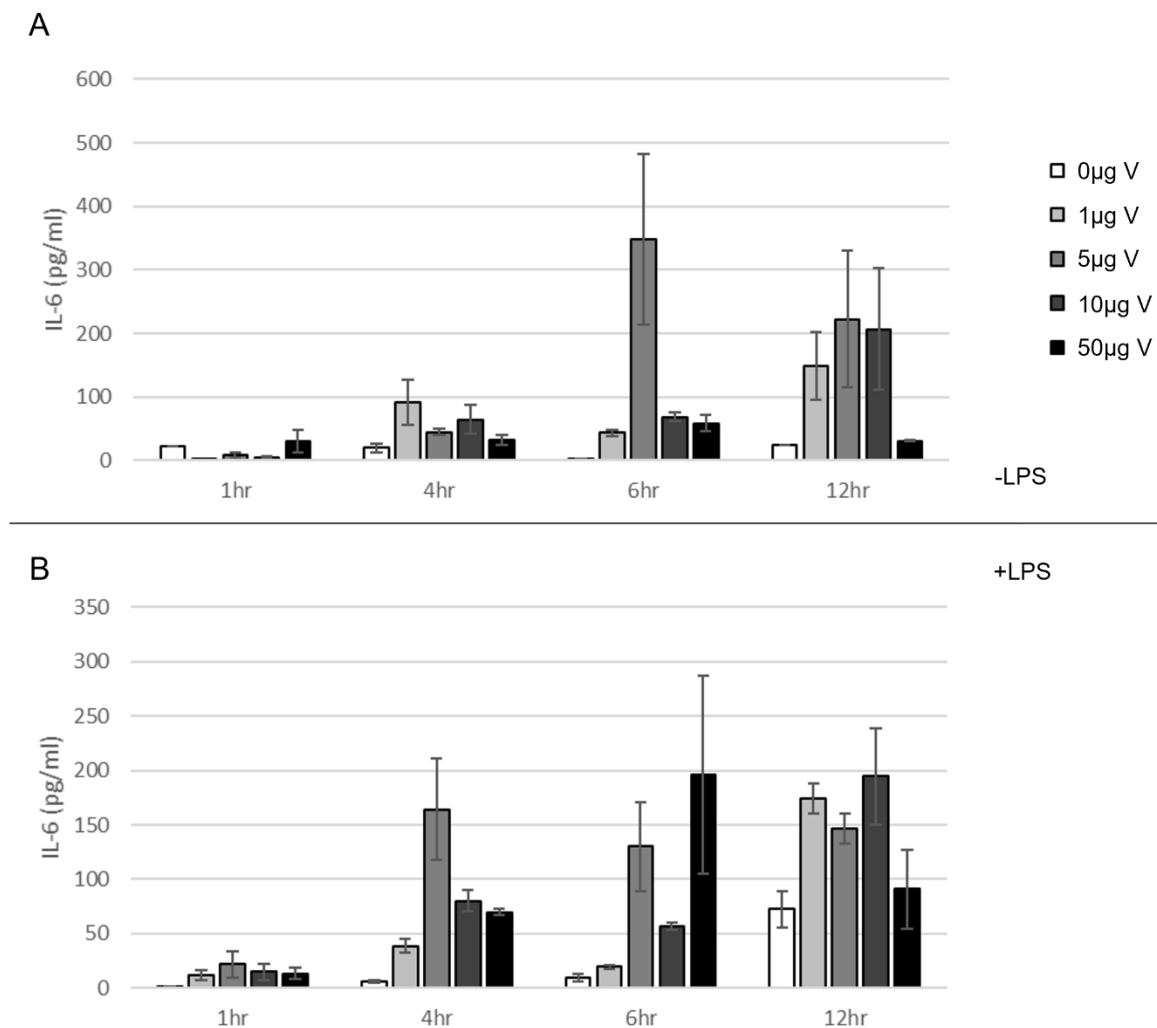


Figure 13 - MM6 secreted level of IL-6 in response to LPS/V-antigen stimulation – Mono-mac 6 (MM6) cells were seeded at a density of 5×10^4 cells/well on 24 well plates and allowed to attach overnight. After a 30min pre-incubation with various concentrations of V-antigen (0µg, 1µg, 5µg, 10µg, 50µg), LPS was added to a final concentration of 100ng/ml or not added at all. After a specified incubation time from the point of LPS addition (or non-addition), the growth media from the cells was harvested and analysed using a 7-plex MSD Multi-spot Assay system kit to determine the level of IL-6 that had been secreted. The data presented is constructed of 3 technical triplicates

A second set of stimulations were performed in technical triplicate to determine whether a new batch of MM6 cells would be more responsive to LPS stimulation. Due to issues with data recovery, only three of the seven cytokines in the 7-plex assay were able to be recovered but as shown in Figure 14, the pooled data of both stimulations show a weak IL-6 response to LPS compared to expected levels. Supplementary Figures S7 and S8, show the data for IL-1 β and TNF α respectively

Figure 14:

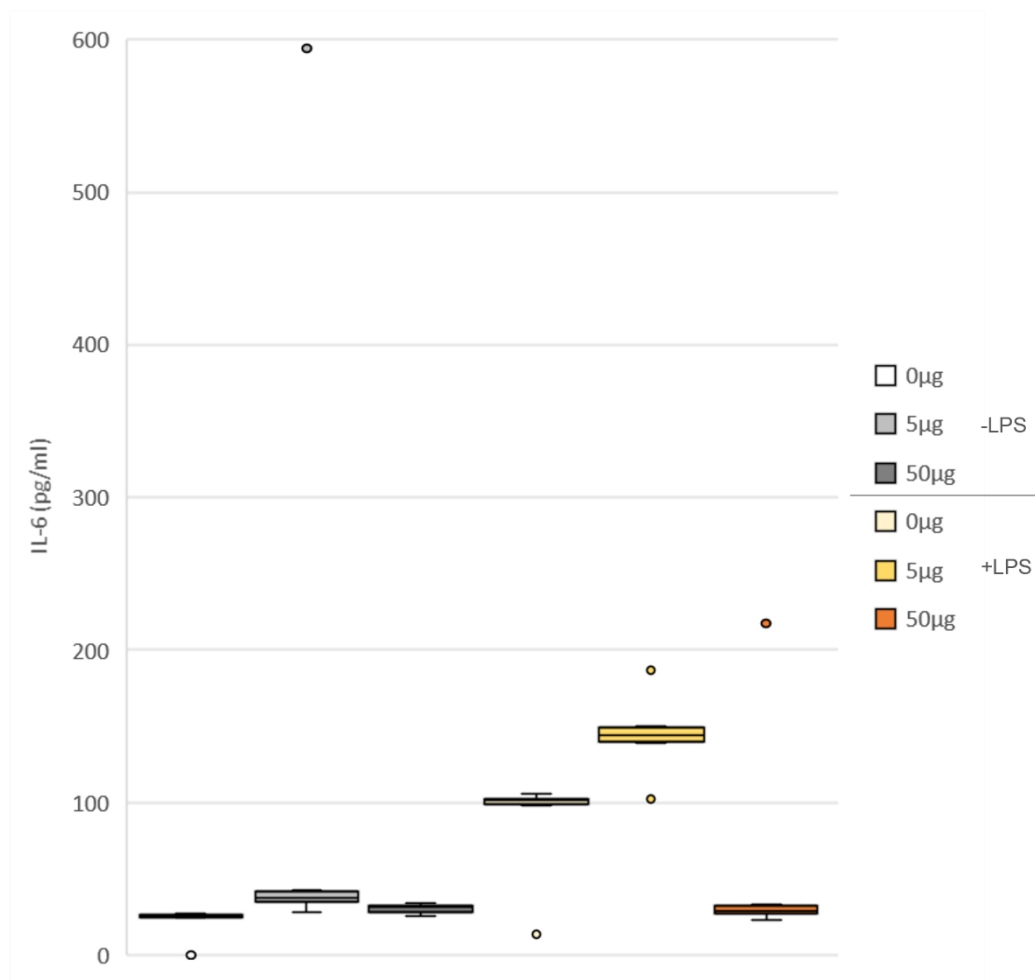


Figure 14 - MM6 secreted level of IL-6 in response to 12hr LPS/V-antigen stimulation – Mono-mac 6 (MM6) cells were seeded at a density of 5×10^4 cells/well on 24 well plates and allowed to attach overnight. After a 30min pre-incubation with various concentrations of V-antigen (0µg, 1µg, 5µg, 10µg, 50µg), LPS was added to a final concentration of 100ng/ml or not added at all. After a specified incubation time from the point of LPS addition (or non-addition) (1hr, 4hr, 6hr, 12hr), the growth media from the cells was harvested and analysed using a 7-plex MSD Multi-spot Assay system kit to determine the level of IL-6 that had been secreted. This data was added to a previous dataset (Figure 13) for n=2 consisting of 6 technical triplicates. Outliers were presented as datapoints that exceeded 1.5 times the interquartile range from the upper/lower quartile

Though there was some indication that V-antigen was affecting the inflammatory response and leading to different levels of secreted cytokines in these stimulations, the poor cytokine response from MM6 cells to LPS as a control and the limitation of a finite V-antigen stock prompted a switch in focus to primary cell work. This is because of the well-documented greater responsiveness of primary cells in comparison to immortalised cell lines.

3.2.5.2: PBMDMs

The limitations of immortalised cell lines compared to primary cells are well-understood and the evidence in 3.2.5.1 suggested that MM6 cells were responding weakly to LPS stimulation. Further stimulations were therefore performed in PBMDMs. These stimulations utilised 4 independent donors of blood from which peripheral monocytes were isolated using anti-CD14 magnetic beads. These were cultivated as reported in 2.1.2 to differentiate them into PBMDMs. As before, technical triplicates were stimulated with various concentrations of V-antigen (0µg, 1µg, 5µg, 10µg, 50µg) for 30min before further stimulated with/without 100ng/ml LPS. These stimulations were then continued for 1hr, 6hr, or 16hr from this point before the growth media was removed for cytokine analysis and the cells were lysed in RLT buffer for future analysis. Figure 15 shows this experimental set-up.

Figure 15:

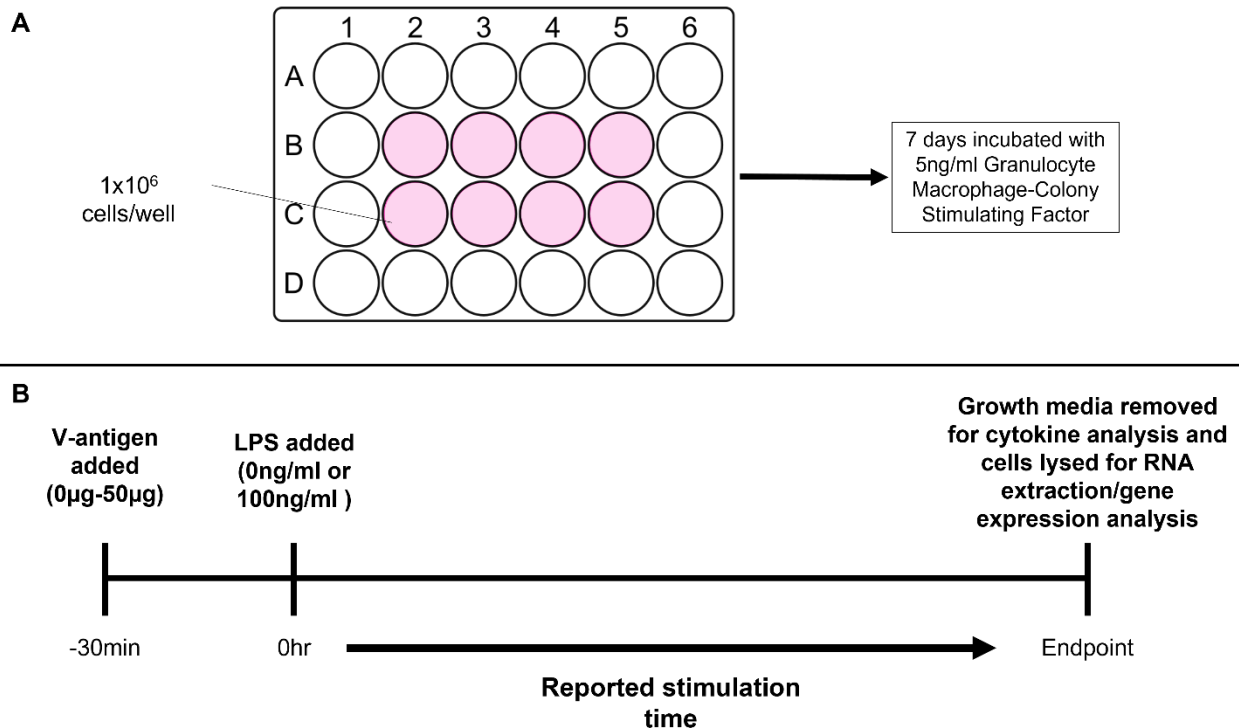


Figure 15 – Experimental design of PBMDM-V-antigen stimulations – A; peripheral blood monocytes harvested from blood donors were seeded at 1x10⁶cells/well in a 24-well plate. These were incubated for 7 days with 5ng/ml granulocyte macrophages-colony stimulating factor to differentiate them into peripheral blood monocyte derived macrophages (PBMDMs). B; PBMDMs were then subjected to a 30min pre-incubation with V-antigen (0µg, 1µg, 5µg, 10µg, 50µg) before LPS was either added to a final concentration of 100ng/ml or not added. This was then incubated for a selected duration (1hr, 6hr, 16hr) before the growth media was removed for cytokine analysis and cells were lysed for RNA analysis

The change in timepoints was made partly due to the availability of primary cells and recombinant V-antigen, but it was also made on the basis of a previous study by *Y.Nedialkov, et al(1997)(147)*, which reported evidence that the secondary immunomodulatory response started at around 6-8hr in mice and so it was decided to extend the final timepoint to 16hr to ensure that V-antigen's secondary immunomodulatory response was able to more substantially influence key changes intracellularly than it would at 12hr. It was also believed that this would avoid extending the stimulations too far and risking a toxic effect on the cells. A separate set of stimulations performed with and without 100ng/ml LPS incubation in combination with, and without, 50µg V-antigen was also run for 16hr and then the cells were analysed by trypan blue assay to determine cell viability. As with the MM6 stimulations, there was no evidence of reduced cell viability in any of the four stimulation conditions.

After collection, the growth media from the PBMDM stimulations was analysed by 7-plex™ MSD Multi-spot assay. The results for IL-1β, IL-6, IL-8, IFNγ, TNFα, and IL-10 are presented in Figures 16 to 21 respectively.

Figure 16:

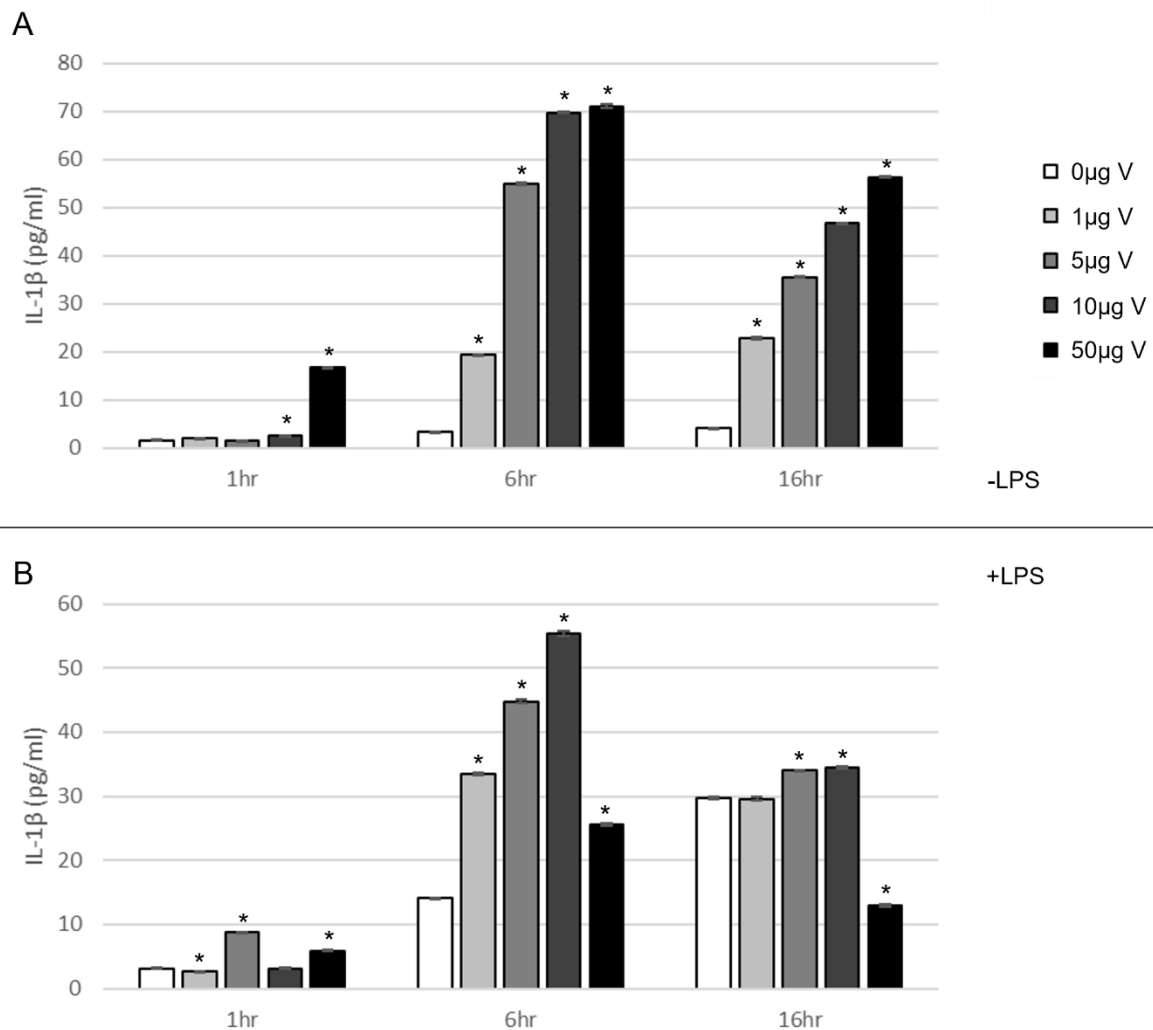


Figure 16 - IL-1 β secretion in PBMDMs in response to V-antigen stimulation (+/- LPS) over 16hr – PBMDMs were set up according to the experimental design in Figure 15 and were pre-incubated with 0 μ g, 1 μ g, 5 μ g, 10 μ g, and 50 μ g V-antigen for 30min before stimulation with A; 0ng/ml LPS or B; 100ng/ml LPS for 1hr, 6hr, and 16hr. The growth media harvested from these stimulations were analysed using a 7-plex MSD Multi-spot Assay system kit to determine the level of IL-1 β that had been secreted. The data from all donors was pooled for each V-antigen concentration and timepoint and a one-way ANOVA was performed using an SPSS statistics package. Statistically significant differences compared to the 0 μ g V-antigen control (*) (p -value = <0.05) were then determined through Tukey's post-hoc analysis. The data presented shows cytokines collected in technical triplicate and $n=4$

In the absence of LPS, V-antigen triggered a dose-dependent secretion of IL-1 β which peaked around 6hr and dropped slightly between 6hr and 16r in all but the 1 μ g V-antigen stimulation (Figure 16A). In the presence of LPS however, 50 μ g V-antigen displayed a lower level of secretion than the other three V-antigen concentrations (Figure 16B). All concentrations still peaked at 6hr but at 16hr, 50 μ g V-antigen stimulations had a lower level of secreted IL-1 β than the LPS only control. All other concentrations of V-antigen displayed a similar trend to the stimulations without LPS – following a dose-dependent secretion and a

drop in secreted levels between 6hr and 16hr. All concentrations except for 1 μ g V-antigen showed a lower secretion of IL-1 β at 6hr in the presence of LPS.

Figure 17:

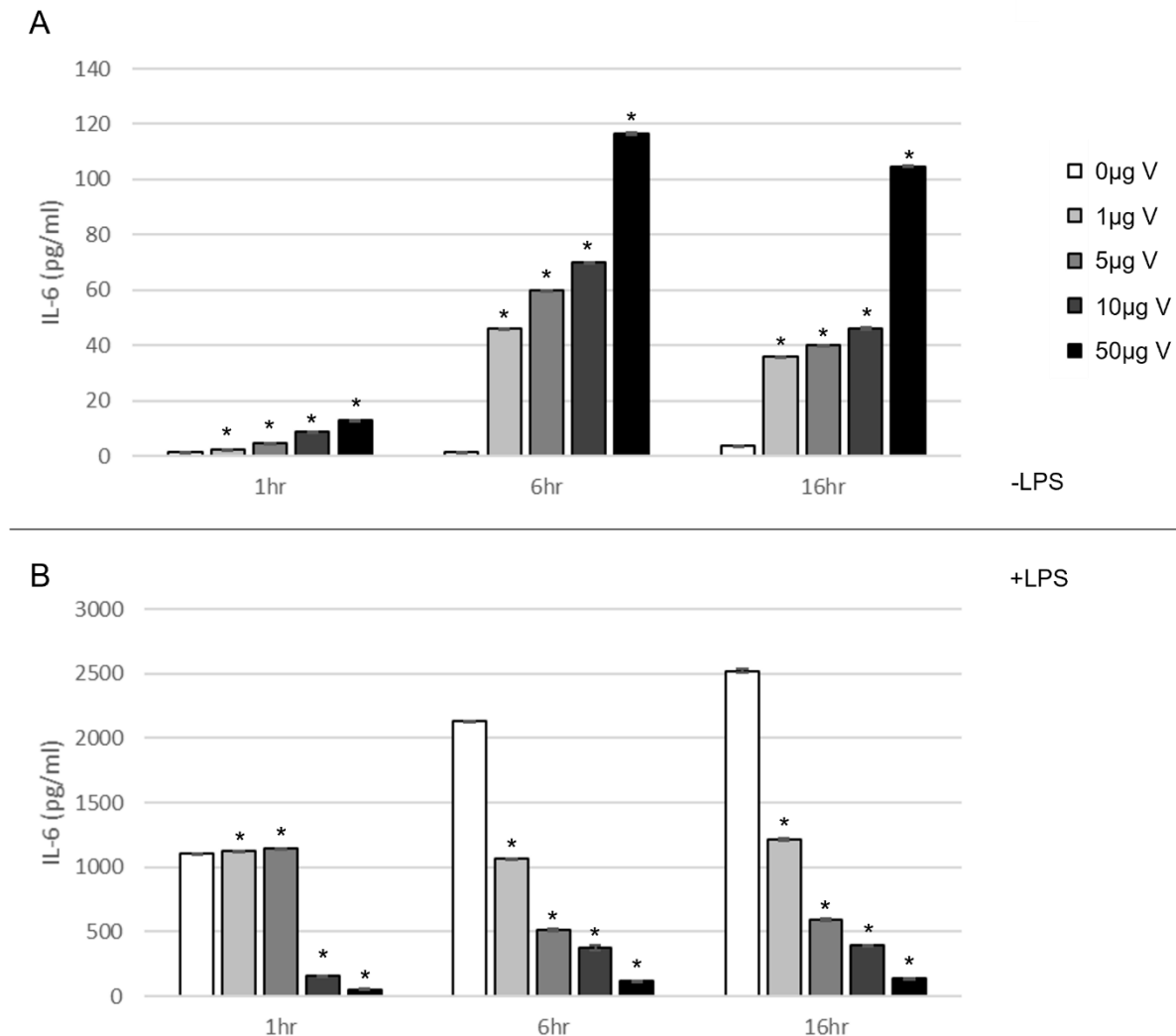


Figure 17 - IL-6 secretion in PBMDMs in response to V-antigen stimulation (+/- LPS) over 16hr – PBMDMs were set up according to the experimental design in Figure 15 and were pre-incubated with 0 μ g, 1 μ g, 5 μ g, 10 μ g, and 50 μ g V-antigen for 30min before stimulation with A; 0ng/ml LPS or B; 100ng/ml LPS for 1hr, 6hr, and 16hr. The growth media harvested from these stimulations were analysed using a 7-plex MSD Multi-spot Assay system kit to determine the level of IL-6 that had been secreted. The data from all donors was pooled for each V-antigen concentration and timepoint and a one-way ANOVA was performed using an SPSS statistics package. Statistically significant differences compared to the 0 μ g V-antigen control (*) (p -value = <0.05) were then determined through Tukey's post-hoc analysis. The data presented shows cytokines collected in technical triplicate and $n=4$

As above, the secretion of IL-6 in response to V-antigen without LPS showed an inflammatory response that arose in a dose-dependent manner (Figure 17A). This inflammatory response peaked at around 6hr and by 16hr, the secreted levels of IL-6 had decreased slightly in all concentrations of V-antigen. All concentrations of V-antigen however, had a rapid and potent inhibition on secretion of IL-6 in the presence of LPS (Figure 17B). At 1hr, 1 μ g and 5 μ g V-antigen stimulations had a similar level of secreted IL-6

to the control, however both 10µg and 50µg stimulations had significantly reduced secreted levels. Control LPS-stimulated cells saw an increase in secreted IL-6 that continued to increase up to 16hr and reached a level over 2-fold higher than even the 1µg V-antigen stimulation at 16hr. Cells treated with 50µg V-antigen saw a ~18-fold lower level of secreted IL-6 in response to 100ng/ml LPS at 16hr.

Figure 18:

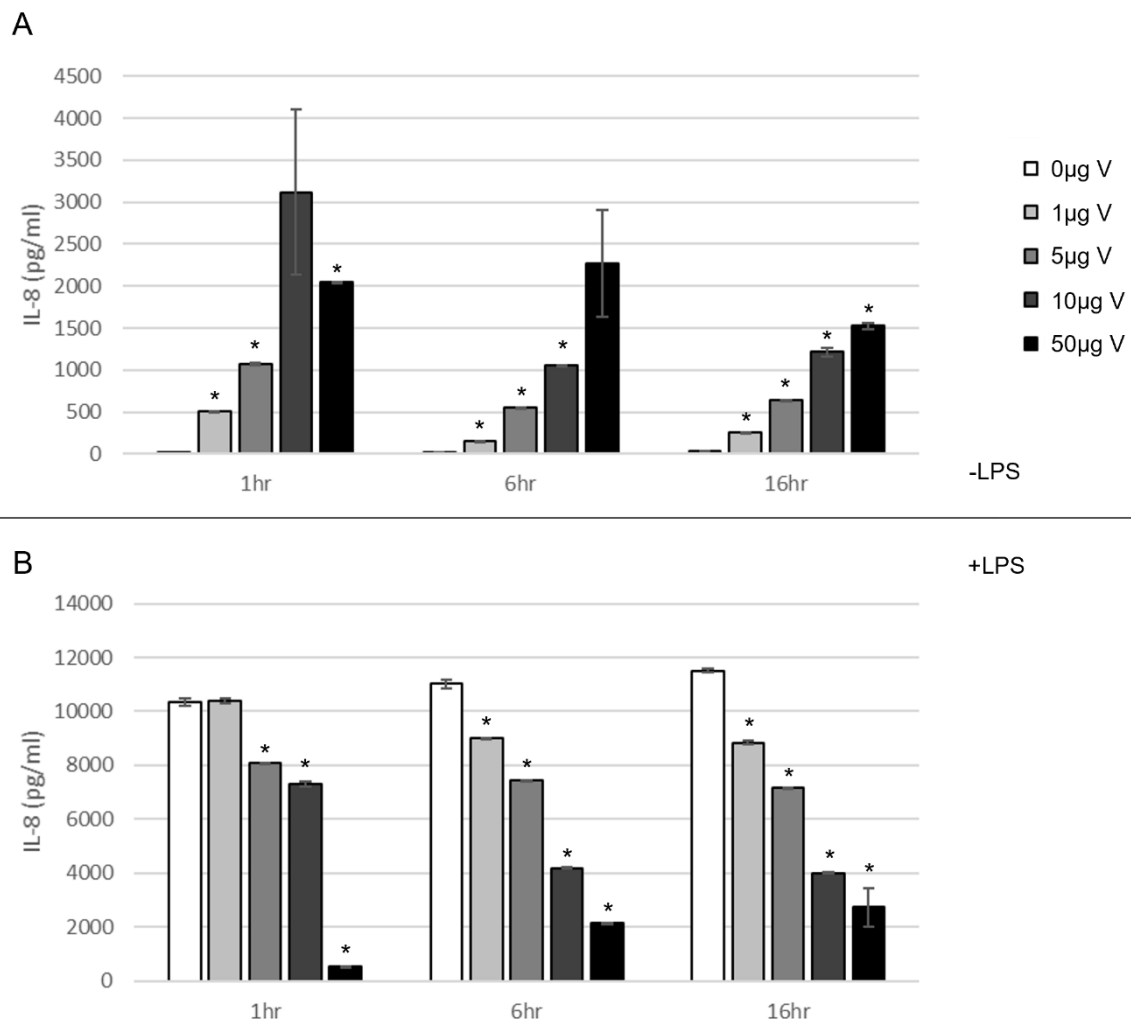


Figure 18 - IL-8 secretion in PBMDMs in response to V-antigen stimulation (+/- LPS) over 16hr – PBMDMs were set up according to the experimental design in Figure 15 and were pre-incubated with 0µg, 1µg, 5µg, 10µg, and 50µg V-antigen for 30min before stimulation with A; 0ng/ml LPS or B; 100ng/ml LPS for 1hr, 6hr, and 16hr. The growth media harvested from these stimulations were analysed using a 7-plex MSD Multi-spot Assay system kit to determine the level of IL-8 that had been secreted. The data from all donors was pooled for each V-antigen concentration and timepoint and a one-way ANOVA was performed using an SPSS statistics package. Statistically significant differences compared to the 0µg V-antigen control (*) (p -value = <0.05) were then determined through Tukey's post-hoc analysis. The data presented shows cytokines collected in technical triplicate and $n=4$

Figure 18A shows IL-8 secretion in the absence of LPS. V-antigen appears to stimulate IL-8 secretion in a roughly dose-dependent manner though the wider variation seen at 1hr 10µg V-antigen and 6hr 50µg V-antigen may require some extra clarity from further

experiments to confirm this. In the presence of LPS though (Figure 18B), V-antigen shows a dose-dependent inhibition that starts as early as 1hr.

Figure 19:

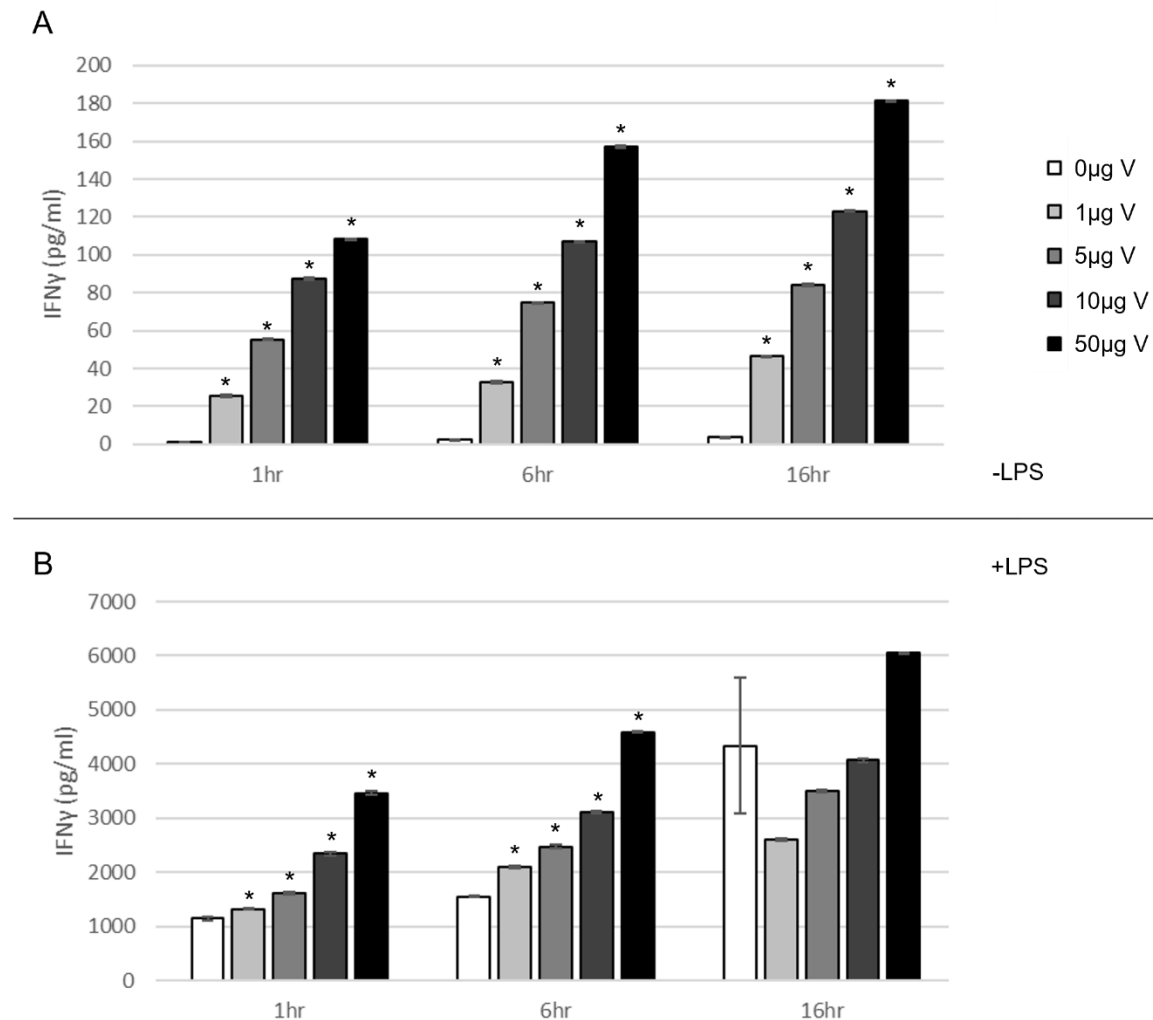


Figure 19 - IFN γ secretion in PBMDMs in response to V-antigen stimulation (+/- LPS) over 16hr – PBMDMs were set up according to the experimental design in Figure 15 and were pre-incubated with 0 μ g, 1 μ g, 5 μ g, 10 μ g, and 50 μ g V-antigen for 30min before stimulation with A; 0ng/ml LPS or B; 100ng/ml LPS for 1hr, 6hr, and 16hr. The growth media harvested from these stimulations were analysed using a 7-plex MSD Multi-spot Assay system kit to determine the level of IFN γ that had been secreted. The data from all donors was pooled for each V-antigen concentration and timepoint and a one-way ANOVA was performed using an SPSS statistics package. Statistically significant differences compared to the 0 μ g V-antigen control (*) (p -value = <0.05) were then determined through Tukey's post-hoc analysis. The data presented shows cytokines collected in technical triplicate and $n=4$

Without LPS, V-antigen stimulates the secretion of IFN γ in a dose-dependent manner (Figure 19A) as with the cytokines above, indicating the initiation of an inflammatory response caused by V-antigen. Under LPS stimulation (Figure 19B), unlike in other cytokines, the same trend is seen with greater secreted levels of IFN γ recorded with increasing concentrations of V-antigen used. At 16hr, there was a greater variation of results in the LPS only control with one donor giving a substantially higher secreted level than the

other two donors. Due to the low *n* number of 4, this gave a high variation that prevented any statistical significance from being achieved (Figure 19B, 16hr).

Figure 20:

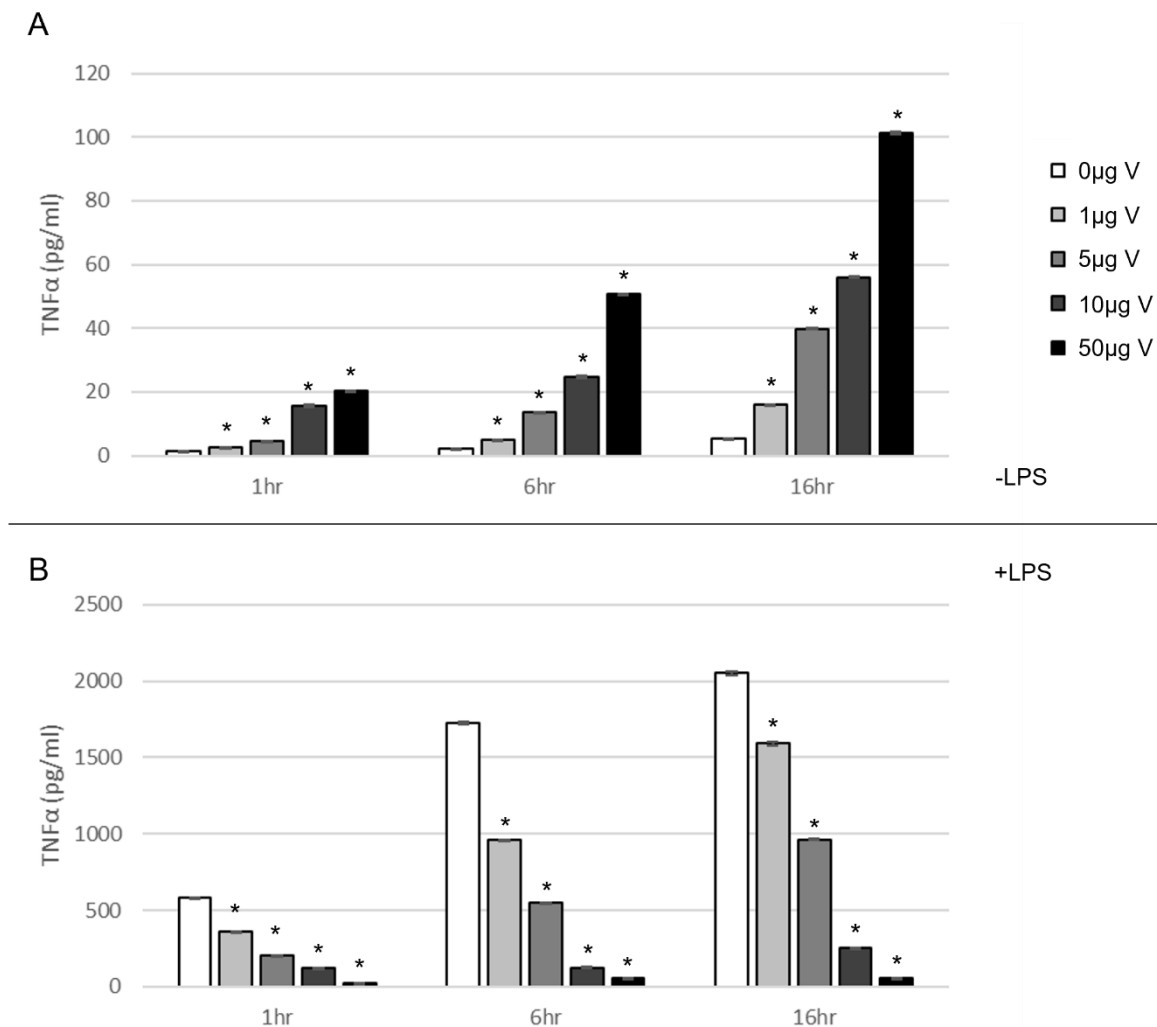


Figure 20 - TNF α secretion in PBMDMs in response to V-antigen stimulation (+/- LPS) over 16hr – PBMDMs were set up according to the experimental design in Figure 15 and were pre-incubated with 0 μ g, 1 μ g, 5 μ g, 10 μ g, and 50 μ g V-antigen for 30min before stimulation with A; 0ng/ml LPS or B; 100ng/ml LPS for 1hr, 6hr, and 16hr. The growth media harvested from these stimulations were analysed using a 7-plex MSD Multi-spot Assay system kit to determine the level of TNF α that had been secreted. The data from all donors was pooled for each V-antigen concentration and timepoint and a one-way ANOVA was performed using an SPSS statistics package. Statistically significant differences compared to the 0 μ g V-antigen control (*) (*p*-value = <0.05) were then determined through Tukey's post-hoc analysis. The data presented shows cytokines collected in technical triplicate and *n*=4

In the absence of LPS, V-antigen stimulated an increasingly higher level of secreted TNF α that corresponded to higher doses of V-antigen (Figure 20A). In the presence of LPS however, this dose response was inverted, and V-antigen reduced secretion of TNF α more potently in a dose-dependent manner (Figure 20B). All concentrations except for 50 μ g showed an increase in TNF α secretion across the 16hr. Instead, 50 μ g peaked at 6hr and plateaued between 6hr and 16hr. The difference in secretion was significant even at 1hr.

Figure 21:

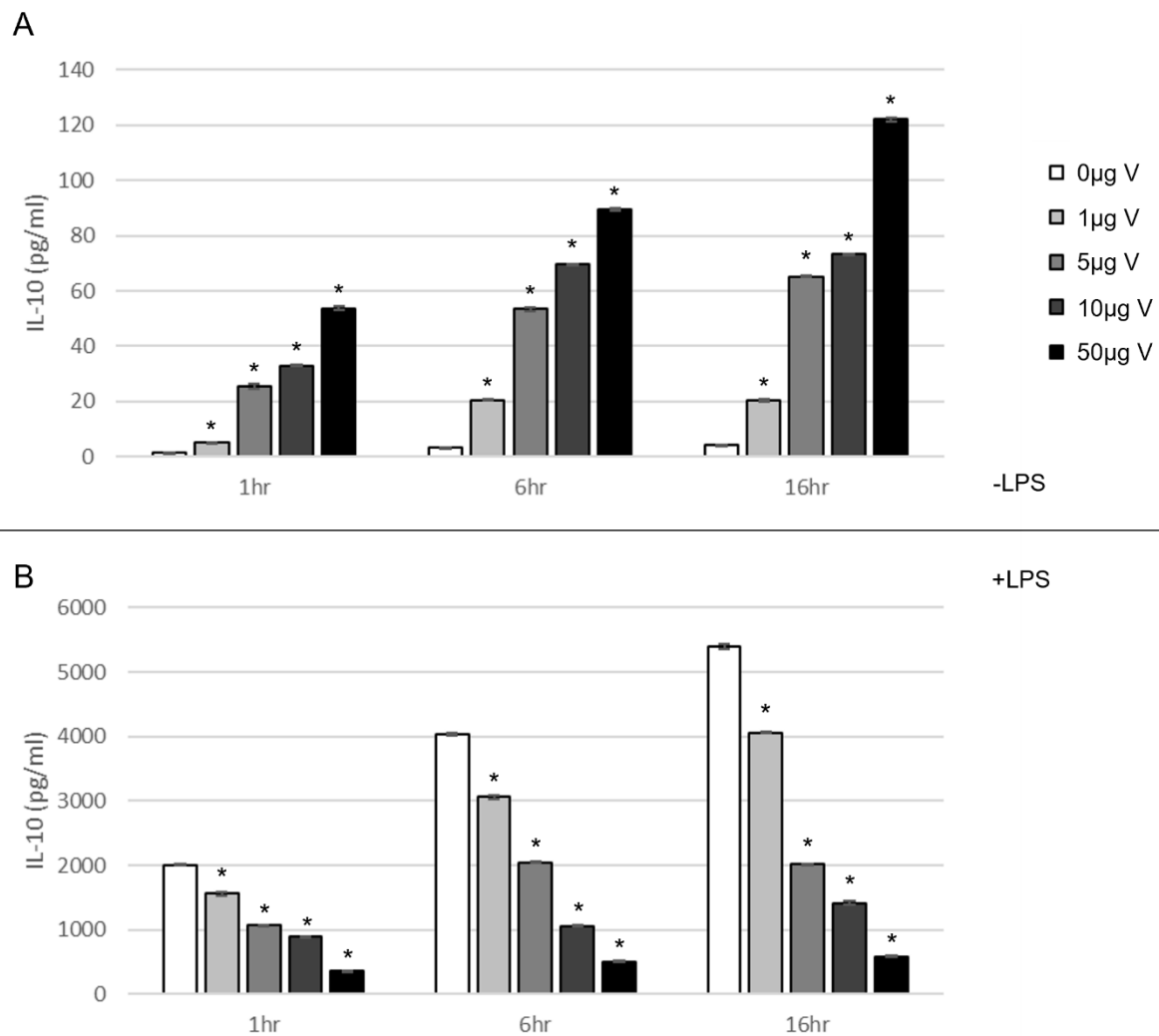


Figure 21 - IL-10 secretion in PBMDMs in response to V-antigen stimulation (+/- LPS) over 16hr – PBMDMs were set up according to the experimental design in Figure 15 and were pre-incubated with 0µg, 1µg, 5µg, 10µg, and 50µg V-antigen for 30min before stimulation with A; 0ng/ml LPS or B; 100ng/ml LPS for 1hr, 6hr, and 16hr. The growth media harvested from these stimulations were analysed using a 7-plex MSD Multi-spot Assay system kit to determine the level of IL-10 that had been secreted. The data from all donors was pooled for each V-antigen concentration and timepoint and a one-way ANOVA was performed using an SPSS statistics package. Statistically significant differences compared to the 0µg V-antigen control (*) (p -value = <0.05) were then determined through Tukey's post-hoc analysis. The data presented shows cytokines collected in technical triplicate and $n=4$

Figure 21A shows that V-antigen stimulates IL-10 in a dose dependent manner in the absence of LPS and like all other presented cytokines except for IFN γ , in the presence of LPS, V-antigen inhibits the secreted level of IL-10 – also in a dose dependent manner. At 16hr, there was an almost 10-fold decrease in secreted IL-10 in the 50µg stimulation compared with the LPS only control.

3.3: Discussion

3.3.1: V-antigen internalises in the absence of *Y.pestis* within 4hr

Conversely to *K.Fields, et al. (1999)*(135), Figure 12 showed clear localisation between V-antigen and EEA1, suggesting that V-antigen has internalised into the early endosome by 4hr. *K.Fields, et al. (1999)*, performed their analysis in the absence of *Y.pestis* using HeLa cells by evaluating the presence/absence of V-antigen in cell lysates and supernatant at 4hr. However, HeLa cells are a cervical epithelium cell line that do not express key surface receptors that have since been shown to interact with V-antigen(132, 149, 151, 152). Therefore, the evidence that V-antigen internalises without *Yersinia spp* in PBMDMs – cells that are relevant to the biology of *Y.pestis* pathogenesis and express key surface receptors that V-antigen interacts with – is more valid than the evidence in HeLa cells.

3.3.2: V-antigen triggers a minor inflammatory response in monocytes

In 3.2.5, cytokine analysis from stimulations of both MM6 cells and PBMDMs was presented. These stimulations were performed both with and without LPS. In stimulations without LPS, it was possible to examine the response of monocytes to V-antigen alone.

For MM6 cells, it was not possible to draw any conclusions due to the preliminary nature of the data. There was a pattern that IL-1 β (Supplementary Figure 1), IL-6 (Figure 14), and TNF α (Supplementary Figure 5) secretion increased in response to 5 μ g and 50 μ g V-antigen at 12hr when compared to unstimulated control cells which would indicate an inflammatory response, however no reliable conclusion can be drawn from MM6 cells due to their lack of responsiveness to LPS and therefore poor relevancy. Stimulations in primary cells showed much more consistent data and substantially more responsiveness to LPS as an inflammatory stimulus and so could be used to generate statistically significant results. Secretion of IL-1 β and IL-6, two major inflammatory mediators, in PBMDMs showed a similar pattern to the MM6 cells with peaks at 6hr and a decrease in secretion after this. V-antigen stimulations also showed a rapid IL-8 response that was triggered within 1hr, as well as IFN γ and TNF α . The level of secretion in the majority of cases, however, was minimal - for example, IFN γ secretion in 50 μ g V-antigen reached 181.16pg/ml at 16hr while 100ng/ml LPS induced IFN γ to 6055.1pg/ml at 16hr (Figure 19).

The response to V-antigen is not an unexpected finding, however, as monocytes should respond to foreign proteins, particularly those of bacterial origin. This has also been reported previously within a mouse study that V-antigen alone triggers an inflammatory response similar to that of introducing 100ng/ml BSA(147). As with that study, which also looked at

cytokine responses over time, there was an initial peak to the inflammation that occurred a few hours after introduction and began to taper off, coinciding with the internalization time shown in Figure 12. The closed nature of the *in vitro* experiment in 3.2.5.1 compared to the mouse study and the differences between an *in vitro* immortalised human cell line stimulation and an *in vivo* mouse inoculation makes it difficult to draw conclusions too closely, however, particularly when the MM6 cells were shown to be poorly responsive to LPS alone.

Interestingly, the level of IL-1 β secreted in response to V-antigen alone appears to be higher than 'LPS only' or 'V-antigen + LPS'. In PBMDMs, only 1 μ g V-antigen (-LPS) had a lower level of IL-1 β at 16hr than the LPS control (Figure 17A). Coincidentally, only 1 μ g V-antigen saw an increase in IL-1 β when co-stimulated with LPS. All other concentrations of V-antigen, besides the 0 μ g V-antigen control, had higher secreted levels of IL-1 β in the absence of LPS. This potentially suggests that the pathway which causes IL-1 β secretion in response to V-antigen is not the same as that which V-antigen inhibits and that LPS preincubation is potentially suppressing it.

The IL-10 response was also recorded as part of the MSD 7-plex cytokine assay. As explained in 1.2.2.3 and 1.2.2.4, previous studies have highlighted IL-10 as potentially the key mechanism to V-antigen's immunomodulatory effects(147, 148, 150-152, 161) though there remains some controversy around this claim(132, 153). In PBMDMs, there was a minor dose-dependent response (Figure 21A) however even with 50 μ g V-antigen, the secreted level of IL-10 at 16hr was 45-fold lower than in LPS-stimulated PBMDMs. Multiple previous studies have reported weak IL-10 responses *in vitro* with one reporting it to be comparable to their stimulations with only 1ng/ml LPS(153). The lack of extensive cytokine evaluation in these studies may have led to an oversight of the proinflammatory cytokines that are also triggered by V-antigen and, as IL-10 is also secreted during inflammatory responses, it means that some reported IL-10 responses may actually be indicators of a natural inflammatory response and not an anti-inflammatory mechanism induced by V-antigen.

3.3.3: V-antigen alters ongoing inflammation in response to LPS, but does not entirely inhibit it

The stimulations in 3.2.5 that were co-stimulated with LPS revealed a clear indication that the recombinant V-antigen used in this study inhibited ongoing inflammation. Nearly all measures of inflammation tested in the cytokine analysis in 3.2.5 showed this effect. IL-1 β

only showed a significant reduction secretion at 16hr in response to LPS when stimulated with 50µg V-antigen (Figure 16B), however all concentrations of V-antigen saw a reduction in IL-1β levels between 6hr and 16hr unlike the LPS-stimulated control which continued to see increasing secretion throughout. *Y.Nedialkov et al, 1997* revealed in their mouse study that the secondary immunomodulation of V-antigen peaked at 48hr and also showed that 10µg gave almost 100% protection from the LD₅₀ dose of LPS in mice at that timepoint(147). This suggests that that the other concentrations of V-antigen might have also suppressed LPS-stimulated IL-1β secretion to a level below the LPS-stimulated control if a later timepoint was examined.

In PBMDMs, IL-1β appeared to show a clear change of rate of induction pre-6hr and post-6hr, which coincides with the rough timing of internalisation of V-antigen (3.3.1) and evidence from *Y.Nedialkov et al, 1997*(147). The secretion of IL-6 (Figure 17B), IL-8 (Figure 18B), and TNFα (Figure 20B) was inhibited in a dose dependent manner too with all tested concentrations of V-antigen leading to significant decreases of secretion over LPS alone. Unexpectedly however, the response was apparent from as little as 1hr post-introduction. IL-8 saw significant decreases in 5µg, 10µg, and 50µg V-antigen stimulations at 1hr (Figure 18B), and IL-6 showed significant decreases at 1hr in both 10µg and 50µg stimulations (Figure 17B).

Conversely to some of the literature surrounding V-antigen, there was no substantial IL-10 response and instead, IL-10 was reduced in a dose-dependent manner (Figure 21B) (147, 149, 150). This suggests that the IL-10 response reported in the literature may have been a result of low-level inflammation triggered by V-antigen rather than specific induction by V-antigen. This does, therefore, means that the rapid, initial immunomodulatory effects of V-antigen seen here in IL-8, IL-6, and TNFα cannot be caused by increased IL-10 induction.

Finally, despite our recombinant V-antigen showing signs of inhibiting the inflammatory response as reported within the literature, it is important to highlight that the more extensive profile of our cytokine analysis revealed that it did not entirely inhibit inflammation. The secretion of IFNγ increased in LPS-stimulated samples when PBMDMs were co-stimulated with V-antigen (Figure 19B). This increase was dose-dependent and significant in all cases and concentrations of V-antigen except for at 16hr where high variance in one of the technical triplicates of one of the control donors prevented statistical significance from being reached. However, unlike in the other cytokines analysed in this study, IFNγ continued to rise steadily in LPS-stimulated cells when co-stimulated with V-antigen and so it is, at least, not inhibiting the secretion of IFNγ and is potentially inducing higher secretion of it.

4: Chapter 4: V-antigen and the inflammasome

4.1: Introduction

4.1.1: Chapter introduction

Chapter 3 confirmed the localisation and functionality of recombinant V-antigen as well as highlighting differences in the cytokine response to LPS in the presence and absence of V-antigen. Following on from this, the same stimulations were further investigated at both a protein- and RNA- level in an attempt to uncover where V-antigen affects the cytokine pathway. Here, IL-1 β was a particular focus due to its importance in not only general inflammation, but specifically sepsis. To achieve this, an investigation into the IL-1 β pathway from secretion to transcription was carried out with the results divided between Chapter 4 and Chapter 5. Chapter 4 focuses on IL-1 β secretion and inflammasome function.

4.1.2: IL-1 β secretion

Pro-IL-1 β is an immature form of IL-1 β and is transcribed from the IL-1 β gene. Pro-IL-1 β mRNA is translated at cytoskeleton-associated polyribosomes(162) and then undergoes a maturation step to produce mature IL-1 β . This step involves proteolytic cleavage by caspase 1 at the site of a formed inflammasome (4.1.3). As inflammasomes are cytoplasmic macrostructures and as pro-IL-1 β is not transcribed at traditional endoplasmic reticulum (ER)-associated ribosomes, IL-1 β is not found within the ER or Golgi body. IL-1 β also has no signal peptide to localise it to either of these organelles(163). IL-1 β , therefore, is prevented from utilising the conventional secretory pathway to exit the cell and instead has to rely on non-conventional means.

Through autophagy, a small proportion of cytosolic IL-1 β is taken up into endosomal vesicles that are then directed to the lysosome. However, further signalling like a calcium influx can cause autolysosomal exocytosis and subsequent release of IL-1 β as part of the lysosomal contents(164, 165). Lysosomal protease inhibitors have shown to increase the level of IL-1 β secreted upon stimulation(166), substantiating this theory, which is known as the 'rescue and redirect' theory.

IL-1 β also appears to be secreted via 'protected release'. This process utilises microvesicles(167) and exosomes(168) to exocytose IL-1 β . Secreted microvesicles containing mature IL-1 β have been identified from numerous innate immune cells as well as platelets(169) with stimulation of the P2X Purinoceptor 7 (P2X7) receptor acting as the trigger for microvesicle release. These microvesicles also contain P2X7 receptor in their membrane and stimulation with extracellular ATP has been shown to cause the microvesicles to spill their contents and release IL-1 β (170). Exosomes, created by the

budding of the late endosome or multivesicular body inwards, contain some contents of the cytosol and can take up cytosolic IL-1 β in a process that has been shown to be dependent on P2X7 receptor stimulation, Apoptosis-associated Speck-like Protein Containing a CARD (ASC), and Nucleotide-binding Oligomerization Domain (NACHT), LRR, and Pyrin Domain (PYD) Domains-containing Protein 3 (NLRP3), but not caspase 1(171). In much the same way as microvesicles, these can be exocytosed from the cell and have their contents spilled to release IL-1 β while in the extracellular environment.

'Terminal release' is the mechanism by which IL-1 β is secreted during pyroptosis. Preventing the fatal osmotic lysis of the cell by using glycerol conditions, it was shown that the release of mature IL-1 β can occur through the pores created in the membrane(172). This was specific to pyroptosis as necrotic cell death and tissue damage only led to the release of pro-IL-1 β upon membrane rupturing(173). Although pro-IL-1 β can be cleaved extracellularly by Neutrophil Proteinase 3(174) to generate an inflammatory response, pyroptosis is the only form of cell death that secretes mature IL-1 β to increase the inflammatory insult during the process of cell death. However, this does not appear to be solely down to pyroptosis as Gasdermin D (GSDMD), a pyroptotic pore-forming protein, was more recently shown to function in non-pyroptotic settings too and act as a gateway to secrete cytosolic IL-1 β in the case of non-lethal hyperactivation(175). This therefore suggests that GSDMD could also be the pore responsible for IL-1 β secretion in the case of pyroptosis.

There is also evidence that the ATP-binding Cassette Transporter A1 (ABCA1) transporter is utilised in another method of IL-1 β secretion as blocking the chloride fluxes that are responsible for the transporter's function inhibits IL-1 β release and enhancing it increased the release(176). It was also shown that a deficiency in ABCA1 reduced the level of IL-1 β secretion in LPS-stimulated macrophages by 30-50% without affecting TNF α or pro-IL-1 β secretion levels(177). This effect however was not seen in monocytes suggesting it may be cell-type specific.

A summary of the IL-1 β secretion pathways is shown in Figure 22.

Figure 22:

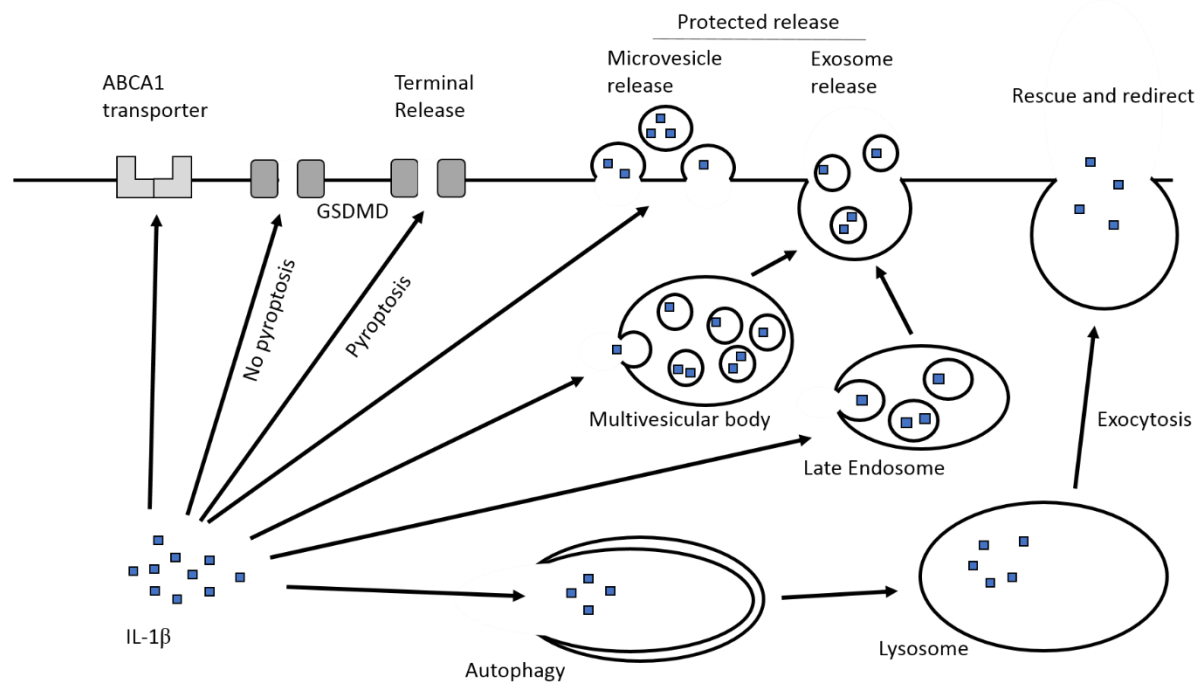


Figure 22 - Summary of IL-1 β secretory pathways – IL-1 β has multiple mechanisms of secretion and has so far been linked to secretion via the ATP-binding cassette transporter A1 (ABCA1) transporter, Gasdermin D (GSDMD) pores - both during and outside of pyroptosis, enveloped release via exosomes and microvesicles, and larger scale exocytosis via autolysosome exocytosis

4.1.3: The inflammasome

An inflammasome is a cyclical structure formed by numerous protein combinations, but all contain the same core principles consisting of repeats of a NLR/ALR and a specific caspase. Those NLR/ALRs without Caspase-recruitment Domain (CARD) regions utilise an adaptor protein like ASC to more effectively recruit their pro-caspase to the inflammasome structure. Once recruited, the pro-caspase is cleaved into its functional state and the inflammasome becomes the hub for caspase activity. This then has specific effects depending upon the cell type, environment, and caspase being utilised and these can range from cytokine maturation to apoptosis to pyroptosis(161).

NLR/ALRs are highly expressed in response to specific proinflammatory stimuli like PAMPs, DAMPs, and cytokines. For example; AIM2 is highly induced by IFNs(178) and NLRP3 is transcribed by NF κ B. AIM2 is activated by dsDNA(179) from DNA viruses and intracellular bacteria, both of which often trigger large IFN γ -driven TH1-style responses. NLRP3 is well characterised as the canonical LPS inflammasome(180) and LPS is also known to be a strong stimulus of the NF κ B pathway. Inflammasome component expression is therefore specialised to specific types of stimuli.

The initial stimulation that triggers the upregulation of inflammasome components and substrates is known as the 'priming signal'. Assembly of the NLR/ALR, adaptor (if needed), and appropriate caspase into the inflammasome structure itself requires a secondary signal known as the 'activating signal'. A wide array of PAMPs and DAMPs can trigger inflammasome formation and are believed to do so through one of three common pathways: ROS formation(181), potassium ion efflux(182), or lysosomal disruption(183). Details on how these three common pathways trigger the assembly of the inflammasome are not known, however. The formation of the inflammasome can also be regulated by a number of other factors. These include; affecting ASC recruitment to the NLRs/ALRs via manipulation of the structure of the mitochondrial-associated membrane (MAM)(184, 185), modulation of ROS production with factors such as with TRIM30(186), the induction of NO which stabilises mitochondria(187), the presence of aryl hydrocarbon receptor (AhR) which inhibits NLRP3 transcription(188), and the alteration of levels autophagy which degrades components and substrates of the inflammasome(189). There are also a number of man-made chemical inhibitors of inflammasome formation and function(190).

The example of the canonical NLRP3/caspase 1 inflammasome is the most studied and is the traditional inflammasome for LPS. Its components are upregulated by NF κ B and it has been shown to be activated by ROS, potassium ion efflux, and lysosomal disruption(181-183, 191). However, within human monocytes, LPS is capable of acting as both the priming signal and the activating signal by utilising a unique connection through TRIF/ Receptor-interacting Serine/Threonine-protein Kinase 1 (RIP1)/Fas-associated Death Domain Protein (FADD)/caspase 8 to trigger inflammasome formation without potassium ion efflux unlike classical activating signals(192). Instead of the classic all-or-nothing response where the potassium efflux triggers the assembly and activation of all inflammasomes within the cell or fails to reach a high enough threshold to trigger any, this unique alternative pathway gives an analogue level of response that correlates to the level of stimulation. The NLRP3 inflammasome recruits pro-caspase 1 which is cleaved to active caspase 1 and this in turn cleaves cytosolic pro-IL-1 β to active IL-1 β . As shown in Figure 23, this process continues until autocleavage of caspase 1 occurs and it is released from the inflammasome as a p20/p10 heterodimer which has minimal cleavage activity.

Figure 23:

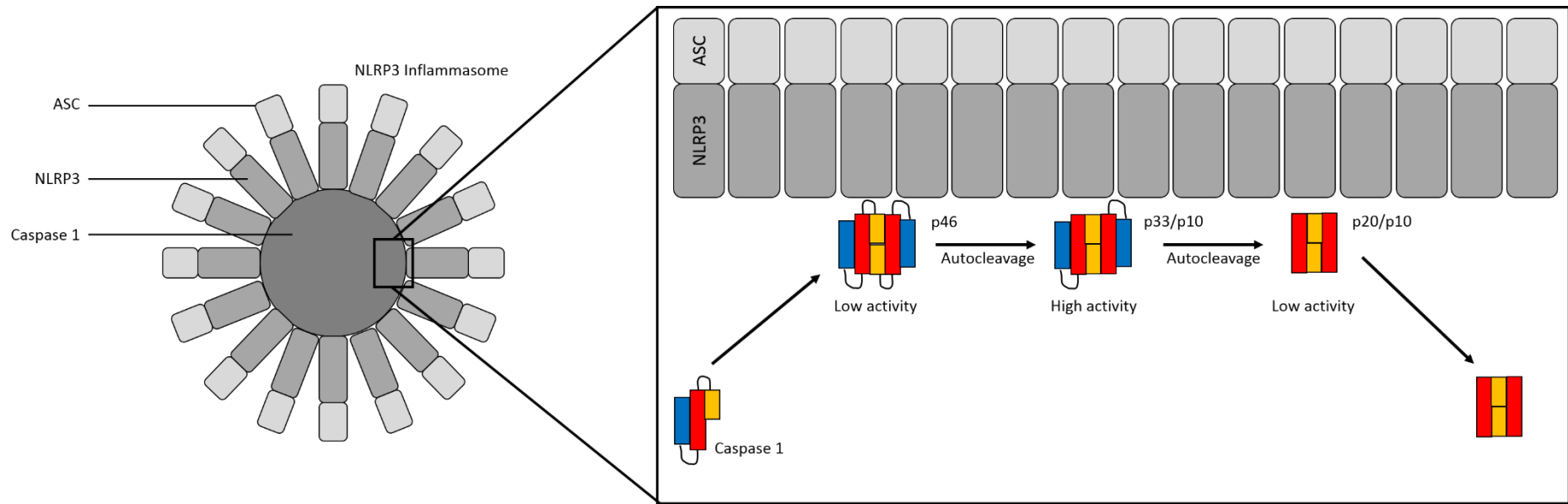


Figure 23 - Caspase 1 cleavage/Inflammasome activity – The function of the inflammasome is to create a site of high density, active caspases. In the case of the NLRP3 inflammasome, the caspase utilised is caspase 1. The central region of high caspase 1 activity is surrounded by NLRP3 – the receptor/trigger molecule for the formation of the inflammasome structure – and then ASC – an adaptor molecule which allows non-CARD-containing NLRs/ALRs like NLRP3 to recruit pro-caspase 1. The presented structure is based upon the work of S.Man et al (2014)(1)

ASC, apoptosis-associated speck-like protein containing a CARD; CARD, caspase-recruitment domain; ALR, AIM2-like receptor; NLR, NOD-like receptor; NLRP3, NACHT, LRR, and PYD domains-containing protein 3

4.1.4: Chapter aims

The aims of the experiments in this chapter are:

- To examine the effect of V-antigen on IL-1 β intracellular processing when under stimulation with LPS
- To determine what, if any, effect V-antigen has on the expression of inflammasome and inflammasome-related genes through large-scaled gene array approaches
- To use the STRING protein interaction database to generate a holistic view of which pathways within the gene array data have altered gene expression under V-antigen stimulation to generate evidence as to the mechanism of action of V-antigen

4.2: Results

4.2.1: Intracellular IL-1 β processing

To investigate the restriction of the IL-1 β pathway seen in Chapter 3, the lysates from the same MM6 stimulations were used for western blotting in an effort to test the secretion, maturation, and transcription of IL-1 β .

At the end of the stimulations performed in 3.2.5.1, the growth media was removed for cytokine analysis and the cells were rapidly lysed in 2x sample buffer (Appendix A). Despite a poor secretory response from the MM6 cells in Chapter 3 in response to LPS alone, Figures 13, 14, and Supplementary Figures 1 - 8 showed there was a much better secretory response to combinations of V-antigen and LPS, and so lysates of these stimulations were examined for intracellular levels of pro-IL-1 β , IL-1 β , and caspase 1 to determine whether the differences in secretory IL-1 β could be attributed to altered processing, reduced secretion, or reduced transcription.

Although, the same number of cells were used for each stimulation, protein quantities in the samples were normalised via western blot by utilising Image-J band intensity analysis on β -2 Microglobulin (β 2M) expression (data not shown). The adjusted loading was then used in future western blots for these samples.

The cellular content of pro-IL-1 β and IL-1 β at each time point and condition was then determined using fluorescent western blotting in denaturing, reducing conditions, with Glyceraldehyde 3-phosphate Dehydrogenase (GAPDH) used as a loading control. The results, presented in Figure 24, show that the '50 μ g V-antigen + LPS' sample had a visibly reduced level of pro-IL-1 β at 6hr and 12hr compared to the other V-antigen + LPS samples. The level of mature IL-1 β was too low in all samples to draw strong conclusions, however there was potentially a reduced quantity in the '50 μ g V-antigen + LPS' sample at 12hr when compared to other quantities of V-antigen + LPS.

It was also clear that, despite the close expression of GAPDH between LPS-stimulated samples, the difference in GAPDH expression between long-term LPS-stimulated samples and non-LPS-stimulated samples was visibly different. This is despite the previous standardization of protein loading around β 2M, another well-established housekeeping gene. It has since been discovered though that GAPDH is involved in the inflammatory response in macrophage/monocytes(193) and so is not an ideal housekeeping gene to use in inflammatory experiments, however due to the normalisation of the protein loading quantities around β 2M, these experiments remain appropriately normalised.

Figure 24:

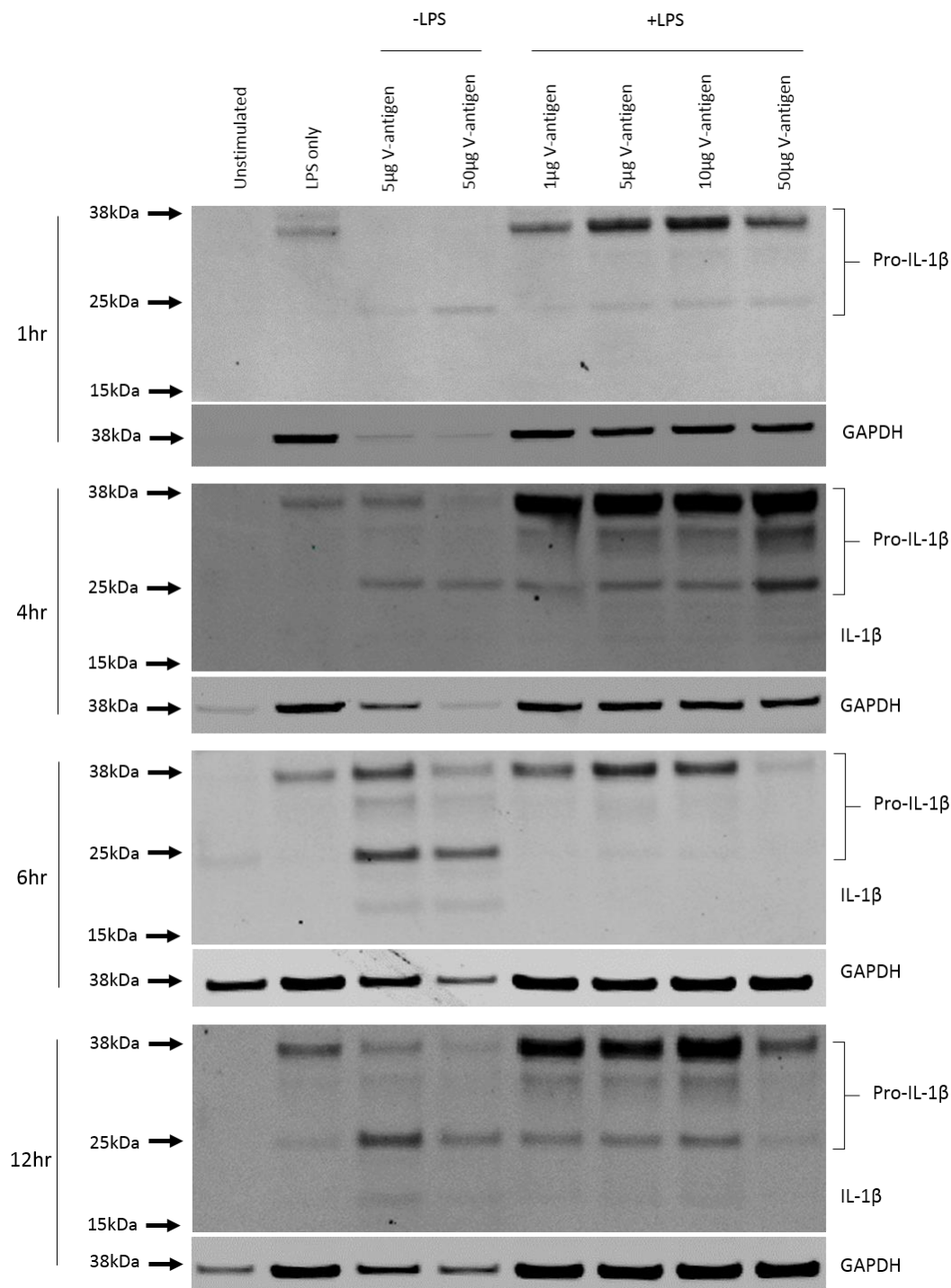


Figure 24 - IL-1 β western blots on LPS/ V-antigen-stimulated MM6 cells – Mono-mac 6 (MM6) cells were seeded at a density of 5×10^4 cells/well on 24 well plates and allowed to attach overnight. After a 30min pre-incubation with various concentrations of V-antigen (0 μ g, 1 μ g, 5 μ g, 10 μ g, 50 μ g), LPS was added to a final concentration of 100ng/ml or not added at all. After a specified incubation time from the point of LPS addition (or non-addition), the cells were lysed in 2x sample buffer (Appendix A). An SDS-PAGE was run in denaturing, reducing conditions using loading quantities determined by β 2M expression (western blot not shown), before being transferred to a nitrocellulose membrane and probed with anti-GAPDH antibody (abcam ab8245) and anti-IL-1 β antibody (R&D AF-401-NA) and then anti-mouse-680 antibody (LiCor 926-68022) and anti-goat-800 antibody (LiCor 926-32214). The resulting blot was then imaged using a LiCor Odyssey fluorescent imaging system where it showed a reduced level of IL-1 β and pro-IL-1 β under 6hr and 12hr '50 μ g V-antigen + 100ng/ml LPS' stimulation compared with other quantities of V-antigen and LPS.

GAPDH, glyceraldehyde 3-phosphate dehydrogenase; IL-1 β , interleukin 1 β

The lack of intracellular build-up of IL-1 β or pro-IL-1 β in '50 μ g V-antigen + LPS' was suggestive of the effects of V-antigen inhibition being localised upstream from secretion and potentially transcription. However, the maturation of IL-1 β was also investigated via further fluorescent western blotting to determine whether there was an inhibition of inflammasome function that could also contribute to the lower levels of mature IL-1 β .

The same western blots were stripped using 2x 10min/RT washes in stripping buffer (Appendix A), 2x 10min/RT washes in PBS, and 2x 5min/RT washes in PBST. They were then re-probed, this time using a caspase 1 antibody that also reported the cleaved subunit; p20. Unfortunately, there was no clear result as to inflammasome function via the cleavage of pro-caspase 1 to its active subunits due to low signal from caspase 1 p20 and so no conclusions could be drawn about cleavage inhibition. The results are shown in Figure 25.

Figure 25:

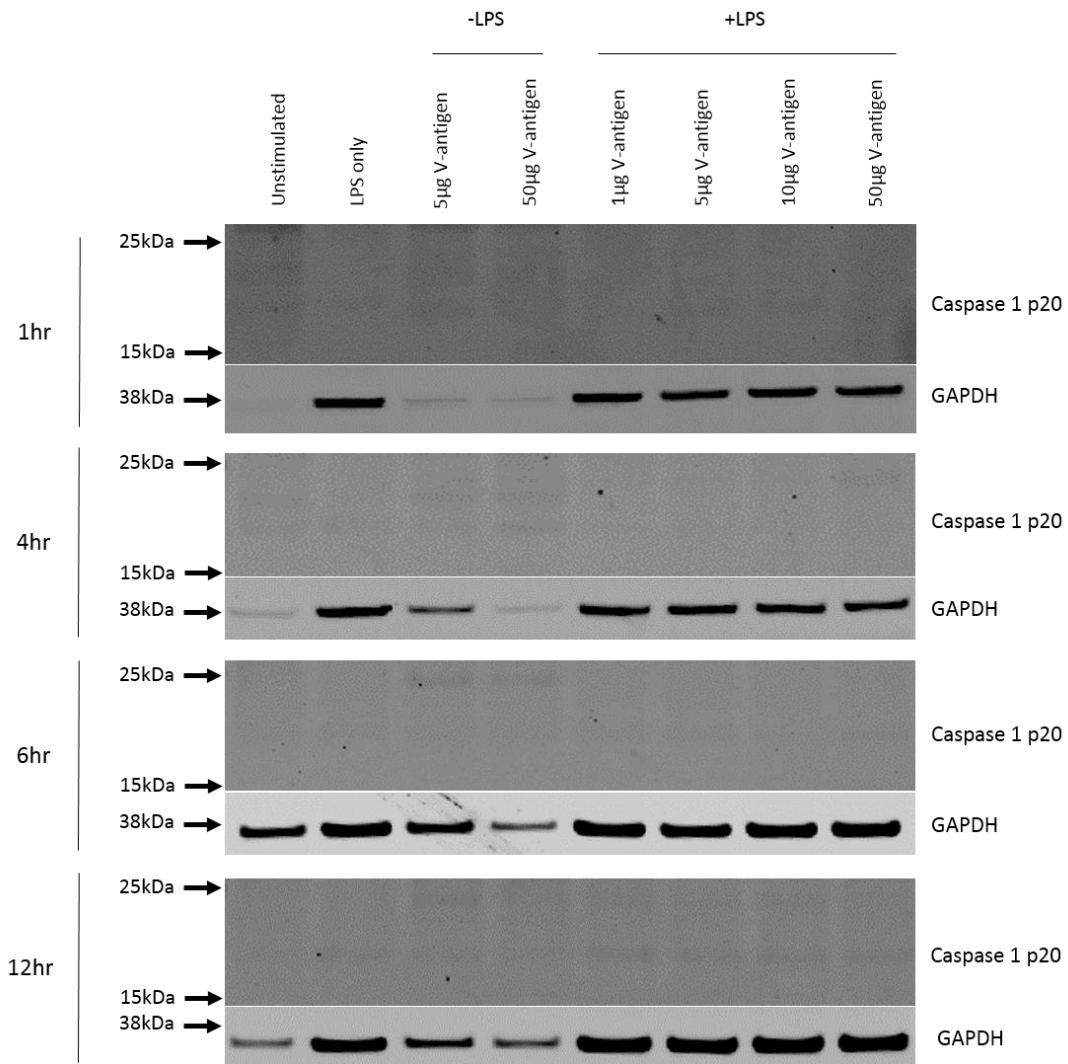


Figure 25 – Caspase 1 western blots on LPS/V-antigen-stimulated MM6 cells – Mono-mac 6 (MM6) cells were seeded at a density of 5×10^4 cells/well on 24 well plates and allowed to attach overnight. After a 30min pre-incubation with various concentrations of V-antigen (0µg, 1µg, 5µg, 10µg, 50µg), LPS was added to a final concentration of 100ng/ml or not added at all. After a specified incubation time from the point of LPS addition (or non-addition), the cells were lysed in 2x sample buffer (Appendix A). An SDS-PAGE was run in denaturing, reducing conditions using loading quantities determined by β 2M expression (western blot not shown), before being transferred to a nitrocellulose membrane and probed (Figure 24). The nitrocellulose membrane was then stripped with stripping buffer (Appendix A) and then re-probed with anti-caspase-1 p20 antibody (R&D MAB6215) and then anti-mouse-680 antibody (LiCor 926-68022). The resulting blot was then imaged using a LiCor Odyssey fluorescent imaging system where it revealed no clear results about caspase 1 p20 levels intracellularly in stimulated MM6 cells

GAPDH, glyceraldehyde 3-phosphate dehydrogenase; IL-1 β , interleukin 1 β

4.2.2: Inflammasome qPCR gene array

4.2.2.1: Gene cluster analysis

A classical western blot approach had failed to yield a conclusion on the effects of V-antigen on caspase 1 cleavage and so ulterior methods to investigate the effect of V-antigen on the inflammasome environment needed to be utilised. As each inflammasome is linked

with specific responses/outcomes, inflammasome-related genes are often controlled through cytokine signalling and PAMP detection, thereby promoting the appropriate response for the stimuli. These responses also extend beyond the cleavage of IL-1 β – as explained in 4.1.3 – and so understanding the full scope of these changes is vital to understanding how V-antigen affects the wider cellular response to LPS. It was also unknown whether V-antigen directly influences any part of this network of proteins to have its immunomodulatory effects or if large data collection techniques would help to isolate its mechanism of action. So, to find whether the altered cytokine profile in Chapter 3 had a substantial impact on the transcription of genes relating to the inflammasome – and whether V-antigen was influencing the processing of cytokines or other cellular processes via inflammasome-related gene expression – the Human Inflammasome Qiagen RT² profiler gene array kit was used.

The gene array consisted of a 384-well plate that contained four copies of primers specific for 84 genes connected to human inflammasomes as well as house-keeping genes that could be used to normalise the four datasets. It also contained quality controls and genomic contamination controls to ensure the qPCR results could be trusted. In addition to NLR/ALR genes, the gene list also contained a number of members of cytokine signalling and PRR pathways as well as target genes to give insight into other related pathways as well. A full list of the target genes in the Human Inflammasome Qiagen RT² profiler gene array is shown in Table 5.

Table 5 - Gene list for the Human Inflammasome Qiagen RT² profiler gene array

<i>AIM2</i>	<i>BCL2</i>	<i>BCL2L1</i>	<i>BIRC2</i>
<i>BIRC3</i>	<i>CARD18</i>	<i>CARD6</i>	<i>CASP1</i>
<i>CASP5</i>	<i>CASP8</i>	<i>CCL2</i>	<i>CCL5</i>
<i>CCL7</i>	<i>CD40LG</i>	<i>CFLAR</i>	<i>CHUK</i>
<i>CIITA</i>	<i>CTSB</i>	<i>CXCL1</i>	<i>CXCL2</i>
<i>FADD</i>	<i>HSP90AA1</i>	<i>HSP90AB1</i>	<i>HSP90B1</i>
<i>IFNB</i>	<i>IFNG</i>	<i>IKBKB</i>	<i>IKBKG</i>
<i>IL12A</i>	<i>IL12B</i>	<i>IL18</i>	<i>IL1B</i>
<i>IL33</i>	<i>IL6</i>	<i>IRAK1</i>	<i>IRF1</i>
<i>IRF2</i>	<i>MAP3K7</i>	<i>MAPK1</i>	<i>MAPK11</i>
<i>MAPK12</i>	<i>MAPK13</i>	<i>MAPK3</i>	<i>MAPK8</i>
<i>MAPK9</i>	<i>MEFV</i>	<i>MYD88</i>	<i>NAIP</i>
<i>NFKB1</i>	<i>NFKBIA</i>	<i>NFKBIB</i>	<i>NLRC4</i>
<i>NLRC5</i>	<i>NLRP1</i>	<i>NLRP12</i>	<i>NLRP3</i>
<i>NLRP4</i>	<i>NLRP5</i>	<i>NLRP6</i>	<i>NLRP9</i>
<i>NLRX1</i>	<i>NOD1</i>	<i>NOD2</i>	<i>P2RX7</i>
<i>PANX1</i>	<i>PEA15</i>	<i>PSTPIP1</i>	<i>PTGS2</i>
<i>PYCARD</i>	<i>PYDC1</i>	<i>MOK</i>	<i>RELA</i>
<i>RIPK2</i>	<i>SUGT1</i>	<i>TAB1</i>	<i>TAB2</i>
<i>TIRAP</i>	<i>TNF</i>	<i>TNFSF11</i>	<i>TNFSF14</i>
<i>TNFSF4</i>	<i>TRAF6</i>	<i>TXNIP</i>	<i>XIAP</i>

The RNA used for the gene array was sourced from the same primary stimulations as used in 3.2.5.2 – an overview of the experimental set-up can be found in Figure 15 – in order to allow for a direct comparison between the gene transcription data and the cytokine data. Immediately after the growth media had been removed for cytokine analysis, cells were lysed in RLT buffer and RNA was isolated and used to generate cDNA (2.2.4) which was then loaded onto the plate in equal concentrations, sealed, and subjected to PCR in a Quantstudio 7 qPCR machine. The resulting qPCR data was then processed through Qiagen's dedicated Geneglobe analysis software (2.4.1) which is calibrated for their RT² profiler gene array kits and provides means to normalise, analyse, compare, and visualise the expression data.

Although each plate could only run four samples at once, data from multiple plates were compiled together to create one large dataset consisting of sixteen individual sets of qPCR data. Each plate contained quality control tests which evaluated each sample for PCR array reproducibility, reverse transcription effectiveness (in regard to the RT² First Strand step), and genomic DNA contamination which were reported in a simple pass/fail message in the Geneglobe analysis software. All samples passed these tests.

The data was then normalised using β 2M gene expression as before as this had previously been reported to be more consistent when testing gene expression in LPS-stimulated monocytes than β -actin (ACTB) and GAPDH which were also available on this plate(194).

The inclusion of four individual donors, all under all four of the stimulation groups ('unstimulated', 'LPS only', 'V-only', 'V+LPS'), allowed the Geneglobe analysis software to run a two-tailed student's t-test (with the assumption that variance within each group was the same) and provide p-values for each change in gene regulation. The full data, using 'unstimulated' as the control group, is provided in Supplementary Table 1 and the expression levels across all sixteen samples is displayed in the clustergram in Figure 26.

Figure 26:

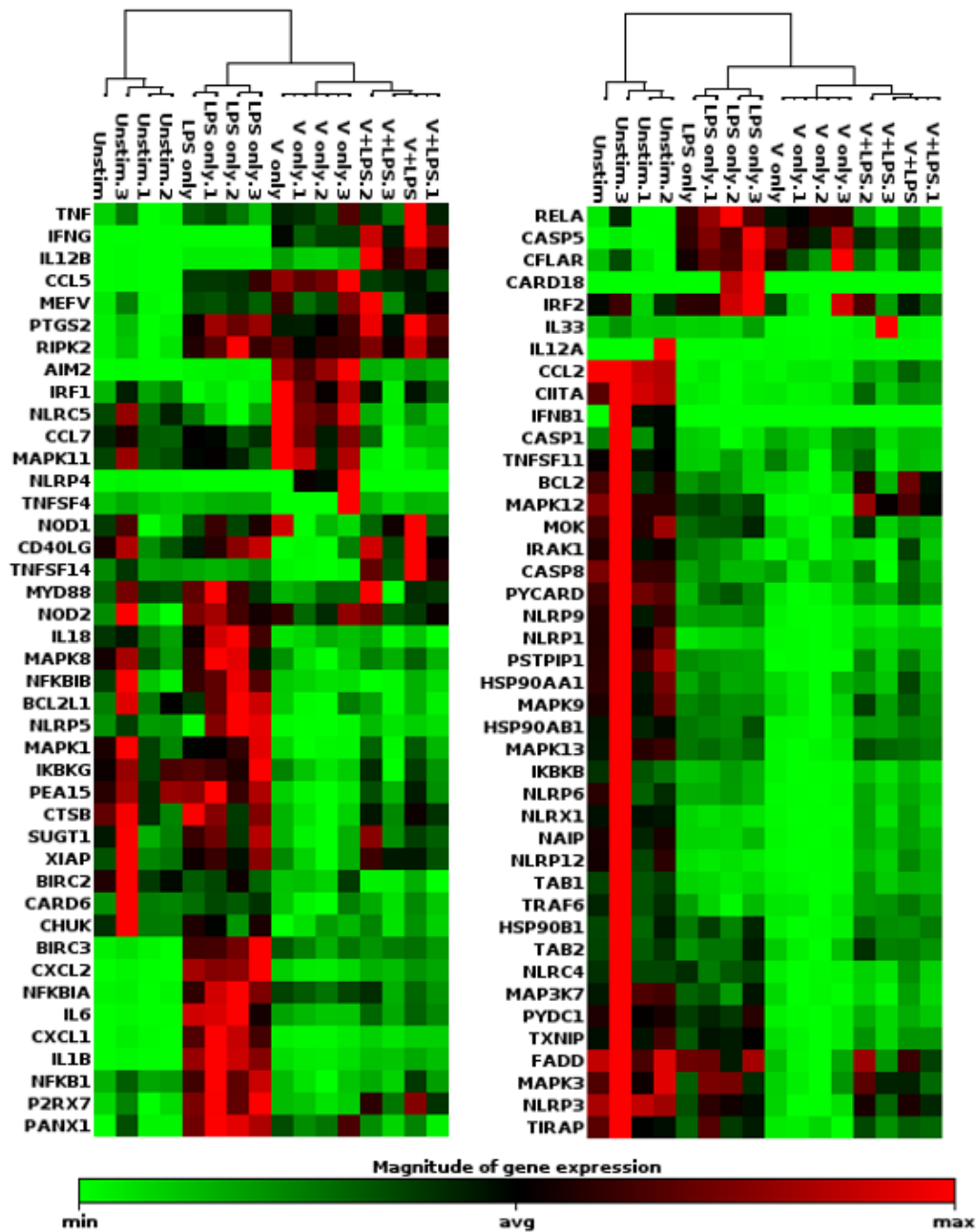


Figure 26 - Clustergram of Qiagen RT² qPCR - Human Inflammasome gene array results for WT V-antigen (+/- LPS) – PBMDMs from 4 separate donors were set up according to the experimental design in Figure 15 with PBMDMs pre-incubated with/without 50µg V-antigen and then stimulated with/without 100ng/ml LPS for 16hr. The cells were then lysed, and the RNA was extracted for qPCR analysis using the Qiagen RT² profiler - Human Inflammasome gene array plate. Using the Qiagen Geneglobe analysis software, a clustergram was generated from the resulting data showing the relative expression of each of the genes across all conditions and donors

Genes that were found to have a >1.5-fold regulation as well as a t-test p-value <0.05 were considered to have increased expression and genes with a <-1.5-fold regulation and a t-test p-value of <0.05 were considered to have decreased expression.

Initially ‘LPS only’ was compared to ‘unstimulated’ controls to investigate whether the donors responded as expected to LPS. The volcano plot in Figure 27 shows a clear

alteration in the gene expression profile and Tables 6 and 7 present the genes which increased and decreased respectively.

Figure 27:

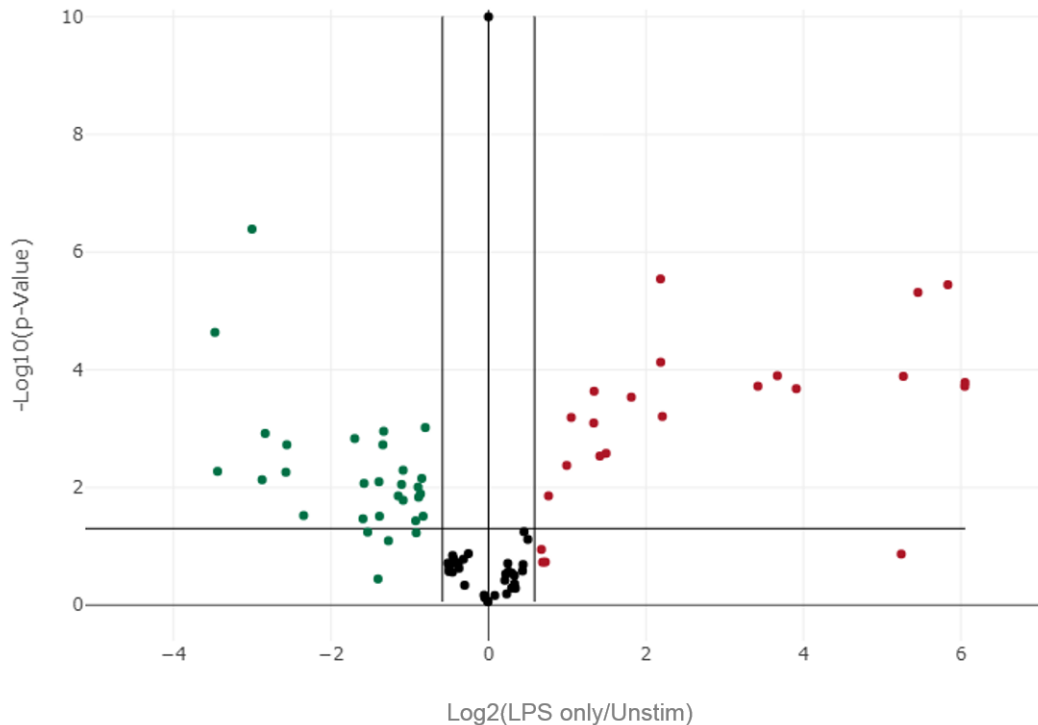


Figure 27 - Volcano plot of 'LPS only' gene expression compared to 'unstimulated' control expression – Inflammasome gene array – PBMDMs from 4 separate donors were set up according to the experimental design in Figure 15 with PBMDMs pre-incubated with/without 50µg V-antigen for 30min and then stimulated with/without 100ng/ml LPS for 16hr. The cells were then lysed, and the RNA was extracted for qPCR analysis using the Qiagen RT² profiler - Human Inflammasome gene array plate. Average gene expression for each gene within 100ng/ml LPS-stimulated PBMDMs (LPS only) and unstimulated control PBMDMs (unstimulated) was determined and compared using a volcano plot generated by the Qiagen Geneglobe analysis software. Genes with a >1.5-fold regulation (red) and genes <-1.5-fold regulation (green) were highlighted and the horizontal line was added to represent the p-value 0.05

Table 6 - Upregulated genes within LPS-stimulated PBMDMs – Inflammasome gene array

Gene Symbol	Fold Regulation	p Value	Comment
AIM2	2.07	0.000647	A
BIRC3	10.71	0.000190	
CASP5	15.02	0.000210	A
CCL5	66.28	0.000165	
CFLAR	2.81	0.002635	
CXCL1	38.53	0.000129	
CXCL2	43.81	0.000005	
IL12B	4.55	0.000003	
IL18	1.70	0.013909	
IL1B	57.00	0.000004	

IL6	66.14	0.000191	A
MEFV	1.99	0.004227	
NFKB1	2.53	0.000803	
NFKBIA	12.71	0.000126	
P2RX7	2.53	0.000232	
PANX1	3.51	0.000292	
PTGS2	4.55	0.000074	
RELA	2.67	0.002926	
RIPK2	4.62	0.000621	

PBMDMs from 4 separate donors were set up according to the experimental design in Figure 15 with PBMDMs pre-incubated with/without 50µg V-antigen for 30min and then stimulated with/without 100ng/ml LPS for 16hr. The cells were then lysed, and the RNA was extracted for qPCR analysis using the Qiagen RT² profiler - Human Inflammasome gene array plate. Average gene expression for each gene within 'LPS only' and 'unstimulated' controls was compared, and a Student's T-test was performed via the Qiagen Geneglobe analysis software. Genes upregulated by LPS (genes with >1.5-fold regulation and <0.05 p-value as determined by Student's T-test) are presented in the table above

'Comments' are: A; the gene's average threshold value is high (>30) in one group and low (<30) in the other, B; the gene's average threshold value is >30 in both samples and the p-value for the fold-change is unavailable or high (p>0.05), C; the gene's average threshold value is above the cut-off or undetected in all samples and so is unreliable and cannot be used

Table 7 - Downregulated genes within LPS-stimulated PBMDMs – Inflammasome gene array

Gene Symbol	Fold Regulation	p Value	Comment
BCL2	-2.21	0.013928	
CASP8	-2.52	0.001110	
CCL2	-8.02	0.000000	
CIITA	-11.11	0.000023	
HSP90AA1	-2.12	0.005097	
IRAK1	-1.82	0.012843	
IRF1	-1.85	0.014642	
MAP3K7	-1.78	0.030844	
MAPK12	-1.86	0.009851	A
MAPK13	-2.12	0.016507	
MAPK9	-2.15	0.008894	
NAIP	-5.95	0.005503	
NLRC5	-1.90	0.036837	
NLRP1	-7.14	0.001207	
NLRP12	-10.86	0.005324	
NLRP3	-1.74	0.000960	
NLRP4	-5.90	0.001882	C
NLRP6	-3.02	0.034091	
NLRP9	-2.99	0.008527	
NLRX1	-7.34	0.007400	
PSTPIP1	-3.25	0.001476	
PYCARD	-2.53	0.001881	
MOK	-1.80	0.007026	A

TAB1	-5.09	0.029976	
TNFSF11	-2.62	0.008008	
TRAF6	-2.61	0.030853	

PBMDMs from 4 separate donors were set up according to the experimental design in Figure 15 with PBMDMs pre-incubated with/without 50 μ g V-antigen for 30min and then stimulated with/without 100ng/ml LPS for 16hr. The cells were then lysed, and the RNA was extracted for qPCR analysis using the Qiagen RT² profiler - Human Inflammasome gene array plate. Average gene expression for each gene within 'LPS only' and 'unstimulated' controls was compared, and a Student's T-test was performed via the Qiagen Geneglobe analysis software. Genes downregulated by LPS (genes with <-1.5-fold regulation and <0.05 p-value as determined by Student's T-test) are presented in the table above

'Comments' are: A; the gene's average threshold value is high (>30) in one group and low (<30) in the other, B; the gene's average threshold value is >30 in both samples and the p-value for the fold-change is unavailable or high (p>0.05), C; the gene's average threshold value is above the cut-off or undetected in all samples and so is unreliable and cannot be used

45 genes were identified as having altered expression with 19 genes increasing in expression and 26 decreasing in expression. These genes were processed through STRING; a protein interaction network database described in 2.4.2 which maps proteins in clusters based on their interactions with each other to generate figures such as those shown in Figures 28 and 29. In large, more varied datasets this creates numerous visible nodes but with our dataset focused exclusively on the inflammasome related genes, this was unlikely to occur. The STRING 'analysis' tab however allows the user to highlight functional clusters within the dataset and provides a False Discovery Rate (FDR) (akin to a p-value) for the probability that the functional cluster has been enriched within the dataset by chance alone. It also provides 'Strength' scores for each cluster which is the $\log_{10}(\text{expected/observed})$ value to show how great the enrichment in the dataset is. Figure 28 is the protein network created from the comparatively upregulated genes which has functional clusters relating to 'response to LPS', 'response to cytokine', and 'response to lipid' highlighted. Predominantly these clusters were made up of cytokine genes and NF κ B genes – two sets of genes expected to be upregulated during LPS stimulation.

Figure 28:

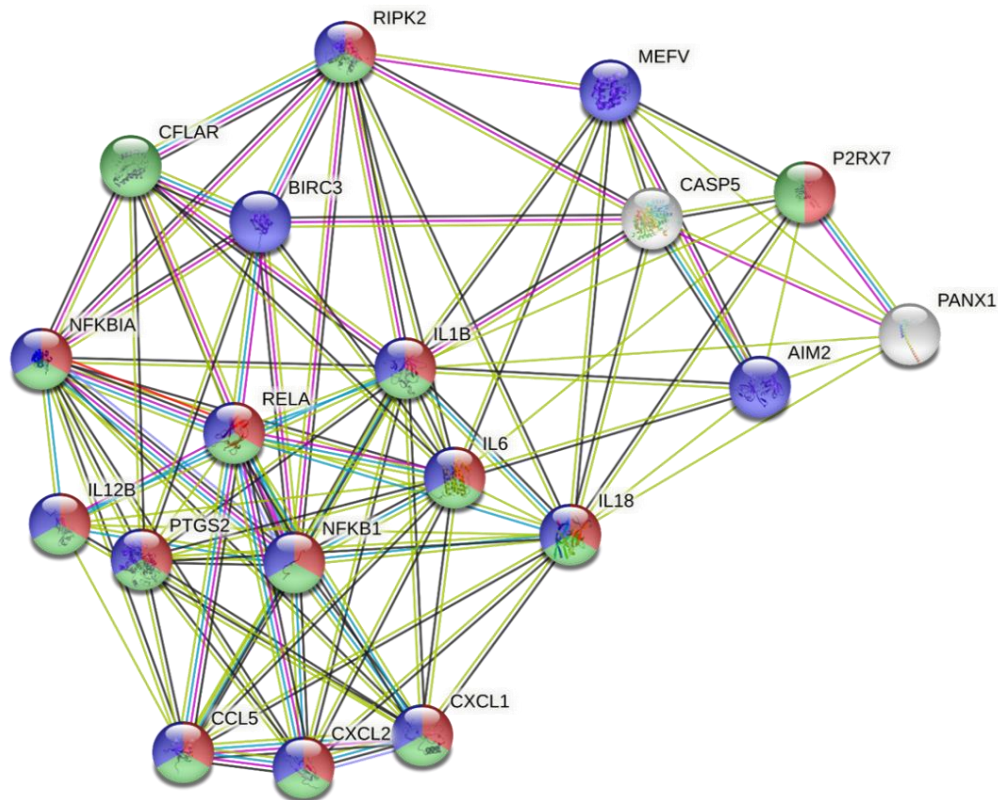


Figure 28 - STRING analysis of LPS-upregulated genes in PBMDMs – Inflammasome gene array – PBMDMs from 4 separate donors were set up according to the experimental design in Figure 15 with PBMDMs pre-incubated with/without 50 μ g V-antigen for 30min and then stimulated with/without 100ng/ml LPS for 16hr. The cells were then lysed, and the RNA was extracted for qPCR analysis using the Qiagen RT² profiler - Human Inflammasome gene array plate. Average gene expression for each gene within 100ng/ml LPS-stimulated PBMDMs (LPS only) and unstimulated control PBMDMs (unstimulated) was calculated and genes with an upregulated expression in 'LPS only', characterised as >1.5-fold regulation of expression and p-value <0.05 (determined by Student's T-test), were processed through the STRING protein interaction network database. Enriched functional clusters within the upregulated gene list were identified by STRING and the functional clusters of 'response to LPS' (red) (FDR = 1.48e-16, Strength = 1.65), 'response to cytokine' (blue) (FDR = 4.68e-14, Strength = 1.17), and 'response to lipid' (green) (FDR = 1.02e-13, Strength = 1.24) are highlighted within the full network presented above

There was an absence of most NLR/ALR genes, except for AIM2, and many were identified within the downregulated genes in Figure 29. NLRP3 could be expected to be an upregulated gene as it is a component of the canonical LPS inflammasome however there is evidence that longer LPS stimulations result in gradual downregulation of NLRP3 expression to protect the cell from excessive inflammation(195). Most NLR/ALR genes also had Cycle Threshold (CT) scores around 30 so were not highly expressed and, while β 2M has been shown to have a low variability across LPS-stimulated monocytes, it is possible that expression levels are less consistent between long LPS stimulations and unstimulated cells. However, due to its reported reliability between LPS-stimulated monocyte samples, β 2M remained our reference gene, as it would provide the most reliable reference gene for the comparison between 'LPS only' and 'V+LPS'.

Downregulated genes are shown in Figure 29 with the highlighted clusters of; 'viral process', 'regulation of cytokine production', and 'MAPK cascade'.

Figure 29:

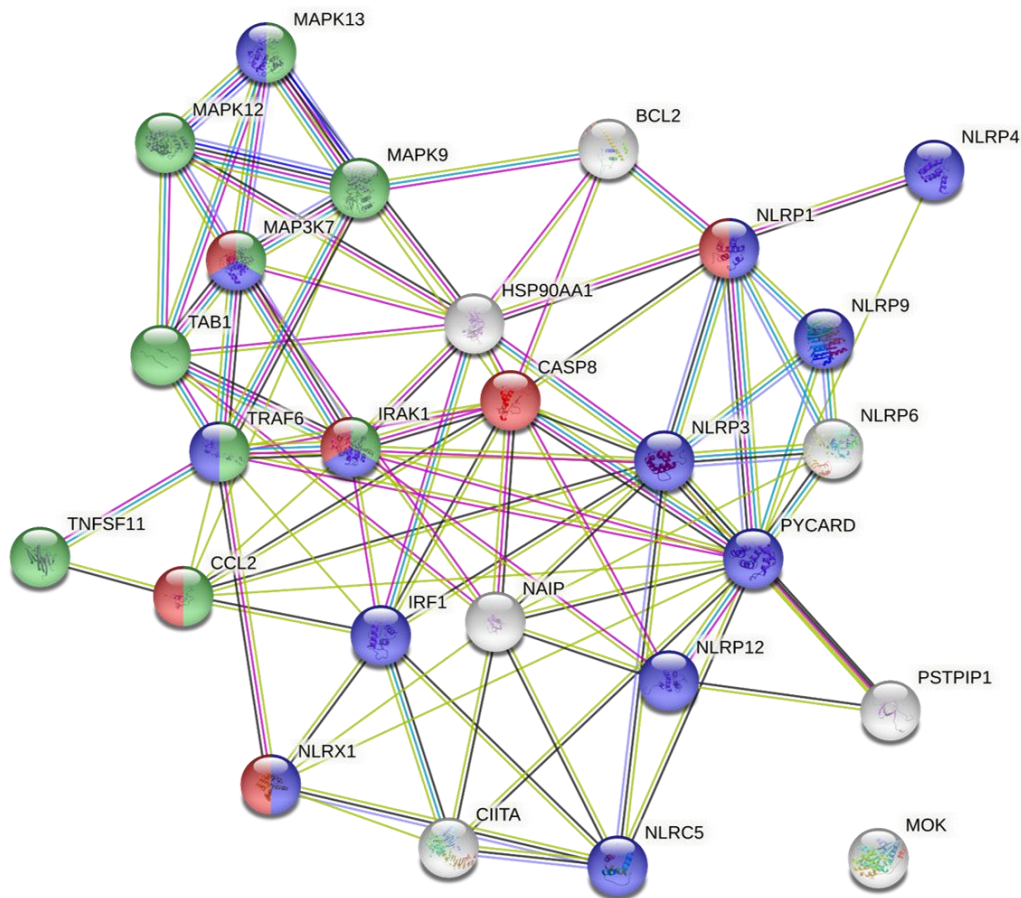


Figure 29 - STRING analysis of LPS-downregulated genes in PBMDMs – Inflammasome gene array – PBMDMs from 4 separate donors were set up according to the experimental design in Figure 15 with PBMDMs pre-incubated with/without 50µg V-antigen for 30min and then stimulated with/without 100ng/ml LPS for 16hr. The cells were then lysed, and the RNA was extracted for qPCR analysis using the Qiagen RT² profiler - Human Inflammasome gene array plate. Average gene expression for each gene within 100ng/ml LPS-stimulated PBMDMs (LPS only) and unstimulated control PBMDMs (unstimulated) was calculated and genes with a downregulated expression in 'LPS only', characterised as <-1.5-fold regulation of expression and p-value <0.05 (determined by Student's T-test), were processed through the STRING protein interaction network database. Enriched functional clusters within the downregulated gene list were identified by STRING and the functional clusters of 'viral process' (red) (FDR = 0.00057, Strength = 0.9), 'regulation of cytokine production' (blue) (FDR = 4.87e-11, Strength = 1.2), and 'MAPK cascade' (green) (FDR = 1.42e-08, Strength = 1.32) are highlighted within the full network presented above

The identification of the 'viral process' cluster in the downregulated genes was not unexpected under LPS stimulation – a bacterial product – though the strength value was relatively low. Interestingly, this cluster included caspase 8 which is the key caspase in the alternative LPS activation pathway in monocytes when there is no other activating signal(192) (4.1.3). This may be due to the β2M normalisation or due to long term stimulation leading to a gradual resistance to the stimulation as with NLRP3. 'Regulation of cytokine production proteins' was also highlighted - The majority of these genes were NLR/ALR genes along with a few members of PRR pathways and MAPKs.

The classical bacterial cytokine response seen in 3.2.5 and the transcriptional evidence of the same response in Figure 28, as well as expected changes in MAPK signalling and the increased expression in genes like Prostaglandin-Endoperoxidase Synthase 2 (PTGS2) and NFkB genes, provided enough certainty that the primary cells were responding to LPS.

Next, a comparison between 'LPS only' and 'V+LPS' was performed. The volcano plot in Figure 30 shows the altered expression of genes when 'V+LPS' is compared to 'LPS only' and Tables 8 and 9 give full lists of the comparatively upregulated and downregulated genes along with their fold change in regulation, t-test p-value, and any clarifying comments about the reliability of their measurement.

Figure 30:

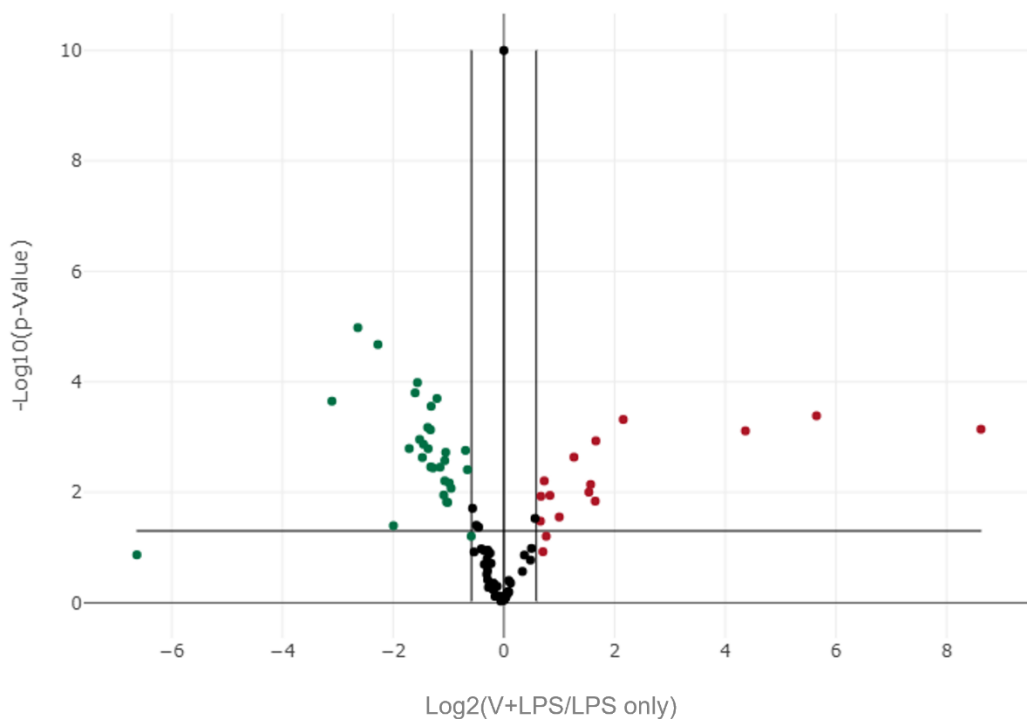


Figure 30 - Volcano plot of 'V+LPS' gene expression compared to 'LPS only' expression – Inflammasome gene array – PBMDMs from 4 separate donors were set up according to the experimental design in Figure 15 with PBMDMs pre-incubated with/without 50µg V-antigen for 30min and then stimulated with/without 100ng/ml LPS for 16hr. The cells were then lysed, and the RNA was extracted for qPCR analysis using the Qiagen RT² profiler - Human Inflammasome gene array plate. Average gene expression for each gene within '50µg V-antigen + 100ng/ml LPS'-stimulated PBMDMs (V+LPS) and 100ng/ml LPS-stimulated PBMDMs (LPS only) was determined and compared using a volcano plot generated by the Qiagen Geneglobe analysis software. Genes with a >1.5-fold regulation (red) and genes <-1.5-fold regulation (green) were highlighted and the horizontal line was added to represent the p-value 0.05

Table 8 - Upregulated genes within LPS-stimulated PBMDMs co-stimulated with V-antigen – Inflammasome gene array

Gene Symbol	Fold Regulation	p Value	Comment
AIM2	4.46	0.000481	
CCL2	2.41	0.002312	
CIITA	2.96	0.007215	
IFNB1	50.13	0.000412	A
IFNG	393.05	0.000722	A
IL12A	3.16	0.001173	
IL12B	20.59	0.000772	A
IRF1	2.00	0.028036	
MAPK12	1.59	0.011814	
NAIP	1.58	0.033297	
NLRP12	2.90	0.009937	
NLRP4	1.66	0.006216	C
TAB1	1.78	0.011394	
TNFSF14	3.14	0.014454	

PBMDMs from 4 separate donors were set up according to the experimental design in Figure 15 with PBMDMs pre-incubated with/without 50µg V-antigen for 30min and then stimulated with/without 100ng/ml LPS for 16hr. The cells were then lysed, and the RNA was extracted for qPCR analysis using the Qiagen RT² profiler - Human Inflammasome gene array plate. Average gene expression for each gene within 'V+LPS' and LPS only' controls was compared, and a Student's T-test was performed via the Qiagen Geneglobe analysis software. Genes upregulated in 'V+LPS' (genes with >1.5-fold regulation and <0.05 p-value as determined by Student's T-test) are presented in the table above.

'Comments' are: A; the gene's average threshold value is high (>30) in one group and low (<30) in the other, B; the gene's average threshold value is >30 in both samples and the p-value for the fold-change is unavailable or high (p>0.05), C; the gene's average threshold value is above the cut-off or undetected in all samples and so in unreliable and cannot be used

Table 9 - Downregulated genes within LPS-stimulated PBMDMs co-stimulated with V-antigen – Inflammasome gene array

Gene Symbol	Fold Regulation	p Value	Comment
BCL2L1	-2.50	0.003475	
BIRC2	-1.62	0.001746	
BIRC3	-2.74	0.001352	
CARD6	-1.58	0.003894	
CASP5	-2.10	0.006213	
CCL7	-1.98	0.006770	
CFLAR	-2.22	0.003513	
CXCL1	-8.61	0.000224	
CXCL2	-4.84	0.000021	
IKBKG	-2.02	0.015283	
IL18	-2.87	0.001106	
IL1B	-6.22	0.000010	
IL6	-3.27	0.001613	
MAP3K7	-2.12	0.011211	

MAPK1	-2.05	0.014919	
MAPK11	-2.31	0.000200	
MAPK8	-1.94	0.008457	
NFKB1	-2.58	0.001622	
NFKBIA	-2.77	0.002348	
NFKBIB	-2.49	0.000277	
NLRC4	-2.43	0.003620	
NLRP5	-3.99	0.040254	
NLRP9	-3.04	0.000158	
PANX1	-2.95	0.000103	
PEA15	-2.10	0.002668	
PYDC1	-2.60	0.000670	
RELA	-2.51	0.000738	
TXNIP	-2.07	0.001891	

PBMDMs from 4 separate donors were set up according to the experimental design in Figure 15 with PBMDMs pre-incubated with/without 50µg V-antigen for 30min and then stimulated with/without 100ng/ml LPS for 16hr. The cells were then lysed, and the RNA was extracted for qPCR analysis using the Qiagen RT² profiler - Human Inflammasome gene array plate. Average gene expression for each gene within 'LPS only' and 'unstimulated' controls was compared, and a Student's T-test was performed via the Qiagen Geneglobe analysis software. Genes downregulated in 'WT+LPS) (genes with <-1.5-fold regulation and <0.05 p-value as determined by Student's T-test) are presented in the table above.

'Comments' are: A; the gene's average threshold value is high (>30) in one group and low (<30) in the other, B; the gene's average threshold value is >30 in both samples and the p-value for the fold-change is unavailable or high (p>0.05), C; the gene's average threshold value is above the cut-off or undetected in all samples and so is unreliable and cannot be used

There were 41 differentially expressed genes were identified with 14 genes identified as upregulated and 27 genes identified as downregulated. As above, these differentially expressed genes were processed through STRING to highlight key functional clusters and Figures 31 and 32 present the findings.

Figure 31 shows identified clusters within the comparatively upregulated gene list. All link heavily with viral-like responses and of the 14 genes, 8 are associated with IFN responses. Higher levels of IFN γ were reported in 3.2.5 (Chapter 3, Figure 19) which explains the 'response to IFN γ ' cluster here. There is also increased IFN β transcription and upregulation of antiviral genes consisting of IRF1 and the antiviral ALR; AIM2.

Figure 31:

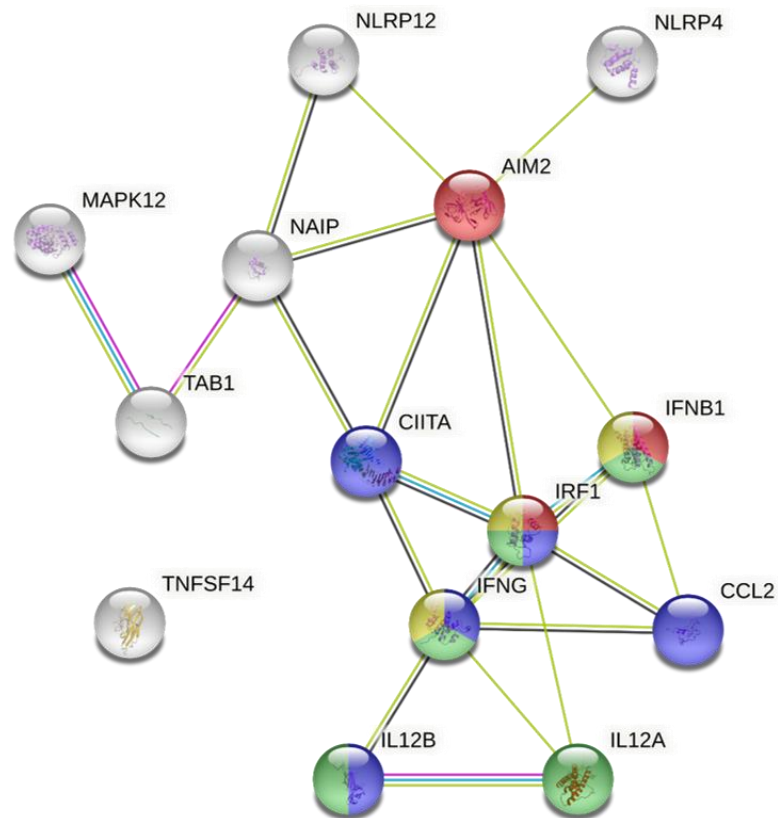


Figure 31 - STRING analysis of V-antigen-upregulated genes in LPS-stimulated PBMDMs – Inflammasome gene array – PBMDMs from 4 separate donors were set up according to the experimental design in Figure 15 with PBMDMs pre-incubated with/without 50 μ g V-antigen for 30min and then stimulated with/without 100ng/ml LPS for 16hr. The cells were then lysed, and the RNA was extracted for qPCR analysis using the Qiagen RT² profiler - Human Inflammasome gene array plate. Average gene expression for each gene within '50 μ g V-antigen + 100ng/ml LPS'-stimulated PBMDMs (V+LPS) and 100ng/ml LPS-stimulated PBMDMs (LPS only) was calculated and genes with an upregulated expression in 'LPS only', characterised as >1.5-fold regulation of expression and p-value <0.05 (determined by Student's T-test), were processed through the STRING protein interaction network database. Enriched functional clusters within the upregulated gene list were identified by STRING and the functional clusters of 'cellular response to IFN β ' (red) (FDR = 4.52e-06, Strength = 2.45), 'cellular response to IFN γ ' (blue) (FDR = 2.05e-06, Strength = 1.65), 'response to virus' (green) (FDR = 1.29e-05, Strength = 1.41), and 'antiviral defence' (yellow) (FDR = 0.0017, Strength = 1.53) are highlighted within the full network above

Figure 32 shows the functional clusters within the downregulated gene list. The 'cellular response to IL-1' cluster also correlates to the reduction in IL-1 β secretion seen in 3.2.5 (Chapter 3, Figure 16) and the reduced transcription of IL-1 β (Table 9). Key classical bacterial inflammatory pathways were also highlighted in the comparatively downregulated group including 'response to bacterium' and 'response to LPS'. These clusters contained classical cytokines, NF κ B components, and numerous MAPKs amongst others.

Figure 32:

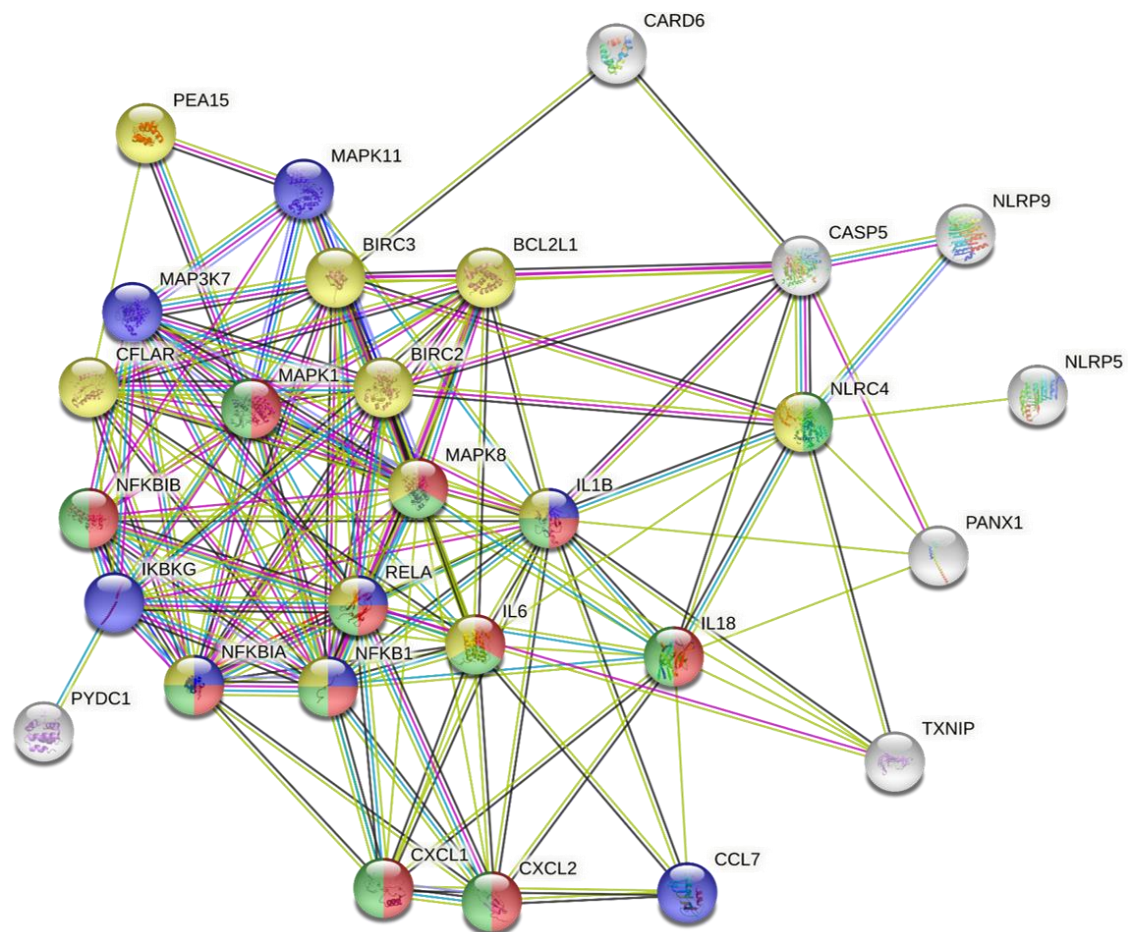


Figure 32 - STRING analysis of V-antigen-downregulated genes in LPS-stimulated PBMDMs – Inflammasome gene array – PBMDMs from 4 separate donors were set up according to the experimental design in Figure 15 with PBMDMs pre-incubated with/without 50 μ g V-antigen for 30min and then stimulated with/without 100ng/ml LPS for 16hr. The cells were then lysed, and the RNA was extracted for qPCR analysis using the Qiagen RT² profiler - Human Inflammasome gene array plate. Average gene expression for each gene within '50 μ g V-antigen + 100ng/ml LPS'-stimulated PBMDMs (V+LPS) and 100ng/ml LPS-stimulated PBMDMs (LPS only) was calculated and genes with a downregulated expression in 'LPS only', characterised as <-1.5-fold regulation of expression and p-value <0.05 (determined by Student's T-test), were processed through the STRING protein interaction network database. Enriched functional clusters within the downregulated gene list were identified by STRING and the functional clusters of 'response to LPS' (red) (FDR = 2.21e-11, Strength = 1.41), 'cellular response to IL-1' (blue) (FDR = 5.79e-10, Strength = 1.65), 'response to bacterium' (green) (FDR = 4.01e-10, Strength = 1.18), and 'negative regulation of apoptotic process' (yellow) (FDR = 2.17e-08, Strength = 0.99) are highlighted within the full network above

4.2.2.2: Expression analysis of key identified genes

A closer investigation into the expression levels of the identified gene clusters across all four conditions was necessary in order to gain a greater understanding of how V-antigen affected the development of the inflammatory response. One major reason for doing this was to better identify genes that showed clear evidence of altering expression in the presence of V-antigen. Direct comparisons between 'LPS only' and 'V+LPS' without this closer investigation hold limitations. For example, a gene identified as downregulated in 'V+LPS' when compared with 'LPS only' could be a gene actively downregulated by V-antigen, but it

could also be a gene that doesn't upregulate in 'V+LPS' but does in 'LPS only', or could upregulate in both but to a significantly lesser degree in 'V+LPS'. Due to the long stimulation times and the closed system nature of the 24 well plates the stimulations were carried out in, the higher level of proinflammatory cytokines (3.2.5) seen in 'LPS only' could be responsible for more extreme gene regulation in either direction when compared with 'V+LPS'. This could lead to a gene controlled by IL-1 β signalling, for example, to appear to be downregulated by V-antigen when in reality it is simply just not upregulating to the same degree as in LPS only due to a lower level of general inflammation. It is therefore important to identify any genes that show distinctly different expression patterns under V-antigen stimulation as these may form a more solid lead for identifying any causal pathways for V-antigen's immunomodulation.

To do this, the same data was analysed further within the Qiagen Geneglobe analysis software but this time at the level of individual genes. Graphs were generated by the software, but due to its limitations of only running t-tests on the resulting data, the p-values generated were then processed through a manual Benjamini-Hochberg posthoc adjustment to account for multiple comparisons (2.4.3).

Firstly, the focus was directed at key cytokines genes. IFN γ and IL-12 (which is associated with IFN γ expression) were both upregulated in all stimulations compared to the unstimulated control cells (Figure 33A/C). For both genes, 'V-only' had a significantly higher expression than 'LPS only' and the combined stimulation had a significantly higher expression than that. The variation of IFN β in the unstimulated control cells was considered too great due to the way the software handles samples with no CT value and so this was removed in Figure 33B for the express purpose of showing the expression changes in the stimulated samples only. The graph shows a clear significant increase in the expression of IFN β , a major antiviral cytokine, under V-antigen stimulation and a significantly higher expression under co-stimulation with both V-antigen and LPS.

The expression of classical bacterial cytokines like IL-1 β , IL-6, and IL-18 (Figure 34) was decreased in both V-antigen stimulations compared to the LPS only condition. While IL-1 β and IL-6 were still upregulated within 'V-only' and 'V+LPS' compared to unstimulated control cells, IL-18 expression was significantly downregulated in both.

Figure 33:

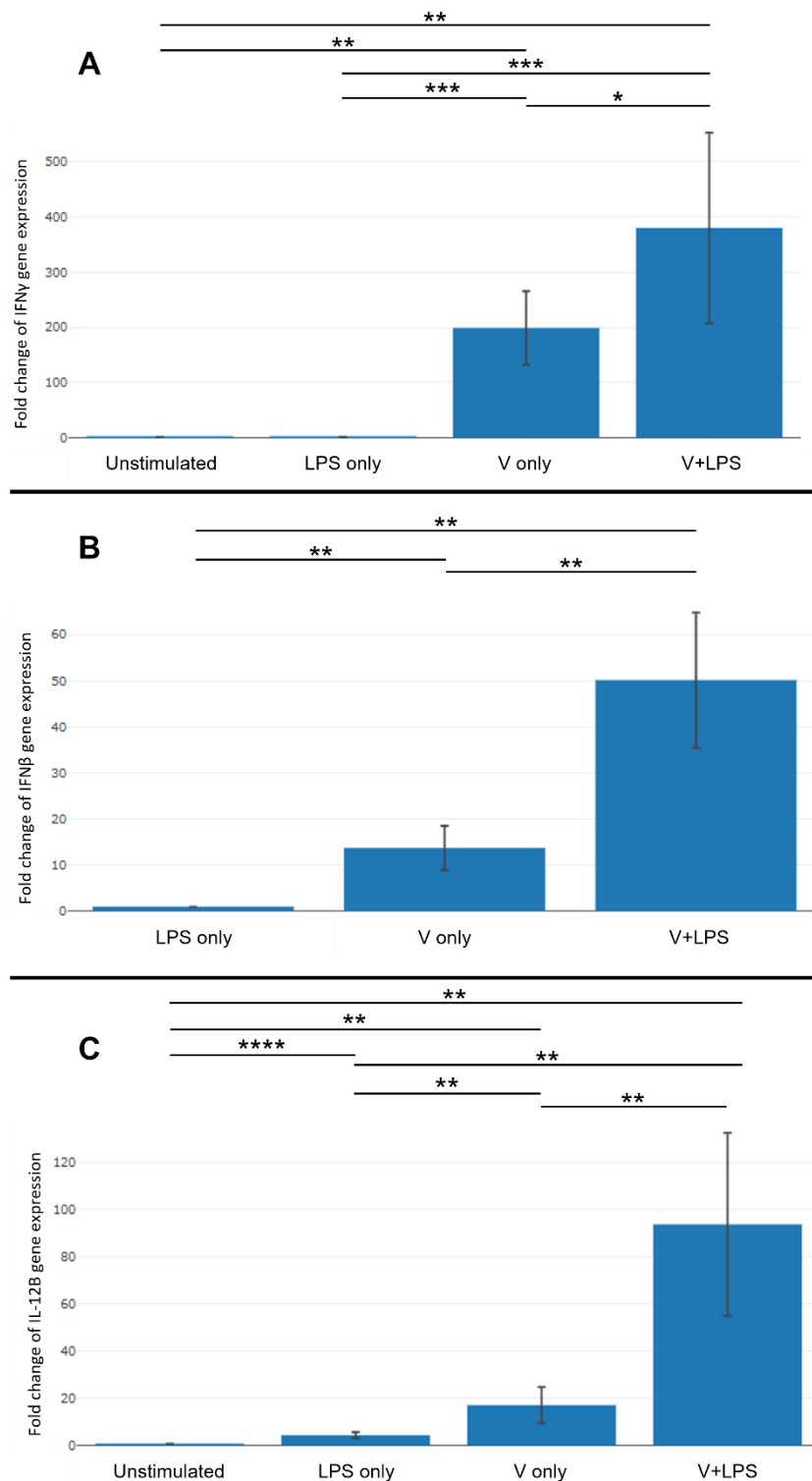


Figure 33 – IFN γ , IFN β , and IL-12B gene expression under stimulation with combinations of LPS and V-antigen – PBMDMs from 4 separate donors were set up according to the experimental design in Figure 15 with PBMDMs pre-incubated with/without 50 μ g V-antigen and then stimulated with/without 100ng/ml LPS for 16hr. The cells were then lysed, and the RNA was extracted for qPCR analysis using the Qiagen RT² profiler - Human Inflammasome gene array plate. Using the Qiagen Geneglobe analysis software, the average expression of A; IFN γ , B; IFN β , and C; IL-12B, was evaluated across all four conditions and displayed as a fold-change from the unstimulated control. Data is presented with standard error bars and indicators for statistical significance(* = <0.05, ** = <0.01, *** = <0.001, **** = <0.0001) as determined by Student's T-test adjusted for multiple comparisons post-hoc with a manual Benjamini-Hochberg correction. Due to high variation in the unstimulated control in the expression of IFN β (B) this data was excluded from the graph and 'LPS only' was used as the control

Figure 34:

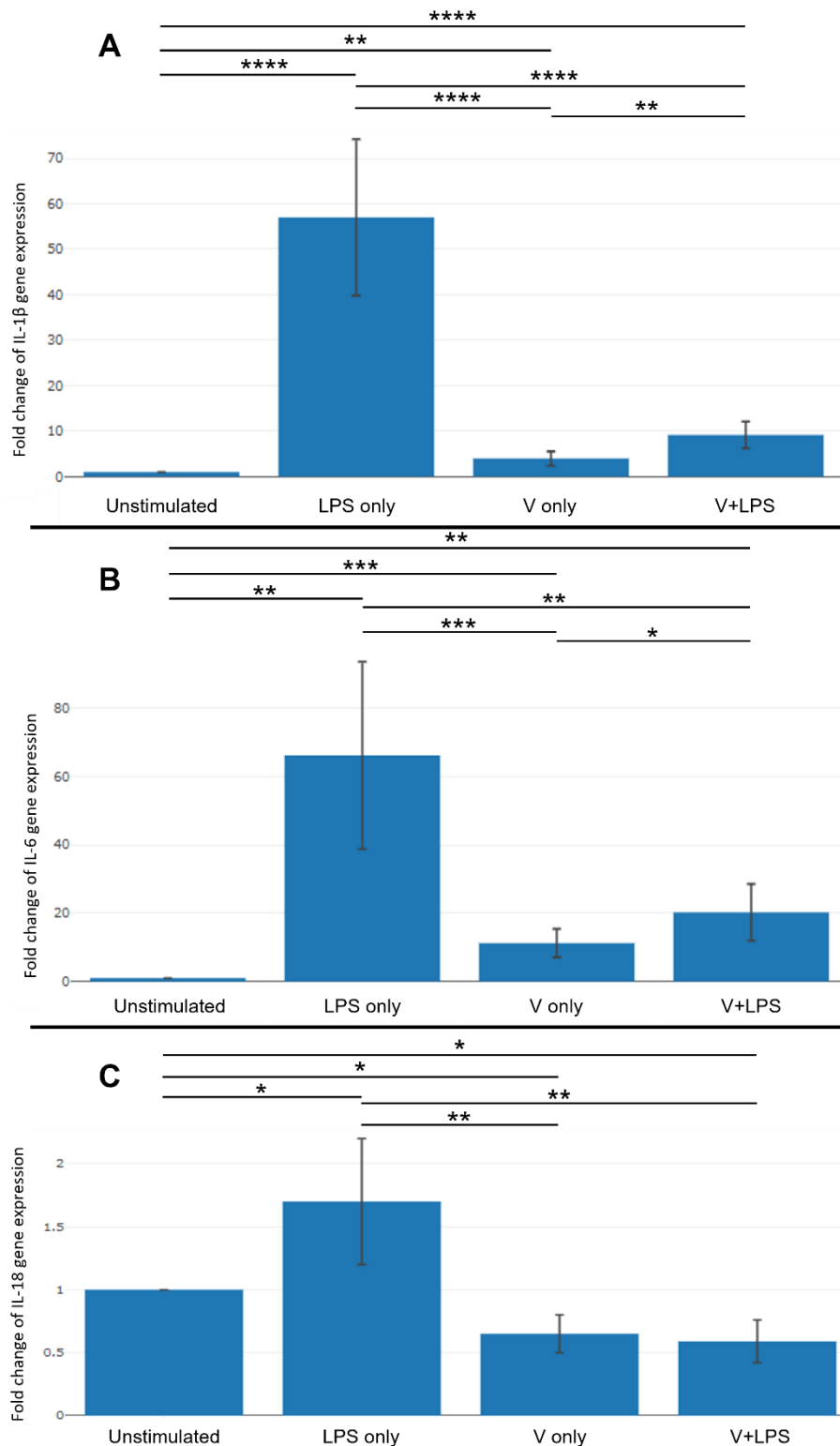


Figure 34 - IL-1 β , IL-6, and IL-18 gene expression under stimulation with combinations of LPS and V-antigen – PBMDMs from 4 separate donors were set up according to the experimental design in Figure 15 with PBMDMs pre-incubated with/without 50 μ g V-antigen and then stimulated with/without 100ng/ml LPS for 16hr. The cells were then lysed, and the RNA was extracted for qPCR analysis using the Qiagen RT² profiler - Human Inflammasome gene array plate. Using the Qiagen Geneglobe analysis software, the average expression of A; IL-1 β , B; IL-6, and C; IL-18, was evaluated across all four conditions and displayed as a fold-change from the unstimulated control. Data is presented with standard error bars and indicators for statistical significance (* = <0.05, ** = <0.01, * = <0.001, **** = <0.0001) as determined by Student's T-test adjusted for multiple comparisons post-hoc with a manual Benjamini-Hochberg correction**

Cytokine analysis in 3.2.5 showed a decrease in secreted TNF α in 'V+LPS' conditions, however the gene expression at 16hr showed no significant change compared to LPS only stimulations (Figure 35). However, compared to unstimulated cells, V-antigen stimulation alone, without LPS, had a significantly increased expression.

Figure 35:

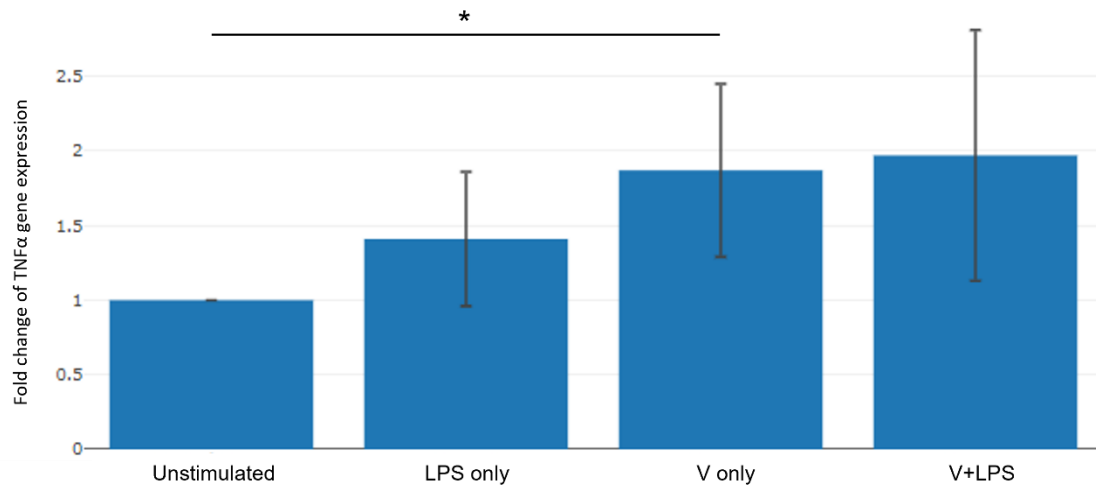


Figure 35 - TNF α gene expression under stimulation with combinations of LPS and V-antigen – PBMDMs from 4 separate donors were set up according to the experimental design in Figure 15 with PBMDMs pre-incubated with/without 50 μ g V-antigen and then stimulated with/without 100ng/ml LPS for 16hr. The cells were then lysed, and the RNA was extracted for qPCR analysis using the Qiagen RT² profiler - Human Inflammasome gene array plate. Using the Qiagen Geneglobe analysis software, the average expression of TNF α was evaluated across all four conditions and displayed as a fold-change from the unstimulated control. Data is presented with standard error bars and indicators for statistical significance(* = <0.05, ** = <0.01, *** = <0.001, **** = <0.0001) as determined by Student's T-test adjusted for multiple comparisons post-hoc with a manual Benjamini-Hochberg correction

This changed cytokine profile and subsequent signalling is likely the reason behind many of the changes in NLR/ALR expression. Two major NLR/ALRs of interest are shown in Figure 36; AIM2, which was identified as an upregulated NLR/ALR gene, and NLR Family CARD Domain-Containing Protein 4 (NLRC4), which was identified as downregulated by V-antigen in LPS-stimulated PBMDMs. AIM2 showed a significant 5.1-fold increase in expression in 'V-only' when compared to 'V+LPS' and a significant 23-fold increase when compared to 'LPS only'. This implies that its expression is heavily promoted by the presence of V-antigen and likely limited in its upregulation under LPS stimulation. This may be because AIM2 is a largely viral inflammasome and LPS is a bacterial product. NLRC4 however showed no significant changes in expression under LPS stimulation alone but in the presence of V-antigen, both with and without LPS co-stimulation, NLRC4 expression was significantly decreased. This was suggestive of a suppressive effect from V-antigen. While previous studies have shown that NLRC4 is inhibited by *Y.pestis*, this phenomenon has not been shown to be caused by V-antigen.

Figure 36:

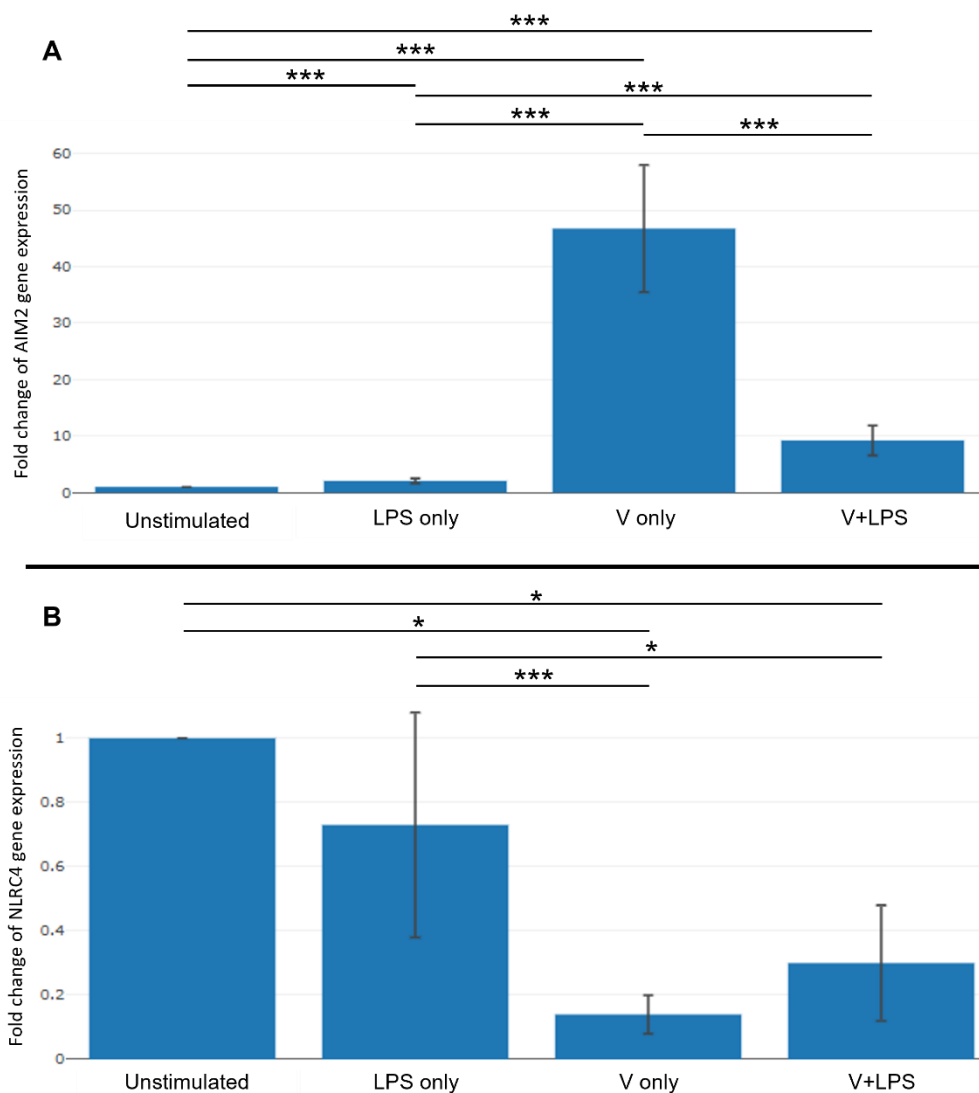


Figure 36 – AIM2 and NLRC4 gene expression under stimulation with combinations of LPS and V-antigen – PBMDMs from 4 separate donors were set up according to the experimental design in Figure 15 with PBMDMs pre-incubated with/without 50µg V-antigen and then stimulated with/without 100ng/ml LPS for 16hr. The cells were then lysed, and the RNA was extracted for qPCR analysis using the Qiagen RT² profiler - Human Inflammasome gene array plate. Using the Qiagen Geneglobe analysis software, the average expression of A; AIM2, and B; NLRC4 was evaluated across all four conditions and displayed as a fold-change from the unstimulated control. Data is presented with standard error bars and indicators for statistical significance(* = <0.05, ** = <0.01, *** = <0.001, **** = <0.0001) as determined by Student's T-test adjusted for multiple comparisons post-hoc with a manual Benjamini-Hochberg correction

The expression of other NLR genes that were identified reliably in Tables 8 and 9 are presented in Supplementary Figure 9.

The expression of IRF1, the major downstream TF for the TRIF pathway, showed a significantly increased expression in both V-antigen stimulations when compared to 'LPS only' – a 3.8-fold increase in expression for 'V only' and 2-fold increase for 'V+LPS' (Figure 37). This corresponded to a decrease in NFκB expression in V-antigen stimulated samples (Supplementary Figure 10).

Figure 37:

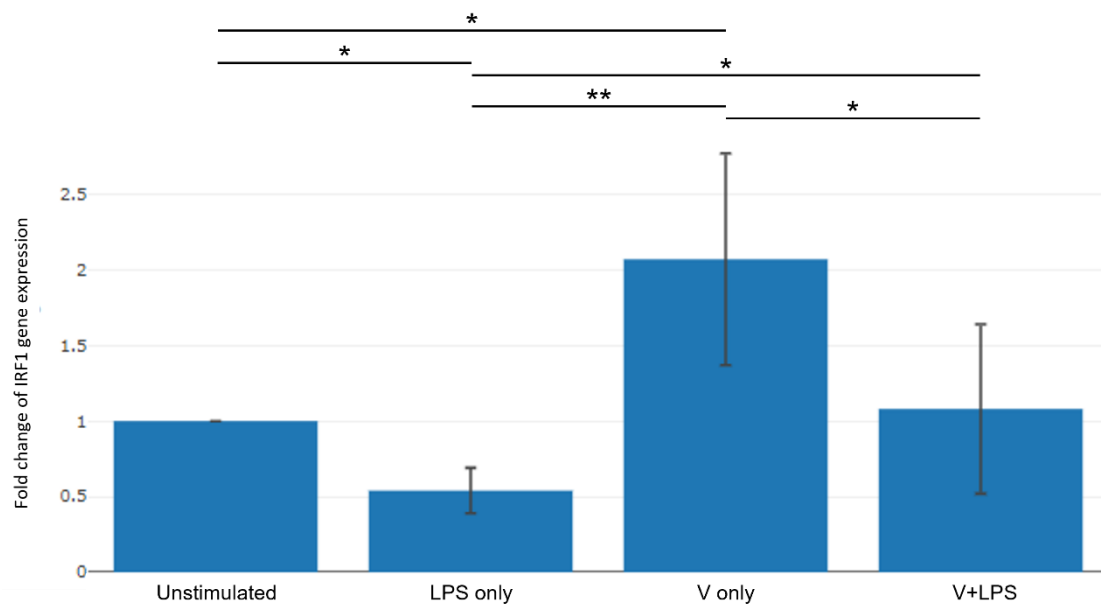


Figure 37 – IRF1 gene expression under stimulation with combinations of LPS and V-antigen – PBMDMs from 4 separate donors were set up according to the experimental design in Figure 15 with PBMDMs pre-incubated with/without 50µg V-antigen and then stimulated with/without 100ng/ml LPS for 16hr. The cells were then lysed, and the RNA was extracted for qPCR analysis using the Qiagen RT² profiler - Human Inflammasome gene array plate. Using the Qiagen Geneglobe analysis software, the average expression of IRF1 was evaluated across all four conditions and displayed as a fold-change from the unstimulated control. Data is presented with standard error bars and indicators for statistical significance(* = <0.05, ** = <0.01, *** = <0.001, **** = <0.0001) as determined by Student's T-test adjusted for multiple comparisons post-hoc with a manual Benjamini-Hochberg correction

MAPK cascade proteins were also regularly seen to have differential expression in Tables 6, 7, 8, and 9. Looking closer at the MAPK genes available on the gene array revealed a largely similar profile of expression across most of the MAPK genes. ERK1/2 and JNK MAPKs (Supplementary Figures 11 and 12 respectively) show their lowest expression in the 'V-only' stimulations and all but MAPK3 and MAPK9 have the highest expression in 'LPS only' when comparing the three stimulated groups. The p38 MAPKs however have a more diverse expression profile. Figure 38 reveals that MAPK11 has its highest expression under 'V-only' conditions and, when stimulated with both V-antigen and LPS, the expression of MAPK11 is actively suppressed – 2-fold and 3-fold lower when compared to 'LPS only' and 'V only' respectively. MAPK12 resembles the expression profiles of ERK1/JNK more closely, however the combination of V-antigen and LPS gave a significantly higher expression than LPS alone, despite the very low expression levels seen in 'V-only'.

Figure 38:

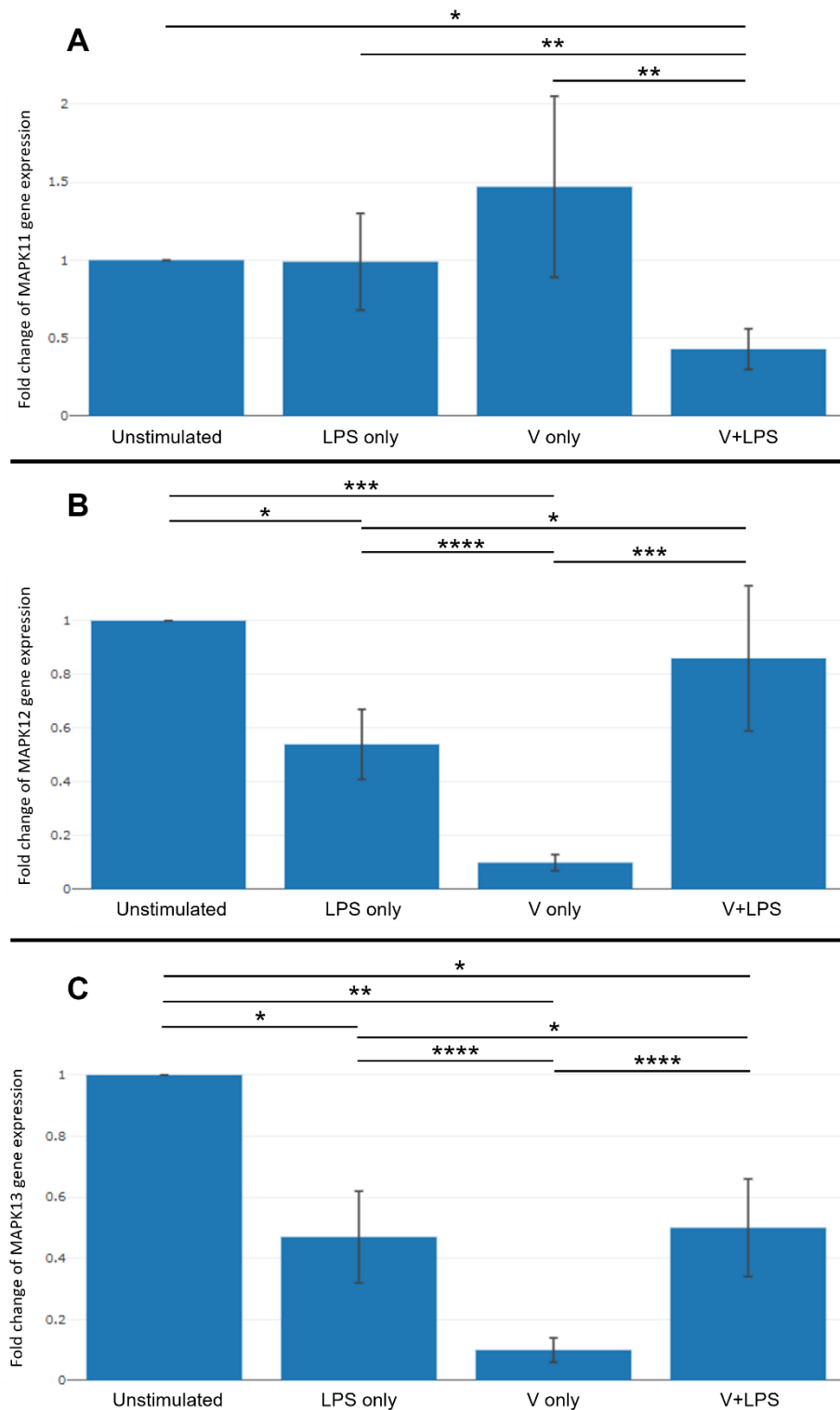


Figure 38 – MAPK11, MAPK12, and MAPK13 gene expression under stimulation with combinations of LPS and V-antigen – PBMDMs from 4 separate donors were set up according to the experimental design in Figure 15 with PBMDMs pre-incubated with/without 50µg V-antigen and then stimulated with/without 100ng/ml LPS for 16hr. The cells were then lysed, and the RNA was extracted for qPCR analysis using the Qiagen RT² profiler - Human Inflammasome gene array plate. Using the Qiagen Geneglobe analysis software, the average expression of A; MAPK11, B; MAPK12, and C; MAPK13, was evaluated across all four conditions and displayed as a fold-change from the unstimulated control. Data is presented with standard error bars and indicators for statistical significance(* = <0.05, ** = <0.01, *** = <0.001, **** = <0.0001) as determined by Student's T-test adjusted for multiple comparisons post-hoc with a manual Benjamini-Hochberg correction

A clear change in MAPK profile - as shown by MAPK11 (Figure 38A) - is indicative of a change in the type of response within LPS-stimulated cells in the presence of V-antigen. This conclusion is supported by the upregulation of classical viral response genes like IRF1 (Figure 37), IFN γ (Figure 33A), IFN β (Figure 33B), IL-12B (Figure 33C), and AIM2 (Figure 36A) as well as the downregulation of classical bacterial response genes like IL-1 β (Figure 34A), IL-6 (Figure 34B), IL-18 (Figure 34C), and NF κ B (Supplementary Figure 10).

4.3: Discussion:

4.3.1: Inhibition of IL-1 β by V-antigen does not appear to affect secretion or maturation

V-antigen begins to internalise within 4hr (3.2.4) and, while other cytokines appeared to show reduced expression under V-antigen co-stimulation within 1hr (3.2.5.2), the cytokine data in 3.2.5.1 and 3.2.5.2 showed that IL-1 β only appeared to show signs of altered secretion at around 6hr. This correlated with the IL-1 β /pro-IL-1 β western blots in Figure 24. The 4hr IL-1 β /pro-IL-1 β western blot showed that inflammatory signalling in response to LPS and 50 μ g V-antigen was at a level above the 'LPS only' control and comparable, or even slightly above, other V-antigen concentrations '+ LPS'. However, at 6hr the level of pro-IL-1 β drastically decreases compared to the other V-antigen concentrations with LPS and the 'LPS only' control and this continues to be the case at the 12hr mark. IL-1 β appeared to show the same clearly visible reduction at 12hr though was not easily identifiable at 6hr. This timing corresponds with the reduced level of secreted IL-1 β detected in Chapter 3; 6-12hr. The reduction of intracellular IL-1 β at these times also suggested that the reduced IL-1 β secretion seen in Chapter 3 was not caused by a blockage in secretion and lie, instead upstream.

There was however no clear inhibition of caspase 1 cleavage (Figure 25). Similar levels of the p20 band of processed caspase 1 appeared to be visible across all stimulated conditions however the expression level was low, and no conclusion could be drawn. The antibody used in the western blot also targeted the p20 region within uncleaved caspase 1 however, due to the nature of multiple isoforms of caspase 1(196) and the risk of interpreting non-specific bands as isoforms, an analysis about the expression levels of different pro-caspase 1 isoforms was not undertaken. Regardless, the drop in pro-IL-1 β seen in Figure 24 appeared to be more indicative of increased degradation of pro-IL-1 β or altered expression of the pro-IL-1 β gene rather than pro-IL-1 β maturation.

4.3.2: V-antigen has a wide effect on the transcriptomic profile of inflammasome-related genes under LPS stimulation

Previous studies have already reported a reduced inflammatory response to LPS in the presence of V-antigen(134) and some studies have also reported changes in the cytokine profile through increased expression of IL-10(147-149, 197) or altered expression of TNF α (130, 149, 153). However, outside of this, the inflammatory response had not been

examined in this level of detail before this study. As discussed in Chapter 3, the changes in cytokine secretion are more complex than simply a systematic reduction of inflammatory cytokines and, as such, 4.2.2 reveals a more complex expression profile too.

The expression of the cytokine genes themselves, with the exception of TNF α , matched with the secretion seen in 3.2.5, corroborating both sets of results further but the gene array in 4.2.2 also included cytokines that weren't examined in the previous chapter. Figure 33 revealed the upregulation of other IFN-related cytokines such as IFN β and IL-12B(198). IL-12B was strongly upregulated in the presence of V-antigen (Figure 33C) though unfortunately, due to undetected reads in some conditions, it was impossible to draw a conclusion for IL-12A expression (data not shown). The increased IFN β expression was of particular interest though due to its strong association with anti-viral responses and, although IFN- β is also upregulated during bacterial challenge(199), its upregulation here occurred despite other classical bacterial inflammatory cytokines being downregulated (Figure 34). Taken in collaboration with the increased expression of IRF1 (Figure 37) and IFN γ (Figure 33A), it appears that the inflammatory profile of the cell shifts to a more viral-like response as was suggested by the STRING functional cluster analysis in Figure 31. The increase in paracrine/autocrine signalling of antiviral cytokines like IFNs and the decrease in signalling from classical bacterial cytokines is likely what gave rise to the majority of the changes in expression seen in 4.2.2, including the upregulation of the antiviral inflammasome AIM2 (Figure 36A) and those genes indicated in the viral-response cluster in Figure 31.

It is not possible to disentangle the effects of altered autocrine/paracrine signalling with any specific effects of V-antigen from the data in 4.2.2 alone. However, there is evidence within the data of transcriptional differences that are not explained by cytokine signalling alone. This includes the change in MAPK expression (Figure 38, Supplementary Figures 11 and 12). As explained in 1.1.2.2, MAPKs act as a signal amplification pathway and will activate in particular combinations and to different degrees based upon the stimuli and its strength. Their gene regulation is highly complex due to their connection to a large number of diverse pathways(200) and, as such, fair evaluation of the source of the altered expression is far beyond the scope of this gene array. It is however possible to acknowledge that p38 expression (Figure 38) does differ compared to other MAPKs, not in the sense of a diminished reaction when compared to LPS, but with a clearly altered expression profile. In this family of MAPKs, V-antigen alone clearly has a marked effect on MAPK expression with very low transcription of MAPK12 and MAPK13 (Figures 38B and 38C) and an increased upregulation of MAPK11 (Figure 38A) over LPS only (non-significant, $p=0.055$) V+LPS (significant) stimulations. All other MAPKs, including ERK1/2 (Supplementary Figure 11) and JNK MAPKs (Supplementary Figure 12) show minimal expression under V-antigen

stimulation alone and an expression profile over the various conditions similar to MAPK12 and MAPK13.

Another set of interesting transcriptional changes brought about by V-antigen were the increased expression of NLR Family Apoptosis Inhibitory Protein (NAIP) (Table 6) and the decreased expression of NLRC4 (Figure 36B). These were of particular note as NAIP is an adaptor protein responsible for interacting with T3SS needle tip proteins like V-antigen and triggering the assembly of the NLRC4 inflammasome(201). In the presence of V-antigen therefore, the upregulation of NAIP (Table 8) was not unexpected. However, as shown in Supplementary Table 1, the upregulation was only in the comparison between 'V+LPS' and 'LPS only' and that the expression of NAIP was minimal under 'V-only' conditions. NLRC4 however was downregulated in the presence of V-antigen both in the presence and absence of LPS (Figure 36B). This is despite the theoretical presumption that it should upregulate and form an active inflammasome in the presence of V-antigen. The only associated transcription factor for NLRC4 is p53(202). Recent evidence has also emerged that type I IFNs inhibit the NLRC4 inflammasome within macrophages though the mechanism is not yet known – whether it is a functional inhibition, inhibition of associated proteins, or transcriptional repression(203). As shown in Chapter 3 and with the gene array data, V-antigen-containing samples have high levels of type I IFNs and so this may be one, if not the, cause of NLRC4 inflammasome inhibition in this case.

There is also the matter of genes of interest that can only be partly analysed due to current knowledge. For example, NLRP12, a gene identified as upregulated by V-antigen during LPS stimulation is known to be an inhibitor of NFκB and of ERK activation (of which MAPK1 appears inhibited (Supplementary Figure 9A)) and also acts as a negative regulator of NOD2 and promotes bacterial tolerance(204, 205). However, there is no current information about the regulation of the NLRP12 gene and so it is unclear whether the regulatory changes are due to the cytokine signalling or whether it is evidence of V-antigen's direct effects.

Therefore, though much of the gene array data confirms and expands the evidence that the inflammatory environment has shifted, it is now clear that the elevated IFN γ response discussed in Chapter 3 was only a part of the change from a classical bacterial response to a more viral response. In addition, the changes to MAPK11 and NLRC4 expression – which both cannot be fully explained by the shift in cytokine profile – offer some potential for future examination as to the mechanism of V-antigen's immunomodulatory effects.

5: Chapter 5: V-antigen and the TLR pathway

5.1: Introduction

5.1.1: Chapter introduction

Continuing from Chapter 4, this chapter focuses on the same stimulations performed on both MM6 and PBMDMs in the previous chapters and the investigation into the IL-1 β pathway. Following on from the conclusions of Chapter 4, V-antigen's mechanism of action is explored further by investigating the TLR signalling pathway to attempt to identify anomalous areas which may explain the reduced level of IL-1 β and other proinflammatory cytokines seen within the V-antigen- and LPS-stimulated samples in Chapter 3.

5.1.2: TLR4 signalling pathway

The TLR4 pathway is triggered by a number of different pathogen stimuli including LPS(206), respiratory syncytial virus fusion protein(207), mouse mammary tumour virus envelope protein(208), and dengue virus Non-structural Protein 1 (NS1)(209). However, in relation to this study, the LPS-TLR4 interaction is the most relevant. LPS binding to TLR4 is mediated by a series of proteins that interact and pass LPS to the TLR4 receptor(210) as shown in Figure 39. CD14 acts not only as a coreceptor for TLR4 surface signalling but it also promotes the endocytosis of activated TLR4 which is necessary for activation of the TRIF pathway(211). LPS-TLR4 binding then triggers TLR4 oligomerization(212) and the recruitment of scaffolding proteins like TIRAP to begin subsequent downstream signalling through the cascade shown in Figure 2 (Chapter 1).

Figure 39:

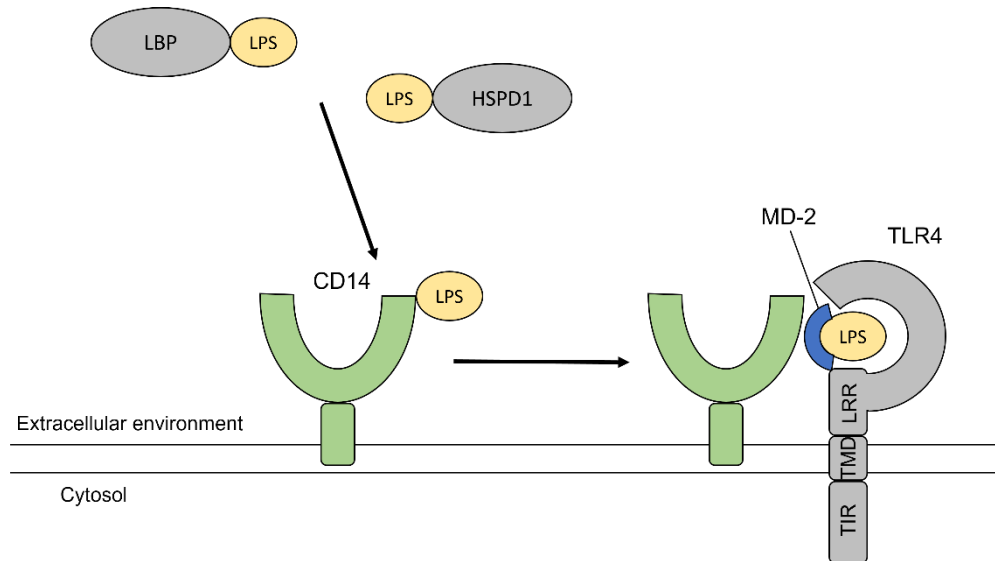


Figure 39 - TLR4-LPS binding process - LPS is endogenously bound by Lipopolysaccharide Binding Protein (LBP) or Heat Shock Protein 60 (HSPD1) before being transferred to CD14 at the surface membrane of receptive cells. CD14 brings LPS into close association with TLR4 and Myeloid Differentiation Protein 2 (MD-2) which forms a tripartite receptor for LPS that triggers downstream signalling.

TIR, Toll/IL-1 receptor; TMD, transmembrane domain; LRR, leucine-rich repeat

Unlike other TLRs, TLR4 utilises both the TRIF and MyD88 pathways in signal transduction likely due to its capability to detect both bacterial and viral stimuli.

5.1.3: Transcription of TLR4-response genes

One of the main goals of PRRs is the transcriptional upregulation of response genes specific to the stimuli that triggers them. As TLR4 detects both viral and bacterial PAMPs and utilises both the MyD88 and TRIF pathways in signal transduction(213, 214), TLR4 stimulation leads to the upregulation of genes linked to both a bacterial response, such as IL-6, IL-1 β (215), and TNF α (216), and a viral response, such as IFN α and IFN β . This is in addition to the upregulation of costimulatory molecules(217) and cell-type-specific genes that are linked to the changes in effector function/morphology. In monocytes and macrophages, this is an increase in phagocytosis(218) and oxidative burst(219). In resident macrophages, this is a heavy production of chemokines(220). In DCs, this is maturation and migration to the draining lymph nodes(221). The control of these genes is managed by regulated TFs that act cooperatively to express the appropriate levels of each gene in response to each specific stimulus. These TFs are: Specificity Protein 1 (Sp1), Activating Protein-1 (AP1), NF κ B, IRF3, IRF5, and IRF7.

Sp1 is a constitutively expressed, ubiquitous TF key for the expression of a number of housekeeping genes(222). Although it is involved in the expression of TLR-response genes, it is not regulated by the pathway for this reason.

AP1 is a family of TFs activated via the MAPK pathways which are triggered by both the MyD88 and TRIF pathways via TRAF6. Both JNK and p38 families of MAPKs are directly triggered by TRAF6, however ERK1/2 is instead regulated via the activity of its Mitogen Activated Protein Kinase Kinase Kinase (MAPKKK); Tumour Progression Locus 2 (TPL2), which is itself regulated by NFκB p105 interaction(14).

NFκB is the archetypal TF for the inflammatory pathway and is one of the key factors in promoting inflammation and survival(154). Constitutively expressed at a considerable level, NFκB is bound by an inhibitory protein; IκBα. Phosphorylation of this inhibitory protein, triggered by MyD88 pathway activation, releases NFκB to translocate to the nucleus and bind to DNA. NFκB then drives the transcription of cytokines and other inflammatory genes as well as the transcription of IκBα(223) ensuring that NFκB activity only continues until upstream signalling stops. NFκB also has a role in the transcription of viral genes like IFNβ which is best expressed with both NFκB and IRF3 acting cooperatively at the promoter site(224). The TRIF pathway therefore has mechanisms to activate NFκB, to a lesser extent than the MyD88 pathway, to allow for the effective transcription of antiviral genes. This occurs through TRIF's interactions with TRAF6 and also with a complex containing Tumour Necrosis Factor Receptor Type 1-associated DEATH Domain Protein (TRADD) and RIP-1 which cleaves caspase 8 and caspase 10 and these subsequently activate the NFκB pathway(5, 225, 226).

IRF3, as the main TF for the TRIF pathway, promotes inflammatory genes much like NFκB but largely genes linking to antiviral responses like IFNs, polyamine production, and type II MHC molecules(227, 228). IRF3 expression is constitutive and its activity is regulated by specific kinases and phosphatases. The constitutive expression allows IRF3 activity to occur quickly after stimulation to drive rapid IFN production. Produced IFNβ then triggers the induction of a complex involving STAT1, STAT2, and IRF9 which activates IRF7(229).

IRF7 also promotes the expression of IFNα/β and so generates a positive feedback loop that drives heavy IFN production(230). IRF7 can also be activated by interaction with MyD88(231).

Finally, IRF5 has been shown to act cooperatively in promoting the expression of proinflammatory cytokines alongside NFκB and is activated by its interaction with MyD88 and TRAF6(232). A deficiency in IRF5 showed a reduced level of TNFα, IL-6, and IL-12 upon stimulation(233).

5.1.4: Chapter aims:

In this chapter, the aims are:

- To investigate the effects of V-antigen on the TLR pathway using western blotting techniques and qPCR gene array
- To attempt to uncover evidence of the causal mechanism of action for V-antigen immunomodulatory effects and inhibition on inflammatory cytokine secretion

5.2: Results

5.2.1: V-antigen's effects on NFκB activation

Chapter 4 concluded that the effects of V-antigen on the IL-1β pathway were likely linked to either the expression of, or increased degradation of, pro-IL-1β. This was due to the evidence shown in Figure 24 (Chapter 4) which showed a reduced intracellular quantity of pro-IL-1β as well as mature IL-1β. To determine which mechanism was the source of the reduced level of pro-IL-1β, a western blot was performed on the lysates from the MM6 stimulations from 3.2.5.1. The loadings were kept consistent with those in 4.2.1 which had been normalised around β2M expression.

Figure 40, shows a western blot, run in denaturing, reducing conditions and probed for phosphorylated IκBα (pIκBα). This was used as an indirect measurement of NFκB activity. IκBα binds NFκB (Figure 2) and, when phosphorylated, releases it to allow NFκB to re-localise to the nucleus and promote transcription (5.1.3). Therefore, the higher the level of pIκBα, the higher the level of free, transcriptionally active NFκB there is expected to be.

Though less visually obvious than the IL-1β western blots (Figure 24, Chapter 4), using the Odyssey in-programme densitometry measurement tool, it was determined that the levels of pIκBα dropped slightly at 6hr in the 50µg V-antigen + LPS sample and at 12hr, the level of IκBα and pIκBα were both reduced. Table 10 shows the densitometry values for the 6hr and 12hr IκBα and pIκBα bands – both at their current density normalised around β2M and when normalised around GAPDH expression.

Figure 40:

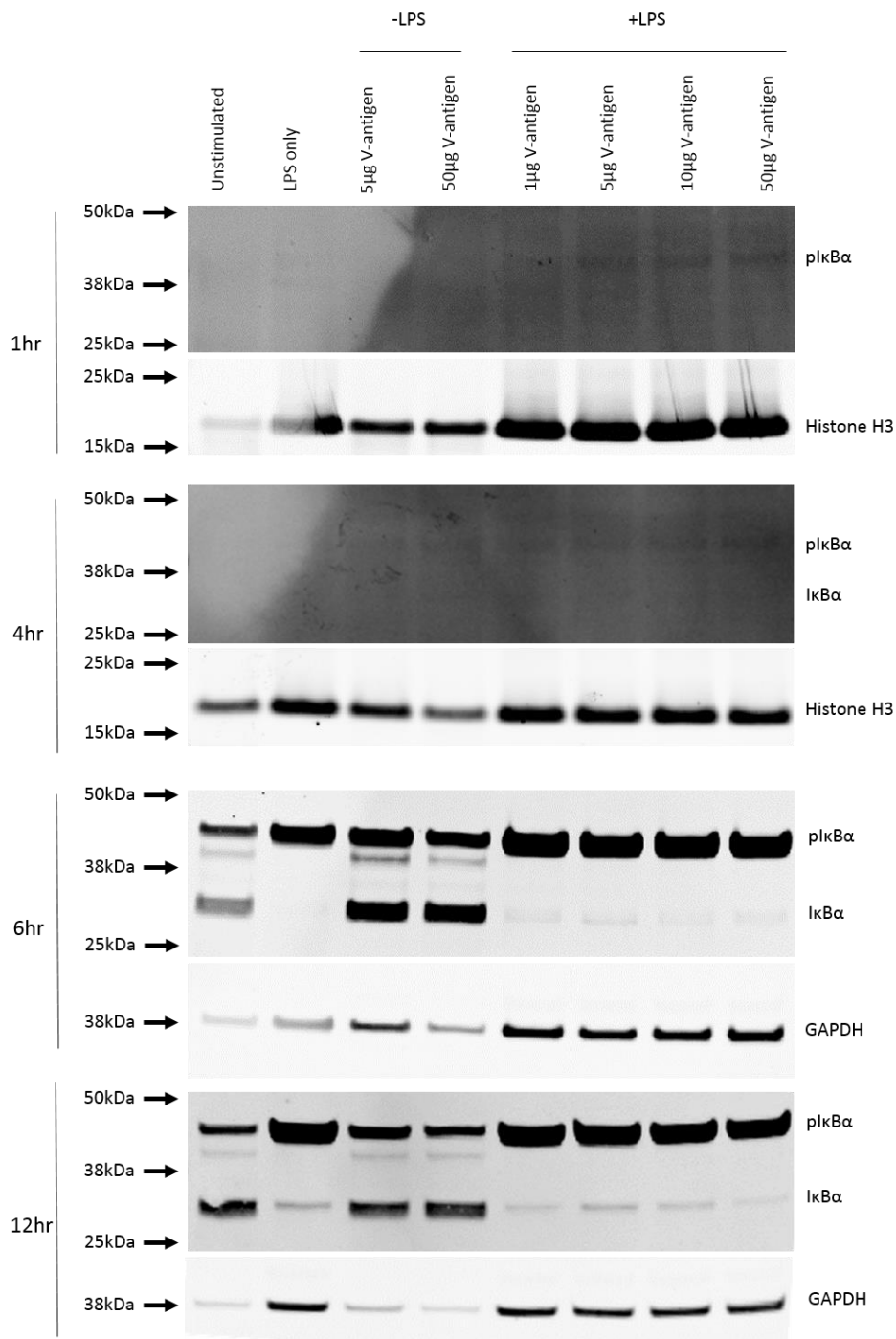


Figure 40 - IκBα western blots on LPS/V-antigen-stimulated MM6 cells – Mono-mac 6 (MM6) cells were seeded at a density of 5×10^4 cells/well on 24 well plates and allowed to attach overnight. After a 30min pre-incubation with various concentrations of V-antigen (0μg, 1μg, 5μg, 10μg, 50μg), LPS was added to a final concentration of 100ng/ml or not added at all. After a specified incubation time from the point of LPS addition (or non-addition), the cells were lysed in 2x sample buffer (Appendix A). An SDS-PAGE was run in denaturing, reducing conditions using loading quantities determined by β2M expression (western blot not shown), before being transferred to a nitrocellulose membrane and probed with anti-GAPDH antibody (abcam ab8245) and pIkBα(S32) (Invitrogen 701271) (6hr/12hr) or anti-histone H3 (abcam ab1791) and pIkBα(S32/S36) (1hr/4hr) and then anti-mouse-680 (LiCor 926-68022) and anti-rabbit-800 (LiCor 926-32213) (6hr/12hr) or anti-rabbit-680 (LiCor 926-68073) and anti-mouse-800 (LiCor 926-32212) (1hr/4hr). The resulting blot was then imaged using a LiCor Odyssey fluorescent imaging system where it showed a reduced level of pIkBα and IκBα under 6hr and 12hr '50μg V-antigen + 100ng/ml LPS' stimulation compared with other quantities of V-antigen and LPS.

GAPDH, glyceraldehyde 3-phosphate dehydrogenase; pIkBα, inhibitor of nuclear factor kappa-light-chain-enhancer of activated B cells α(phosphorylated); IκBα, inhibitor of nuclear factor kappa-light-chain-enhancer of activated B cells α

Table 10 - Densitometry of western blots probed for pIkBa/IkBa/GAPDH after 6hr and 12hr LPS+V-antigen stimulation

Sample	6hr				12hr			
	1µg V +LPS	5µg V +LPS	10µg V +LPS	50µg V +LPS	1µg V +LPS	5µg V +LPS	10µg V +LPS	50µg V +LPS
pIkBa	197.13	176.85	185.41	167.89	86.64	83.67	85.52	67.71
IkBa	0.50	0.56	0.28	0.34	0.39	0.65	0.41	0.16
GAPDH	31.69	24.81	27.72	28.88	14.17	12.49	12.75	12.11
Adjusted pIkBa	154.33	176.85	165.95	144.23	74.04	81.12	81.22	67.71
Adjusted IkBa	0.39	0.56	0.25	0.28	0.33	0.63	0.39	0.16
Adjusted GAPDH	24.81	24.81	24.81	24.81	12.11	12.11	12.11	12.11

Mono-mac 6 (MM6) cells were seeded at a density of 5x10⁴ cells/well on 24 well plates and allowed to attach overnight. After a 30min pre-incubation with various concentrations of V-antigen (0µg, 1µg, 5µg, 10µg, 50µg), LPS was added to a final concentration of 100ng/ml or not added at all. After a specified incubation time from the point of LPS addition (or non-addition), the cells were lysed in 2x sample buffer (Appendix A). An SDS-PAGE was run in denaturing, reducing conditions using loading quantities determined by β2M expression (western blot not shown), before being transferred to a nitrocellulose membrane and probed with anti-GAPDH antibody (abcam ab8245) and pIkBa(S32) (Invitrogen 701271). This blot is shown in Figure 40. Densitometry analysis on the resulting western blot bands for pIkBa, IkBa, and GAPDH for the 6hr and 12hr stimulations was performed using the Odyssey in-programme densitometry tool. An additional adjustment to the values was also made to normalise the densitometry around GAPDH expression for each timepoint to provide an additional normalised expression for additional robustness (adjusted values)

GAPDH, glyceraldehyde 3-phosphate dehydrogenase; pIkBa, inhibitor of nuclear factor kappa-light-chain-enhancer of activated B cells α(phosphorylated); IkBa, inhibitor of nuclear factor kappa-light-chain-enhancer of activated B cells α

The reduction of phosphorylated IkBa within the '50µg V-antigen + LPS' sample signified a reduction at, or upstream of, IkBa phosphorylation. The reduction in IkBa at 12hr was likely due to reduced transcription of the IkBa gene as a result of lower NFκB activation as seen from the reduced level of pIkBa at the 6hr mark. The reduced expression of pro-IL-1β /IL-1β (Figure 24) therefore appeared to be the result of inhibited signalling within the TLR pathway.

5.2.2: TLR pathway qPCR gene array

5.2.2.1: Gene cluster analysis

To investigate the transcription of a wide scope of the components and products of the TLR pathway, a Qiagen RT² profiler gene array specific for the human TLR pathway was used. The Human TLR Pathway Qiagen RT² profiler gene array kit, much like the Human Inflammasome gene array in 4.2.2, contained a 384-well plate which consisted of 4 copies of primers specific for 84 genes connected to the human TLR pathway as well as house-keeping genes to normalise the datasets, and quality/contamination controls to ensure the validity of the qPCR results. The gene list consisted of transcribed targets of the TLR pathway TFs as well as members and transcribed targets of the IFN γ pathway and TNF α pathway. A diagram of the pathways and their connections to the TLR pathway are shown in Figure 41. A full list of the target genes in the Qiagen RT² profiler gene array – human TLR pathway is shown in Table 11.

Table 11 - Gene list for Human TLR Pathway Qiagen RT² Profiler gene array

<i>BTK</i>	<i>CASP8</i>	<i>CCL2</i>	<i>CD14</i>
<i>CD180</i>	<i>CD80</i>	<i>CD86</i>	<i>CHUK</i>
<i>CLEC4E</i>	<i>CSF2</i>	<i>CSF3</i>	<i>CXCL10</i>
<i>ECSIT</i>	<i>EIFAK2</i>	<i>ELK1</i>	<i>FADD</i>
<i>FOS</i>	<i>HMGB1</i>	<i>HRAS</i>	<i>HSPA1A</i>
<i>HSPD1</i>	<i>IFNA1</i>	<i>IFNB1</i>	<i>IFNG</i>
<i>IKBKB</i>	<i>IL10</i>	<i>IL12A</i>	<i>IL1A</i>
<i>IL1B</i>	<i>IL2</i>	<i>IL6</i>	<i>CXCL8</i>
<i>IRAK1</i>	<i>IRAK2</i>	<i>IRAK4</i>	<i>IRF1</i>
<i>IRF3</i>	<i>JUN</i>	<i>LTA</i>	<i>LY86</i>
<i>LY96</i>	<i>MAP2K3</i>	<i>MAP2K4</i>	<i>MAP3K1</i>
<i>MAP3K7</i>	<i>MAP4K4</i>	<i>MAPK8</i>	<i>MAPK8IP3</i>
<i>MYD88</i>	<i>NFKB1</i>	<i>NFKB2</i>	<i>NFKBIA</i>
<i>NFKBIL1</i>	<i>NFRKB</i>	<i>NR2C2</i>	<i>PELI1</i>
<i>PPARA</i>	<i>PRKRA</i>	<i>PTGS2</i>	<i>REL</i>
<i>RELA</i>	<i>RIPK2</i>	<i>SARM1</i>	<i>SIGIRR</i>
<i>TAB1</i>	<i>TBK1</i>	<i>TICAM1</i>	<i>TICAM2</i>
<i>TIRAP</i>	<i>TLR1</i>	<i>TLR10</i>	<i>TLR2</i>
<i>TLR3</i>	<i>TLR4</i>	<i>TLR5</i>	<i>TLR6</i>
<i>TLR7</i>	<i>TLR8</i>	<i>TLR9</i>	<i>TNF</i>
<i>TNFSF1A</i>	<i>TOLLIP</i>	<i>TRAF6</i>	<i>UBE2N</i>

Figure 41:

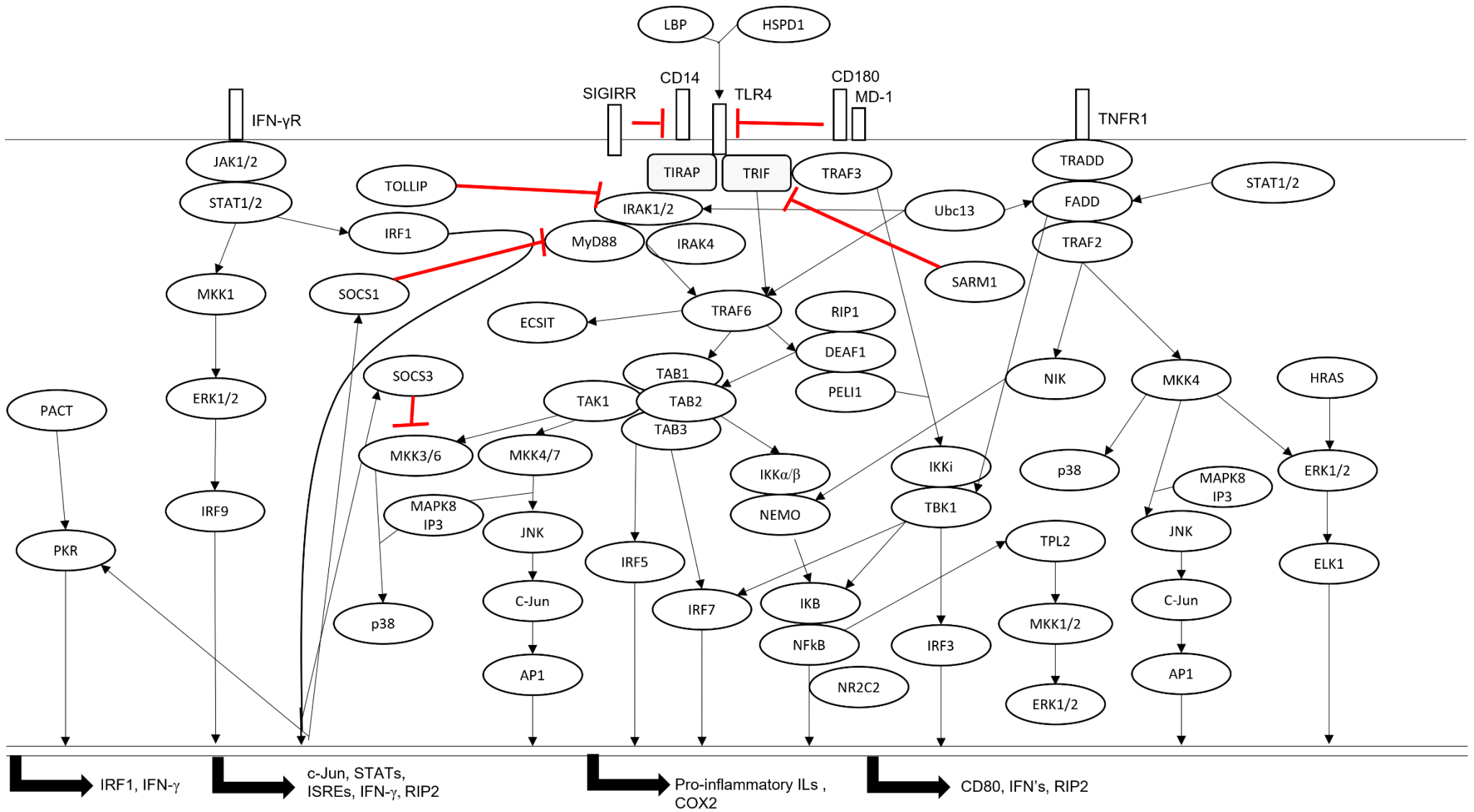


Figure 41 - TLR/TNF α /IFN γ pathways – A representation of the interconnected pathways represented by genes on the Human TLR Pathway Qiagen RT² profiler gene array and examples of the gene products they promote.

IFN γ R, interferon γ receptor; JAK1/2, janus kinase 1/2; STAT1/2, signal transducer and activator of transcription 1/2; PKR, protein kinase R; PACT, protein activator of interferon protein kinase EIF2AK2; ISREs, interferon stimulated response elements; RIPK2, ;COX2, cyclooxygenase 2; CD14/180, cluster of differentiation 14/180; LBP, lipopolysaccharide binding protein; HSP60, heat shock protein 60; TLR, Toll-like receptor; TIRAP, TIR-domain-containing adaptor protein; TRIF, TIR-domain-containing adaptor-inducing interferon- β ; TRAF2/3/6, tumour necrosis factor receptor-associated factor2/ 3/6; IRAK1/4, IL-1 receptor-associated kinase 1/4; MyD88, myeloid differentiation primary response protein 88; ECSIT, evolutionarily conserved signalling intermediate in Toll pathway, mitochondrial; RIP1, receptor-interacting serine/threonine-protein kinase 1; DEAF1, deformed epithelial autoregulatory factor-1; PELI1, pellino E3 ubiquitin protein ligase 1; TAK1, TGF β -activated kinase 1; TAB1/2/3, TGF β -activated kinase 1 binding protein 1/2/3; MKK1/2/3/4/6/7, Mitogen activated protein kinase kinase 1/2/3/4/6/7; JNK, c-Jun N-terminal kinase; AP1, activating protein-1; IRF1/3/5/7/9, interferon regulatory factor 1/3/5/7/9; IKK α / β /i, Inhibitor of kappa kinase α / β /i; NEMO, nuclear factor κ B essential modulator; TBK1, TANK binding kinase; TPL2, tumour progression locus 2; IKB, inhibitor of nuclear factor kappa-light-chain-enhancer of activated B cells; NF κ B, nuclear factor kappa-light-chain-enhancer of activated B cells; NR2C2, nuclear receptor subfamily 2 group C member 2; ERK1/2, extracellular signal-regulated kinase 1/2; TOLLIP, Toll-interacting protein; SOCS1/3, suppressor of cell signalling 1/3; SIGIRR, single Ig IL-1-related receptor; MD-1, myeloid differentiation protein 1/2; Ubc13, ubiquitin-conjugating enzyme E2 N; SARM1, sterile alpha and TIR motif containing 1; TNFR1, tumour necrosis factor receptor 1/2; TRADD, tumour necrosis factor receptor type 1-associated DEATH domain protein; FADD, Fas-associated death domain protein; NIK, NF κ B-inducing kinase; ELK1, ETS-like protein 1

The plate was set-up exactly as in 4.2.2, using the same RNA from the same samples and the same equipment. The data was also analysed using the same techniques for consistency. The data for the TLR pathway plates was compiled into a single datasheet and processed through the Qiagen analysis software (2.4.1) which checked the quality control tests for PCR array reproducibility, reverse transcription effectiveness (in regard to the RT² First Strand step), and genomic DNA contamination. All samples passed these quality checks. The data was then normalised once more using β 2M expression as the reference gene. As each stimulation had four individual donors, the Geneglobe analysis software was able to perform a two-tailed student's t-test and provide p-values for each change in gene regulation. The full data, using 'unstimulated' as the control group, is provided in Supplementary Table 2 and the relative expression levels across all donors and conditions are displayed in the clustergram in Figure 42.

Figure 42:

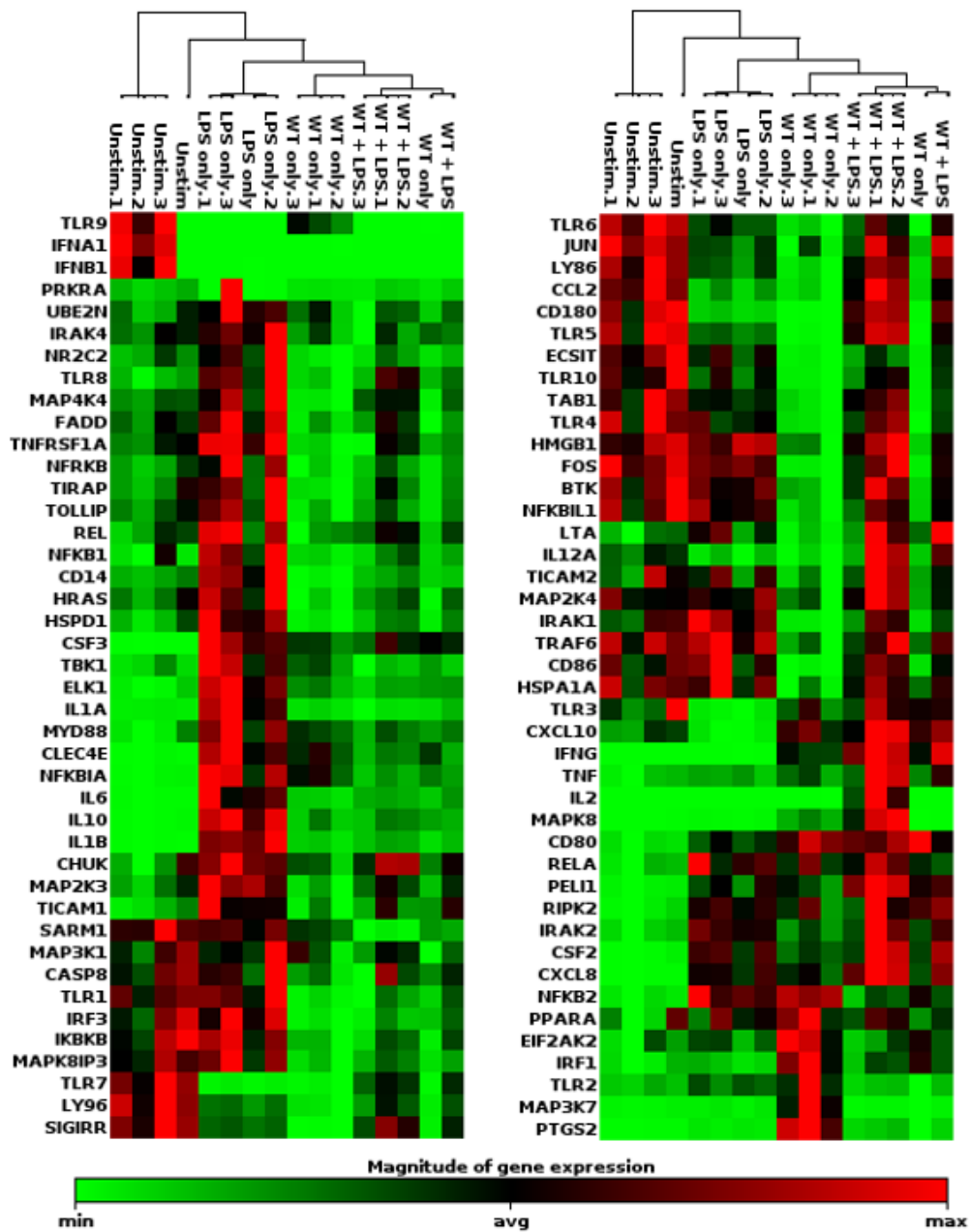


Figure 42 - Clustergram of Qiagen RT² qPCR - Human TLR pathway gene array results for WT V-antigen (+/- LPS) – PBMDMs from 4 separate donors were set up according to the experimental design in Figure 15 with PBMDMs pre-incubated with/without 50µg V-antigen and then stimulated with/without 100ng/ml LPS for 16hr. The cells were then lysed, and the RNA was extracted for qPCR analysis using the Qiagen RT² profiler - Human TLR pathway gene array plate. Using the Qiagen Geneglobe analysis software, a clustergram was generated from the resulting data showing the relative expression of each of the genes across all conditions and donors

In all comparisons, genes that were found to have a >1.5-fold change in regulation with a t-test p-value <0.05 were considered to have increased expression and genes with a <-1.5-fold change of regulation and a t-test p-value of <0.05 were considered to have decreased expression.

Initially 'LPS only' was compared to 'unstimulated' to investigate whether the donors responded as expected to LPS. The volcano plot in Figure 43 shows a clear alteration in the gene expression profile with Tables 12 and 13 presenting the genes with increased and decreased expression respectively.

Figure 43:

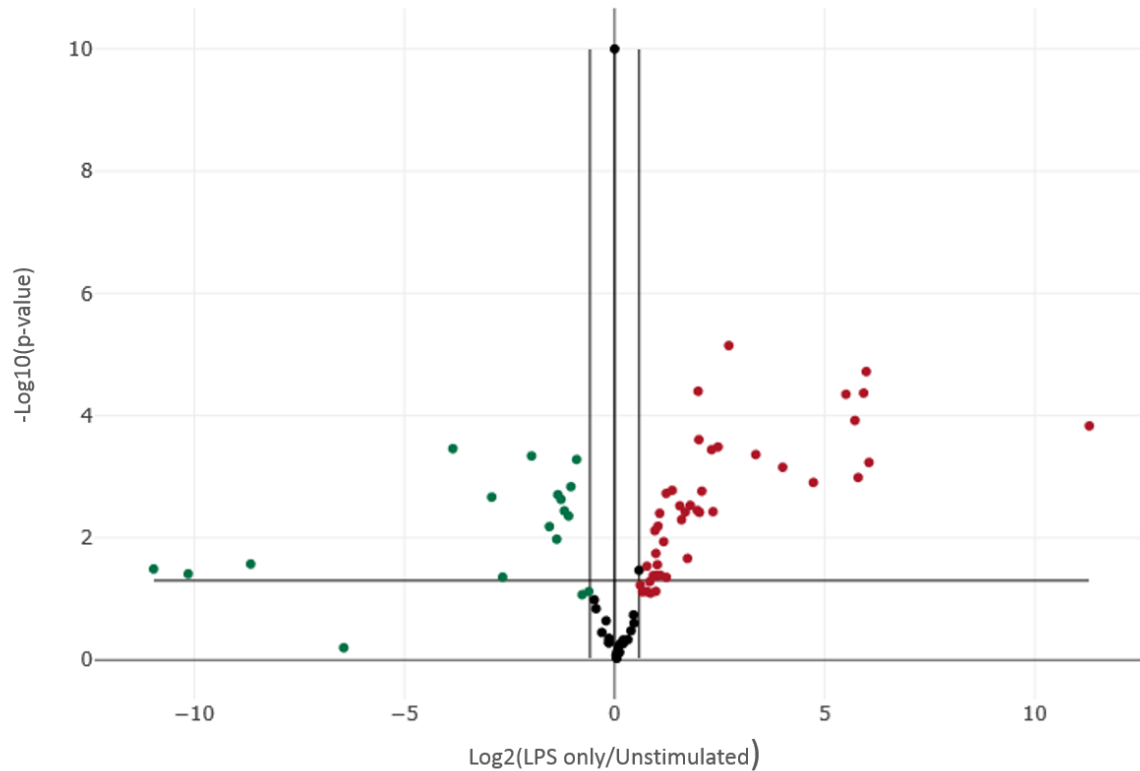


Figure 43 - Volcano plot of 'LPS only' gene expression compared to 'unstimulated' control expression – TLR pathway gene array – PBMDMs from 4 separate donors were set up according to the experimental design in Figure 15 with PBMDMs pre-incubated with/without 50 μ g V-antigen for 30min and then stimulated with/without 100ng/ml LPS for 16hr. The cells were then lysed, and the RNA was extracted for qPCR analysis using the Qiagen RT² profiler - Human Inflammasome gene array plate. Average gene expression for each gene within 100ng/ml LPS-stimulated PBMDMs (LPS only) and unstimulated control PBMDMs (unstimulated) was determined and compared using a volcano plot generated by the Qiagen Geneglobe analysis software. Genes with a >1.5-fold regulation (red) and genes <-1.5-fold regulation (green) were highlighted and the horizontal line was added to represent the p-value 0.05

Table 12 - Upregulated genes within LPS-stimulated PBMDMs – TLR pathway gene array

Gene Symbol	Fold Regulation	p-value	Comment
CD14	4.21	0.001725	
CD80	4.01	0.000248	
CHUK	2.25	0.011557	
CLEC4E	66.34	0.000584	
CSF2	52.62	0.000120	A
CSF3	2512.67	0.000147	A
ELK1	10.25	0.000433	
FADD	1.70	0.029137	
HRAS	2.02	0.027540	
HSPD1	4.05	0.003829	
IL10	60.76	0.000043	
IL1A	16.00	0.000702	A
IL1B	63.37	0.000019	
IL2	1.94	0.007633	
IL6	55.46	0.001030	A
CXCL8	45.36	0.000045	
IRAK2	3.96	0.000040	
MAP2K3	2.34	0.001874	
MAP4K4	2.12	0.040952	
MAPK8	2.93	0.002998	
MYD88	5.07	0.003730	
NFKB1	3.33	0.021705	
NFKB2	5.50	0.000326	
NFKBIA	26.51	0.001242	
NFRKB	2.35	0.044327	
NR2C2	1.99	0.041281	
PELI1	3.48	0.002939	
PTGS2	4.95	0.000360	
REL	1.99	0.042389	
RELA	3.90	0.003560	
RIPK2	6.58	0.000007	
TBK1	3.21	0.003767	
TICAM1	2.04	0.006453	
TLR2	2.59	0.001669	
TLR8	3.02	0.005053	
TNFRSF1A	2.10	0.003971	
TOLLIP	1.89	0.041407	
UBE2N	1.97	0.018004	

PBMDMs from 4 separate donors were set up according to the experimental design in Figure 15 with PBMDMs pre-incubated with/without 50µg V-antigen for 30min and then stimulated with/without 100ng/ml LPS for 16hr. The cells were then lysed, and the RNA was extracted for qPCR analysis using the Qiagen RT² profiler - Human TLR pathway gene array plate. Average gene expression for each gene within 'LPS only' and 'unstimulated' controls was compared, and a Student's T-test was performed via the Qiagen Geneglobe analysis software.

Genes upregulated by LPS (genes with >1.5-fold regulation and <0.05 p-value as determined by Student's T-test) are presented in the table above

'Comments' are: A; the gene's average threshold value is high (>30) in one group and low (<30) in the other, B; the gene's average threshold value is >30 in both samples and the p-value for the fold-change is unavailable or high ($p>0.05$), C; the gene's average threshold value is above the cut-off or undetected in all samples and so in unreliable and cannot be used

Table 13 - Downregulated genes within LPS-stimulated PBMDMs – TLR pathway gene array

Gene Symbol	Fold Regulation	p-value	Comment
CCL2	-3.94	0.000457	
CD180	-7.60	0.002154	
CXCL10	-2.93	0.006545	
IFNA1	-404.53	0.026879	A
IFNB1	-1133.09	0.038854	A
IL12A	-2.14	0.004400	
JUN	-1.87	0.000522	
LY86	-2.29	0.003612	
LY96	-2.55	0.001966	
SIGIRR	-2.42	0.002350	
TLR3	-6.34	0.043871	A
TLR5	-2.60	0.010538	
TLR6	-2.06	0.001455	
TLR7	-14.40	0.000347	
TLR9	-2005.39	0.032361	A

PBMDMs from 4 separate donors were set up according to the experimental design in Figure 15 with PBMDMs pre-incubated with/without 50 μ g V-antigen for 30min and then stimulated with/without 100ng/ml LPS for 16hr. The cells were then lysed, and the RNA was extracted for qPCR analysis using the Qiagen RT² profiler - Human TLR pathway gene array plate. Average gene expression for each gene within 'LPS only' and 'unstimulated' controls was compared, and a Student's T-test was performed via the Qiagen Geneglobe analysis software. Genes downregulated by LPS (genes with <-1.5-fold regulation and <0.05 p-value as determined by Student's T-test) are presented in the table above

'Comments' are: A; the gene's average threshold value is high (>30) in one group and low (<30) in the other, B; the gene's average threshold value is >30 in both samples and the p-value for the fold-change is unavailable or high ($p>0.05$), C; the gene's average threshold value is above the cut-off or undetected in all samples and so in unreliable and cannot be used

53 genes were identified as differentially expressed. Of these, 38 were upregulated and 15 were downregulated. Figure 44 highlights the location of these genes within the TLR/TNF α /IFN γ signalling pathways.

Figure 44:

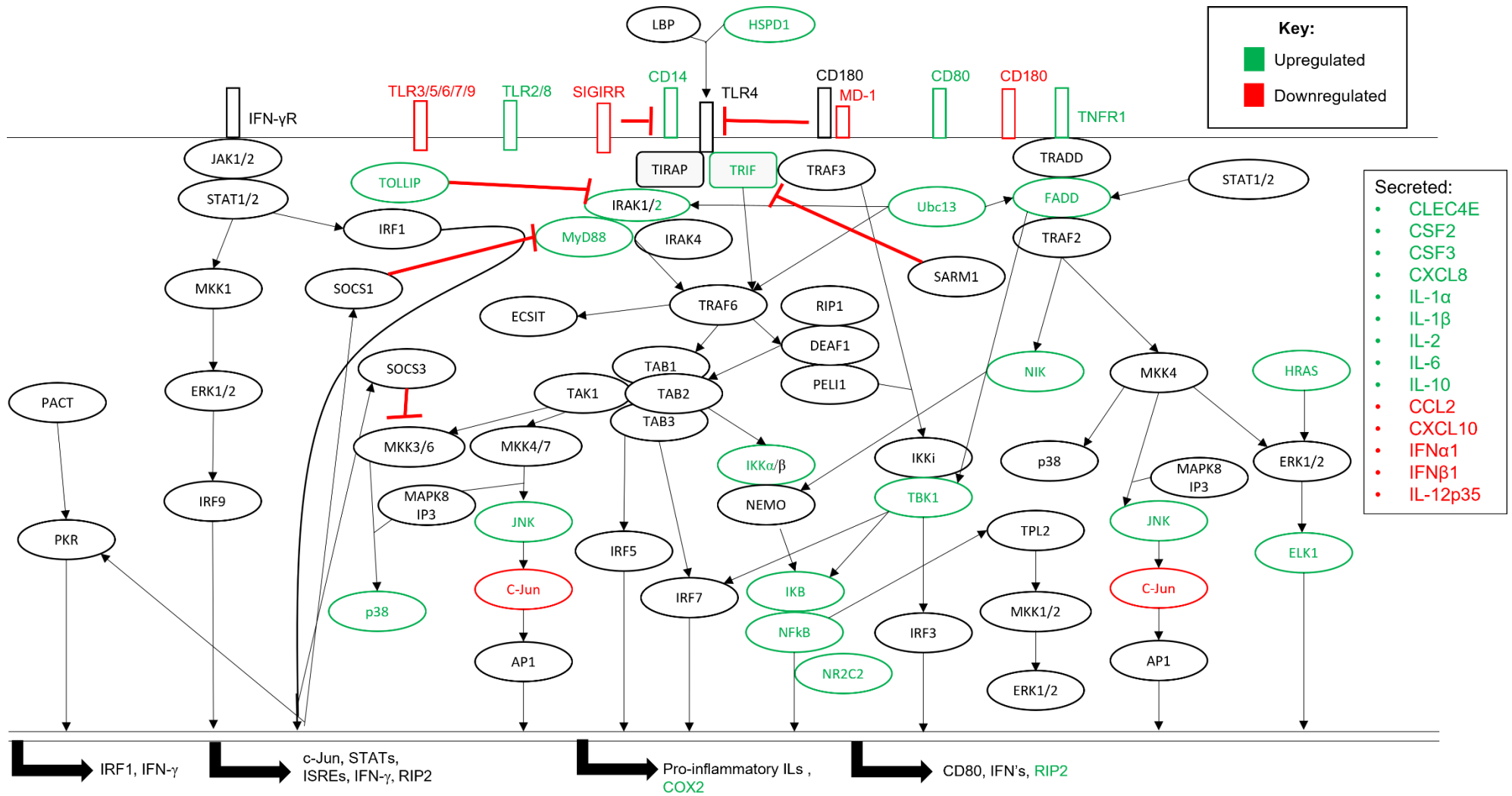


Figure 44 - Differentially expressed genes in LPS-stimulated PBMDMs – PBMDMs from 4 separate donors were set up according to the experimental design in Figure 15 with PBMDMs pre-incubated with/without 50µg V-antigen for 30min and then stimulated with/without 100ng/ml LPS for 16hr. The cells were then lysed, and the RNA was extracted for qPCR analysis using the Qiagen RT² profiler - Human TLR pathway gene array plate. Average gene expression for each gene within 'LPS only' and 'unstimulated' controls was compared, and a Student's T-test was performed via the Qiagen Geneglobe analysis software. Genes upregulated or downregulated by LPS (genes with >1.5-fold regulation or <-1.5-fold regulation respectively and <0.05 p-value as determined by Student's T-test) are presented with their location in the IFN γ /TLR/TNF α pathway

IFN γ R, interferon γ receptor; JAK1/2, janus kinase 1/2; STAT1/2, signal transducer and activator of transcription 1/2; PKR, protein kinase R; PACT, protein activator of interferon protein kinase EIF2AK2; ISREs, interferon stimulated response elements; RIPK2, ;COX2, cyclooxygenase 2; CD14/180, cluster of differentiation 14/180; LBP, lipopolysaccharide binding protein; HSP60, heat shock protein 60; TLR, Toll-like receptor; TIRAP, TIR-domain-containing adaptor protein; TRIF, TIR-domain-containing adaptor-inducing interferon- β ; TRAF2/3/6, tumour necrosis factor receptor-associated factor2/ 3/6; IRAK1/4, IL-1 receptor-associated kinase 1/4; MyD88, myeloid differentiation primary response protein 88; ECSIT, evolutionarily conserved signalling intermediate in Toll pathway, mitochondrial; RIP1, receptor-interacting serine/threonine-protein kinase 1; DEAF1, deformed epithelial autoregulatory factor-1; PELI1, pellino E3 ubiquitin protein ligase 1; TAK1, TGF β -activated kinase 1; TAB1/2/3, TGF β -activated kinase 1 binding protein 1/2/3; MKK1/2/3/4/6/7, Mitogen activated protein kinase kinase 1/2/3/4/6/7; JNK, c-Jun N-terminal kinase; AP1, activating protein-1; IRF1/3/5/7/9, interferon regulatory factor 1/3/5/7/9; IKK α / β /i, Inhibitor of kappa kinase α / β /i; NEMO, nuclear factor κ B essential modulator; TBK1, TANK binding kinase; TPL2, tumour progression locus 2; IKB, inhibitor of nuclear factor kappa-light-chain-enhancer of activated B cells; NF κ B, nuclear factor kappa-light-chain-enhancer of activated B cells; NR2C2, nuclear receptor subfamily 2 group C member 2; ERK1/2, extracellular signal-regulated kinase 1/2; TOLLIP, Toll-interacting protein; SOCS1/3, suppressor of cell signalling 1/3; SIGIRR, single Ig IL-1-related receptor; MD-1, myeloid differentiation protein 1/2; Ubc13, ubiquitin-conjugating enzyme E2 N; SARM1, sterile alpha and TIR motif containing 1; TNFR1, tumour necrosis factor receptor 1/2; TRADD, tumour necrosis factor receptor type 1-associated DEATH domain protein; FADD, Fas-associated death domain protein; NIK, NF κ B-inducing kinase; ELK1, ETS-like protein 1; CLEC4E, c-type lectin domain containing 4E; CSF2/3, colony-stimulating factor 2/3; CXCL8/10, C-X-C ligand motif 8/10; CCL2, C-C motif ligand 2; IFN, interferon; IL, interleukin

The upregulated and downregulated genes were analysed separately using the STRING protein interaction database which maps proteins into nodes based on their interactions with each other to generate figures such as those shown in Figures 45 and 46. It also lists functional clusters within the dataset and presents FDRs (akin to a p-value) for the probability that the functional cluster has been enriched within the dataset by chance alone. It also provides 'Strength' scores for each cluster ($\log_{10}(\text{expected/observed})$) to show how great the enrichment in the dataset is.

Figure 45 reveals a robust detection of functional clusters associated with the 'LPS response' and 'carbohydrate-derivative binding' with LPS receptor/detection proteins like CD14 and Heat Shock Protein 60 (HSPD1), TLR signalling proteins like Pellino E3 Ubiquitin Ligase 1 (PELI1), NF κ B, MyD88, and Interleukin 1 Receptor Associated Kinase 2 (IRAK2), cytokines like IL-1 β , IL-10, and IL-6, and MAPK proteins all showing increased expression. Figure 46 shows genes with decreased expression with highlighted functional clusters of 'regulation of LPS-mediated signalling pathway' like CD180 and Lymphocyte Antigen 86 (LY86) and 'virus response' proteins such as viral TLRs, IFNs, and CXCL10.

Figure 45:

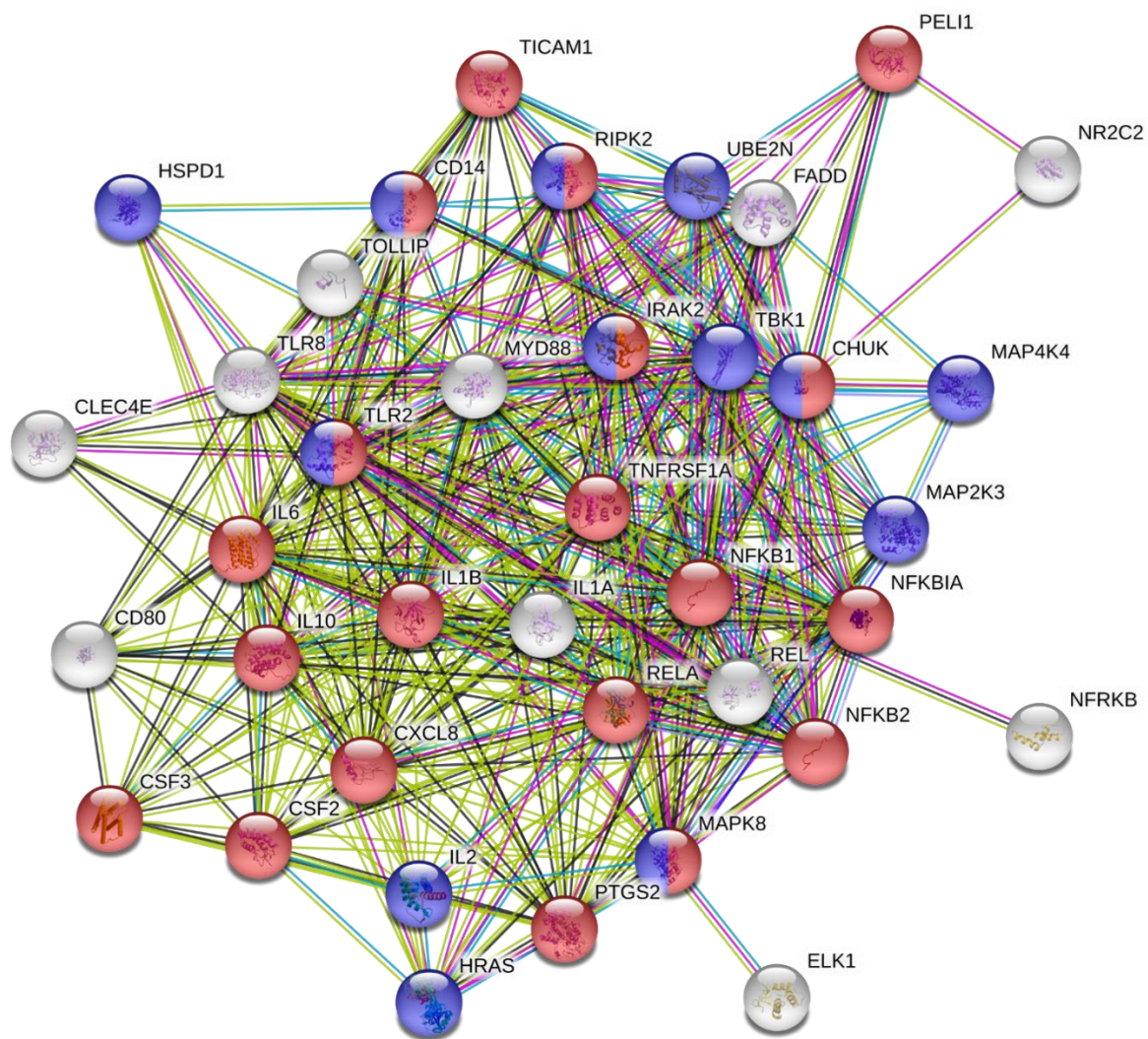


Figure 45 -STRING analysis of LPS-upregulated genes in PBMDMs – TLR pathway gene array – PBMDMs from 4 separate donors were set up according to the experimental design in Figure 15 with PBMDMs pre-incubated with/without 50µg V-antigen for 30min and then stimulated with/without 100ng/ml LPS for 16hr. The cells were then lysed, and the RNA was extracted for qPCR analysis using the Qiagen RT² profiler - Human TLR pathway gene array plate. Average gene expression for each gene within 100ng/ml LPS-stimulated PBMDMs (LPS only) and unstimulated control PBMDMs (unstimulated) was calculated and genes with an upregulated expression in 'LPS only', characterised as >1.5-fold regulation of expression and p-value <0.05 (determined by Student's T-test), were processed through the STRING protein interaction network database. Enriched functional clusters within the upregulated gene list were identified by STRING and the functional clusters of 'response to LPS' (red) (FDR = 1.78e-27, Strength = 1.58) and 'carbohydrate derivative binding' (blue) (FDR = 0.0016, Strength = 1.34) are highlighted within the full network presented above

Figure 46:

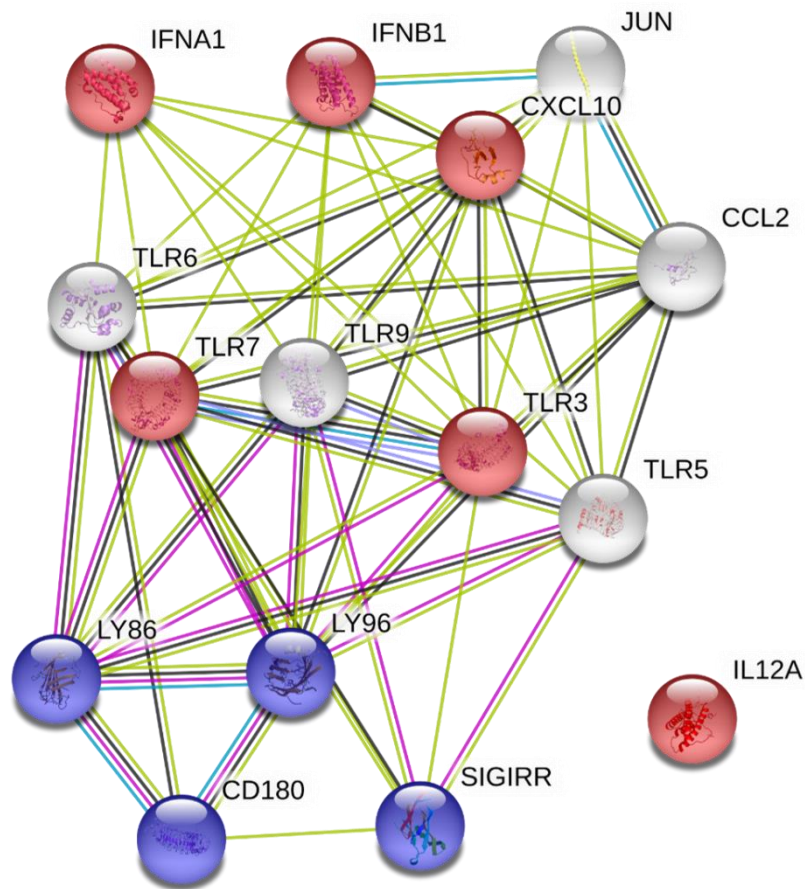


Figure 46 -STRING analysis of LPS-downregulated genes in PBMDMs – TLR pathway gene array – PBMDMs from 4 separate donors were set up according to the experimental design in Figure 15 with PBMDMs pre-incubated with/without 50 μ g V-antigen for 30min and then stimulated with/without 100ng/ml LPS for 16hr. The cells were then lysed, and the RNA was extracted for qPCR analysis using the Qiagen RT² profiler - Human TLR pathway gene array plate. Average gene expression for each gene within 100ng/ml LPS-stimulated PBMDMs (LPS only) and unstimulated control PBMDMs (unstimulated) was calculated and genes with a downregulated expression in 'LPS only', characterised as <-1.5-fold regulation of expression and p-value <0.05 (determined by Student's T-test), were processed through the STRING protein interaction network database. Enriched functional clusters within the downregulated gene list were identified by STRING and the functional clusters of 'response to virus' (red) (FDR = 4.74e-07, Strength = 1.49) and 'regulation of LPS-mediated signalling pathway' (blue) (FDR = 2.35e-06, Strength = 2.3) are highlighted within the full network presented above

The altered expression from LPS stimulation correlated with what would be expected of LPS-stimulated PBMDMs with upregulated functional clusters of 'response to LPS' and 'carbohydrate derivative binding' being highlighted with a low FDR and high strength values. This, along with the additional data of the cytokine response in 3.2.5.2 and the Human Inflammasome Qiagen RT² profiler gene array in 4.2.2, confirmed that the cells were responding appropriately.

Next, 'V+LPS' was compared to 'LPS only'. The volcano plot shown in Figure 47, which compares 'V+LPS' gene expression to 'LPS only' gene expression, shows a clear difference

gene expression profile. The full list of genes that increase and decrease in expression under V-antigen co-stimulation, along with fold regulation change and t-test p-value, is presented in Tables 14 and 15 and their location within the TLR/TNF α /IFN γ signalling pathways are presented in Figure 48.

Figure 47:

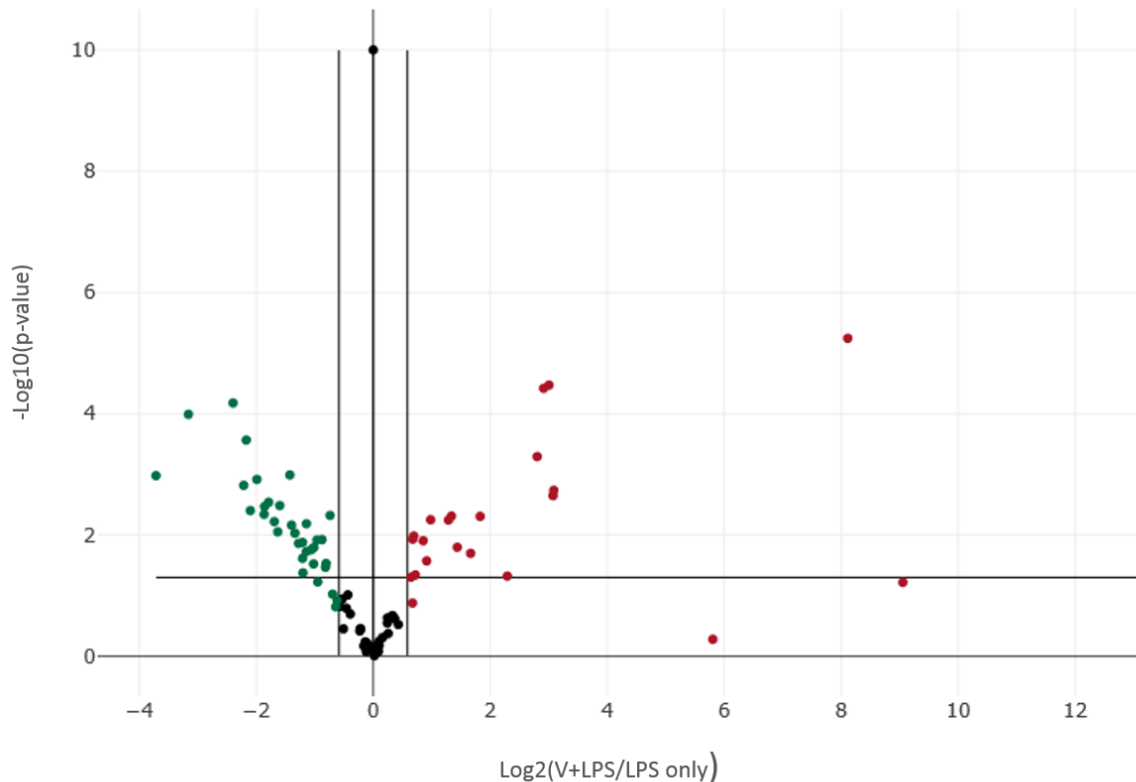


Figure 47 - Volcano plot of V+LPS gene expression compared to LPS only expression – TLR pathway gene array – PBMDMs from 4 separate donors were set up according to the experimental design in Figure 15 with PBMDMs pre-incubated with/without 50 μ g V-antigen for 30min and then stimulated with/without 100ng/ml LPS for 16hr. The cells were then lysed, and the RNA was extracted for qPCR analysis using the Qiagen RT² profiler - Human TLR pathway gene array plate. Average gene expression for each gene within '50 μ g V-antigen + 100ng/ml LPS'-stimulated PBMDMs (V+LPS) and 100ng/ml LPS-stimulated PBMDMs (LPS only) was determined and compared using a volcano plot generated by the Qiagen Geneglobe analysis software. Genes with a >1.5-fold regulation (red) and genes <-1.5-fold regulation (green) were highlighted and the horizontal line was added to represent the p-value 0.05.

Table 14 - Upregulated genes within LPS-stimulated PBMDMs co-stimulated with V-antigen – TLR pathway gene array

Gene Symbol	Fold Regulation	p-value	Comment
CCL2	3.55	0.004922	
CD180	7.52	0.000038	
CD80	1.61	0.010380	
CXCL10	6.97	0.000508	
IFNB1	8.41	0.002241	
IFNG	276.19	0.000006	A
IL12A	3.17	0.020077	

CXCL8	1.59	0.011698	
IRF1	1.88	0.026710	
JUN	1.56	0.049473	
LY86	1.97	0.005594	
MAPK8	4.89	0.047642	
PELI1	1.81	0.012378	
PTGS2	2.52	0.004871	
SIGIRR	1.65	0.045531	
TLR3	8.48	0.001832	A
TLR5	2.44	0.005645	
TLR7	8.01	0.000034	
TNF	2.70	0.015915	

PBMDMs from 4 separate donors were set up according to the experimental design in Figure 15 with PBMDMs pre-incubated with/without 50µg V-antigen for 30min and then stimulated with/without 100ng/ml LPS for 16hr. The cells were then lysed, and the RNA was extracted for qPCR analysis using the Qiagen RT² profiler - Human TLR pathway gene array plate. Average gene expression for each gene within 'V+LPS' and LPS only' controls was compared, and a Student's T-test was performed via the Qiagen Geneglobe analysis software. Genes upregulated in 'V+LPS' (genes with >1.5-fold regulation and <0.05 p-value as determined by Student's T-test) are presented in the table above.

'Comments' are: A; the gene's average threshold value is high (>30) in one group and low (<30) in the other, B; the gene's average threshold value is >30 in both samples and the p-value for the fold-change is unavailable or high (p>0.05), C; the gene's average threshold value is above the cut-off or undetected in all samples and so is unreliable and cannot be used

Table 15 - Downregulated genes within LPS-stimulated PBMDMs co-stimulated with V-antigen – TLR pathway gene array

Gene Symbol	Fold Regulation	p-value	Comment
CD14	-4.64	0.001516	
CLEC4E	-3.63	0.003385	
CSF3	-1.75	0.029378	
ELK1	-3.97	0.001211	
FADD	-1.76	0.034006	
HRAS	-2.02	0.015969	
HSPD1	-3.03	0.003264	
IKBKB	-1.84	0.011898	
IL10	-4.50	0.000272	
IL1A	-13.12	0.001049	
IL1B	-5.27	0.000066	
IL6	-3.65	0.004553	
IRAK4	-1.95	0.012038	
IRF3	-3.23	0.006016	
MAP2K3	-1.67	0.004743	
MAP3K7	-2.03	0.029935	
MAPK8IP3	-2.53	0.009311	
MYD88	-2.31	0.013223	

<i>NFKB1</i>	-2.42	0.013718	
<i>NFKB2</i>	-2.21	0.006509	
<i>NFKBIA</i>	-4.29	0.003952	
<i>NFRKB</i>	-2.30	0.041990	
<i>NR2C2</i>	-2.31	0.024240	
<i>SARM1</i>	-8.93	0.000102	A
<i>TBK1</i>	-3.45	0.002881	
<i>TLR1</i>	-3.10	0.008843	
<i>TLR2</i>	-2.69	0.001020	
<i>TNFRSF1A</i>	-2.63	0.006876	
<i>TOLLIP</i>	-2.21	0.018795	
<i>UBE2N</i>	-2.08	0.017456	

PBMDMs from 4 separate donors were set up according to the experimental design in Figure 15 with PBMDMs pre-incubated with/without 50µg V-antigen for 30min and then stimulated with/without 100ng/ml LPS for 16hr. The cells were then lysed, and the RNA was extracted for qPCR analysis using the Qiagen RT² profiler - Human TLR pathway gene array plate. Average gene expression for each gene within 'LPS only' and 'unstimulated' controls was compared, and a Student's T-test was performed via the Qiagen Geneglobe analysis software. Genes downregulated in 'WT+LPS' (genes with <-1.5-fold regulation and <0.05 p-value as determined by Student's T-test) are presented in the table above.

'Comments' are: A; the gene's average threshold value is high (>30) in one group and low (<30) in the other, B; the gene's average threshold value is >30 in both samples and the p-value for the fold-change is unavailable or high (p>0.05), C; the gene's average threshold value is above the cut-off or undetected in all samples and so in unreliable and cannot be used

Figure 48:

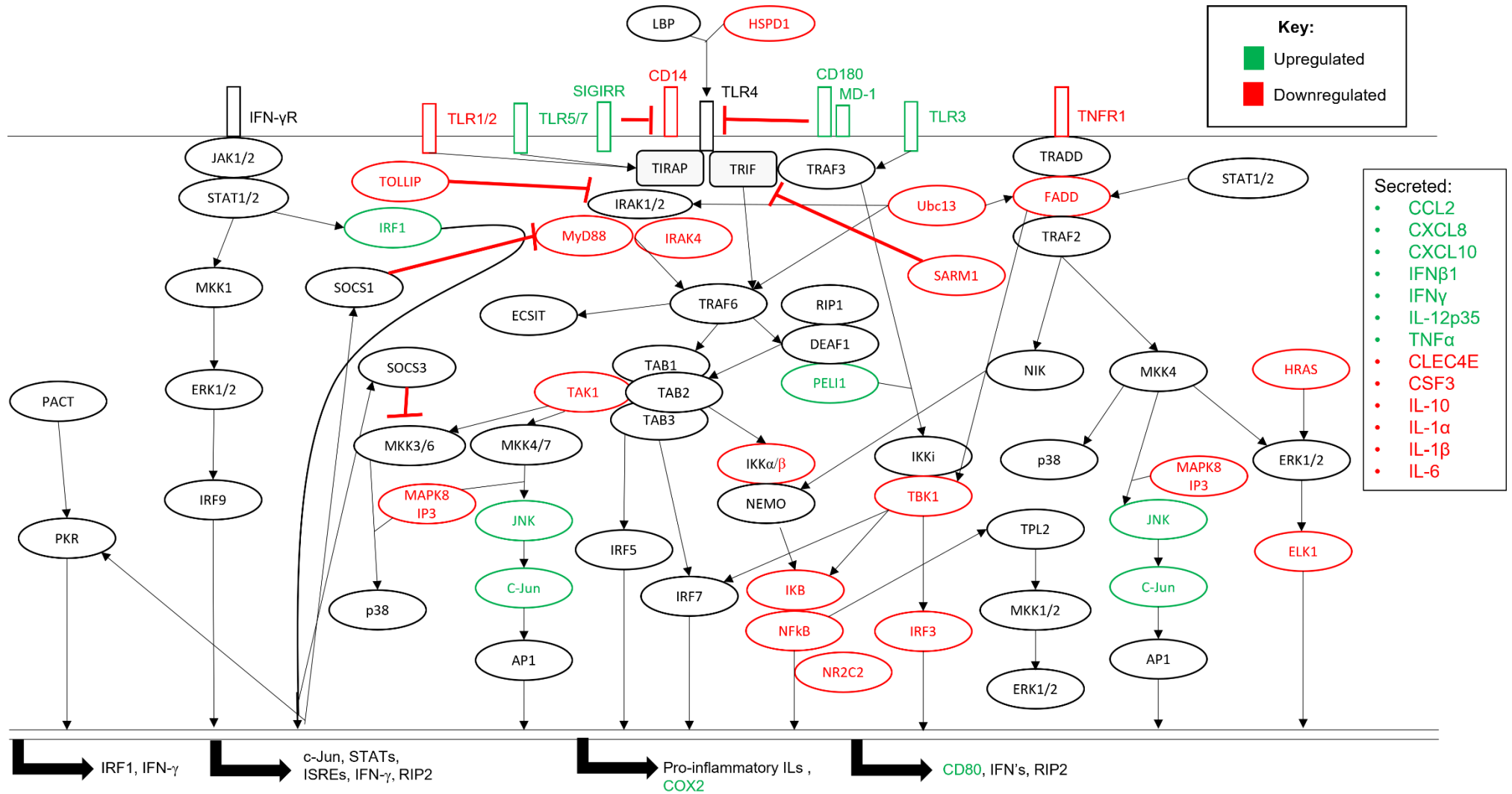


Figure 48 - Differentially expressed genes in LPS-stimulated PBMDMs co-stimulated with V-antigen – PBMDMs from 4 separate donors were set up according to the experimental design in Figure 15 with PBMDMs pre-incubated with/without 50µg V-antigen for 30min and then stimulated with/without 100ng/ml LPS for 16hr. The cells were then lysed, and the RNA was extracted for qPCR analysis using the Qiagen RT² profiler - Human TLR pathway gene array plate. Average gene expression for each gene within 'V+LPS' and 'LPS only' control was compared, and a Student's T-test was performed via the Qiagen Geneglobe analysis software. Genes upregulated or downregulated by LPS (genes with >1.5-fold regulation or <-1.5-fold regulation respectively and <0.05 p-value as determined by Student's T-test) are presented with their location in the IFN γ /TLR/TNF α pathway

IFN γ R, interferon γ receptor; JAK1/2, janus kinase 1/2; STAT1/2, signal transducer and activator of transcription 1/2; PKR, protein kinase R; PACT, protein activator of interferon protein kinase EIF2AK2; ISREs, interferon stimulated response elements; RIPK2, ;COX2, cyclooxygenase 2; CD14/180, cluster of differentiation 14/180; LBP, lipopolysaccharide binding protein; HSP60, heat shock protein 60; TLR, Toll-like receptor; TIRAP, TIR-domain-containing adaptor protein; TRIF, TIR-domain-containing adaptor-inducing interferon- β ; TRAF2/3/6, tumour necrosis factor receptor-associated factor2/ 3/6; IRAK1/4, IL-1 receptor-associated kinase 1/4; MyD88, myeloid differentiation primary response protein 88; ECSIT, evolutionarily conserved signalling intermediate in Toll pathway, mitochondrial; RIP1, receptor-interacting serine/threonine-protein kinase 1; DEAF1, deformed epithelial autoregulatory factor-1; PELI1, pellino E3 ubiquitin protein ligase 1; TAK1, TGF β -activated kinase 1; TAB1/2/3, TGF β -activated kinase 1 binding protein 1/2/3; MKK1/2/3/4/6/7, Mitogen activated protein kinase kinase 1/2/3/4/6/7; JNK, c-Jun N-terminal kinase; AP1, activating protein-1; IRF1/3/5/7/9, interferon regulatory factor 1/3/5/7/9; IKK α / β /i, Inhibitor of kappa kinase α / β /i; NEMO, nuclear factor κ B essential modulator; TBK1, TANK binding kinase; TPL2, tumour progression locus 2; IKB, inhibitor of nuclear factor kappa-light-chain-enhancer of activated B cells; NF κ B, nuclear factor kappa-light-chain-enhancer of activated B cells; NR2C2, nuclear receptor subfamily 2 group C member 2; ERK1/2, extracellular signal-regulated kinase 1/2; TOLLIP, Toll-interacting protein; SOCS1/3, suppressor of cell signalling 1/3; SIGIRR, single Ig IL-1-related receptor; MD-1, myeloid differentiation protein 1/2; Ubc13, ubiquitin-conjugating enzyme E2 N; SARM1, sterile alpha and TIR motif containing 1; TNFR1, tumour necrosis factor receptor 1/2; TRADD, tumour necrosis factor receptor type 1-associated DEATH domain protein; FADD, Fas-associated death domain protein; NIK, NF κ B-inducing kinase; ELK1, ETS-like protein 1; CLEC4E, c-type lectin domain containing 4E; CSF3, colony-stimulating factor 3; CXCL8/10, C-X-C ligand motif 8/10; CCL2, C-C motif ligand 2; IFN, interferon; IL, interleukin

A total of 49 genes were differentially expressed with 19 genes classed as having increased expression in the presence of V-antigen and 30 classed as having decreased expression. The STRING analysis on the upregulated and downregulated genes is shown in Figure 49 and Figure 50 respectively. The upregulated genes provided a high-level of confidence that the functional cluster of 'response to virus' was enriched. Viral TLRs, IFNs, PELI1, and CXCL10 were all upregulated while 'response to bacterium' and 'MyD88-dependent Toll-like receptor signalling pathway' were both identified as enriched functional clusters within the downregulated gene list. This included genes like NFκB, bacterial TLRs, LPS receptor/detection proteins like CD14 and HSPD1, as well as members of the signalling pathway like MyD88, IRAK4, and TANK Binding Kinase (TBK1). It was also noted that some inhibitory molecules for LPS detection like CD180, LY86, and Single Ig IL-1-Related Receptor (SIGIRR) were also upregulated.

Figure 49:

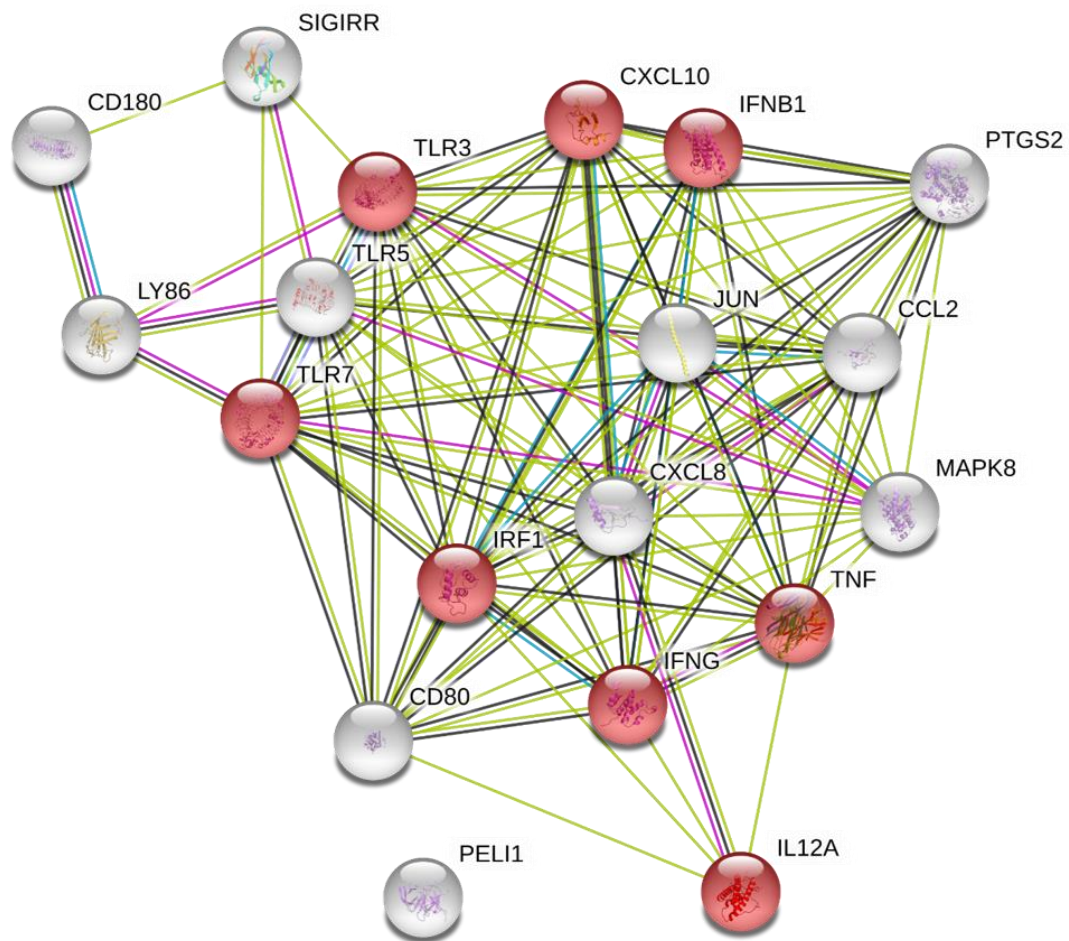


Figure 49 - STRING analysis of V-antigen-upregulated genes in LPS-stimulated PBMDMs –TLR pathway gene array – PBMDMs from 4 separate donors were set up according to the experimental design in Figure 15 with PBMDMs pre-incubated with/without 50 μ g V-antigen for 30min and then stimulated with/without 100ng/ml LPS for 16hr. The cells were then lysed, and the RNA was extracted for qPCR analysis using the Qiagen RT² profiler - Human TLR pathway gene array plate. Average gene expression for each gene within '50 μ g V-antigen + 100ng/ml LPS'-stimulated PBMDMs (V+LPS) and 100ng/ml LPS-stimulated PBMDMs (LPS only) was calculated and genes with an upregulated expression in 'LPS only', characterised as >1.5-fold regulation of expression and p-value <0.05 (determined by Student's T-test), were processed through the STRING protein interaction network database. Enriched functional clusters within the upregulated gene list were identified by STRING and the functional clusters of 'response to virus' (red) (FDR = 7.91e-08, Strength =1.45) is highlighted

Figure 50:

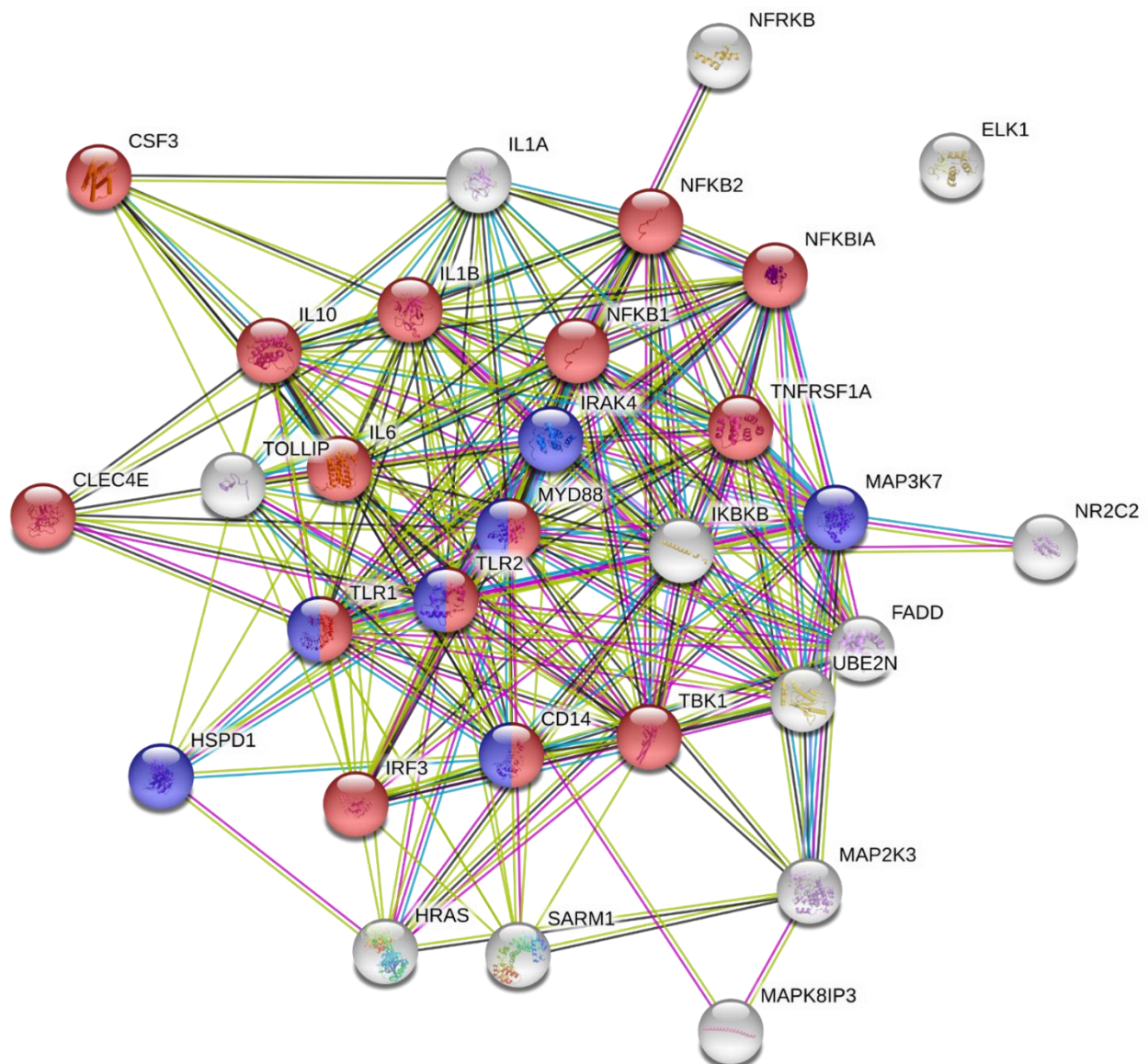


Figure 50 - STRING analysis of V-antigen-downregulated genes in LPS-stimulated PBMDMs – TLR pathway gene array – PBMDMs from 4 separate donors were set up according to the experimental design in Figure 15 with PBMDMs pre-incubated with/without 50µg V-antigen for 30min and then stimulated with/without 100ng/ml LPS for 16hr. The cells were then lysed, and the RNA was extracted for qPCR analysis using the Qiagen RT² profiler - Human TLR pathway gene array plate. Average gene expression for each gene within '50µg V-antigen + 100ng/ml LPS'-stimulated PBMDMs (V+LPS) and 100ng/ml LPS-stimulated PBMDMs (LPS only) was calculated and genes with a downregulated expression in 'LPS only', characterised as <-1.5-fold regulation of expression and p-value <0.05 (determined by Student's T-test), were processed through the STRING protein interaction network database. Enriched functional clusters within the downregulated gene list were identified by STRING and the functional clusters of 'response to bacterium' (red) (FDR = 6.96e-15, Strength = 1.24) and 'MyD88-dependent Toll-like receptor signalling pathway' (blue) (FDR = 5.51e-11, Strength = 2.14) are highlighted

5.2.2.2: Expression analysis of key identified genes

As in 4.2.2.2, it was important to explore the expression of individual genes beyond functional cluster analysis. Analysis of this kind would allow for the identification of genes

that were transcribed substantially differently under V-antigen stimulation and may provide leads to further the investigation into V-antigen's mechanism of action.

Initially, genes from the functional cluster 'viral response' were investigated. These included cytokines that could be stimulated by both viral and bacterial stimuli and so the focus within that cluster was on proteins within the TRIF pathway and those linked to IFN signalling. TLR3, a viral-PAMP PRR and the only TLR to exclusively use the TRIF pathway was expressed at a significantly higher level within the 'V+LPS' sample compared with 'LPS only'. When expression was compared across all four conditions (Figure 51A) there was no evidence of any significant difference between the unstimulated control and V-antigen-stimulated samples. 'LPS only' had a non-significantly reduced expression of TLR3 (0.16-fold change, p-value = 0.08774) when compared to the unstimulated control whereas 'V-only' had no significant changes in expression compared to the unstimulated control (0.95-fold change, p-value = 0.74734). However, although V-antigen alone did not affect TLR3 expression, when LPS was co-stimulated with V-antigen, TLR3 was prevented from downregulating (1.34-fold change compared to unstimulated, p-value = 0.74215).

IRF1, shown in Figure 41 as a key downstream TF of the IFN γ pathway, was also highlighted as an upregulated gene. Stimulation with LPS alone did not increase IRF1 expression with any significance, however both V-antigen samples saw significant increases in expression when compared to the unstimulated control and 'LPS only' (Figure 51B). The greatest expression of IRF1 was under V-antigen stimulation alone (5.2-fold change compared to the unstimulated control) while in the presence of LPS co-stimulation, this only reached an upregulation of 2.46-fold compared to the unstimulated control suggesting that V-antigen stimulation upregulates IRF1 expression but that is restricted by the presence of LPS.

PELI1 was also found to be a gene with increased expression in 'V+LPS' compared with 'LPS only'. It was not highlighted within the 'viral response' functional cluster in Figure 49 however recent studies have shown that PELI1 is an important E3 ubiquitin ligase for the TRIF pathway(234) as well as being involved in the MyD88 pathway. When compared over all conditions (Figure 51C), the expression of PELI1 showed a cumulative effect for both LPS and V-antigen with both stimuli trigger increased expression (3.5-fold) and an even greater expression (6.5-fold) when combined.

Figure 51:

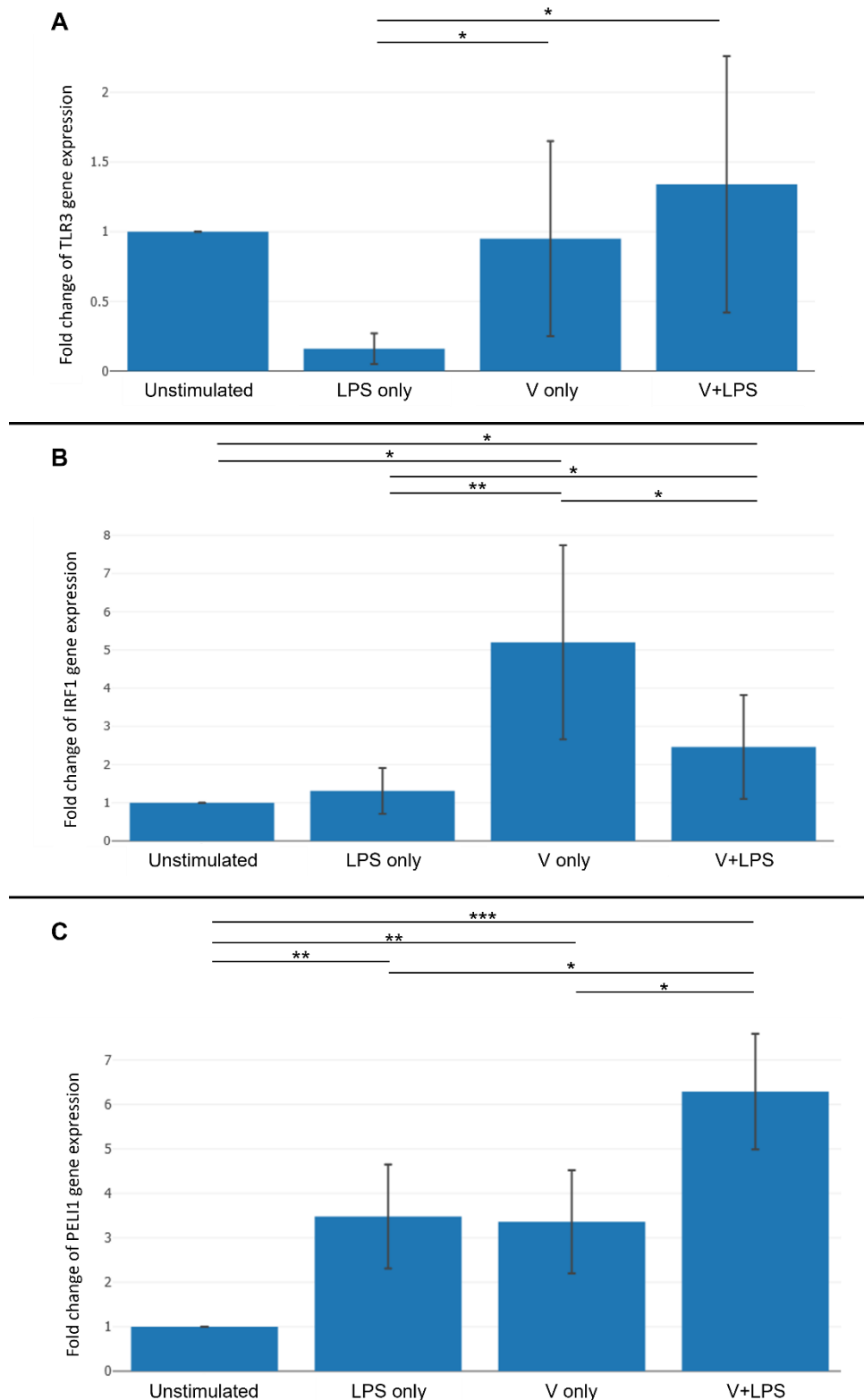


Figure 51 – TLR3, IRF1, and PELI1 gene expression under stimulation with combinations of LPS and V-antigen – PBMDMs from 4 separate donors were set up according to the experimental design in Figure 15 with PBMDMs pre-incubated with/without 50 μ g V-antigen and then stimulated with/without 100ng/ml LPS for 16hr. The cells were then lysed, and the RNA was extracted for qPCR analysis using the Qiagen RT² profiler - Human TLR pathway gene array plate. Using the Qiagen Geneglobe analysis software, the average expression of A; TLR3, B; IRF1, and C; PELI1, was evaluated across all four conditions and displayed as a fold-change from the unstimulated control. Data is presented with standard error bars and indicators for statistical significance(* = <0.05, ** = <0.01, *** = <0.001, **** = <0.0001) as determined by Student's T-test adjusted for multiple comparisons post-hoc with a manual Benjamini-Hochberg correction

IFN γ belongs to the IFN family; a family of cytokines largely responsible for anti-viral responses, and despite also having important roles in bacterial responses and in leukocyte development/activation, it is heavily involved in the anti-viral response too. CXCL10 is a largely-IFN γ -induced chemokine and acts as an important chemokine in viral infections. Figures 52A and 52B show that IFN γ and CXCL10 both have significantly higher expression in the presence of V-antigen alone and even higher expression in the presence of V-antigen and LPS together. IFN γ in particular had a significant increase of over 200-fold on the unstimulated control and 'LPS only' expression. CXCL10, however, did not show significance in its 2.38-fold upregulation between the unstimulated control and 'V+LPS' but it was significantly upregulated compared to 'LPS only' which itself was downregulated compared to the unstimulated control.

Figure 52:

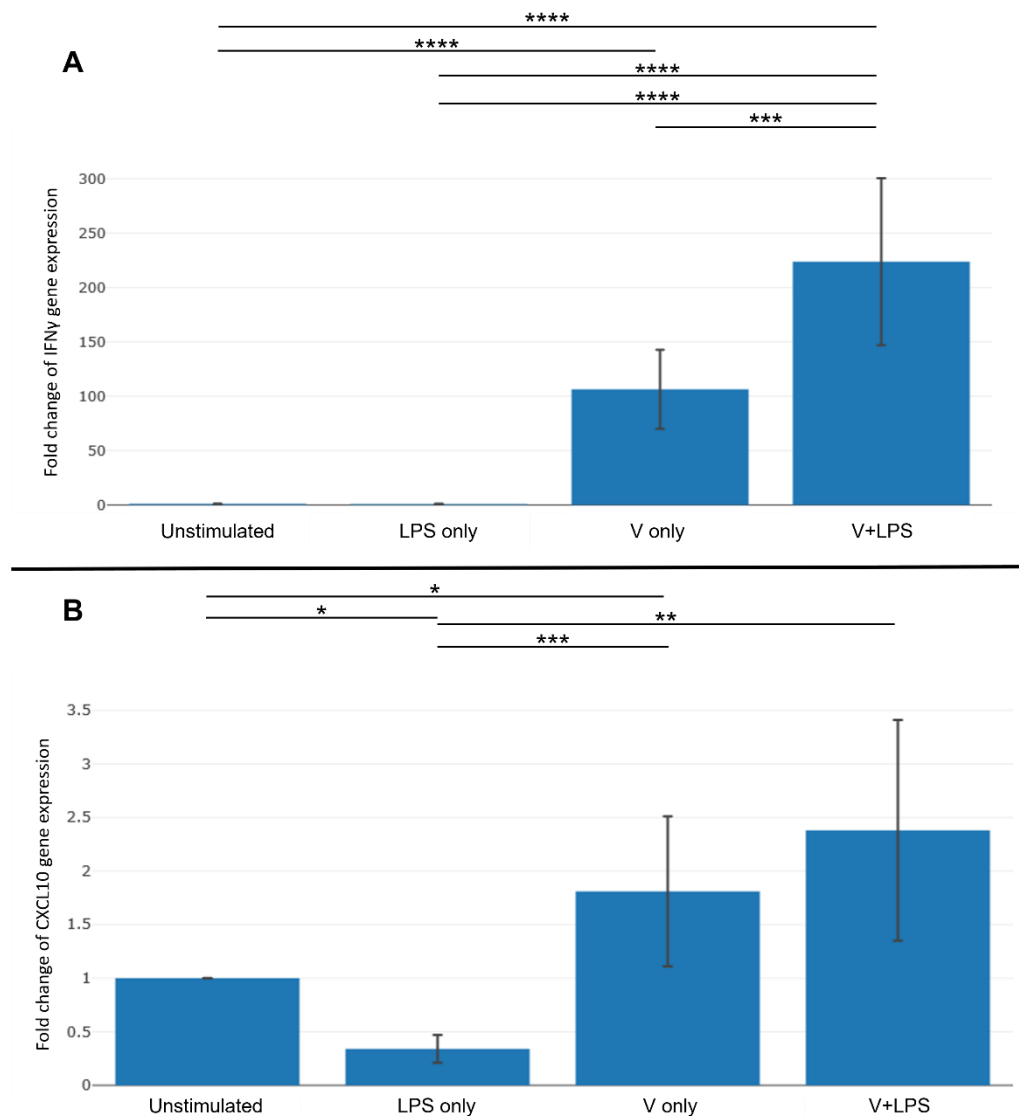


Figure 52 - IFN γ , and CXCL10 gene expression under stimulation with combinations of LPS and V-antigen – PBMDMs from 4 separate donors were set up according to the experimental design in Figure 15 with PBMDMs pre-incubated with/without 50 μ g V-antigen and then stimulated with/without 100ng/ml LPS for 16hr. The cells were then lysed, and the RNA was extracted for qPCR analysis using the Qiagen RT² profiler - Human TLR pathway gene array plate. Using the Qiagen Geneglobe analysis software, the average expression of A; IFN γ and B; CXCL10 was evaluated across all four conditions and displayed as a fold-change from the unstimulated control. Data is presented with standard error bars and indicators for statistical significance (* = <0.05, ** = <0.01, *** = <0.001, **** = <0.0001) as determined by Student's T-test adjusted for multiple comparisons post-hoc with a manual Benjamini-Hochberg correction

These changes in gene expression reveals that the co-stimulation of V-antigen alters the inflammatory response triggered by LPS in a way that induces higher expression of TRIF/viral response-associated genes at 16hr. The same gene array data revealed a downregulation of genes associated to the functional clusters: 'response to bacterium' and 'MyD88-dependent Toll like receptor signalling pathway' (Figure 50), and so analysis was also performed on key genes within these clusters in the same way as those above.

Two key genes that were identified as downregulated by V-antigen co-stimulation are genes that are involved in the initial binding and receptor interaction of LPS: CD14 and HSPD1. Under LPS-stimulation alone both genes saw significantly upregulated expression of ~4-fold change over the expression of the unstimulated control. When co-stimulated with V-antigen though, both genes failed to upregulate, and when PBMDMs were stimulated with V-antigen alone, both genes saw downregulated expression – significantly for CD14 (0.15-fold (p-value = 0.00922)) and non-significantly for HSPD1 (0.38-fold (p-value = 0.09632)).

Figure 53:

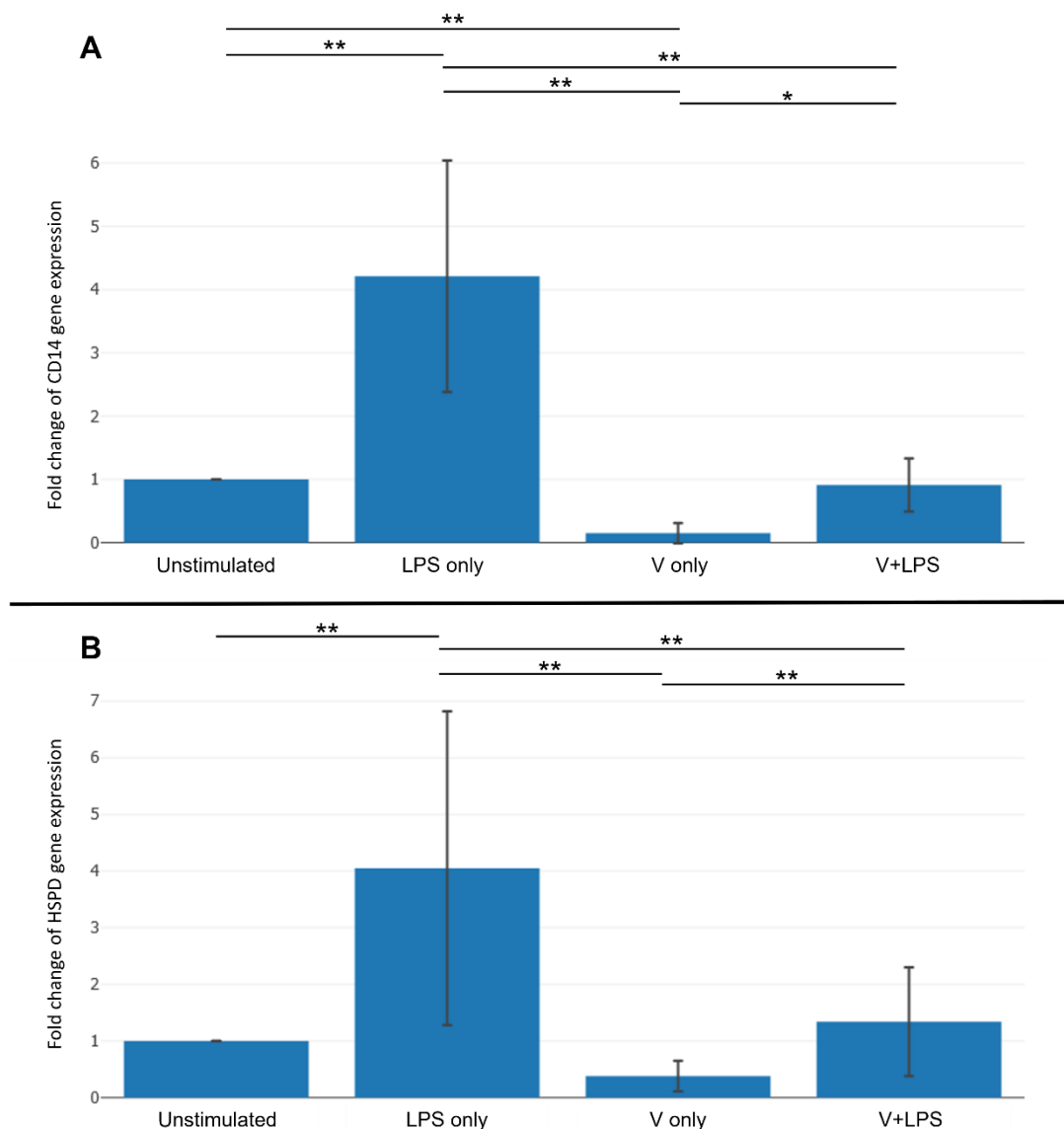


Figure 53 – CD14 and HSPD1 gene expression under stimulation with combinations of LPS and V-antigen – PBMDMs from 4 separate donors were set up according to the experimental design in Figure 15 with PBMDMs pre-incubated with/without 50µg V-antigen and then stimulated with/without 100ng/ml LPS for 16hr. The cells were then lysed, and the RNA was extracted for qPCR analysis using the Qiagen RT² profiler - Human TLR pathway gene array plate. Using the Qiagen Geneglobe analysis software, the average expression of A; CD14 and B; HSPD1 was evaluated across all four conditions and displayed as a fold-change from the unstimulated control. Data is presented with standard error bars and indicators for statistical significance(* = <0.05, ** = <0.01, *** = <0.001, **** = <0.0001) as determined by Student's T-test adjusted for multiple comparisons post-hoc with a manual Benjamini-Hochberg correction

Further examination of the expression of key MyD88 pathway proteins revealed a general reduced level of responsiveness to LPS-induced gene expression changes when PBMDMs were co-stimulated with V-antigen. This included the NF κ B genes; NFKB1, NFKB2, and NFKBIA (Supplementary Figure 14), as well as MyD88, IRAK4, and TBK1 (Supplementary Figure 15). However, this reduced responsiveness could be due to reduced autocrine and paracrine signalling from the inhibited cytokine response seen in V-antigen co-stimulated PBMDMs over 16hr (3.2.5.2).

TLR signalling inhibitory proteins were also looked at closer as five were reported as either upregulated or downregulated when LPS-stimulated PBMDMs were co-stimulated with V-antigen. SARM1 and Toll-interacting Protein (TOLLIP) were both downregulated by V-antigen co-stimulation while CD180, LY86, and SIGIRR were all upregulated. CD180 and LY86 are competitive LPS receptors that function like CD14 and MD-2 respectively but do not instigate downstream signalling upon binding LPS. As with the MyD88 pathway proteins mentioned above, CD180 and LY86 showed a reduced level of response to LPS when V-antigen was present. LPS reduces the expression of both of these surface proteins but when V-antigen is co-stimulated with it, the expression of both is far more comparable to the unstimulated control (Supplementary Figure 16). SIGIRR and TOLLIP, two proteins involved in TLR4 signalling inhibition and MyD88 dependent signalling inhibition respectively, show the same characteristic. While SIGIRR was downregulated under LPS conditions and TOLLIP was upregulated, both genes showed no significant difference in expression between the unstimulated control when co-stimulated with LPS and V-antigen (Supplementary Figure 17). All four inhibitory proteins were expressed minimally in 'V only' compared with unstimulated controls. This failure to up- or downregulate like in the LPS-only stimulation may be due to reduced autocrine/paracrine cytokine signalling rather than the direct mechanism of action from V-antigen.

SARM1, however, showed a more interesting change in regulation. There was no significant change between the unstimulated control and LPS stimulated PBMDMs (Figure 54) but in the presence of V-antigen alone, and V-antigen and LPS in combination, SARM1 is significantly downregulated. This downregulation is most significant under co-stimulation. As SARM1 is a TRIF-exclusive inhibitory protein, it is possible that this could allow for greater TRIF-dependent signalling and so may also tie in to the viral-like response reported by STRING (Figure 49).

Figure 54:

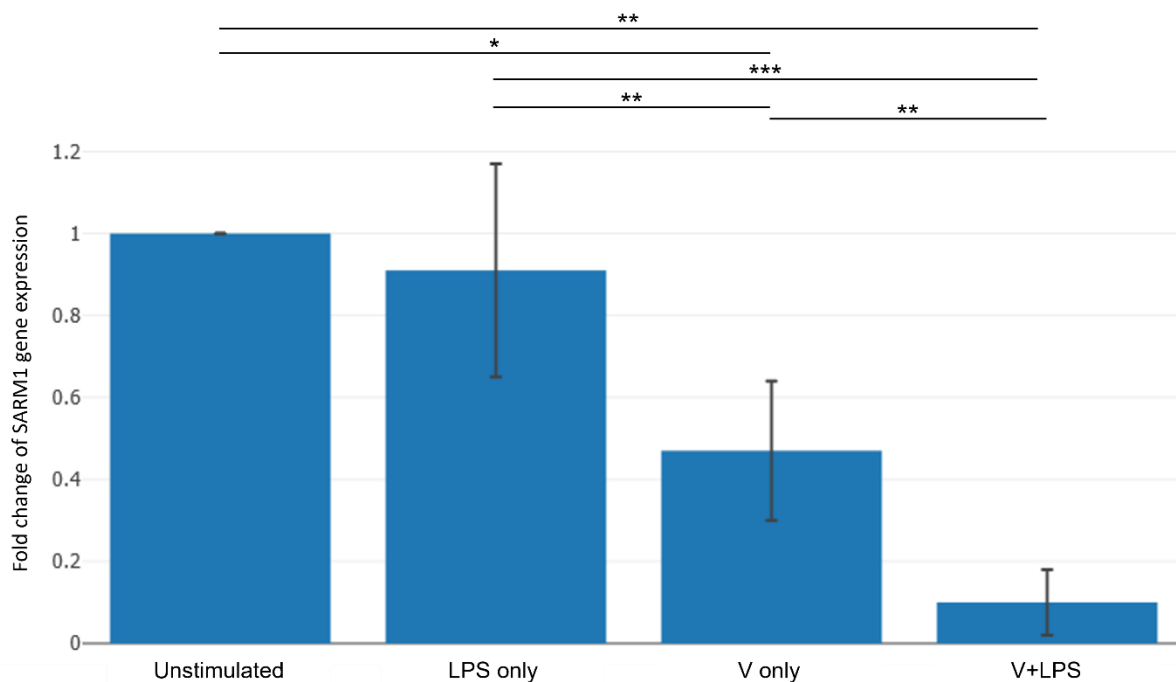


Figure 54 – SARM1 gene expression under stimulation with combinations of LPS and V-antigen – PBMDMs from 4 separate donors were set up according to the experimental design in Figure 15 with PBMDMs pre-incubated with/without 50µg V-antigen and then stimulated with/without 100ng/ml LPS for 16hr. The cells were then lysed, and the RNA was extracted for qPCR analysis using the Qiagen RT² profiler - Human TLR pathway gene array plate. Using the Qiagen Geneglobe analysis software, the average expression of SARM1 was evaluated across all four conditions and displayed as a fold-change from the unstimulated control. Data is presented with standard error bars and indicators for statistical significance(* = <0.05, ** = <0.01, *** = <0.001, **** = <0.0001) as determined by Student's T-test adjusted for multiple comparisons post-hoc with a manual Benjamini-Hochberg correction

Therefore, taking the full scope of the expression data into account, the suggestion that there is an increase in the expression of 'viral response' genes within 'V+LPS' stimulated monocytes appeared to be related mostly to the increase in IFN γ and the suppression of the usual LPS response. There is some evidence to suggest that V-antigen alone generates a more viral-like response with IRF1 expression increasing 5-fold compared to the 1.5-fold and 2.5-fold of 'LPS only' and 'V+LPS' as well as large significant increases in IFN γ and CXCL10 and there are also signs that the specific suppression of SARM1 expression by V-antigen could allow for higher levels of TRIF pathway signalling. This evidence is supported by data from 4.2.2 which also showed a more viral response with IFN-related genes and upregulated IFN β expression (Figure 33B, Chapter 4) as well as by the cytokine data from 3.2.5.2 which revealed a potential increase in IFN γ secretion (Figure 19, Chapter 3).

5.2.3: Comparison between Inflammasome and TLR qPCR gene arrays

common genes

The Human Inflammasome Qiagen RT² gene array (Chapter 4) and the Human TLR Pathway Qiagen RT² gene array (Chapter 5) have 23 common genes between them. As the same RNA was used for each plate, the expression of these genes should be highly comparable between the two plates. An examination of the 23 genes in both sets of plates was therefore undertaken, comparing the changes in fold regulation and whether there was significance between 'LPS only' and 'V+LPS', to determine whether the results were reliable. Table 16 shows the results of the comparison. Any comments relating to the quality of the CT data is presented in brackets next to the fold regulation value.

Table 16 - Fold regulation and significance of common genes between the Qiagen RT² 'TLR pathway' and 'Inflammasome' gene arrays

Gene	TLR plate fold regulation	Significant?	Inflammasome plate fold regulation	Significant?
<i>CCL2</i>	3.55	Y	2.41	Y
<i>CHUK</i>	-1.16	N	-1.48	Y
<i>FADD</i>	-1.76	Y	-1.24	N
<i>IFNB</i>	8.41	Y	50.13 (A)	Y
<i>IFNG</i>	276.19 (A)	Y	393.05 (A)	Y
<i>IKBKB</i>	-1.84	Y	-2.02	Y
<i>IL12A</i>	3.17	Y	3.16	Y
<i>IL1B</i>	-5.27	Y	-6.22	Y
<i>IL6</i>	-3.65	Y	-3.27	Y
<i>IRAK1</i>	-1.62	N	-1.14	N
<i>IRF1</i>	1.88	Y	2.00	Y
<i>MAP3K7</i>	-2.03	Y	-2.12	Y
<i>MAPK8</i>	4.89	Y	-1.94	Y
<i>MYD88</i>	-2.31	Y	-1.23	N
<i>NFKB1</i>	-2.42	Y	-2.58	Y
<i>NFKBIA</i>	-4.29	Y	-2.77	Y
<i>PTGS2</i>	2.52	Y	1.06	N
<i>RELA</i>	-1.12	N	-2.51	Y
<i>RIPK2</i>	1.07	N	-1.02	N
<i>TAB1</i>	1.18	N	1.78	Y
<i>TIRAP</i>	-1.93	N	-1.28	N
<i>TNF</i>	2.70	Y	1.39	N
<i>TRAF6</i>	-1.17	N	1.48	Y

PBMDMs from 4 separate donors were set up according to the experimental design in Figure 15 with PBMDMs pre-incubated with/without 50µg V-antigen for 30min and then stimulated with/without 100ng/ml LPS for 16hr. The cells were then lysed, and the RNA was extracted for qPCR analysis using both the Qiagen RT² profiler - Human Inflammasome gene array plate and Qiagen RT² profiler - Human TLR gene array plate. Average gene expression for genes within 'V+LPS' and the 'LPS only' control was compared and the statistical significance was determined by a Student's T-test performed by the Qiagen Geneglobe analysis software. Genes common between the two plates were then examined for similarities in their results as to whether they fell within the same boundaries of; downregulated (<-1.5-fold regulation), upregulated (>1.5-fold regulation), or no change (-1.5-1.5-fold regulation), and significant (p-value = <0.05) or non-significant (p-value = 0.05 or >0.05). Comments on the

reliability of the data, as flagged by the Geneglobe analysis software, are presented in brackets alongside the fold-regulation value.

'Comments' are: A; the gene's average threshold value is high (>30) in one group and low (<30) in the other

Variation between the plates was evident however due to the criteria set for defining upregulated and downregulated genes, only 7 genes were categorised differently between the plates. In the cases of FADD, MYD88, PTGS2, Transcription Factor p65 (RELA), TGF β Activated Kinase 1 Binding Protein 1 (TAB1), and TNF, this was seen as a shift in the fold regulation and occasionally the significance however the change in fold-regulation was still in the same relative direction from the control – i.e., an upregulated gene with a higher fold regulation in one plate than the other but still >1-fold regulation in both. MAPK8 however showed a significant increase in the TLR plate and yet a significant decrease in the inflammasome plate and was the only gene to show such extreme differences.

Despite this, the other 16 genes showed far closer consistency and were categorized the same way in both analyses. Within this group are numerous key genes of interest including IRF1, IFN genes, key cytokines like IL-6 and IL-1 β , and CCL2.

5.2.4: TGF β

5.2.4.1: TGF β 1

TGF β is a family of three cytokines; TGF β 1, TGF β 2, and TGF β 3, which belong to the TGF β superfamily. These cytokines function through a family of downstream signalling proteins known as Mothers Against Decapentaplegic Homologs (SMADs). TGF β has a wide set of roles including control of cell cycle progression and differentiation - particularly within osteoclasts and mesenchymal stem cells, as well as pro- and anti-apoptotic signals in cells throughout the body. TGF β 1 is the most common member of the TGF β family and is a highly conserved protein with 100% sequence homology between human, bovine, simian, porcine, and chicken proteins as well as a 99% homology between humans and mice. It is cleaved intracellularly by golgi Furin to form mature TGF β 1 and a Latency Associated Peptide (LAP) which stay associated after cleavage to form an inactive heterodimer. Active TGF β 1 is mature TGF β 1 that is dissociated from LAP; a process that occurs through protein conformational changes or proteolytic processing.

TGF β 1 is an anti-inflammatory cytokine as it inhibits the differentiation of Th1/Th2 effector T-cells, promotes the development of T-reg cells, and suppresses the proliferation of T- and B-cells. It also inhibits the function of monocytes, macrophages, and DCs, inhibits the

ability of CD8 T-cells and NK cells to exocytose granules, and suppresses pro-inflammatory cytokine signalling. It also inhibits iNOS and MMP-12 function within macrophages(235). Monocytes and macrophages are large secretors of TGF β 1, secreting it in response to apoptotic cell debris to restrict autoinflammation. In particular, the inhibition of IL-2, IL-4, and IFN γ responses has been noted by studies on the anti-inflammatory properties of TGF β 1. The suppression of cytokine signalling arises through the interaction of SMAD2/3 with Suppressor of Cytokine Signalling 1 (SOCS1) – an inhibitor of JAK1 and JAK2 activity, and of MyD88-signalling via MyD88 degradation(236). This leads to a reduction in MyD88-dependent signalling and the signalling of cytokines such as IL-6 and IFN γ . An exception, however, is within human monocytes where SOCS1 does not inhibit STAT1 DNA binding, leaving the IFN γ pathway fully functional while restricting the MyD88 pathway(237). In all cell types though, the TRIF pathway is not specifically targeted by TGF β 1 and as such, TLR3 stimuli see no change in response in the presence of TGF β 1 whereas TLR2, TLR4, and TLR5 stimuli all do.

TGF β 1 was of interest to this study due to its MyD88-specific inhibition and, in human monocytes, a lack of restraint on IFN γ signalling which correlated with what had been observed in 3.2.5.2 and 4.2.2. The use of human monocytes and therefore the lack of IFN γ control by SOCS1 could explain the increased IFN γ response seen in 3.3.5.2 and Figure 52A which would not be expected in other TGF β 1-stimulated cell types. This would also reduce the effect of TGF β 1 as an anti-inflammatory because as well as TGF β 1 having an inhibitory effect on IFN γ signalling (via SOCS1), IFN γ has an inhibitory effect on TGF β (238). Therefore, as this study utilises human monocytes, it is possible that a less potent immunosuppressive effect is being observed if TGF β is indeed involved in V-antigen's mechanism of action.

TGF β 1 also utilises the JNK and p38 MAPK pathways via Transforming Growth Factor β -Activated Kinase 1(TAK1) – TAK1/MAP Kinase Kinase 4(MKK4)/JNK and TAK1/MKK3(/6)/p38(239, 240). In 4.2.2, there was a potential increase seen in p38 MAPK expression under V-antigen stimulation – in particular MAPK11 (without LPS) (Figure 38A, Chapter 4) and MAPK12 (with LPS) (Figure 38B, Chapter 4). However, it did not show an increase in expression of JNK MAPKs (Supplementary Figure 12). The TLR pathway gene array did show altered expression of MAP3K7(aka TAK1) (Figure 55) though the expression was lower in V-antigen co-stimulated PBMDMs than in those stimulated with LPS alone. Under the stimulation of V-antigen alone however, TAK1 expression was 18.8-fold higher than in 'LPS-only' and 38.2-fold higher than in 'V+LPS'.

Figure 55:

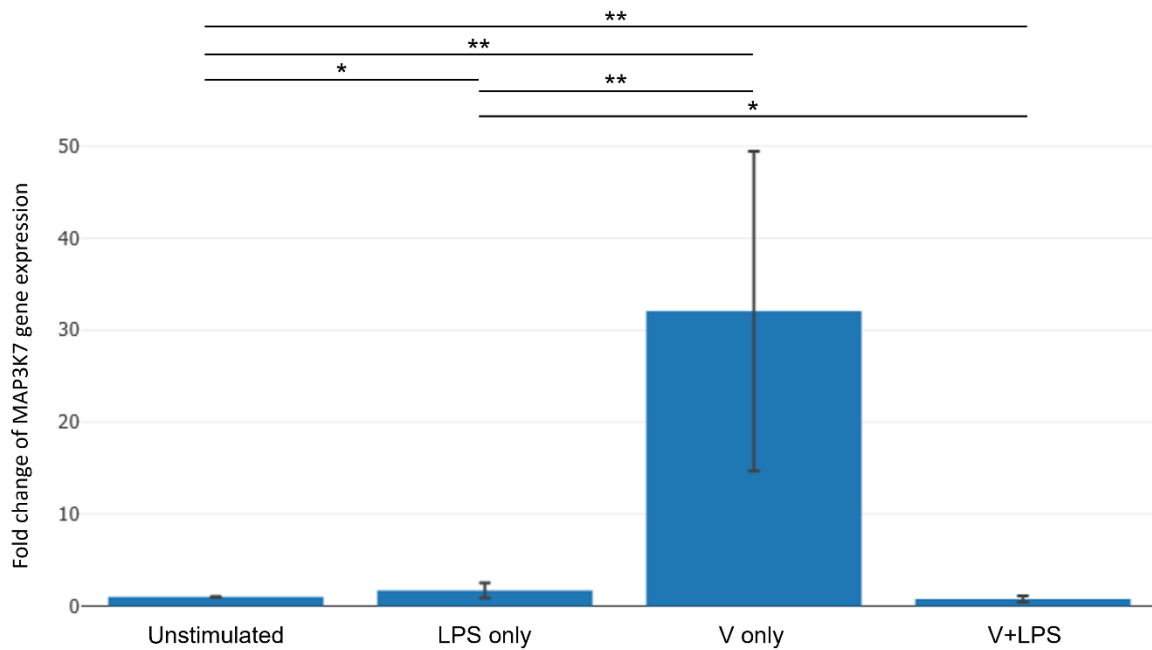


Figure 55 – MAP3K7 gene expression under stimulation with combinations of LPS and V-antigen – PBMDMs from 4 separate donors were set up according to the experimental design in Figure 15 with PBMDMs pre-incubated with/without 50µg V-antigen and then stimulated with/without 100ng/ml LPS for 16hr. The cells were then lysed, and the RNA was extracted for qPCR analysis using the Qiagen RT² profiler - Human TLR pathway gene array plate. Using the Qiagen Geneglobe analysis software, the average expression of MAP3K7 was evaluated across all four conditions and displayed as a fold-change from the unstimulated control. Data is presented with standard error bars and indicators for statistical significance (* = <0.05, ** = <0.01, *** = <0.001, **** = <0.0001) as determined by Student's T-test adjusted for multiple comparisons post-hoc with a manual Benjamini-Hochberg correction

5.2.4.2: Evidence of TGFβ involvement

TGFβ1 has previously been shown to reduce cellular levels of CD14 via transcriptional repression(241). V-antigen stimulation, with and without LPS, shows a downregulated expression of CD14 according to the TLR pathway gene array data in Figure 53A. To prove whether this led to reduced protein levels within V-antigen-stimulated cells, the same lysates used for the western blots in Chapter 4 (4.2.1, Figures 24 and 25) and Chapter 5 (Figure 40) were examined for CD14 quantity via western blot. Equal quantities of protein were run in denaturing, reducing conditions and probed using antibodies for CD14 and β2M. The resulting western blot is displayed in Figure 56.

Figure 56:

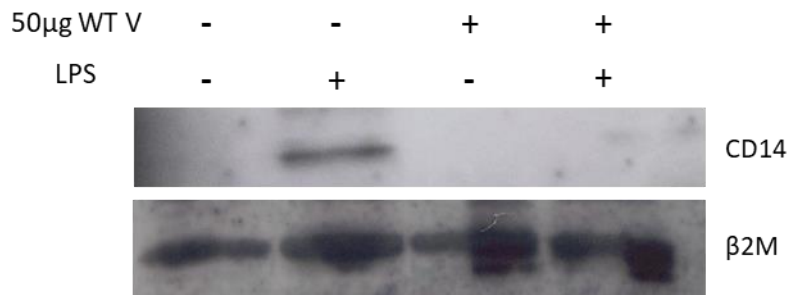


Figure 56 - CD14 western blot on LPS/V-antigen-stimulated MM6 cells – Mono-mac 6 (MM6) cells were seeded at a density of 5×10^4 cells/well on 24 well plates and allowed to attach overnight. After a 30min pre-incubation with/without 50µg V-antigen, LPS was added to a final concentration of 100ng/ml or not added at all. After a specified incubation time from the point of LPS addition (or non-addition), the cells were lysed in 2x sample buffer (Appendix A). An SDS-PAGE was run in denaturing, reducing conditions using loading quantities determined by β2M expression (western blot not shown), before being transferred to a nitrocellulose membrane and probed with anti-β2M antibody (MyBioSource MBS246617) and anti-CD14 antibody (MyBioSource MBS178874) and then anti-mouse-HRP antibody (Dako P0260). The resulting blot was developed using ECL reagents and x-ray film where it showed that the cellular content of CD14 was only detectable in MM6 cells when stimulated by LPS without 50µg V-antigen co-stimulation

CD14, cluster of differentiation 14; β2M, β-2 microglobulin

Figure 56 shows a clear band at the expected size for CD14 (~55kDa) which does not appear in the unstimulated or V-antigen samples (+/- LPS). This correlates with the expression data in Figure 53A.

TGFβ1 is also upregulated at an mRNA level in response to inflammatory stimuli such as LPS(242). Therefore, a western blot was performed on further lysate from the stimulations in 3.3.5.1 and the same conditions probing for TGFβ1. The results are shown in Figure 57.

Figure 57:

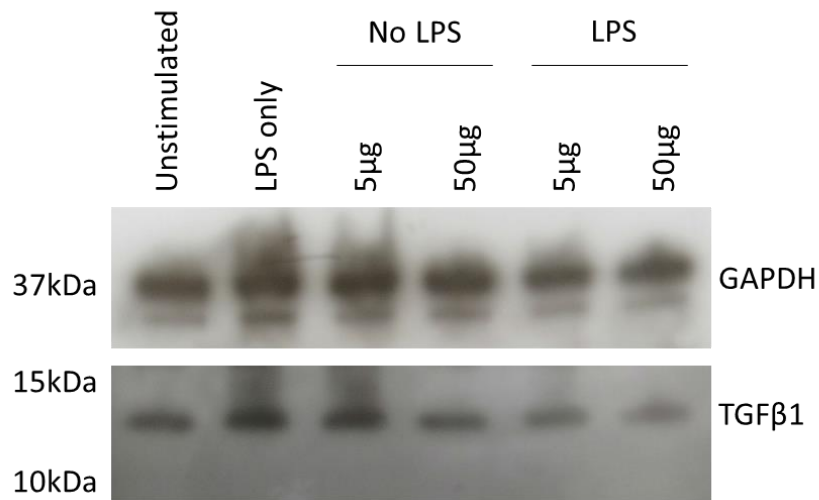


Figure 57 - TGFβ1 western blot on LPS/V-antigen-stimulated MM6 cells – Mono-mac 6 (MM6) cells were seeded at a density of 5×10^4 cells/well on 24 well plates and allowed to attach overnight. After a 30min pre-incubation with/without V-antigen (5μg, 50μg), LPS was added to a final concentration of 100ng/ml or not added at all. After a specified incubation time from the point of LPS addition (or non-addition), the cells were lysed in 2x sample buffer (Appendix A). An SDS-PAGE was run in denaturing, reducing conditions using loading quantities determined by β2M expression (western blot not shown), before being transferred to a nitrocellulose membrane and probed with anti-GAPDH antibody (Abcam ab8245) and anti-TGFβ1 antibody (Cell Signalling Technology #3709) and then anti-mouse-HRP antibody (Dako P0260) and anti-rabbit-HRP antibody (Dako P044801-2). The resulting blot was developed using ECL reagents and x-ray film where it showed that there was no discernible difference in the cellular content of TGFβ1 in MM6 cells at difference concentrations of V-antigen or in the presence or absence of 100ng/ml LPS

GAPDH, glyceraldehyde 3-phosphate dehydrogenase; TGFβ1, transforming growth factor β1

Despite studies reporting an upregulation of TGFβ1 mRNA in response to inflammatory stimuli, none of the samples tested here showed any detectable alteration in intracellular TGFβ1 levels at 12hr, either to LPS or V-antigen.

As TGFβ exists as an inactive, cleaved subunit, there was potential for the activation of the TGFβ molecules to be altered rather than the expression. There was also the chance that the PBMDMs were more responsive than the MM6 cells which may not experience the effects as strongly. This was backed up by the evidence in 3.2.5 where the responsiveness and immunosuppression seen in PBMDMs was shown to be far greater than that in MM6 cells. To see whether any change in secreted, mature TGFβ1 could be detected in PBMDMs, the growth media of three of the four donors used in 4.2.2 and 5.2.2 was analysed. Each sample was analysed in a technical triplicate using the Human/Mouse TGF-beta 1 ELISA Ready-SET-Go kit (eBioscience) and mean secretion levels were established for each donor at each stimulation (2.3.9). The results are shown in Figure 58.

Figure 58:

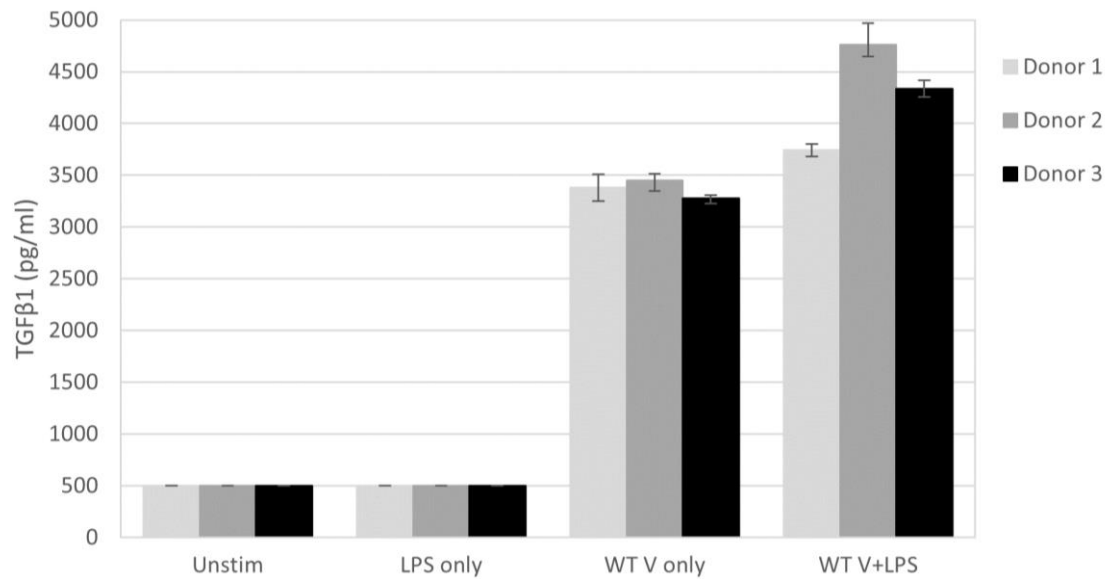


Figure 58 - Secreted mature TGFβ1 ELISA on the growth media of LPS/V-antigen-stimulated PBMDMs – PBMDMs from 3 donors were set up according to the experimental design in Figure 15 and pre-incubated with/without 50µg V-antigen before being stimulated with 0ng/ml or 100ng/ml LPS for 16hr. The growth media was removed and tested using the Human/Mouse TGF-beta 1 ELISA Ready-SET-Go kit (eBioscience) with the results shown for each donor tested in technical triplicates. The graph is presented with 95% confidence interval bars. A two-way ANOVA (with repeated measures) identified a statistical significant interaction between donors and conditions ($F(6, 12) = 798.106$ (p -value = <0.001)). The stimulation conditions were reported as significant (p -value = <0.001) and that of the donors was reported as significant also (p -value = <0.001)

TGFβ1, transforming growth factor β1

The lower detection limit was 500pg/ml within this experiment as determined by the standard curve. No registered levels of mature, secreted TGFβ1 were seen in either the unstimulated or LPS controls after 16hr of stimulation while both V-antigen stimulations, however, had substantial levels of TGFβ1 in their growth media. The control values were assumed to be at the detection limit to offer as robust an analysis as was possible with negative readings. The lack of variation within the control samples for this reason made it difficult to run reliable statistics, however a two-way ANOVA (with repeated measures) identified a significant interaction between the stimulation conditions and the donors - $F(6, 12) = 798.106$ (p -value = <0.001). Both the conditions (p -value = <0.001) and the donors (p -value = <0.001) were reported as having a significant effect on TGFβ secretion.

As the initial statistics had reduced reliability due to the lack of detectable TGFβ from the unstimulated and LPS-stimulated samples, a further two-way ANOVA (with repeated measures) was performed between 'WT V-only' and 'WT V+LPS'. In these results a significant interaction between donors and conditions was also seen: $F(2, 4) = 742.831$ (p -

value = <0.001) and both the conditions (p-value = <0.001) and the donors (p-value = <0.001) were identified as having a significant effect on TGF β secretion.

5.3: Discussion

5.3.1: V-antigen inhibits the transcription of pro-IL-1 β by inhibiting the

TLR pathway:

The pIkBa/IkBa western blot was performed on the same lysate as the pro-IL-1 β /IL-1 β western blots in Chapter 4 (Figure 24) and so, despite the unclear 1hr and 4hr western blots, it is known that the same '50 μ g V-antigen + LPS' sample saw a potentially higher, but at least similar, transcription rate of pro-IL-1 β than other 'V-antigen + LPS' samples. This therefore would have required a similar or larger level of active NF κ B in each 'V-antigen + LPS' sample up to 4hr, in theory. However, at 6hr and 12hr, as with the pro-IL-1 β /IL-1 β western blots, the level of both pIkBa and IkBa begins to decrease compared to the expression in other V-antigen and LPS samples (Table 10) as well as the 'LPS only' control (Figure 40). As the transcription of IkBa is controlled by NF κ B activity, this reduced level was predicted to be caused by a reduction in active NF κ B which was being activated through LPS/TLR4 signalling. Therefore, the reduction in pro-IL-1 β (Figure 24, Chapter 4), another gene controlled largely by NF κ B, was predicted to be caused by the same reduction in NF κ B, rather than an increase in degradation of pro-IL-1 β which could also have led to a reduced intracellular level as well.

5.3.2: V-antigen promotes a TRIF-dominant response to LPS

TLR4 stimulation activates both the TRIF and MyD88 pathways leading to a balanced activation of predominantly-TRIF pathway TFs like IRF3 and predominantly-MyD88 pathway TFs like NF κ B. A key difference between the 'V+LPS' and 'LPS only' samples in 5.2.2 was the decrease in the expression of MyD88 pathway genes (Figure 50) and the increase in viral-response genes (Figure 49) as identified by functional clustering. Although some genes expressed at a level comparable to unstimulated controls or between the level of unstimulated controls and LPS only samples, some genes expressed within the V-antigen samples clearly expressed far more differentially than just being a lesser form of the upregulation/downregulation seen in 'LPS only'. Genes such as NFKB1, NFKB2, NFKBIA, IRAK4, MyD88, and TBK1 were all identified as being significantly downregulated in the presence of V-antigen but, at closer inspection, appear to just show a generalised failure to upregulate to the same degree as they do with LPS alone, likely due to reduced signalling within the TLR pathway and reduced autocrine/paracrine signalling from cytokines. IRF1, IFN γ , and CXCL10 were identified within the 'viral response' functional cluster and all three showed a more interestingly altered expression with IRF1 and IFN γ showing significantly

greater transcription than LPS only and CXCL10 showing upregulation in the presence of V-antigen despite 'LPS only' showing a downregulation. The MyD88 pathway and NFκB – the major TF of the MyD88 pathway – therefore show signs of being generally suppressed which cannot purely be accredited to reduced LPS detection despite CD14 and HSPD1 both having a significant downregulation in V-antigen-stimulated PBMDMs and a failure to upregulate in 'V+LPS' PBMDMs. This is because viral response genes are upregulated and this suggests that, despite reduced LPS detection, the signal from TLR4 is not proportionately transducing down the MyD88 and TRIF pathways. The inhibition of the MyD88 pathway and more prominent expression of TRIF-pathway-associated genes and viral response genes suggests instead that the MyD88 pathway is being selectively inhibited, allowing for an altered balance in the ratio of MyD88:TRIF signalling to give a more prominent TRIF signal by comparison. This in turn pushes the cell into a more viral-associated response with an upregulation of TRIF-pathway components, upregulation of viral chemokines/cytokines, and the downregulation of SARM1 – a TRIF-specific inhibitor.

The large upregulation of IFN γ is also explained by the same theory. An increase in type 1 IFNs like IFN β 1 (Table 14) increases the level of IFN γ via STAT4(243). The lack of control of the IFN γ pathway within human monocytes due to the inability of SOCS1 to inhibit STAT1 as it does in epithelial cells, could also explain why TNF α transcription could be significantly higher(244) in V-antigen samples (Table 14) though due to the difference in expression data between the inflammasome gene array and the TLR gene array (Table 16), further investigation would be required to conclusively show whether TNF α transcription is significantly increased or not.

Targeting the TLR pathway, and specifically the MyD88-dependent pathway, is not uncommon in pathogenic bacteria like *Yersinia pestis*. In fact, *Yersinia pestis* already has documented effector proteins that affect the TLR pathway with YopJ and YopP both inhibiting TAK1(245), MKK3/6(246), MEK2, and IKK(247) by using acetylation within the activation loops of the kinases to prevent activation. YpTIR, another *Y.pestis* virulence protein binds and prevents the activation of MyD88 directly(248). Many other pathogenic species like *Shigella*(249), *Salmonella*(250), *E.coli*(251), and *Chlamydia*(252) all have systems to target and inhibit TLR signalling.

5.3.3: V-antigen utilises TGF β to suppress TLR signalling, cytokine signalling, and subsequent inflammation

The transcriptional changes seen in 5.2.2 suggest a suppression of the MyD88 pathway; a mechanism also shown by TGF β -mediated immunosuppression. TGF β functions through downstream effector proteins such as SOCS1 which, as discussed in 5.3.2, has no effect on suppressing the IFN γ pathway in human monocytes. There are also signs of TGF β involvement from the potentially upregulated transcription of TGF β -associated MAPKs(239, 240) (Figures 38 and 55) which cannot be explained by signalling in the TLR4/IFN γ /TNF α pathways. Further evidence is the reduced levels of CD14 mRNA and protein (Figures 53A and 56) - which have been identified as a trait of TGF β stimulation(253) - and the significantly increased secretion of mature TGF β in PBMDM V-antigen stimulations (Figure 58). This occurs despite no obvious signs of increased TGF β translation (Figure 57), at least in MM6 cells.

It has not been proven whether the induction of TGF β is caused by a direct involvement of V-antigen in the TGF β pathway or whether V-antigen influences another pathway or protein that then causes TGF β maturation and secretion. Targeting the TGF β pathway directly though is not unheard of within bacterial infections - group A *Streptococcus* has previously been shown to utilise the secretion of TGF β to promote the development of Th17 and Treg cells which then hinders an effective immune response to *Streptococci*(254). Regardless of which mechanism it utilises though, the paracrine/autocrine stimulation of active TGF β 1 would cause immunosuppression.

Previous papers analysing V-antigen's effects on cytokine signalling have been largely short-term or limited in their cytokine analysis. They have also largely ignored the internalisation of V-antigen despite early studies suggesting that this was the case. This may be due to the lack of clear evidence supporting internalised V-antigen's role in immunomodulation specifically but could also be due to one study which reported that V-antigen did not internalise without *Yersinia* bacteria present(135). However, unpublished data from Prof Kathy Triantafilou and Dr Martha Triantafilou and the data shown in 3.2.4 (Figure 12, Chapter 3) reveals that the internalisation of recombinant V-antigen into monocytes occurs in the absence of *Y.pestis*. The failure of other studies to include the long-term effects of V-antigen internalisation has generated misleading conclusions from a number of studies where the correlation between V-antigen and the short, rapid IL-10 response was the only immunomodulation considered. This creates some difficulty when analysing V-antigen immunomodulation studies; most are short stimulations that stop before the internalisation of V-antigen and so before the internalisation and change in IL-1 β

secretion seen in Chapter 3, and those which are longer studies often use only a basic panel of cytokines like IL-10 and TNF α .

One of the few long term *in vitro* studies, for example; A.Sing, *et al.* 2005(150) shows that V-antigen promoted a reduced level of TNF α secretion in mouse macrophages when their media was sampled at 21hr (3hr pre-incubation with V-antigen followed by 18hr of 1mg/ml zymosan A stimulation). They also reported that using primary cells from an IL-10 $^{-/-}$ mouse line prevented that reduction in TNF α . However, IL-10 is induced by inflammation naturally (Figure 21B, Chapter 3) and, while 3.3.2 presents evidence that IL-10 may not be responsible for V-antigen's initial immunomodulation, removing it from the system by using IL-10 $^{-/-}$ mouse cells would remove an anti-inflammatory cytokine that also naturally restricts ongoing inflammation. In a closed system such as an *in vitro* cell culture assay as was performed by the group and with a high concentration of stimuli as was used, the unrestricted inflammation coupled with subsequently higher paracrine/autocrine signalling differences could mask the effects of V-antigen's immunomodulation in IL10 $^{-/-}$ cells so that by the point of measuring at 21hr, there is a greater level of TNF α compared to IL-10 $^{+/+}$ cells. This therefore creates a confounding factor in their experiment and without a more diverse cytokine profile, it is impossible to determine whether the IL-10 $^{-/-}$ cells are protected from V-antigen's effects or just respond more strongly to inflammatory stimuli.

Infection/survival studies in the presence/absence of V-antigen remain relevant but still fail to include that V-antigen has multiple roles within infection. These include multiple interactions with both host and bacterial proteins but also include both the IL-10 and TGF β mechanisms of immunomodulation. It is therefore not possible to determine the causative mechanism by which survival is changed by simply looking at the absence/presence of the protein and claims that survival is exclusively affected by the loss of one specific role is not proven by these studies(134).

In vitro mutation studies, both long and short term also lose validity due to the risk that they interfered with the internalisation and/or the internal interactions of V-antigen; something which was not addressed or considered within any studies of this type(150, 153). As before, this creates the potential to confound results unfairly and attribute outcomes incorrectly to the loss of a single function/interaction. *In vivo* studies that mutated proposed TLR2-binding sites also lose validity for the same reasons – internal interactions were not considered or proven to be unaffected(150, 153).

The theory proposed here, therefore, does fit into the current literature. IL-10 has been shown in multiple studies to be highly important in *Yersinia pestis* infection and that IL-10 $^{-/-}$ mice are protected from V-antigen+ *Yersinia pestis* to the same degree as infection with

LcrV- *Y.pestis*(148, 151). It is also already known that IL-10 is an important part of the wider immunosuppressive TGF β response *in vivo*. TGF β induces IL-10 transcription and secretion from naïve T-cells and Th1 T-cells(255, 256) and IL-10 is vital for the expansion of TGF β -induced T-cells and the induction of further TGF β secretion from these cells(257). TGF β and IL-10 work in tandem, and only in tandem, to suppress TLR-pathway-mediated B-cell activation(235). While TGF β has a mild immunosuppressive effect on innate cells, its importance in an *in vivo* system with a functioning adaptive immune system and an experiment that runs over the course of days or even weeks, cannot be understated(258). This is especially as the generated IL-10 would then impact and inhibit the inflammatory response in innate cells on top of the direct effects of TGF β . IL-10 $^{-/-}$ mice will therefore have a severely inhibited TGF β response in survival studies which allows them to respond far more effectively to pathogens like in *Yersinia* challenge experiments. This knowledge, alongside the evidence from Chapter 3 (Figure 21) and evidence from previous papers both *in vivo* and *in vitro*(147, 148), shows that while IL-10 is highly important in the immunomodulatory effects of V-antigen long term, the level induced within the first phase of immunomodulation prior to internalisation cannot be responsible for these effects. In this regard, an immunomodulatory response mediated by TGF β fits entirely with previous findings.

Within the context of *Y.pestis* lifecycle, inhibition of MyD88 specifically and not TRIF also makes biological sense as *Y.pestis* produces tetraacylated LPS at 37°C which is far less stimulatory to TLR4 than hexaacylated LPS(127) and so TRIF activation is minimal in *Y.pestis* infection. TLR-, and specifically MyD88-pathway inhibition is also performed by other *Y.pestis* proteins as mentioned in 5.3.2. Inhibition of the IFN γ would be important too as IFN γ is a key signalling molecule for monocyte/macrophage activation and promotes phagocytic killing. As *Y.pestis* is a facultative intracellular pathogen, this is an important process to inhibit.

Therefore, the induction of TGF β as an anti-inflammatory mechanism of action fits not only the evidence presented in this chapter but also the current literature on V-antigen, TGF β , and *Yersinia pestis*.

6: Chapter 6: Fragments of V-antigen

6.1: Introduction

6.1.1: Chapter introduction

Chapters 3-5 examined the inflammatory response of monocytes and PBMDMs to LPS in the presence and absence of WT V-antigen. Both cytokine signalling and inflammatory-gene expression were examined, and an altered inflammatory response in the presence of V-antigen was characterised. V-antigen however is a multifunctional protein that has multiple roles within *Yersinia* infection and numerous protein interactors, both bacterial and host. In the interest of therapeutic applications, this poses the potential for numerous unknown side effects. Isolating the immunomodulatory region from the WT protein therefore creates a far more appealing potential therapeutic.

In this chapter, peptide fragments corresponding to a central portion of the V-antigen protein were subjected to the same analyses of cytokines and inflammatory-gene expression with the purpose of generating comparable datasets to that of the WT protein. Comparisons were then drawn between the individual fragments and the WT to establish whether any of the fragments retained their immunomodulatory capabilities.

6.1.2: Defined regions of V-antigen

Protein structure is invariably tied to protein function and therefore understanding the structure of a protein can help identify functional regions. The full structure of V-antigen was detailed by *U.Derewenda, et al. 2004*(131) who showed that it has a 'dumbbell-like structure' made of two globular domains and a certain 'grip' region consisting of a coiled coil of $\alpha 7$ (aa148-183) and $\alpha 12$ (aa279-317) (Figure 59A). The whole protein contains at least 12 α -helixes in total and 9 β -sheets and contains an internal cysteine loop at aa261-281. Analysis of multiple primary sequences revealed a hypervariable region across aa40-61(150) and a set of highly conserved regions at aa160-175 and aa257-320(259) that correlate with the coiled coil 'grip' domain. Another hypervariable site has also been reported at aa225-232 however this has been disputed(260).

Functionally, there have also been several regions highlighted by previous studies. V-antigen's association with the YopB/YopD pore, for example, has been attributed to aa127-195(261) and its interaction with LcrG has been attributed to two alpha-helix regions; aa152-165 and aa290-311(262). The TLR2 binding site has been repeatedly identified as lying within the regions aa31-57 and aa203-205(149, 150, 152) and one study specifically

highlighted the role of aa33, 34, 42, 204, and 205 as the residues responsible for TLR2 binding(152). However, a later mutational study performed on these residues saw no difference in TLR2 binding mechanics when they were individually or collectively mutated(153) so it is unclear if these residues are indeed involved. A similar set of regions – aa41-43 and aa203-205 – were also reported to be responsible for CD14 binding(144).

While many of the studies above have identified regions through site mutation, others have identified a loss of function, or no loss of function, via deletion of specific regions. For example, it is possible for V-antigen to still induce IL-10 secretion when the first 67 residues of the N-terminus are deleted(142). A deletion of aa25-40 led to reduced LcrV secretion from *Y.pestis* whereas a deletion of aa108-125 abolished it entirely(263), both without affecting regulation of the LCR gene operon. Deleting the region that spans aa188-207 however led to the total repression of the LCR operon, even in low calcium conditions. Also, it was noted that deletion of residues aa271-300 prevented V-antigen from inhibiting the inflammatory response and abolished the lethality associated with V-antigen-expressing *Y.pestis*(264).

Finally, immunological studies have also highlighted two specific regions of importance within V-antigen. These were two epitopes that provoked a protective host response when targeted by the immune system (1.2.2.1). One protective epitope, considered the minor protective epitope, is located between aa2-135 whilst the major protective epitope is located between aa135-275, crossing the two highly conserved regions and the α 7 coiled coil 'grip' domain(142, 265).

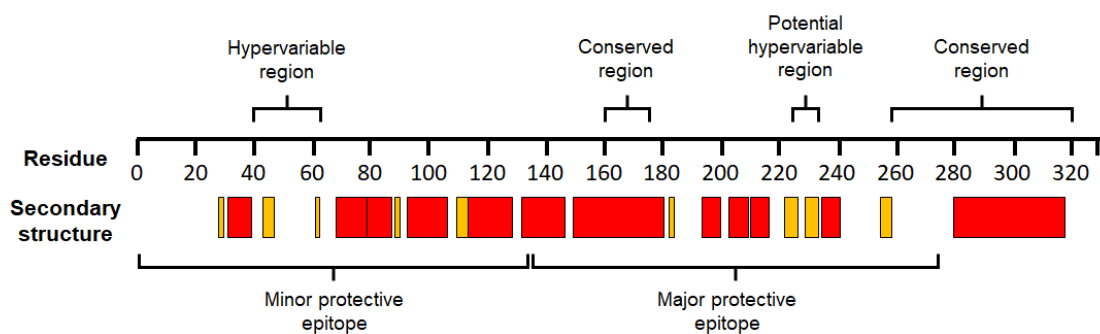
Key regions of V-antigen structure have been highlighted in Figure 59.

Figure 59:

A



B



C

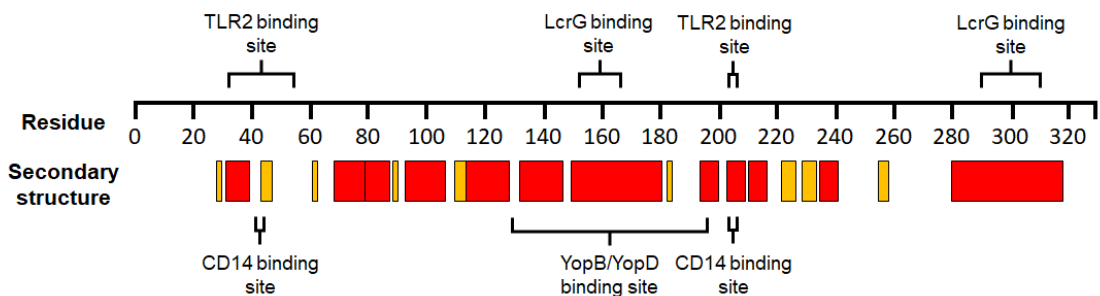


Figure 59 – The tertiary structure of V-antigen and key functional regions – A; The tertiary structure of WT V-antigen as determined by S.Chaudhury, et al. 2013, with secondary structures highlighted using the RCSB Protein Data Bank online resource – beta-sheets (yellow) and alpha folds (red). **B;** Key structural regions within V-antigen including both protective epitopes and noted sites of residue variability and conservation. **C;** Key interaction sites within V-antigen’s structure as reported by previous studies

6.1.3: V-antigen fragments in this study

The V-antigen fragments used in this chapter were developed by Dr Claire Vernazza who produced gene fragments that correspond to a central epitope of V-antigen between aa135-275(265). This epitope covers the major protective epitope (Figure 59 and Figure 60). The plasmid that expresses them are the same as that described in 3.2.1 as well as the GST-tag attached to the fragments. The fragment details are presented in Table 17 and Figure 60.

Table 17 - Recombinant V-antigen fragment details

Fragment name	Region encoded (aa)
pV1	135-275
pV2	168-275
pV3	175-275
pV4	135-268
pV5	135-262
pV6	135-275 Δ 218-234

The encoded region of each V-antigen fragment (pV1-pV6) and the residues each fragment correlates to from the WT V-antigen protein

Figure 60:

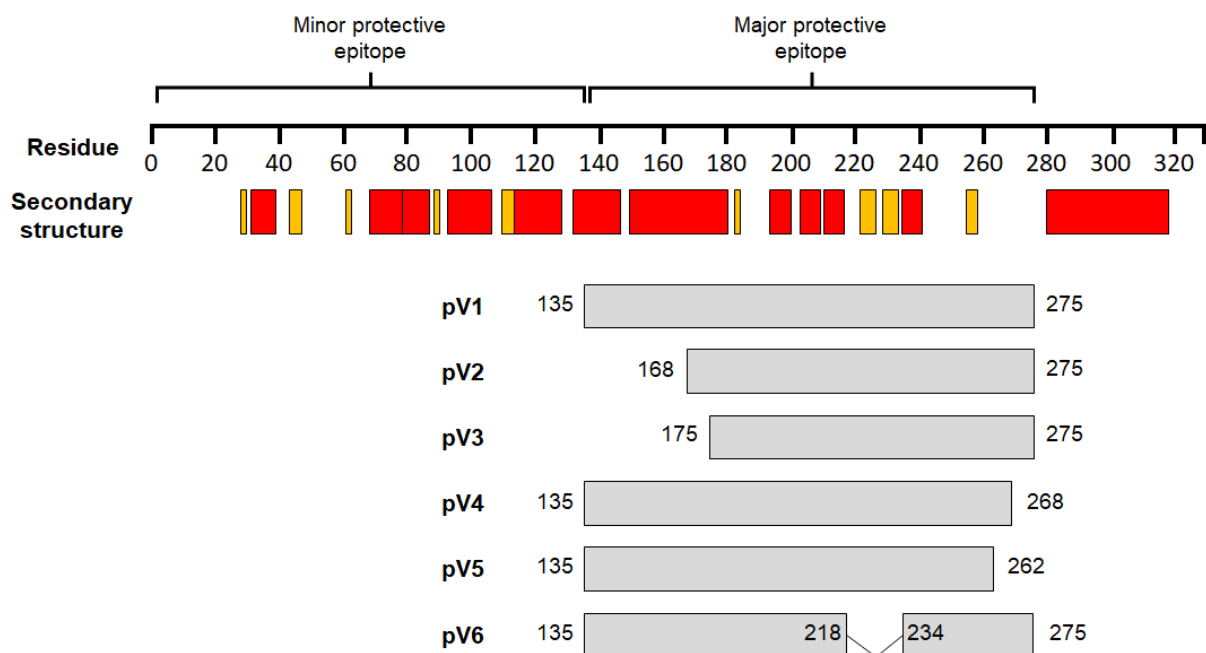


Figure 60 – Location of V-antigen fragments (pV1-pV6) within the WT V-antigen structure – The V-antigen fragments used within this study are located over the major protective epitope (aa 135-275) within WT V-antigen. Presented are the secondary structural elements of WT V-antigen – beta-sheets (yellow) and alpha folds (red) – as well as the location of the V-antigen fragments alongside these

pV1 represents the full protective epitope. pV2 and pV3 were both identified as containing the same protective capabilities in a previous study by the same group(159). pV4 and pV5 omit parts of a loop structure between 262-275 to different degrees – pV5 removes the full loop structure and pV4 leaves part of the structure to cover a potentially lipophilic region of the peptide. Finally, pV6 covers the full 135-275 region but with a central deletion between 218-234 which removes two β -sheets that were not believed to be involved in the antibody binding.

6.1.4: Chapter aims

The aims of the experiments in this chapter are:

- To generate peptide fragments associated with the major protective epitope of V-antigen that can be used to compare responses with the WT protein
- To create a comparative dataset of the inflammatory response to LPS in the presence and absence of each of these fragments using the same techniques outlined in chapters 3, 4, and 5
- To utilise the results of these experiments to determine whether any of the V-antigen fragments retain the ability to modulate the inflammatory response like the WT protein

6.2: Results

6.2.1: Purification of fragments

The V-antigen fragments were expressed via the same method as the WT protein. *E.coli* transformed with the respective plasmids were grown and then incubated for 6hr with IPTG to induce fragment-gene expression. The fragments were then purified through GST-tag column purification and passed through columns filled with Pierce™ Endotoxin Removal Resin to remove remaining LPS from the sample. This process is fully detailed in 3.2.3. Figure 10 (Chapter 3) shows proteins at the expected size of the monomeric and multimeric fragments, confirming the presence of the fragments in the final sample after purification.

6.2.2: Cytokine analysis

To draw comparisons between the fragments and the WT V-antigen, similar stimulations to those in 3.2.5 needed to be run. PBMDMs from 3 independent donors were stimulated with 50µg of each of the fragments for 30min, before 100ng/ml LPS was added and left to incubate with the cells for 16hr at 37°C/5% CO₂ (Figure 15). Alongside this, controls of unstimulated cells, LPS-only stimulated cells (100ng/ml), and V-antigen fragment-only-stimulated cells were also run to the same timings as shown in Figure 15. After the stimulation, the growth media was removed for cytokine analysis and the cells were either lysed in 2x sample buffer in preparation for future protein analysis (2 of the donors) or analysed for cell viability by trypan blue. No indication of reduced cell viability was seen in any of the conditions.

The secreted cytokine concentration was then measured using the 7-plex™ MSD Multi-spot assay which detected a panel of 6 proinflammatory cytokines (IL-1β, IL-6, IL-12p70, IL-8, IFNγ and TNFα) and 1 anti-inflammatory cytokine (IL-10). Unfortunately, due to contamination of the pV4 and pV5 stimulations and insufficient protein yield to repeat the experiment, it was not possible to continue with their data collection and so they were excluded from the analysis and comparison with WT V-antigen. Figures 61 to 66 show the cytokine graphs for IL-1β, IL-6, IL-8, IFNγ, TNFα, and IL-10 for pV1, pV2, pV3, and pV6.

Figure 61:

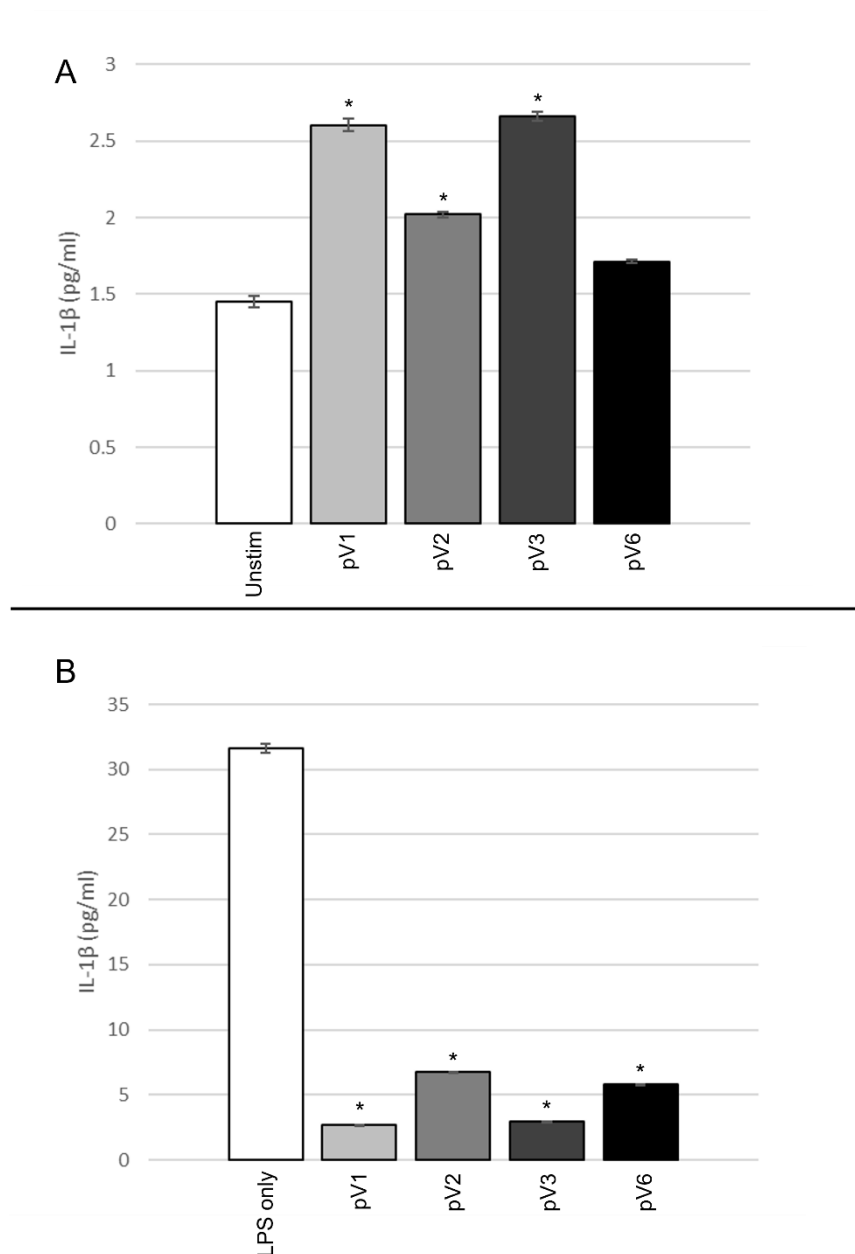


Figure 61 - IL-1 β secretion in PBMDMs in response to V-antigen fragment stimulation (+/- LPS) – PBMDMs were set up according to the experimental design in Figure 15 and were pre-incubated with/without 50 μ g V-antigen fragments (pV1-pV6) before stimulation with A; 0ng/ml LPS or B; 100ng/ml LPS for 16hr. The growth media harvested from these stimulations were analysed using a 7-plex MSD Multi-spot Assay system kit to determine the level of IL-1 β that had been secreted. The data from all donors was pooled for each V-antigen fragment and a one-way ANOVA was performed using an SPSS statistics package. Statistically significant differences compared to the 0 μ g V-antigen control (*) (p -value = <0.05) were then determined through Tukey's post-hoc analysis. The data presented shows cytokines collected in technical triplicate and $n=3$

All 4 of the tested fragments stimulated very little IL-1 β secretion in the absence of LPS despite having significantly higher levels of expression than the unstimulated control (Figure 61A). In LPS-stimulated samples though, all 4 of the fragments reduced the level of secreted

IL-1 β in the samples. In particular, pV1 and pV3 had very strong inhibition of the IL-1 β response (Figure 61B).

Figure 62:

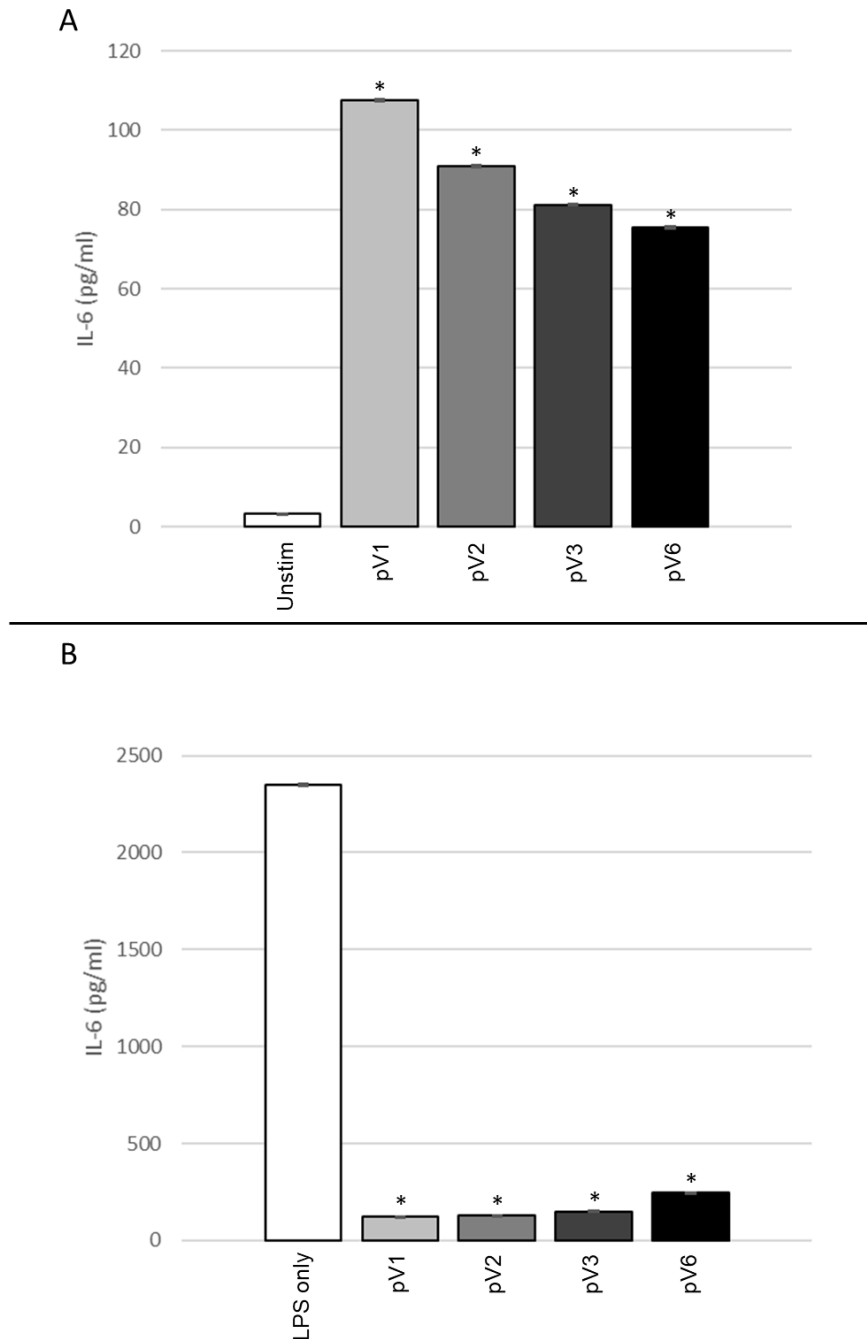


Figure 62 - IL-6 secretion in PBMDMs in response to V-antigen fragment stimulation (+/- LPS) – PBMDMs were set up according to the experimental design in Figure 15 and were pre-incubated with/without 50 μ g V-antigen fragments (pV1-pV6) before stimulation with A; 0ng/ml LPS or B; 100ng/ml LPS for 16hr. The growth media harvested from these stimulations were analysed using a 7-plex MSD Multi-spot Assay system kit to determine the level of IL-6 that had been secreted. The data from all donors was pooled for each V-antigen fragment and a one-way ANOVA was performed using an SPSS statistics package. Statistically significant differences compared to the 0 μ g V-antigen control (*) (p-value = <0.05) were then determined through Tukey's post-hoc analysis. The data presented shows cytokines collected in technical triplicate and n=3

IL-6 however, evidenced that the fragments still stimulated an inflammatory response when incubated with PBMDMs with all the fragments showing a significantly higher level of secreted IL-6 (Figure 62A). LPS-stimulated PBMDMs though saw a significantly reduced level of secreted IL-6 when co-stimulated with any of the V-antigen fragments (Figure 62B).

Figure 63:

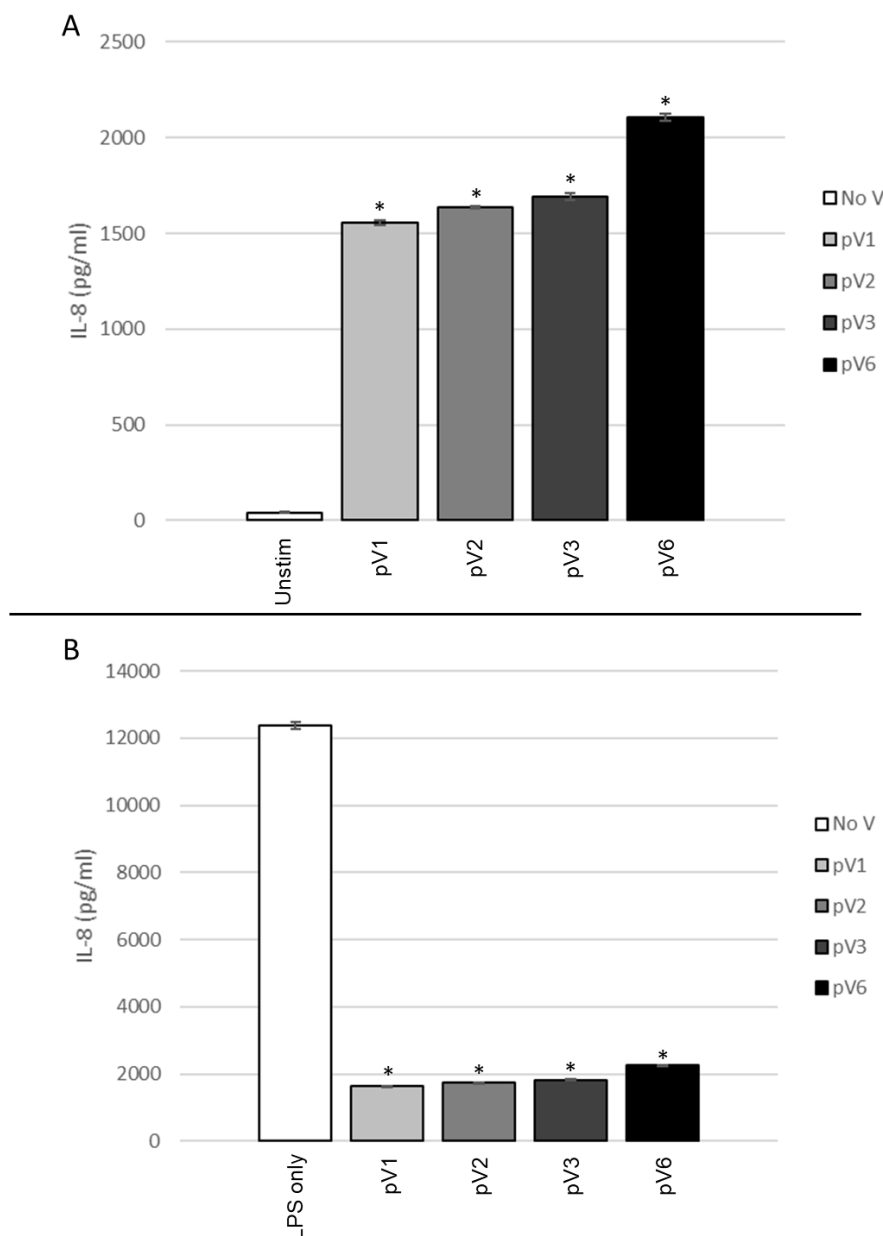


Figure 63 - IL-8 secretion in PBMDMs in response to V-antigen fragment stimulation (+/- LPS) – PBMDMs were set up according to the experimental design in Figure 15 and were pre-incubated with/without 50µg V-antigen fragments (pV1-pV6) before stimulation with A; 0ng/ml LPS or B; 100ng/ml LPS for 16hr. The growth media harvested from these stimulations were analysed using a 7-plex MSD Multi-spot Assay system kit to determine the level of IL-8 that had been secreted. The data from all donors was pooled for each V-antigen fragment and a one-way ANOVA was performed using an SPSS statistics package. Statistically significant differences compared to the 0µg V-antigen control (*) (p-value = <0.05) were then determined through Tukey's post-hoc analysis. The data presented shows cytokines collected in technical triplicate and n=3

As above, all of the recombinant fragments show an ability to trigger IL-8 secretion in the absence of LPS (Figure 63A) and yet, in the presence of it, suppress IL-8 secretion significantly (Figure 63B).

Figure 64:

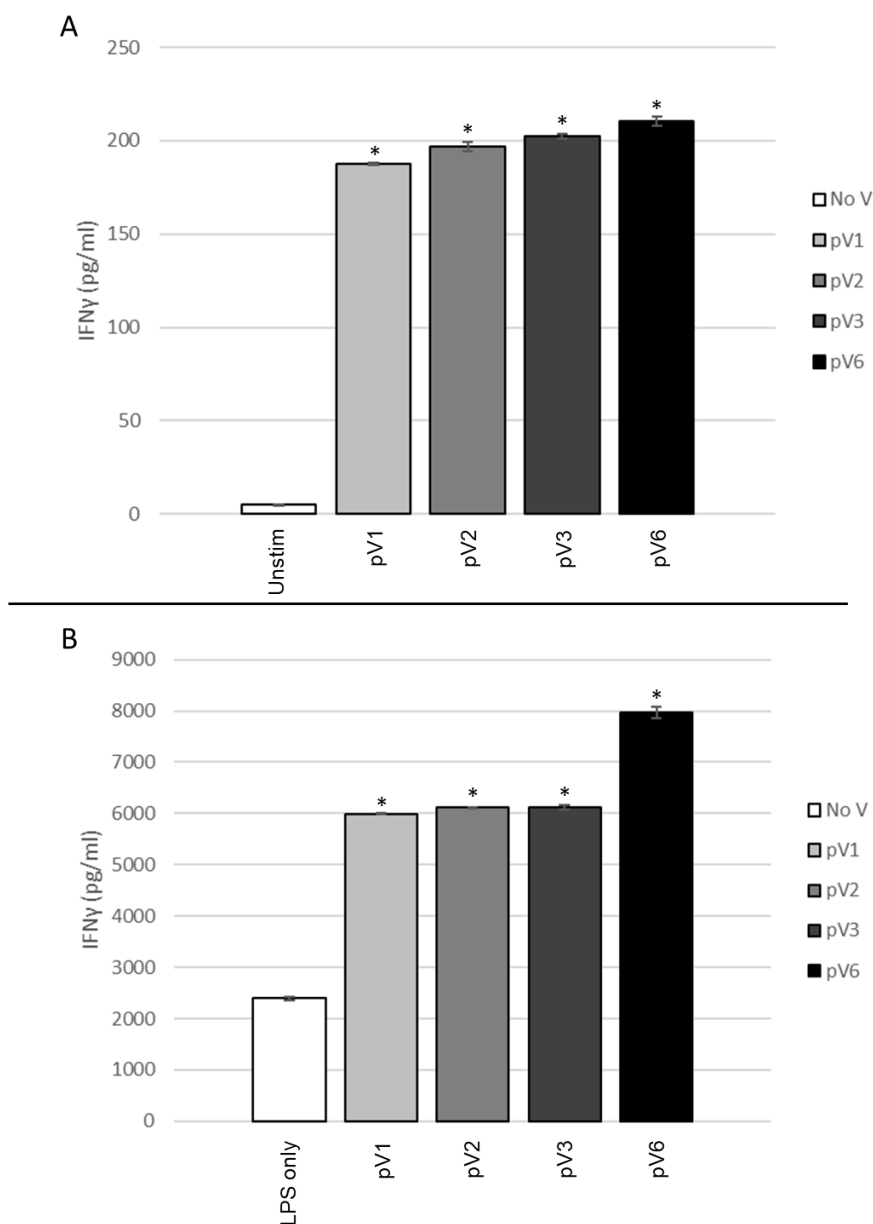


Figure 64 - IFN γ secretion in PBMDMs in response to V-antigen fragment stimulation (+/- LPS) – PBMDMs were set up according to the experimental design in Figure 15 and were pre-incubated with/without 50 μ g V-antigen fragments (pV1-pV6) before stimulation with A; 0ng/ml LPS or B; 100ng/ml LPS for 16hr. The growth media harvested from these stimulations were analysed using a 7-plex MSD Multi-spot Assay system kit to determine the level of IFN γ that had been secreted. The data from all donors was pooled for each V-antigen fragment and a one-way ANOVA was performed using an SPSS statistics package. Statistically significant differences compared to the 0 μ g V-antigen control (*) (p -value = <0.05) were then determined through Tukey's post-hoc analysis.

The data presented shows cytokines collected in technical triplicate and $n=3$

All four fragments also induce IFN γ secretion without co-stimulation with LPS (Figure 64A). However, unlike with the other cytokines analysed above, in the presence of LPS, all four fragments induce a significantly higher secretion of IFN γ than LPS-stimulated control cells (Figure 64B). The difference is a roughly 2.4-fold increase, except for in the case of pV6 which shows a 3.2-fold increase.

Figure 65:

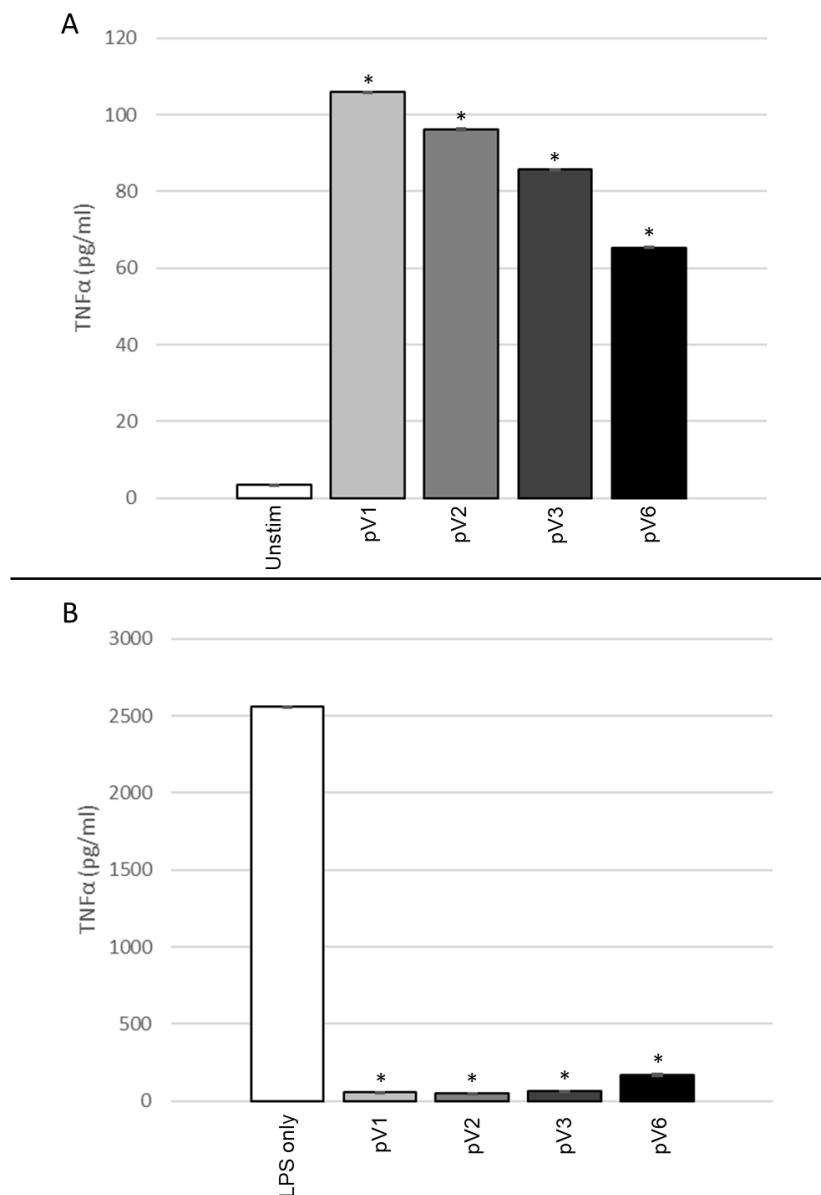


Figure 65 - TNF α secretion in PBMDMs in response to V-antigen fragment stimulation (+/- LPS) – PBMDMs were set up according to the experimental design in Figure 15 and were pre-incubated with/without 50 μ g V-antigen fragments (pV1-pV6) before stimulation with A; 0ng/ml LPS or B; 100ng/ml LPS for 16hr. The growth media harvested from these stimulations were analysed using a 7-plex MSD Multi-spot Assay system kit to determine the level of TNF α that had been secreted. The data from all donors was pooled for each V-antigen fragment and a one-way ANOVA was performed using an SPSS statistics package. Statistically significant differences compared to the 0 μ g V-antigen control (*) (p -value = <0.05) were then determined through Tukey's post-hoc analysis. The data presented shows cytokines collected in technical triplicate and $n=3$

The levels of TNF α (Figure 65) show a similar trend to the IL-6 graphs (Figure 62) with each of the fragments showing a significant increase over the unstimulated control when incubated without LPS. The response is similar too in that pV1 shows the highest levels of secretion, then pV2, pV3, and finally pV6. However, when co-incubated with LPS, all of the fragments reduce secretion of TNF α . In that instance, pV2 has the lowest level of TNF α , then pV1, pV3, and pV6.

Figure 66:

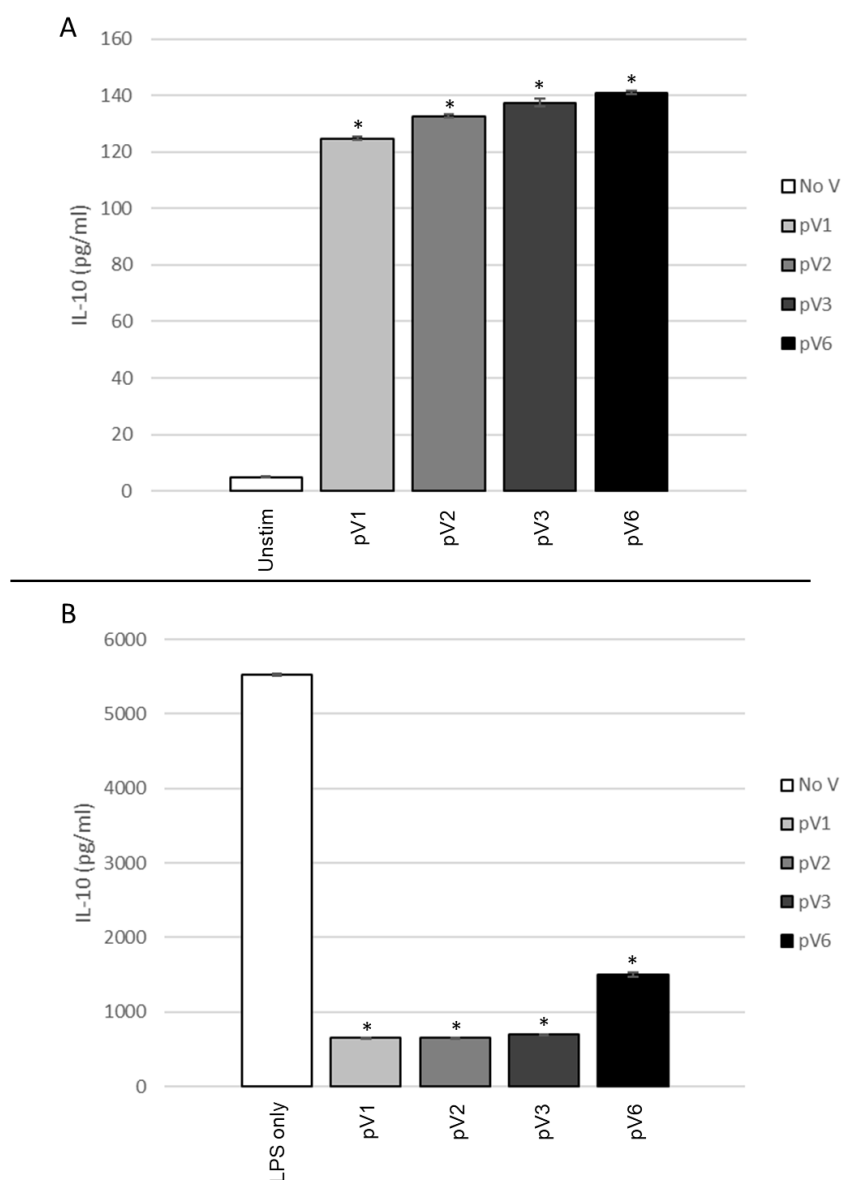


Figure 66 - IL-10 secretion in PBMDMs in response to V-antigen fragment stimulation (+/- LPS) – PBMDMs were set up according to the experimental design in Figure 15 and were pre-incubated with/without 50 μ g V-antigen fragments (pV1-pV6) before stimulation with A; 0ng/ml LPS or B; 100ng/ml LPS for 16hr. The growth media harvested from these stimulations were analysed using a 7-plex MSD Multi-spot Assay system kit to determine the level of IL-10 that had been secreted. The data from all donors was pooled for each V-antigen fragment and a one-way ANOVA was performed using an SPSS statistics package. Statistically significant differences compared to the 0 μ g V-antigen control (*) (p -value = <0.05) were then determined through Tukey's post-hoc analysis. The data presented shows cytokines collected in technical triplicate and $n=3$

Secretion of IL-10 is induced to a significantly higher degree within PBMDMs stimulated with the V-antigen fragments alone (Figure 66A) but when co-stimulated with LPS, the level of IL-10 is significantly lower than control cells that are stimulated with LPS alone (Figure 66B). The secreted level of IL-10 in pV6 is not reduced to the same degree as pV1, pV2, and pV3 though is still significantly reduced over the control.

6.2.3: TLR-related gene analysis

A separate set of stimulations to those run in 6.2.2 were performed with the same set-up as is shown in Figure 15. These were performed under the same conditions and also for 16hr LPS-stimulation with the exception that, due to donor cell availability, 6 independent donors were used – 3 for pV1 and pV2, and 3 for pV3 and pV6. At the endpoint of the stimulation, the cells were lysed in RLT buffer and cDNA was generated from the isolated RNA. This was subsequently loaded onto the Human TLR Qiagen RT² profiler gene array along with SYBR green PCR reagents and subjected to 40 rounds of PCR in a qPCR thermocycler according to the protocol in 2.2.4. A full table of the genes within the gene array are given in Table 11 (Chapter 5).

The resulting data was then handled and analysed in the same way as the WT data in 4.2.2 to ensure the datasets were comparable. This included normalising genes around the β 2M gene and categorising genes as upregulated or downregulated only when they have a p-value of <0.05 and a fold-regulation of >1.5 or <-1.5 respectively. Figures 67 and 68 show clustergrams of relative gene expression levels for each gene. The full data as compared to the unstimulated controls are available in Supplementary Tables 3 and 4.

Figure 67:

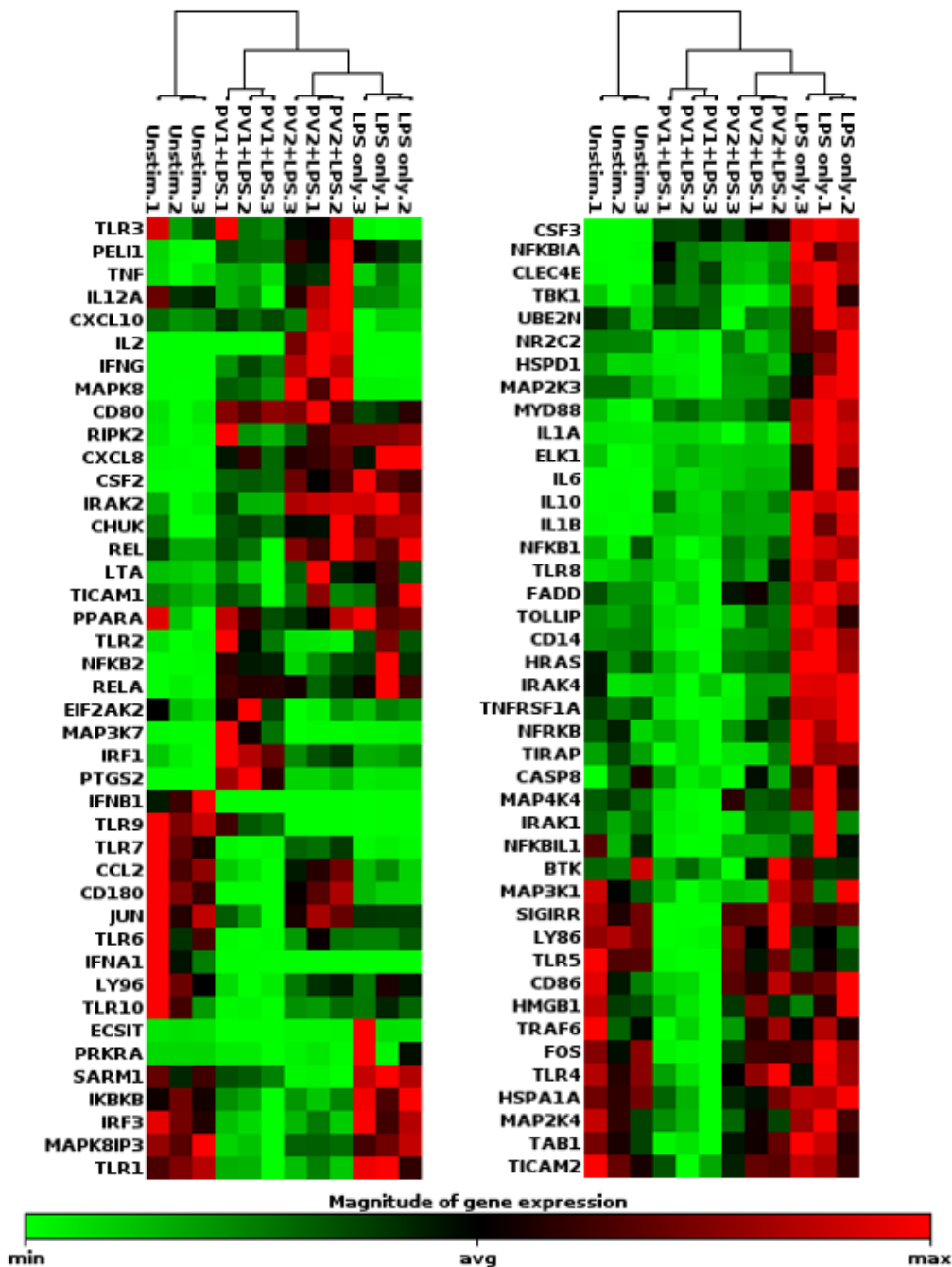


Figure 67 - Clustergram of Qiagen RT² qPCR - Human TLR pathway gene array results for pV1/pV2 (+LPS) – PBMDMs from 3 separate donors were set up according to the experimental design in Figure 15 with PBMDMs pre-incubated with/without 50µg V-antigen fragments (pV1/pV2) and then stimulated with 0ng/ml or 100ng/ml LPS for 16hr. The cells were then lysed, and the RNA was extracted for qPCR analysis using the Qiagen RT² profiler - Human TLR pathway gene array plate. Using the Qiagen Geneglobe analysis software, a clustergram was generated from the resulting data showing the relative expression of each of the genes across all conditions and donors

Figure 68:

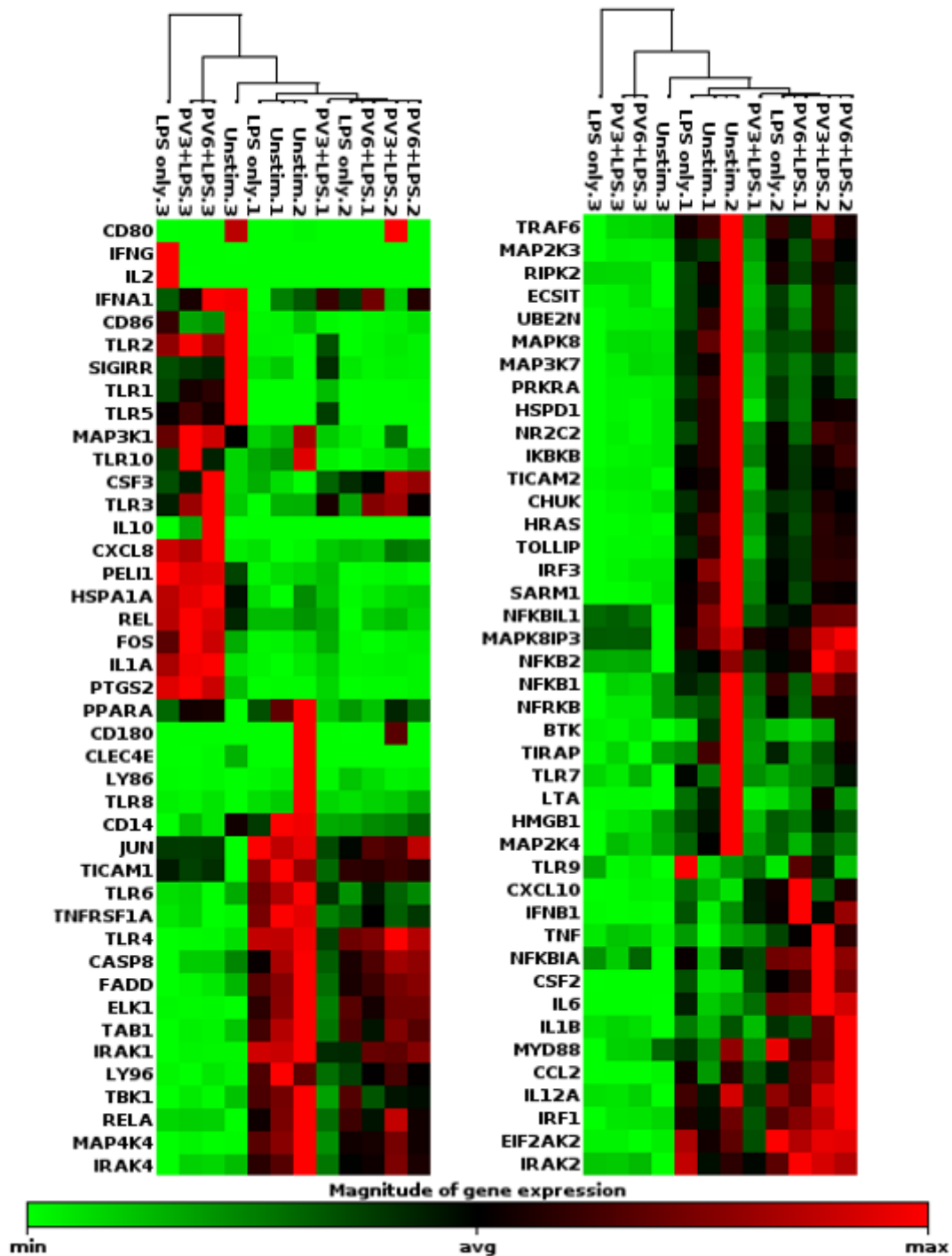


Figure 68 -Clustergram of Qiagen RT² qPCR - Human TLR pathway gene array results for pV3/pV6 (+LPS) – PBMDMs from 3 separate donors were set up according to the experimental design in Figure 15 with PBMDMs pre-incubated with/without 50µg V-antigen fragments (pV3/pV6) and then stimulated with 0ng/ml or 100ng/ml LPS for 16hr. The cells were then lysed, and the RNA was extracted for qPCR analysis using the Qiagen RT² profiler - Human TLR pathway gene array plate. Using the Qiagen Geneglobe analysis software, a clustergram was generated from the resulting data showing the relative expression of each of the genes across all conditions and donors

As in 4.2.2, volcano plots were generated using the Qiagen Geneglobe Analysis software to show graphically the gene expression changes between the LPS only control and the unstimulated control. This was performed to ensure that the donors were responding appropriately to LPS stimulation and causing clear transcriptional changes within the cells. The volcano plot for the pV3/pV6 dataset (Figure 69) reveals that the donors used for the pV3 and pV6 plate did not generate an appropriate response. Although there appears to be numerous genes which have altered expression, there are only two genes that do so with significance and could be reliably classified as up- or downregulated. This suggests an abnormally high level of variability within the dataset and so it could not be analysed any further.

Figure 69:

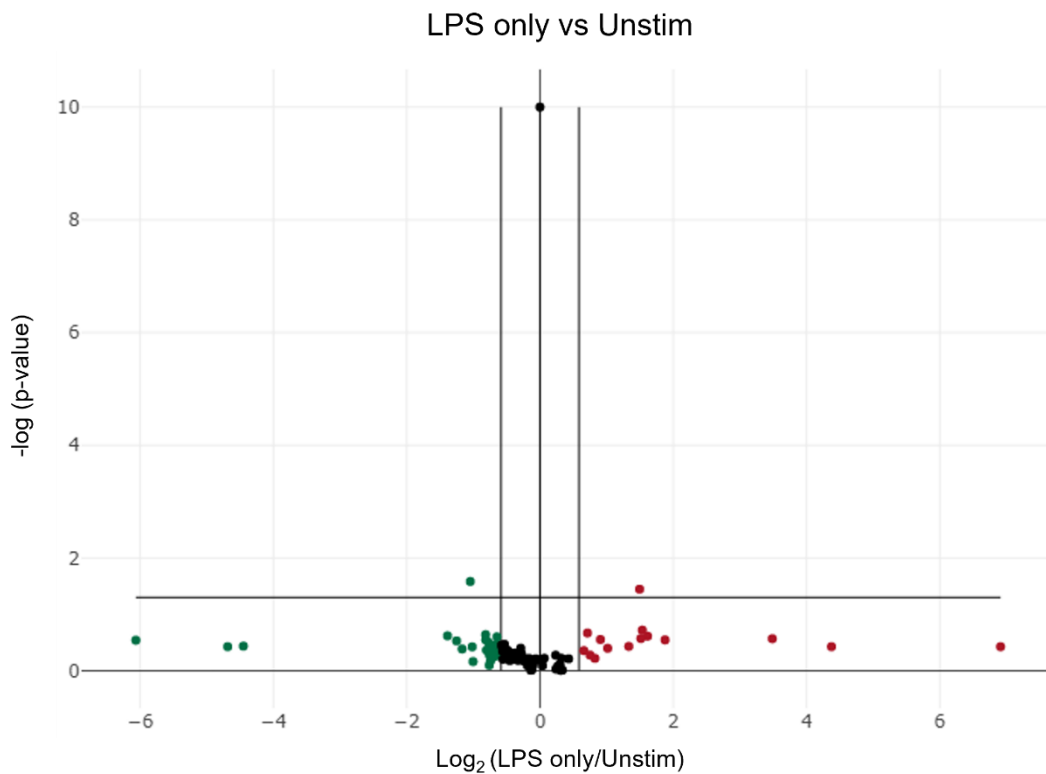


Figure 69 - Volcano plot of 'LPS only' gene expression compared to 'unstimulated' control expression (pV3/pV6 plate) – TLR pathway gene array – PBMDMs from 3 separate donors were set up according to the experimental design in Figure 15 with PBMDMs pre-incubated with/without 50 μ g V-antigen fragments (pV3/pV6) for 30min and then stimulated with 0ng/ml or 100ng/ml LPS for 16hr. The cells were then lysed, and the RNA was extracted for qPCR analysis using the Qiagen RT² profiler - Human TLR pathway gene array plate. Average gene expression for each gene within 100ng/ml LPS-stimulated PBMDMs (LPS only) and unstimulated control PBMDMs (unstimulated) was determined and compared using a volcano plot generated by the Qiagen Geneglobe analysis software. Genes with a >1.5-fold regulation (red) and genes <-1.5-fold regulation (green) were highlighted and the horizontal line was added to represent the p-value 0.05

The same analysis was performed on the pV1/pV2 dataset and this time, the change in gene expression between LPS stimulated cells and unstimulated cells was much more

reliable. Figure 70 is the volcano plot showing the change in gene expression between LPS-stimulated and unstimulated control cells and Tables 18 and 19 give the full list of genes that were identified as being upregulated or downregulated in response to LPS. STRING analysis of the upregulated genes revealed clusters of: 'response to bacterium' and 'response to LPS' at a high strength and a low FDR. The full protein network, with these clusters highlighted, is presented in Figure 71.

Figure 70:

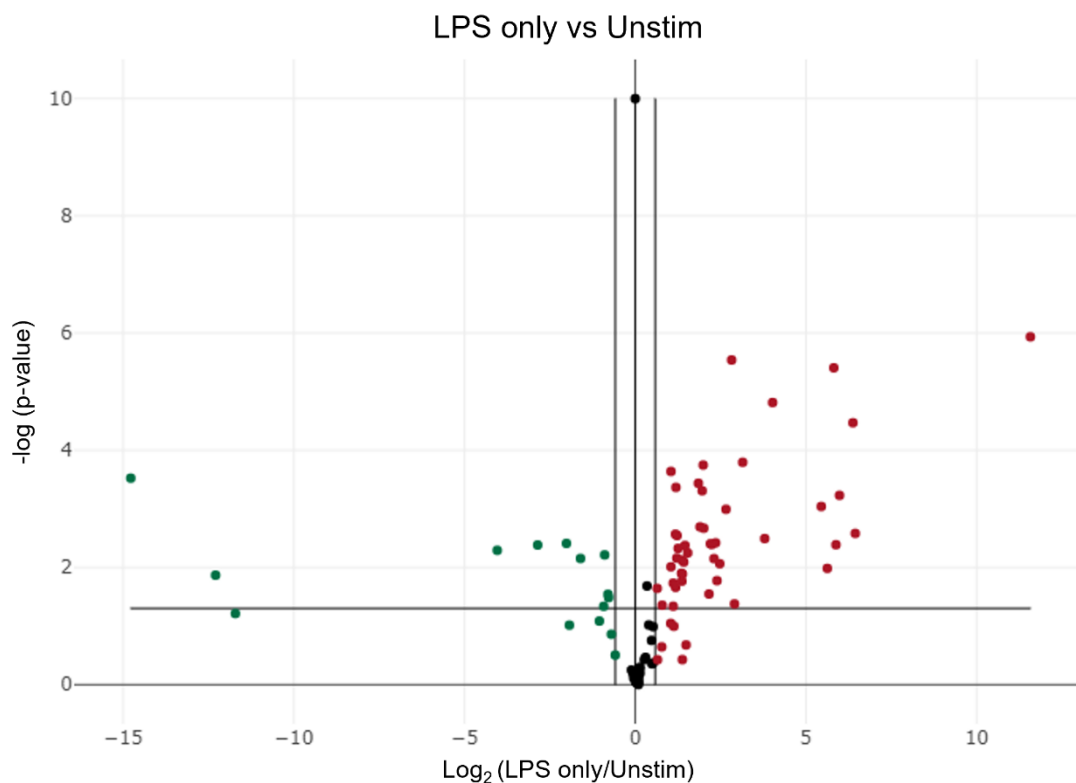


Figure 70 - Volcano plot of 'LPS only' gene expression compared to 'unstimulated' control expression (pV1/pV2 plate) – TLR pathway gene array – PBMDMs from 3 separate donors were set up according to the experimental design in Figure 15 with PBMDMs pre-incubated with/without 50µg V-antigen fragments (pV1/pV2) for 30min and then stimulated with 0ng/ml or 100ng/ml LPS for 16hr. The cells were then lysed, and the RNA was extracted for qPCR analysis using the Qiagen RT² profiler - Human TLR pathway gene array plate. Average gene expression for each gene within 100ng/ml LPS-stimulated PBMDMs (LPS only) and unstimulated control PBMDMs (unstimulated) was determined and compared using a volcano plot generated by the Qiagen Geneglobe analysis software. Genes with a >1.5-fold regulation (red) and genes <-1.5-fold regulation (green) were highlighted and the horizontal line was added to represent the p-value 0.05

Table 18 - Upregulated genes within LPS-stimulated PBMDMs (pV1/pV2 plate)

Gene Symbol	Fold Regulation	p Value	Comment
CD14	3.60	0.000366	
CD80	4.73	0.004045	
CHUK	4.02	0.002140	
CLEC4E	83.05	0.000034	
CSF2	87.06	0.002623	A

CSF3	3047.46	0.000001	A
ELK1	13.84	0.003213	A
FADD	2.28	0.000430	
HRAS	2.34	0.002856	
HSPD1	5.26	0.016803	
IL10	56.29	0.000004	
IL1A	16.25	0.000015	A
IL1B	63.18	0.000588	
IL2	2.16	0.045917	
IL6	58.83	0.004094	A
CXCL8	49.34	0.010380	
IRAK2	3.89	0.000491	
IRAK4	2.39	0.004722	
IRF1	2.27	0.021908	
LTA	2.60	0.012916	
MAP2K3	2.58	0.017153	
MAP3K7	2.06	0.009752	
MAP4K4	2.16	0.018517	
MAPK8	5.56	0.008648	
MYD88	8.85	0.000160	
NFKB1	3.73	0.002028	
NFKB2	7.50	0.041893	
NFKBIA	43.67	0.000911	
NFRKB	2.90	0.005649	A
NR2C2	2.32	0.006920	
PELI1	5.11	0.003797	
PTGS2	6.31	0.001017	
REL	2.59	0.007446	
RELA	4.95	0.007063	
RIPK2	7.07	0.000003	
SARM1	1.56	0.022757	
TBK1	4.59	0.003941	
TIRAP	2.26	0.002708	
TLR2	4.47	0.028406	
TLR8	3.97	0.000179	
TNFRSF1A	2.07	0.000230	
TOLLIP	2.68	0.008100	
UBE2N	2.55	0.012597	

PBMDMs from 3 separate donors were set up according to the experimental design in Figure 15 with PBMDMs pre-incubated with/without 50µg V-antigen fragments (pV1/pV2) for 30min and then stimulated with 0ng/ml or 100ng/ml LPS for 16hr. The cells were then lysed, and the RNA was extracted for qPCR analysis using the Qiagen RT² profiler - Human TLR pathway gene array plate. Average gene expression for each gene within 'LPS only' and 'unstimulated' controls was compared, and a Student's T-test was performed via the Qiagen Geneglobe analysis software. Genes upregulated by LPS (genes with >1.5-fold regulation and <0.05 p-value as determined by Student's T-test) are presented in the table above

'Comments' are: A; the gene's average threshold value is high (>30) in one group and low (<30) in the other, B; the gene's average threshold value is >30 in both samples and the p-value for the fold-change is unavailable or high (p>0.05), C; the gene's average threshold value is above the cut-off or undetected in all samples and so is unreliable and cannot be used

Table 19 - Downregulated genes within LPS-stimulated PBMDMs (pV1/pV2 plate)

Gene Symbol	Fold Regulation	p Value	Comment
CCL2	-4.04	0.003888	
CD180	-7.25	0.004138	
CXCL10	-3.04	0.007023	
IFNB1	-5016.87	0.013548	A
IL12A	-1.72	0.032744	
JUN	-1.74	0.028707	
LY86	-1.86	0.006109	
TLR5	-1.90	0.046020	
TLR7	-16.47	0.005102	
TLR9	-28071.09	0.000299	A

PBMDMs from 3 separate donors were set up according to the experimental design in Figure 15 with PBMDMs pre-incubated with/without 50µg V-antigen fragments (pV1/pV2) for 30min and then stimulated with 0ng/ml or 100ng/ml LPS for 16hr. The cells were then lysed, and the RNA was extracted for qPCR analysis using the Qiagen RT² profiler - Human TLR pathway gene array plate. Average gene expression for each gene within 'LPS only' and 'unstimulated' controls was compared, and a Student's T-test was performed via the Qiagen Geneglobe analysis software. Genes downregulated by LPS (genes with <-1.5-fold regulation and <0.05 p-value as determined by Student's T-test) are presented in the table above

'Comments' are: A; the gene's average threshold value is high (>30) in one group and low (<30) in the other, B; the gene's average threshold value is >30 in both samples and the p-value for the fold-change is unavailable or high (p>0.05), C; the gene's average threshold value is above the cut-off or undetected in all samples and so in unreliable and cannot be used

Figure 71:

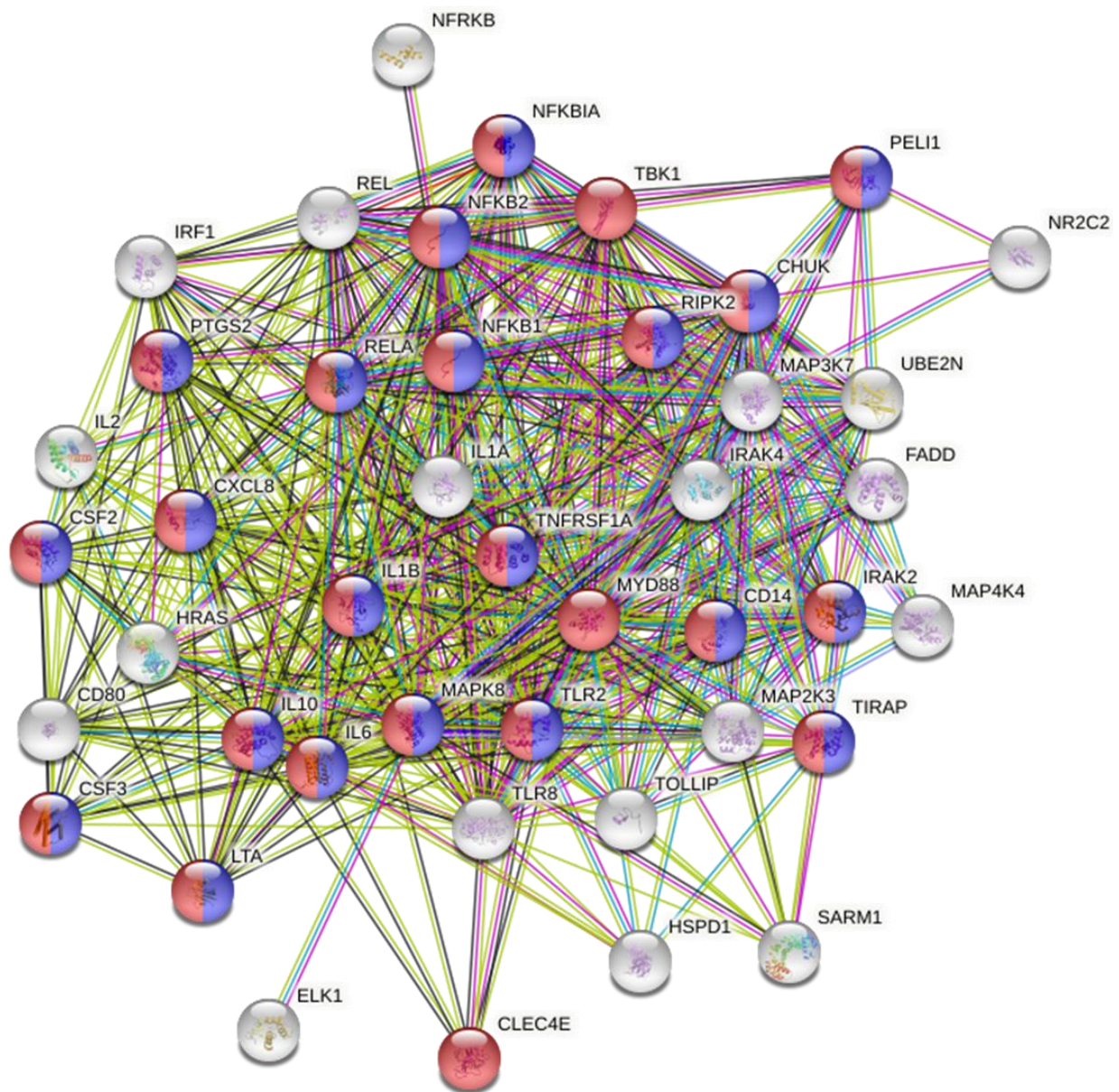


Figure 71 - STRING analysis of LPS-upregulated genes in PBMDMs – TLR pathway gene array – PBMDMs from 3 separate donors were set up according to the experimental design in Figure 15 with PBMDMs pre-incubated with/without 50µg V-antigen fragments (pV1/pV2) for 30min and then stimulated with 0ng/ml or 100ng/ml LPS for 16hr. The cells were then lysed, and the RNA was extracted for qPCR analysis using the Qiagen RT² profiler - Human Inflammasome gene array plate. Average gene expression for each gene within 100ng/ml LPS-stimulated PBMDMs (LPS only) and unstimulated control PBMDMs (unstimulated) was calculated and genes with an upregulated expression in 'LPS only', characterised as >1.5-fold regulation of expression and p-value <0.05 (determined by Student's T-test), were processed through the STRING protein interaction network database. Enriched functional clusters within the upregulated gene list were identified by STRING and the functional clusters of 'response to bacterium' (red) (FDR = 4.59e-24, Strength = 1.29) and 'response to lipopolysaccharide' (blue) (FDR = 1.11e-24, Strength = 1.51) are highlighted within the full network above

The evidence in Figure 71 and Tables 18 and 19 showed that the donor cells on the pV1 and pV2 plates responded appropriately to LPS. It was therefore decided that analysis of the pV1 and pV2 stimulations could be reliably performed.

Volcano plots in Figures 72 and 73 show the altered gene expression seen in LPS-stimulated PBMDMs when co-stimulated with pV1 and pV2 respectively. These are reported as expression changes compared with LPS-stimulated control cells. Full lists of the upregulated and downregulated genes are listed in Tables 20, 21, 22, and 23.

Figure 72:

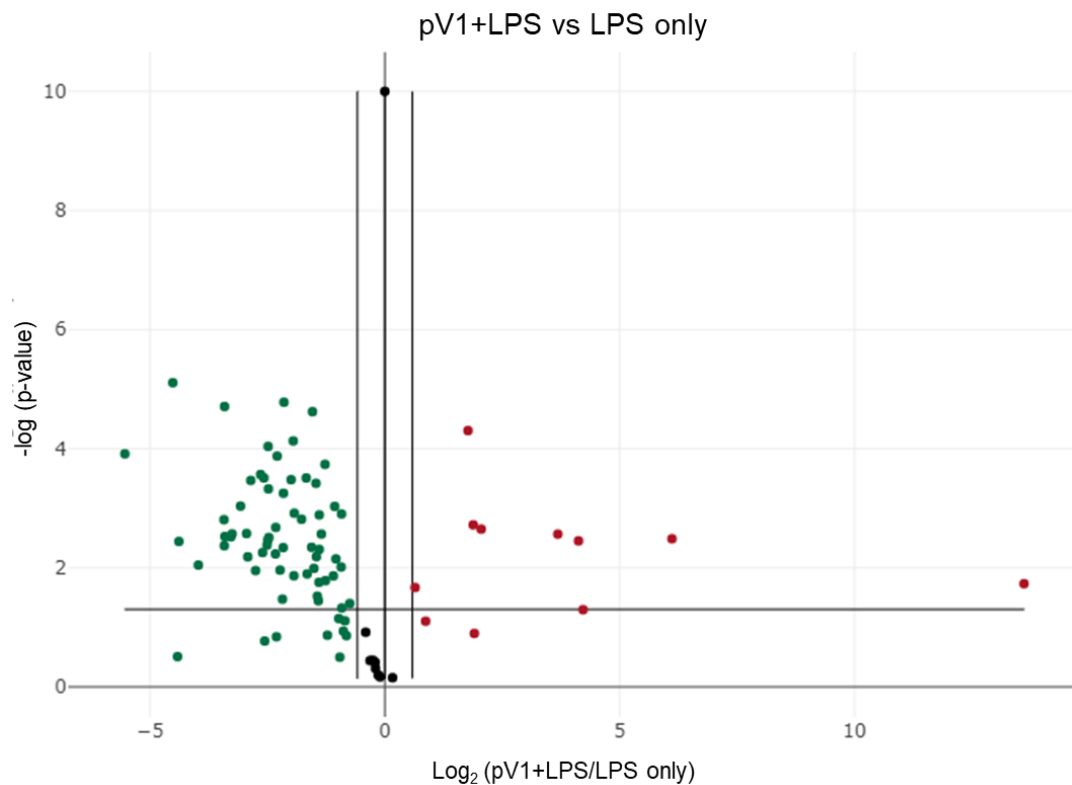


Figure 72 - Volcano plot of 'pV1+LPS' gene expression compared to 'LPS only' control expression (pV1/pV2 plate) – TLR pathway gene array – PBMDMs from 3 separate donors were set up according to the experimental design in Figure 15 with PBMDMs pre-incubated with/without 50 μ g V-antigen fragments (pV1/pV2) for 30min and then stimulated with 0ng/ml or 100ng/ml LPS for 16hr. The cells were then lysed, and the RNA was extracted for qPCR analysis using the Qiagen RT² profiler - Human TLR pathway gene array plate. Average gene expression for each gene within '50 μ g pV1 + 100ng/ml LPS'-stimulated PBMDMs (pV1+LPS) and 100ng/ml LPS-stimulated PBMDMs (LPS only) was determined and compared using a volcano plot generated by the Qiagen Geneglobe analysis software. Genes with a >1.5-fold regulation (red) and genes <-1.5-fold regulation (green) were highlighted and the horizontal line was added to represent the p-value 0.05

Table 20 - Upregulated genes within LPS-stimulated PBMDMs co-stimulated with pV1

Gene Symbol	Fold Regulation	p Value	Comment
CD80	1.56	0.021465	
CXCL10	4.15	0.002243	
IFNB1	3.41	0.000050	
IFNG	69.18	0.003260	A
IRF1	3.68	0.001905	
MAPK8	12.84	0.002724	
PTGS2	17.43	0.003530	
TLR9	12494.79	0.018538	A

PBMDMs from 3 separate donors were set up according to the experimental design in Figure 15 with PBMDMs pre-incubated with/without 50µg V-antigen fragments (pV1/pV2) for 30min and then stimulated with 0ng/ml or 100ng/ml LPS for 16hr. The cells were then lysed, and the RNA was extracted for qPCR analysis using the Qiagen RT² profiler - Human TLR pathway gene array plate. Average gene expression for each gene within 'pV1+LPS' and 'LPS only' controls was compared, and a Student's T-test was performed via the Qiagen Geneglobe analysis software. Genes upregulated by LPS (genes with >1.5-fold regulation and <0.05 p-value as determined by Student's T-test) are presented in the table above

'Comments' are: A; the gene's average threshold value is high (>30) in one group and low (<30) in the other, B; the gene's average threshold value is >30 in both samples and the p-value for the fold-change is unavailable or high (p>0.05), C; the gene's average threshold value is above the cut-off or undetected in all samples and so is unreliable and cannot be used

Table 21 - Downregulated genes within LPS-stimulated PBMDMs co-stimulated with pV1

Gene Symbol	Fold Regulation	p Value	Comment
BTK	-1.68	0.039818	
CASP8	-2.85	0.010261	
CD14	-46.39	0.000122	
CD180	-10.69	0.004262	
CD86	-10.61	0.002986	
CHUK	-1.90	0.001249	
CLEC4E	-2.63	0.001297	
CSF2	-2.40	0.016428	
CSF3	-2.42	0.000183	
ELK1	-5.69	0.004170	
FADD	-3.87	0.000074	
FOS	-10.74	0.001560	
HRAS	-6.26	0.000272	
HSPA1A	-3.42	0.001531	
HSPD1	-15.68	0.009016	
IFNA1	-2.67	0.035892	
IKBKB	-2.95	0.004534	
IL10	-7.23	0.000341	
IL1A	-10.66	0.000020	
IL1B	-8.41	0.000923	
IL2	-6.74	0.011157	
IL6	-7.56	0.006551	
IRAK2	-2.55	0.002717	
IRAK4	-2.91	0.000024	
IRF3	-7.70	0.002663	

LTA	-2.71	0.030071	
LY86	-4.48	0.004585	
LY96	-4.70	0.010956	
MAP2K3	-6.08	0.005561	
MAP2K4	-2.63	0.004922	
MAP3K1	-1.89	0.047351	
MAP4K4	-9.53	0.002703	
MAPK8IP3	-3.81	0.001212	
MYD88	-3.19	0.000311	
NFKB1	-5.60	0.000092	
NFKBIA	-2.64	0.017550	
NFKBIL1	-4.53	0.033670	
NFRKB	-5.96	0.000311	
NR2C2	-5.00	0.002101	
REL	-3.15	0.012706	
SARM1	-2.76	0.000382	
SIGIRR	-22.86	0.000008	
TAB1	-5.63	0.003438	
TBK1	-2.14	0.013714	
TICAM2	-1.91	0.009724	
TIRAP	-3.99	0.000332	
TLR1	-5.02	0.005857	
TLR10	-9.70	0.003025	
TLR4	-3.83	0.013624	
TLR5	-20.89	0.003616	A
TLR6	-4.47	0.000561	
TLR8	-4.90	0.000133	
TNFRSF1A	-4.44	0.000017	
TOLLIP	-5.54	0.003100	
TRAF6	-2.75	0.006517	
UBE2N	-2.06	0.007110	

PBMDMs from 3 separate donors were set up according to the experimental design in Figure 15 with PBMDMs pre-incubated with/without 50µg V-antigen fragments (pV1/pV2) for 30min and then stimulated with 0ng/ml or 100ng/ml LPS for 16hr. The cells were then lysed, and the RNA was extracted for qPCR analysis using the Qiagen RT² profiler - Human TLR pathway gene array plate. Average gene expression for each gene within 'pV1+LPS' and 'LPS only' controls was compared, and a Student's T-test was performed via the Qiagen Geneglobe analysis software. Genes downregulated by LPS (genes with <-1.5-fold regulation and <0.05 p-value as determined by Student's T-test) are presented in the table above

'Comments' are: A; the gene's average threshold value is high (>30) in one group and low (<30) in the other, B; the gene's average threshold value is >30 in both samples and the p-value for the fold-change is unavailable or high (p>0.05), C; the gene's average threshold value is above the cut-off or undetected in all samples and so is unreliable and cannot be used

Figure 73:

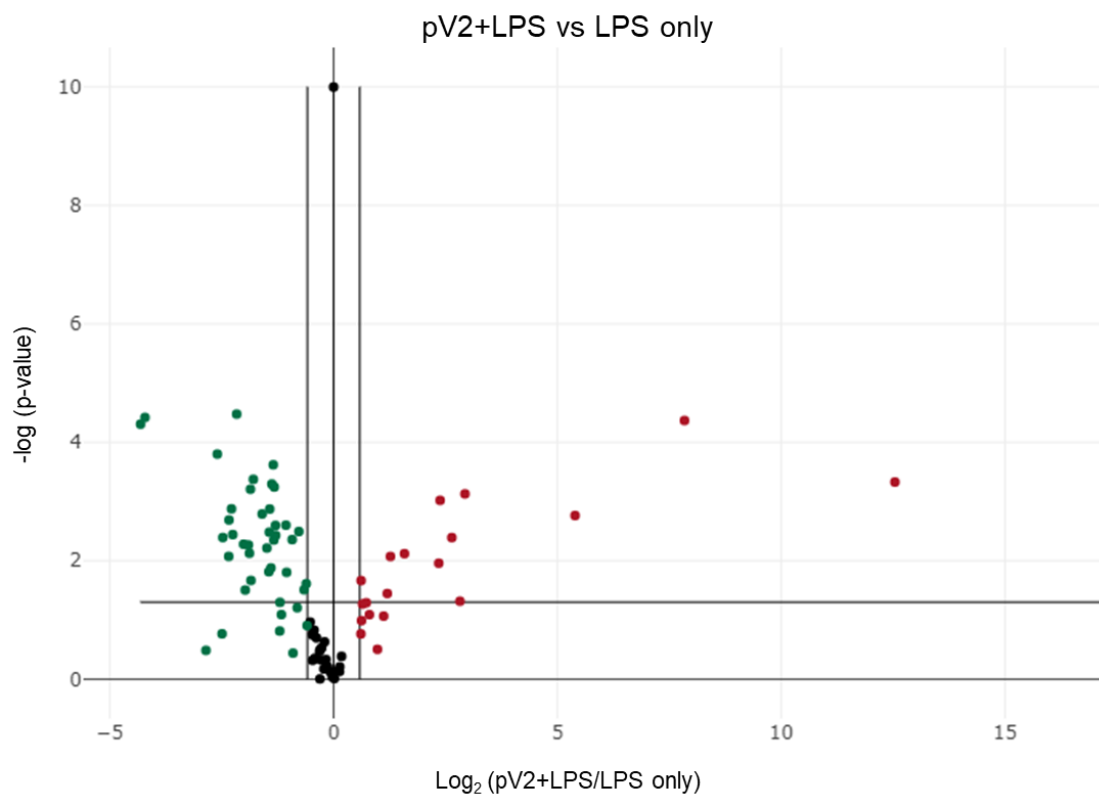


Figure 73 - Volcano plot of 'pV2+LPS' gene expression compared to 'LPS only' control expression (pV1/pV2 plate) – TLR pathway gene array – PBMDMs from 3 separate donors were set up according to the experimental design in Figure 15 with PBMDMs pre-incubated with/without 50µg V-antigen fragments (pV1/pV2) for 30min and then stimulated with 0ng/ml or 100ng/ml LPS for 16hr. The cells were then lysed, and the RNA was extracted for qPCR analysis using the Qiagen RT² profiler - Human TLR pathway gene array plate. Average gene expression for each gene within '50µg pV2 + 100ng/ml LPS'-stimulated PBMDMs (pV2+LPS) and 100ng/ml LPS-stimulated PBMDMs (LPS only) was determined and compared using a volcano plot generated by the Qiagen Geneglobe analysis software. Genes with a >1.5-fold regulation (red) and genes <-1.5-fold regulation (green) were highlighted and the horizontal line was added to represent the p-value 0.05

Table 22 - Upregulated genes within LPS-stimulated PBMDMs co-stimulated with pV2

Gene Symbol	Fold Regulation	p Value	Comment
CCL2	3.00	0.007605	
CD180	6.24	0.004065	
CXCL10	7.08	0.048238	
IFNB1	5.20	0.000956	
IFNG	229.18	0.000043	A
IL12A	2.41	0.008478	
IL2	5960.33	0.000469	A
JUN	1.53	0.021620	
MAPK8	42.09	0.001724	
PTGS2	2.30	0.035816	
TLR3	5.10	0.011028	A
TLR7	7.65	0.000743	

PBMDMs from 3 separate donors were set up according to the experimental design in Figure 15 with PBMDMs pre-incubated with/without 50µg V-antigen fragments (pV1/pV2) for 30min and then stimulated with 0ng/ml or 100ng/ml LPS for 16hr. The cells were then lysed, and the RNA was extracted for qPCR analysis using the Qiagen RT² profiler - Human TLR pathway gene array plate. Average gene expression for each gene within 'pV2+LPS' and 'LPS only' controls was compared, and a Student's T-test was performed via the Qiagen Geneglobe analysis software. Genes upregulated by LPS (genes with >1.5-fold regulation and <0.05 p-value as determined by Student's T-test) are presented in the table above

'Comments' are: A; the gene's average threshold value is high (>30) in one group and low (<30) in the other, B; the gene's average threshold value is >30 in both samples and the p-value for the fold-change is unavailable or high (p>0.05), C; the gene's average threshold value is above the cut-off or undetected in all samples and so is unreliable and cannot be used

Table 23 - Downregulated genes within LPS-stimulated PBMDMs co-stimulated with pV2

Gene Symbol	Fold Regulation	p Value	Comment
CD14	-3.46	0.000422	
CLEC4E	-6.06	0.000158	
CSF3	-2.09	0.002511	
ELK1	-5.56	0.004057	
FADD	-1.71	0.003212	
HRAS	-2.51	0.000569	
HSPA1A	-1.53	0.024430	
HSPD1	-3.60	0.021524	
IKBKB	-2.52	0.004471	
IL10	-4.48	0.000033	
IL1A	-19.87	0.000050	
IL1B	-4.86	0.001330	
IL6	-5.07	0.008458	
IRAK4	-2.54	0.000240	
IRF3	-4.03	0.005267	
MAP2K3	-2.72	0.015335	
MAP2K4	-1.58	0.030954	
MAP3K7	-2.07	0.015719	
MAPK8IP3	-1.90	0.004396	
MYD88	-2.69	0.001341	

<i>NFKB1</i>	-2.60	0.000506	
<i>NFKBIA</i>	-5.05	0.002051	
<i>NFRKB</i>	-2.46	0.002534	
<i>NR2C2</i>	-2.81	0.006108	
<i>SARM1</i>	-18.55	0.000038	A
<i>TBK1</i>	-4.76	0.003622	
<i>TIRAP</i>	-3.02	0.001624	
<i>TLR1</i>	-3.68	0.007482	
<i>TLR2</i>	-3.93	0.031250	
<i>TLR8</i>	-2.45	0.003724	
<i>TNFRSF1A</i>	-2.70	0.003298	
<i>TOLLIP</i>	-2.64	0.013244	
<i>UBE2N</i>	-3.74	0.005416	

PBMDMs from 3 separate donors were set up according to the experimental design in Figure 15 with PBMDMs pre-incubated with/without 50µg V-antigen fragments (pV1/pV2) for 30min and then stimulated with 0ng/ml or 100ng/ml LPS for 16hr. The cells were then lysed, and the RNA was extracted for qPCR analysis using the Qiagen RT² profiler - Human TLR pathway gene array plate. Average gene expression for each gene within 'pV2+LPS' and 'LPS only' controls was compared, and a Student's T-test was performed via the Qiagen Geneglobe analysis software. Genes downregulated by LPS (genes with <-1.5-fold regulation and <0.05 p-value as determined by Student's T-test) are presented in the table above

'Comments' are: A; the gene's average threshold value is high (>30) in one group and low (<30) in the other, B; the gene's average threshold value is >30 in both samples and the p-value for the fold-change is unavailable or high (p>0.05), C; the gene's average threshold value is above the cut-off or undetected in all samples and so is unreliable and cannot be used

Only 8 genes were identified as upregulated in 'pV1+LPS' when compared to 'LPS only' controls. Despite the low number of genes, STRING analysis of these showed an enrichment of the functional clusters: 'cellular response to IFNβ', 'defence response to virus', and 'positive regulation of cytokine production' (Figure 74).

Figure 74:

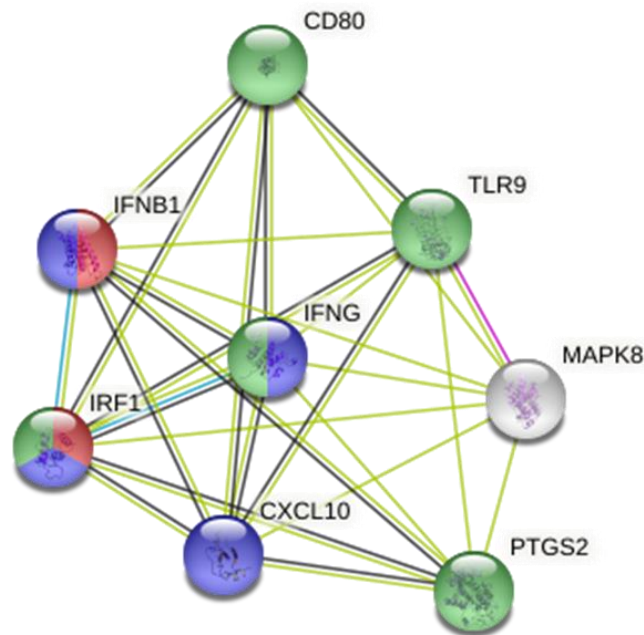


Figure 74 - STRING analysis of pV1-upregulated genes in LPS-stimulated PBMDMs – TLR pathway gene array – PBMDMs from 4 separate donors were set up according to the experimental design in Figure 15 with PBMDMs pre-incubated with/without 50µg V-antigen fragment (pV1/pV2) for 30min and then stimulated with 0ng/ml or 100ng/ml LPS for 16hr. The cells were then lysed, and the RNA was extracted for qPCR analysis using the Qiagen RT² profiler - Human TLR pathway gene array plate. Average gene expression for each gene within '50µg pV1 + 100ng/ml LPS'-stimulated PBMDMs (pV1+LPS) and 100ng/ml LPS-stimulated PBMDMs (LPS only) was calculated and genes with an upregulated expression in 'pV1+LPS', characterised as >1.5-fold regulation of expression and p-value <0.05 (determined by Student's T-test), were processed through the STRING protein interaction network database. Enriched functional clusters within the upregulated gene list were identified by STRING and the functional clusters of 'cellular response to interferon-beta' (red) (FDR = 0.00028, Strength = 2.51), 'defence response to virus' (blue) (FDR = 1.91e-05, Strength = 1.73), and 'positive regulation of cytokine production' (green) (FDR = 1.44e-05, Strength = 1.50) are highlighted within the full network above

In contrast, a total of 56 genes had downregulated expression and STRING analysis of these highlighted; 'cellular response to bacterial lipopeptide', 'detection of LPS', 'MyD88-dependent TLR pathway', and 'regulation of cytokine biosynthetic process' as enriched functional clusters (Figure 75).

Figure 75:

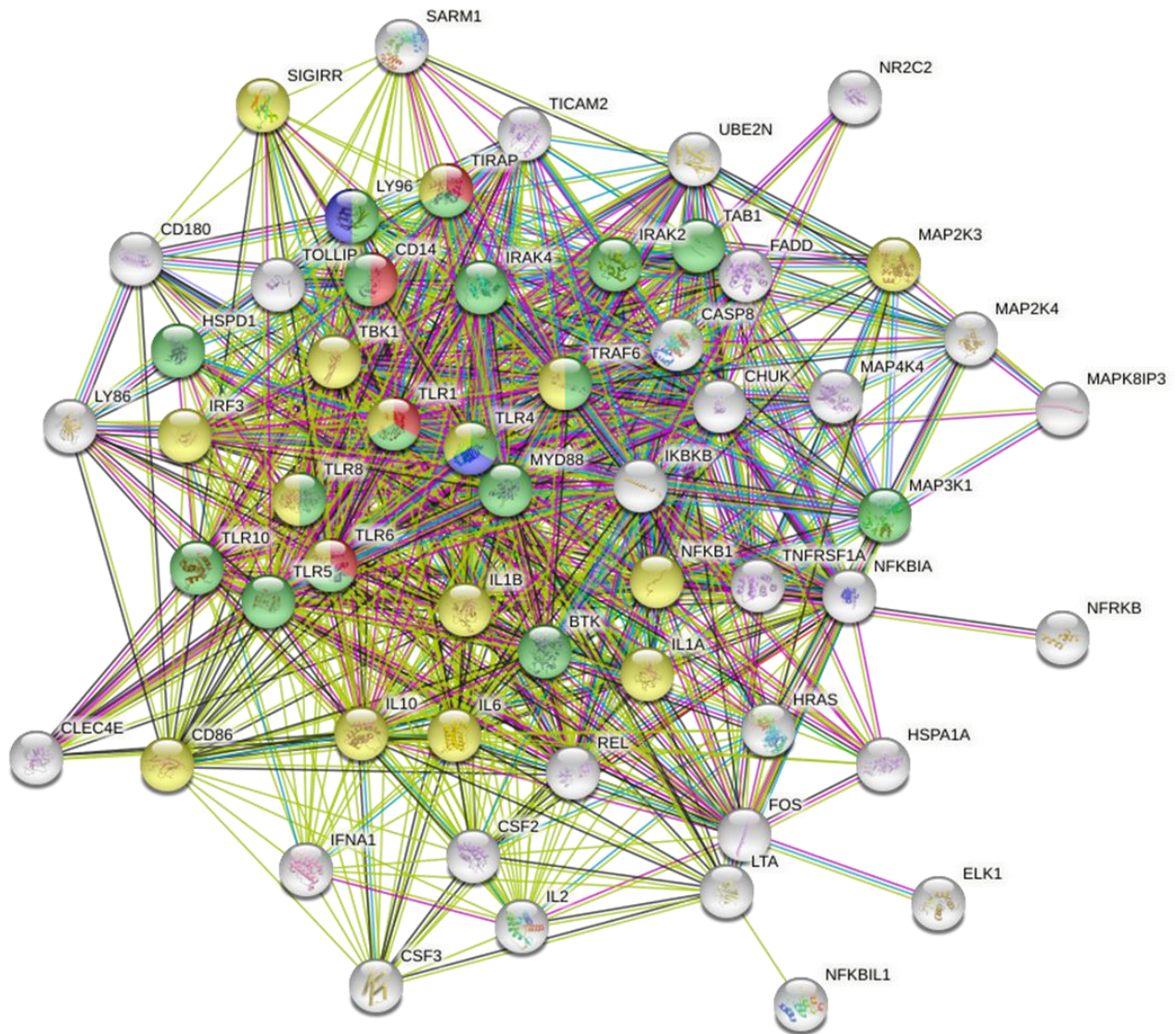


Figure 75 - STRING analysis of pV1-downregulated genes in LPS-stimulated PBMDMs – TLR pathway gene array – PBMDMs from 4 separate donors were set up according to the experimental design in Figure 15 with PBMDMs pre-incubated with/without 50µg V-antigen fragment (pV1/pV2) for 30min and then stimulated with 0ng/ml or 100ng/ml LPS for 16hr. The cells were then lysed, and the RNA was extracted for qPCR analysis using the Qiagen RT² profiler - Human TLR pathway gene array plate. Average gene expression for each gene within '50µg pV1 + 100ng/ml LPS'-stimulated PBMDMs (pV1+LPS) and 100ng/ml LPS-stimulated PBMDMs (LPS only) was calculated and genes with a downregulated expression in 'LPS only', characterised as <-1.5-fold regulation of expression and p-value <0.05 (determined by Student's T-test), were processed through the STRING protein interaction network database. Enriched functional clusters within the downregulated gene list were identified by STRING and the functional clusters of 'cellular response to lipopolysaccharide' (red) (FDR = 1.03e-07, Strength = 2.37), 'detection of lipopolysaccharide' (blue) (FDR = 0.00055, Strength = 2.24), 'MyD88-dependent toll-like receptor signalling pathway' (green) (FDR = 2.38e-30, Strength = 2.26), and 'regulation of cytokine biosynthetic process' (yellow) (FDR = 5.06e-22, Strength = 1.77) are highlighted within the full network above

In pV2 co-stimulated samples, 12 genes were upregulated compared to LPS-only controls (Table 22). When processed through STRING, the functional clusters of; 'positive regulation of the IFN α biosynthetic process', 'cellular response to IFN β ', 'response to virus', and 'response to bacterium' were reported (Figure 76). These were similar to pV1 however

included the 'response to bacterium' functional cluster which was not present in pV1's functional enrichment analysis.

Figure 76:

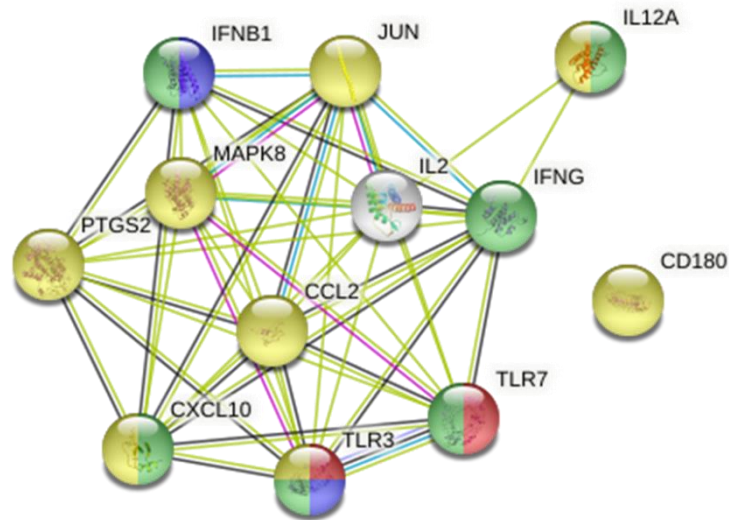


Figure 76 - STRING analysis of pV2-upregulated genes in LPS-stimulated PBMDMs – TLR pathway gene array – PBMDMs from 4 separate donors were set up according to the experimental design in Figure 15 with PBMDMs pre-incubated with/without 50µg V-antigen fragment (pV1/pV2) for 30min and then stimulated with 0ng/ml or 100ng/ml LPS for 16hr. The cells were then lysed, and the RNA was extracted for qPCR analysis using the Qiagen RT² profiler - Human TLR pathway gene array plate. Average gene expression for each gene within '50µg pV2 + 100ng/ml LPS'-stimulated PBMDMs (pV2+LPS) and 100ng/ml LPS-stimulated PBMDMs (LPS only) was calculated and genes with an upregulated expression in 'pV1+LPS', characterised as >1.5-fold regulation of expression and p-value <0.05 (determined by Student's T-test), were processed through the STRING protein interaction network database. Enriched functional clusters within the upregulated gene list were identified by STRING and the functional clusters of 'positive regulation of interferon alpha biosynthetic process' (red) (FDR = 6.83e-05, Strength = 2.81), cellular response to interferon-beta' (blue) (FDR = 0.00034, Strength = 2.34), 'response to virus' (green) (FDR = 1.92e-07, Strength = 1.56), 'response to bacterium' (yellow) (FDR = 1.54e-08, Strength = 1.37) are highlighted within the full network above

Finally, the 33 genes that were identified as downregulated returned functional clusters of; 'cellular response to triacyl bacterial lipopeptide', 'MyD88-dependent toll-like receptor signalling pathway', and 'toll-like receptor signalling pathway' (Figure 77). Similar to the functional clusters in Figure 75, these were largely specific to the MyD88 pathway and bacterial responses.

Figure 77:

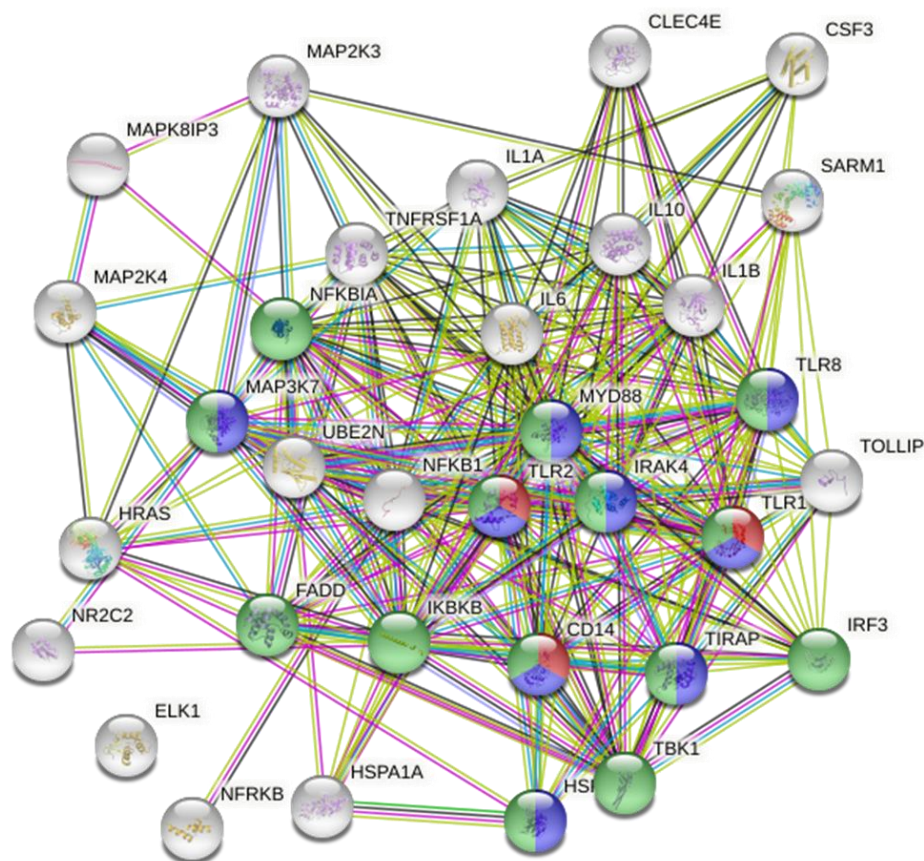


Figure 77 - STRING analysis of pV2-downregulated genes in LPS-stimulated PBMDMs – TLR pathway gene array – PBMDMs from 4 separate donors were set up according to the experimental design in Figure 15 with PBMDMs pre-incubated with/without 50 μ g V-antigen fragment (pV1/pV2) for 30min and then stimulated with 0ng/ml or 100ng/ml LPS for 16hr. The cells were then lysed, and the RNA was extracted for qPCR analysis using the Qiagen RT² profiler - Human TLR pathway gene array plate. Average gene expression for each gene within '50 μ g pV2 + 100ng/ml LPS'-stimulated PBMDMs (pV2+LPS) and 100ng/ml LPS-stimulated PBMDMs (LPS only) was calculated and genes with a downregulated expression in 'LPS only', characterised as <-1.5-fold regulation of expression and p-value <0.05 (determined by Student's T-test), were processed through the STRING protein interaction network database. Enriched functional clusters within the downregulated gene list were identified by STRING and the functional clusters of 'cellular response to triacyl bacterial lipopeptide' (red) (FDR = 8.11e-07, Strength = 2.77), 'MyD88-dependent toll-like receptor signalling pathway' (blue) (FDR = 6.61e-16, Strength = 2.21), and 'Toll-like receptor signalling pathway' (green) (FDR = 3.52e-22, Strength = 1.98) are highlighted within the full network above

6.2.4: TGFB induction

The fragments showed clear signs of altering the inflammatory response to LPS, and the functional clusters reported in Figures 74-77 showed a pattern of upregulated viral response genes and a downregulation of bacterial response genes much like the WT in Chapter 5. The clearest indication of WT V-antigen's effect on the inflammatory response was the induction of TGF β in Figure 58 (Chapter 5). As a central feature of what is now hypothesized to be the mechanism of action of V-antigen, or at least a sign thereof, determining whether the fragments had the ability to induce the maturation and secretion of TGF β was important to determining whether they retained their immunosuppressant characteristics. Therefore,

the growth media that had been harvested from the stimulations in order to run the cytokine analysis in 6.2.2 was also tested for TGF β . This was done using the Human/Mouse TGF-beta 1 ELISA Ready-SET-Go kit – the same kit as used for the WT stimulations in 5.2.4.2 – to detect matured TGF β that had been secreted into the growth media during the stimulations. The full protocol is described in 2.3.9.

The results are presented in Figure 78. As previously (5.2.4.2), the unstimulated and LPS-stimulated controls produced no detectable levels of TGF β 1 and so were once again assumed to be at the limit of detection which was 500pg/ml. All of the V-antigen fragments however, triggered the secretion of mature TGF β 1 above the detection limit with pV1 inducing the highest secretion both with and without LPS co-stimulation.

Figure 78:

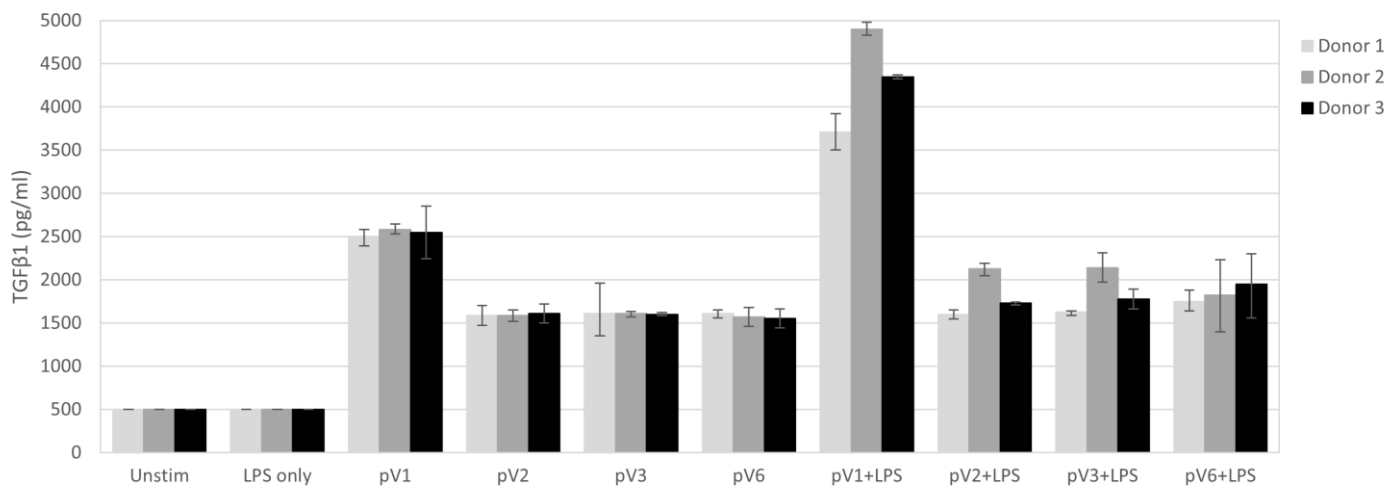


Figure 78 - Secreted mature TGF β 1 ELISA on the growth media of LPS/V-antigen-stimulated PBMDMs – PBMDMs from 3 donors were set up according to the experimental design in Figure 15 and pre-incubated with/without 50 μ g V-antigen fragment (pV1-pV6) before being stimulated with 0ng/ml or 100ng/ml LPS for 16hr. The growth media was removed and tested using the Human/Mouse TGF-beta 1 ELISA Ready-SET-Go kit (eBioscience) with the results shown for each donor tested in technical triplicates. The graph is presented with 95% confidence interval bars. A two-way ANOVA (with repeated measures) identified a statistical significant interaction between donors and conditions ($F(18,36) = 32.163$ (p -value = <0.001)). Both the donor (p -value = <0.001) and the stimulation condition (p -value = <0.001) were identified as significant factors in the level of TGF β secretion

A two way ANOVA (with repeated measures) identified the statistical significance of the difference between stimulation conditions as $F(9,18) = 5365.549$ (p -value = <0.001) which is a strongly significant indication that the stimulation affects the secretion of mature TGF β 1. The same ANOVA also determined the significance of the effect of the donor on the results with a value of $F(2,4) = 170.260$ (p -value = <0.001). This confirms that there is significant

difference between the donors. When combined to see whether the two variables interacted, the resulting F value was $F(18,36) = 32.163$ (p-value = <0.001), rejecting the null hypothesis that the two variables did not interact.

The SPSS programme also performed Mauchly's test of sphericity on the data. This is a measure of equal variance between multiple groups. However, small sample sizes are notoriously difficult to assume the sphericity of and so a Greenhouse-Geisser adjustment is commonly used. This adjusts the degrees of freedom used in the ANOVA to account for the potential differences in the variance of the data, and therefore gives a more conservative indication of the potential significance. When the TGF β 1 secretion data was adjusted via the Greenhouse-Geisser method, the significance for none of the variables changed; the significance between conditions was $F(1.979,3.959) = 5365.549$ (p-value= <0.001), the significance between donors was $F(1.501,3.001) = 170.260$ (p-value <0.001), and the significance of both combined was $F(1.507,3.014) = 32.163$ (p-value=0.01).

To ensure that the significance seen in the 'conditions' variable was not unfairly affected by the original ANOVA containing both LPS and non-LPS-stimulated samples together, the ANOVA was also repeated on LPS-stimulated and non-LPS-stimulated conditions separately. The results are shown below in Table 24.

Table 24 - Two-way ANOVA (with repeated measures) results for PBMDM TGF β 1 secretion in response to V-antigen fragments

Absence/Presence of LPS	Variable	Sphericity assumed	Greenhouse-Geisser
LPS-stimulated samples	Condition	$F(4,8) = 10092.228$ (p-value= $<0.001^*$)	$F(1.985,3.970) = 10092.228$ (p-value= $<0.001^*$)
	Donor	$F(2,4) = 209.078$ (p-value= $<0.001^*$)	$F(1.145,2.289) = 209.078$ (p-value=0.003*)
	Condition*Donor	$F(8,16) = 32.347$ (p-value= $<0.001^*$)	$F(1.281,2.562) = 32.347$ (p-value=0.016*)
Non-LPS stimulated samples	Condition	$F(4,8) = 2583.434$ (p-value= $<0.001^*$)	$F(1.480,2.959) = 2583.434$ (p-value= $<0.001^*$)
	Donor	$F(2,4) = 0.467$ (p-value=0.657)	$F(1.025,2.050) = 0.467$ (p-value=0.568)
	Condition*Donor	$F(8,16) = 0.741$ (p-value=0.656)	$F(1.392,2.784) = 0.741$ (p-value=0.505)

PBMDMs from 3 donors were set up according to the experimental design in Figure 15 and pre-incubated with/without 50 μ g V-antigen fragment (pV1-pV6) before being stimulated with 0ng/ml or 100ng/ml LPS for 16hr. The growth media was removed and tested using the Human/Mouse TGF-beta 1 ELISA Ready-SET-Go kit (eBioscience) with the results shown for each donor tested in technical triplicates. The graph is presented with 95% confidence interval bars. A two-way ANOVA (with repeated measures) was performed using an SPSS statistics programme and the F-values and p-values of those results are presented here, both with the assumption of sphericity and with the Greenhouse-Geisser adjustment. Significant results are indicated by **

Even removing the V-antigen and LPS controls from the statistics, as in 5.2.4.2, to ensure that the lack of detectable signal and therefore the lack of variance in the controls does not unfairly influence the analysis, reveals a statistically significant interaction between the donors and the stimulation conditions used ($F(14,28) = 29.753$ ($p\text{-value} = <0.001$)). Under the Greenhouse-Geisser method this still remains significant ($F(1.501, 3.002) = 29.753$ ($p\text{-value} = 0.011$)). With sphericity assumed or with the conservative Greenhouse-Geisser method, both the donor choice and the stimulation conditions have a significant impact on the level of TGF β secretion seen ($p\text{-value} = <0.001$ for all).

6.3: Discussion

6.3.1: The central protective epitope of V-antigen is responsible for V-antigen's immunomodulatory effects on cytokine secretion

Isolating functional regions from multifunctional virulence proteins has previously been achieved and so the isolation of the immunomodulatory site for V-antigen is not without precedent. For example, the SdrI protein of *Staphylococcus saprophyticus* is a multifunctional transmembrane protein that is involved in colonisation which had its fibronectin-binding domain isolated by *T.Sakinç, et al. 2009* (266). To test whether the V-antigen fragments also retained the functionality of the WT protein, each was tested at the same quantity as the WT protein on the same type of cells in stimulations run as similarly to the WT as possible. The results were a highly comparable response. Each V-antigen fragment showed signs of stimulating an inflammatory response when introduced without LPS (Figures 61-66). The only exception to this was a low induced level of IL-1 β in the absence of LPS (Figure 61) which, at a maximum increase of 1.8-fold over the unstimulated controls (pV1 and pV3), was unlike the 14-fold increase seen in 50 μ g WT V-antigen stimulation (Figure 16A, Chapter 3).

Out of the four fragments tested, pV6 appeared to consistently show the least inhibited responses in LPS-stimulated samples (Figures 61B-66B). This fragment had been developed to cover the same region as pV1 however omitting two β -sheets (aa214-234) which were not considered to be part of the epitope for protective antibodies. Evidently, the two β -sheets do appear to show importance in the immunomodulatory effects of V-antigen regardless of their antigenic properties, from what is seen in the comparison between pV6 to pV1.

As with the WT protein, IFN γ secretion is increased when the V-antigen fragments are co-stimulated with LPS (Figure 64B). In Chapter 5, this was predicted to be indicative of the overall mechanism of V-antigen's immunomodulation due to inhibition of the MyD88 pathway leading to proportionally greater TRIF-pathway signalling and so an IFN-predominant response. If this hypothesis is upheld, then the greater IFN γ secretion shown in Figure 64B and suppression of the other measured cytokines (Figures 61B-63B, Figures 65B & 66B) would suggest that each of the four V-antigen fragments was capable of functioning like the WT protein in its immunomodulation. It also suggests that each of the four V-antigen fragments is capable of internalising despite missing substantial regions of the WT protein and so it may potentially also be the case that the central epitope is involved in protein internalisation as well or is capable of utilising another pathway to enter the cell.

6.3.2: pV1 and pV2 induce similar gene expression changes to WT V-

antigen

6.3.2.1: pV1:

The stimulations for WT V-antigen and those of the generated fragments were performed on different PBMDM donors and so comparison of the two had to be done with the acknowledgement that donor variability could have influenced gene expression as well. Focusing on the more holistic view of functional clusters though gave a more robust approach initially as it was able to look at the type of responses affected rather than just the individual genes within it.

In the WT TLR pathway gene array (5.2.2), STRING identified 'response to virus' as a key upregulated functional cluster (Figure 49, Chapter 5). The discussion in 5.3.2 evaluated that this appeared to be due to the unbalancing of the standard TLR4 MyD88:TRIF signalling ratio into a response that appeared predominantly TRIF-orientated instead. This shift to a more TLR3/viral-like response causes a greater induction of viral-like genes and therefore shows a pattern similar to what was highlighted by STRING in Figure 49 (Chapter 5). Gene expression data from the pV1 stimulations returned the functional clusters of 'response to IFN β ' and 'defence response to virus' (Figure 74). Like the WT cluster, these are also viral response-related and could signify a shift towards a TRIF-predominant response in a similar fashion to the WT protein. Likewise, the clusters of 'cellular response to bacterial lipopeptide' and 'MyD88-dependent TLR signalling pathway' identified in pV1's downregulated gene list (Figure 75) correlated strongly with the WT's downregulated functional clusters of 'response to bacterium' and 'MyD88-dependent TLR signalling' (Figure 50, Chapter 5). These comparisons, together with the cytokine data evaluated in 6.3.1, suggest that pV1 is having a similar overall response to the WT protein.

Also, within the analysis of the WT stimulations in Chapter 5 (5.3.2) was a number of key genes that were highlighted as members of these functional clusters which, under closer examination of their expression in 5.2.2.2, showed an obvious influence from V-antigen's presence. These genes included upregulated TRIF/viral response-associated genes such as IRF1 (Figure 51B, Chapter 5), IFN γ (Figure 52A, Chapter 5), IFN β (Figure 33B, Chapter 4), CXCL10 (Figure 52B, Chapter 5), and TLR3 (Figure 51A, Chapter 5), as well as downregulated bacterial response-associated genes like NF κ B genes (Supplementary Figure 10, Chapter 5), TBK1 (Supplementary Figure 15C, Chapter 5), IL-6 (Figure 34B, Chapter 4), and IL-1 β (Figure 34A, Chapter 4). There was also evidence to show that

SARM1; a TRIF pathway inhibitor, was downregulated in V-antigen stimulations (Figure 54, Chapter 5) along with LPS detection proteins; CD14 (Figure 53A, Chapter 5) and HSPD1 (Figure 53B, Chapter 5). While the exact same level of analysis could not be performed due to a lack of a condition pertaining to the fragment without LPS co-stimulation, it was possible to compare whether the genes had upregulated or downregulated accordingly in the presence of LPS. The stimulations performed using pV1 showed a high level of similarity across all of these genes (Tables 20 and 21) and almost all of the genes listed were upregulated or downregulated in the same manner as in the WT stimulations. The only exception to this was TLR3 which showed a non-significant upregulation within pV1 stimulations, unlike the significant upregulation in the WT. Both the WT and pV1 stimulations also saw a decrease in MyD88 (Supplementary Figure 15A, Chapter 5, and Table 21) however due to the inconsistency of its expression when compared with the expression data in the Human Inflammasome gene array (Table 16, Chapter 5), further validation experiments would need to be carried out to confirm this.

Other genes that weren't highlighted in those key clusters but that also added to the similarities between the WT V-antigen and pV1 stimulations included CD80 which was identified as an upregulated gene in both stimulations and, though it was not included in the antiviral functional clusters, it is known to play an important role in innate-adaptive communications in viral responses as well as bacterial ones(267). Another commonly upregulated gene identified was MAPK8. This was also identified by the TLR pathway gene array in WT stimulations (Table 12, Chapter 5) however, as explained in 5.2.3, MAPK8 expression in WT stimulations could not be concluded due to an inconsistent reading across the TLR pathway gene array and the inflammasome gene array.

The WT stimulations did however identify 12 upregulated genes that were not upregulated in pV1 stimulations. These were; CCL2, CD180, IL12A, CXCL8, JUN, LY86, PELI1, SIGIRR, TLR3, TLR5, TLR7, and TNF (Table 12, Chapter 5). Of these 12, CD180, SIGIRR, and TLR5 were instead identified as downregulated genes within pV1 stimulations (Table 21). LY86 and CD180 are both involved in inhibition of TLR4-LPS signalling in myeloid cells(268). CCL2 and CXCL8 are both chemoattractants and may be upregulated due to donor response differences. Evidence of this is the ~500pg/ml difference in TNF α secreted levels for the LPS-stimulated control cells used in the fragment stimulations and those used in the WT stimulations (Figure 20B, Chapter 3, and Figure 65). The higher inflammatory signalling from cells used in the pV1 stimulations may have affected the comparison to the pV1-stimulated cells. This could also be true of JUN; a proinflammatory TF. PELI1 is a signalling protein important in both the MyD88 and TRIF pathway(234) and SIGIRR is a regulatory protein for the MyD88 pathway. There were also only 5 genes that

weren't commonly downregulated between both pV1 and WT V-antigen; HSPA1A, MAP2K4, TIRAP, and TLR8 downregulated only in pV1 and NFκB2 downregulated only in WT V-antigen. The potential reasons behind these differences are numerous and are discussed in greater detail in 6.3.4.

6.3.2.2: pV2:

The stimulations on pV2 were carried out alongside pV1 using the same donors and the same conditions. Therefore, they form a more direct comparison between each other than even the comparison to the WT protein. The key upregulated functional clusters identified by STRING (Figure 76) for pV2 were; 'cellular response to IFNβ', 'response to virus', 'positive regulation of IFNα biosynthetic process', and 'response to bacterium'. While most of these correlated strongly with the WT and pV1 precedent of viral- and IFN-responses, the presence of 'response to bacterium' as one of the highest functional clusters was not. However, despite making up 8 of the 12 proteins in the upregulated gene list, the cluster had lower strength than the other three categories due to the large number of proteins encompassed within the functional group. This meant that the 'expected observations' value was far higher for it than the other three functional clusters. All of the genes identified within the 'response to bacterium' were also present in the upregulated gene list for WT V-antigen; CD180, IL12A, JUN, CCL2, MAPK8, PTGS2, TLR3, and CXCL10 (Table 14, Chapter 5). However, due to the larger number of upregulated genes in the WT stimulations (19 as opposed to 12 with pV2) and the low strength value of the functional cluster in pV2, it is possible that the functional cluster registered as too low in strength to appear in the analysis for the WT upregulated gene list.

The downregulated gene list for pV2 revealed functional clusters of; 'cellular response to triacyl bacterial lipopeptide', 'MyD88-dependent TLR signalling pathway', and 'TLR signalling pathway' (Figure 77). These once again matched closely to the WT downregulated functional clusters of 'response to bacterium' and 'MyD88-dependent TLR signalling' (Figure 50, Chapter 5).

As in the pV1 analysis in 6.3.2.1, the similarities between pV2 and the key genes linked to the WT clusters were also examined. Most of the genes were similarly expressed and were found in the same category of expression changes (Upregulated – IFNγ, IFNβ, CXCL10, and TLR3; downregulated – MyD88, NFκB genes, TBK1, IL-6, IL-1β, SARM1, CD14, and HSPD1. The only gene that was not identified in the same category was IRF1

which had a non-significant increase in pV2 stimulations (p-value=0.053) (data not presented).

Only 7 genes were identified that were upregulated in the WT stimulations that were not upregulated in pV2 stimulations. These were; CD80, CXCL8, IRF1, LY86, PELI1, SIGIRR, TLR5, and TNF. CD180 was upregulated in pV2 stimulations and, as mentioned in 6.3.2.1, CD180 and LY86 function together to regulate TLR4-LPS signalling and so likely have similar regulation. At closer examination, LY86's expression did increase above the 1.5-fold threshold however this increase was not significant (p-value=0.081) (data not presented) so, while it did not appear in the upregulated gene list, LY86 may have had reached significance with a higher *n* number. Unlike in pV1, none of the genes found in the WT upregulated gene list are found in the downregulated gene list in pV2. However, the downregulated gene list of pV2 was substantially larger than that of WT V-antigen, with 56 genes being identified as significantly downregulated whereas only 30 were identified in WT V-antigen. All of the downregulated genes seen in WT stimulations were found to be downregulated in pV2 except for MAP3K7, NFκB2, and TLR2.

Comparing pV1 and pV2 (Tables 20 and 22), only 5 genes were commonly upregulated; CXCL10, IFNβ, IFNγ, MAPK8, and PTGS2. Both MAPK8 and PTGS2 were identified as being upregulated in the WT TLR pathways gene array but were also both identified as giving inconsistent results when compared to the data from the inflammasome gene array(5.2.3). Further evaluation by manual qPCR would be ideal as both of these genes are reported as being induced by TGFβ in previous studies(237, 269) and so could be important validity genes for V-antigen's mechanism of action. The other three genes; CXCL10, IFNβ, and IFNγ are also upregulated by WT V-antigen and are clear indicators of an IFN-based viral response which is considered to be indicative to V-antigen's influence over the LPS response. With regards to downregulated genes, pV1 had a total of 33 genes when compared with the LPS control whereas pV2 had 56. All except for two genes from the pV1 downregulated gene list were also present in pV2's downregulated gene list. These two were MAP3K7 and TLR2. MAP3K7 is of particular interest as this was highlighted as a downregulated gene in the WT stimulations and, as discussed in 5.2.4.1, is a MAPK related to the TGFβ response.

Taken with the cytokine data from 6.2.2, it appears that both pV1 and pV2 induce a similar response to the WT V-antigen protein. The cytokine data was able to reveal a clear immunomodulatory effect from the fragments however it could only reveal a snapshot of the current levels of secreted cytokines and only of those within the 7-plex kit. The qPCR gene array data revealed a more detailed view at how key inflammatory pathways were affected

and showed that the same MyD88 pathway-specific suppression was present in the fragments as had first been seen in the WT. This confirmed that the fragments were acting in a similar manner to the WT and not influencing cytokine secretion via an ulterior method.

6.3.3: The central epitope of V-antigen is responsible for inducing TGFβ1

secretion

One of the key findings of Chapter 5 was the evidence that WT V-antigen stimulated the secretion of TGFβ1 from PBMDMs and it was hypothesized that this was, at least in part, the mechanism of action by which V-antigen induced MyD88 signalling pathway inhibition. The recombinant fragments were also tested for their capability to induce TGFβ1 secretion (Figure 78) as a means to also evaluate whether they retained the same functional properties as the WT. The results clearly showed that all four of the tested fragments were capable of inducing mature TGFβ1 secretion to varying degrees and also that pV1 induced the highest secreted level at 16hr both in the presence and absence of LPS.

The results of the two-way ANOVA with repeated measures revealed that in the absence of LPS, the donors did not have significant differences in their responses and that the only differences in the secreted levels of TGFβ1 was due to the fragments they were stimulated with (Table 24). By comparison, when cells were co-stimulated LPS, donor variability became a significant factor in the affecting TGFβ1 secretion. This, however, is not unexpected as it is well documented that there is substantial heterogeneity in individual responses to LPS in monocytes(270).

As the WT stimulations were carried out on PBMDMs from a different set of donors to the fragment stimulations, comparing the exact concentration of TGFβ1 must be done with the consideration that donor variability, even in triplicate, could have played a role in the differences seen. With that in mind, WT V-antigen without LPS appeared to stimulate a greater concentration of mature TGFβ1 at 16hr than any of its recombinant fragments. It also showed a marked increase in TGFβ1 secretion to 3750-4750pg/ml when LPS was co-stimulating. Out of all four of the recombinant fragments, pV1 showed the highest level of secreted TGFβ1 and, unlike the other three fragments, it also had a visible increase in TGFβ1 secretion when in the presence of LPS. Under LPS co-stimulation, pV1 induced TGFβ1 levels similar to that of the WT protein.

6.3.4: Considerations

It is important to highlight specific limitations that must be considered when evaluating the comparisons between WT V-antigen and the recombinant fragments.

Firstly, the different sizes of each protein mean that using a consistent quantity of 50µg in stimulations does not normalise the quantity of active units added to each stimulation. The comparisons could therefore be partially confounded by different doses of V-antigen's immunomodulatory site. This could have various effects such as a stronger immunomodulatory effect or a more potent inflammatory reaction within the early hours of the stimulation and this could influence cytokine secretion or gene expression even at the 16hr timepoint.

Secondly, it was not possible to determine whether the kinetics of the fragments were altered compared to the WT protein. In Chapter 3, it was determined that WT V-antigen internalised within 4hr and cytokine data (Figures 16-21, Chapter 3), as well as data from previous studies(147), showed that the major immunomodulatory effects of V-antigen occur after internalisation. As the data within Chapter 6 appears to show considerable similarities between the fragments and the WT protein, it can be assumed that the recombinant fragments are still internalising. However, it is not known whether the fragments internalise faster or slower or at a similar rate to WT V-antigen and so it is not possible to determine whether the set 16hr time point is the most valid timepoint to measure from. Ideally, the best comparison would be at a set timepoint post-internalisation rather than post-introduction so further investigation of the kinetics of the fragments would be needed to perform a more comparable analysis.

Finally, as mentioned previously, the use of a different set of donors for the WT and fragments as well as for the fragment cytokine data in 6.2.2/6.2.4 and the gene arrays in 6.2.3 adds the potential for donor variability to skew results. This is clear in the poor LPS response given by the donors used for the pV3/pV6 plate in 6.2.3 (Figure 57) but has also been reported in the literature(270) and was seen statistically in the two-way ANOVA in 6.2.4 (Table 24).

It is however important to clarify that these considerations do not affect the conclusion that the recombinant fragments retain to some extent, the immunomodulatory effects of V-antigen. However, they do impact how accurate direct comparisons are and more detailed future experiments would need to address these limitations.

7: Chapter 7: Discussion

7.1: Study summary

The focus of this study was to investigate the effect V-antigen has on LPS-induced inflammation. As an already-documented immunomodulatory protein, V-antigen is understood to inhibit inflammation triggered by a number of stimuli like LPS and Zymosan A and also cause a greatly diminished immune response to *Yersinia* infection(271). However, most of the previous studies on V-antigen's immunomodulatory effects focused on the survival rates of infected mice or the short-term IL-10 response that V-antigen potentially induces. Evidence of a secondary, delayed immunomodulatory response was present within the literature but no study had ever attempted to uncover the mechanism of it, even though the short-lived IL-10 response could not realistically provide the long-term and potent immunosuppression shown by V-antigen. As well as the mechanism of action not being investigated, data about the impact of V-antigen on cytokine signalling was minimal, particularly during the potential secondary wave of immunosuppression. It was for these reasons that this study was designed to detail how the inflammatory response was affected at a both a secreted cytokine- and gene expression-level up to, and during, the beginning of the secondary response.

V-antigen stimulations in both immortalised MM6s and primary PBMDMs were carried out using a 30min preincubation of V-antigen to allow for the protein to dissipate and bind with cells but not internalise (Figure 15). The cells were then incubated with 100ng/ml LPS for 1-16hr and at the end of the stimulations, the growth media was removed for cytokine analysis. MM6 cells were lysed in sample buffer and tested for protein expression while RNA was extracted from the 16hr PBMDM stimulations to analyse the expression levels of genes relating to inflammasomes and the TLR/IFN γ /TNF α pathways. This design was chosen to create a holistic view of how the cellular response to LPS changes in the presence/absence of V-antigen.

A second important aspect of V-antigen is that it is a multifunctional protein which has multiple specific roles and interactions both with host proteins and *Yersinia* proteins. The region responsible for the immunomodulatory effects had never previously been identified or isolated from the WT protein. Part of this study therefore looked to express, purify, and test a series of peptide fragments that correlate to a highly conserved protective epitope of V-antigen. To do this, pre-developed plasmids containing these gene fragments were expressed and the proteins were isolated. These were then subjected to similar experiments as those performed on WT V-antigen, though this time exclusively on primary PBMDMs, to

see whether the cytokine secretion and gene expression correlated between any of the fragments and the WT.

Over the course of this project, I uncovered evidence of V-antigen's mechanism of action which could explain the peculiarities seen in other V-antigen studies and confirm the presence of a secondary, long-term immunomodulatory response. I also uncovered evidence that the central protective epitope of V-antigen (aa135-275) is responsible for this effect and that this region could be isolated from the WT protein while still retaining the ability to modulate the inflammatory response.

Considering the thesis aims given in 1.4, this study has achieved its aims of; providing a more extensive cytokine profile for the effects of V-antigen on LPS-driven inflammation, investigating the effect of V-antigen on key inflammatory pathways with large scale gene arrays, identifying, at least in part, the mechanism of action that V-antigen functions by, and isolating the functional region that causes this.

In conclusion, this study has investigated the effects of V-antigen on inflammation and highlighted three major novel findings; that V-antigen has a secondary anti-inflammatory effect post-internalisation, that TGF β is involved in V-antigen's immunomodulatory effects, and that the central protective epitope of V-antigen is responsible for these effects. These findings, as well as evidence from the cytokine profiles, gene expression, and current knowledge of TGF β function can be used to begin a dialogue about the potential use for V-antigen and its mechanism of action as a therapeutic against inflammatory disorders. The rest of this discussion shall therefore be dedicated to that dialogue as well as discussing the limitations and future directions of this study.

7.2: Considerations about the use of MM6 cells and PBMDMs

The choice to use monocyte and monocyte-derived macrophages in this study has been highlighted in 3.1.1. Their importance within inflammation as heavy cytokine secretors – and their importance in inflammatory disorders(272-274) – meant that evidence of inflammatory suppression within these cells would give far greater insight into to V-antigen's immunomodulatory capabilities and therefore its potential as a therapeutic.

Inevitably, as with all models, there are limitations that must be considered when evaluating the data that comes from them and the use of monocytes in this study was no exception. MM6 cells, for example, have a low cellular level of CD14(275). They have been well characterised as being reliable cell lines and ones that have many similarities with mature primary monocytes but the reduced expression of CD14 could have affected LPS

signalling and so responsiveness to LPS. There are also studies that have shown that V-antigen binds to CD14(149) and so a lower CD14 content could have reduced the effectiveness of V-antigen compared to primary cells as well. This may explain the lack of reliable response to LPS seen in MM6 stimulation as shown by the low secretion of cytokines in 3.2.5.1.

The choice of monocytes also had a unique impact on the evaluation of the immunomodulatory effects of V-antigen. In other cell lines, such as epithelial cells, SOCS1 functions through inhibiting JAK1/JAK2 activity(237), inhibiting MyD88-pathway signalling(236), and inhibiting STAT1 from promoting upregulation of genes in response to IFN γ (238). Monocytes and macrophages still experience inhibitory effects from SOCS1 but monocyte/macrophage SOCS1 does not inhibit STAT1-mediated gene promotion. This means that monocytes experience a reduced inhibitory effect through this pathway. SOCS1 is used by anti-inflammatory cytokines like IL-10, TGF β (237), and IL-4(276). Though this is not believed to have prevented the discovery of new aspects of V-antigen's mechanism of action, it is entirely possible that V-antigen's immunomodulatory effects could be even stronger in other cell types or in multicellular environments like in *in vivo* studies. The literature appears to support this too as *in vivo* studies often show strongly protective responses *in vivo*(147, 151) and yet *in vitro* studies often show weak responses or no immunomodulation at all(132, 153).

The other limitation of using MM6 cells was highlighted in 3.1.1 – the limitation of responsiveness of immortalised cell lines compared to primary cells. Comparing the cytokine data in 3.2.5, PBMDMs have a far higher cytokine response to LPS in the 'LPS only' control. This was particularly true for TNF α which had a ~150-fold greater secreted concentration in primary cells at 6hr, and IL-6 which had ~210-fold greater concentration at 6hr too. For this reason, primary cells were used where possible however not all evidence was gathered from primary cells - namely the IL-1 β , Caspase p20, and plkB α western blots in Chapters 4 and 5 - due to their availability.

7.3: V-antigen's mechanism of action

7.3.1: V-antigen has a complex effect on inflammation

Full details of the effects of V-antigen on cytokines secretion and transcription is presented in the chapter discussions for Chapters 3-5, however a brief summary of the main findings of this study are also presented below.

V-antigen internalises in monocytes, in the absence of *Yersinia spp*, by 4hr post-introduction and once internalised, it is capable of interacting with host factors to trigger its secondary immunomodulation. Chapter 3 analysed the effects on cytokine secretion in however PBMDMs and concluded that V-antigen had a potent ability to inhibit cytokine secretion. The secreted levels of proinflammatory cytokines like IL-1 β , IL-6, and IL-8 were consistently lower in V-antigen stimulated cells as well as the anti-inflammatory cytokine IL-10. However, IFN γ secretion was significantly increased. PBMDMs also showed an unexpectedly potent primary immunomodulatory effect that started as quickly as 1hr after V-antigen introduction for some cytokines and this primary immunomodulation did not appear to be caused by IL-10.

Western blotting revealed a reduced level of intracellular IL-1 β and pro-IL-1 β , as well as I κ B α and pI κ B α , and when transcription was analysed by qPCR gene arrays, V-antigen appeared to have a MyD88 pathway-specific inhibitory effect as well as hallmarks of TGF β induction. This included the reduced expression of MyD88 pathway genes and bacteria response-like genes, and yet an increased expression of viral response-like genes. MyD88 suppression is indicative of the anti-inflammatory effects of TGF β , however there were other indicators in the qPCR gene expression data that also suggested that TGF β signalling was being induced. This included the increased expression of MAPK11 (Chapter 4) which is regulated by TAB1 (also upregulated) which is itself regulated by TAK1 – a MAP3K that is well-documented to be triggered by TGF β signalling. The downregulated expression of NLRC4 in the presence of V-antigen is also a potential indication of TGF β intervention too. As the NLR responsible for generating the inflammasome triggered by T3SS needle tip proteins (of which V-antigen is), its upregulation would be expected in the presence of V-antigen. However, the only currently identified TF for NLRC4 is p53 which is itself inhibited by PTGS2 expression – another TGF β -upregulated gene which was shown to be upregulated in Chapter 5. Further evidence included the downregulated expression of CD14 mRNA as identified through qPCR and the reduced cellular content of translated CD14 as determined by western blotting. Upon testing the growth media for the secreted level of mature, active TGF β 1, it was determined that V-antigen stimulation led to a significant increase in TGF β secretion.

TGF β as an anti-inflammatory inhibits the MyD88 signalling pathway and also the IFN γ signalling pathway through SOCS1 which inhibits STAT1-driven gene upregulation. As explained in 7.2, only human monocytes do not have the regulatory control of SOCS1 over the IFN γ pathway. This could also diminish V-antigen's immunomodulatory effect as IFN γ has previously been shown to inhibit IL-10 production in monocytes and so may reduce the strength of this anti-inflammatory paracrine/autocrine signalling(277). TGF β also, in *in vivo*

situations, induces a potent anti-inflammatory environment that is not achievable in a monoculture of monocytes (5.2.4.1 and 5.3.3). Therefore, the complex effects V-antigen has on inflammation in human monocytes may appear less so in studies performed *in vivo* or in multi-cell systems or in single-cell systems that don't use human monocytes. In those cases, restriction on IFN γ expression and a more substantial anti-inflammatory effect from a stronger anti-inflammatory environment triggered by TGF β and IL-10 in tandem may give V-antigen a stronger anti-inflammatory effect and less of an antiviral response-like shift in gene expression.

7.3.2: V-antigen's immunomodulation and the wider literature

Evaluating the concordance of this study's results with those in the wider literature has several difficulties. V-antigen has not been extensively studied for its immunomodulation and detailed investigation into its effects on inflammation has not been previously attempted *in vitro* before. Studies that do investigate the immunomodulatory effects of V-antigen do not consider the secondary immunomodulatory effects post-internalisation and so do not appropriately control for it and often these provide very limited cytokine profiles to compare against. However, there is still some potential to evaluate our data with that of previous work to surmise both the current understanding of V-antigen's effects and why the findings of this study could explain some of the limitations and results seen in other studies.

Firstly, evaluating *in vitro* studies revealed critical differences in IL-10 induction between different sources. One study, *A.Sing, et al. 2002(148)*, witnessed IL-10 secretion of roughly 130pg/ml in MM6 cells after an 18hr incubation with 5 μ g V-antigen. The cytokine data collected from PBMDMs in Figure 21A revealed a similar secretion of IL-10 in V-antigen-only stimulations. However, while these two results correlate, both of these represent a low level of IL-10 compared to control samples stimulated with 100ng/ml LPS in Figure 21B (5400pg/ml) and only being similar to the study's own control of just 1ng/ml LPS. Importantly though, the wider scope of the cytokine analysis in our evaluation of V-antigen identified a trend of increasing IFN γ (Figure 19A) and TNF α (Figure 20A) over 16hr in the same V-only stimulations and so the increase in IL-10 cannot be ruled out as inflammation-related rather than a specific anti-inflammatory IL-10 response induced by V-antigen.

Not all studies report IL-10 induction though. Another study, this time in murine macrophages, did not show any significant increases in IL-10 secretion after 18hr(153). However, both this study, and the one mentioned above, showed a reduction of TNF α in response to inflammatory stimuli however. This correlates to our theory that the IL-10

response induced early in the V-antigen stimulation is weak and not the primary source of immunomodulation, and also corroborates our findings that TNF α induction by inflammatory stimuli was suppressed by V-antigen in PBMDMs (Figure 20B). The murine macrophage study also tested mutations at a predicted TLR2-binding site but found no significant difference in IL-10 induction at 18hr with 5 μ g/ml and 10 μ g/ml mutant V-antigen. However, they saw increased TNF α secretion to a level comparable with their 500ng/ml LPS control in mutant V-antigen stimulations. The study did not investigate whether internalisation dynamics were altered which, after an 18hr stimulation, would have seen the WT protein internalised. This may have been prevented in the mutant V-antigen and that could have caused it to act solely as an inflammatory stimulant, something witnessed in the non-LPS stimulated V-antigen stimulations in Chapter 3 (3.3.2) before internalisation.

The use of IL-10 $^{-/-}$ cells or anti-IL-10 antibodies as a means of examining whether a lack of IL-10 prevented V-antigen from exerting immunomodulatory effects is also to be challenged. As mentioned in 5.3.3, IL-10 is an important regulator of inflammation that is induced by inflammatory stimuli like LPS and Zymosan A(278). An abolition of IL-10 will generate altered inflammatory dynamics and cytokine induction, particularly in a closed cell culture system and over longer stimulations, and so without appropriate controls these results are not valid. Unfortunately, no IL-10-depleted LPS-stimulated control was performed and so it is impossible to fully conclude that the increase in TNF α secretion was the result of blocking V-antigen's mechanism of action and not just altering the inflammatory conditions, despite this matching with the data presented in Figure 30B(148, 153).

Other studies remain too short and limited for effective comparison and have limited information to draw conclusions on. *A.Sing, et al. 2002B(149)*, presented data of IL-10 induction by V-antigen at 2hr post-introduction with a macrophage cell line however, IL-10 was the only cytokine tested for in the experiment and so whether it was induced by an anti-inflammatory or pro-inflammatory response is unknown. The data presented in Chapter 3 in this project suggests that the response would be inflammatory though the study itself assumes that it is an anti-inflammatory mechanism. The study is also too short to evaluate the secondary immunomodulation induced by V-antigen.

In vivo studies have presented more of an opportunity to insert our findings, particularly about TGF β . In part this is because of the longer nature of these studies but it also due to the consistency of the results between studies. The most striking of these is the importance of IL-10 in the immunomodulation of V-antigen long-term *in vivo*. V-antigen+ *Yersinia pestis* and *Yersinia enterocolitica* shows a consistently higher lethality in mouse studies as well as greater tissue infiltration compared with V-antigen $^{-/-}$ *Yersinia*(132, 134). This

immunomodulation is potent enough to give 100% protection from an LD50 dose of LPS(147) and removal of V-antigen or sequestering it via antibody intervention protects from a lethal dose of *Y.pestis*(151, 152). These studies take place over the course of at least 24hr but extend up to 14 days and so fit comfortably after the window of V-antigen's internalisation which shows that IL-10 must become an important mediator in the anti-inflammatory properties of V-antigen during the secondary phase of its immunomodulation. The discrepancies between even the longer-term stimulations *in vitro* and the *in vivo* studies also suggest that either there is a highly delayed and substantial IL-10 response that arises *in vitro* that has not yet been identified/reported or that the multicellular system of *in vivo* studies exacerbates the anti-inflammatory effect of V-antigen to include IL-10 and that this is not present in *in vitro* studies. As explained in 5.3.3, TGF β is an inducer of IL-10 secretion, particularly from T-cells, and can stimulate the development of Treg cells by promoting the TF; FoxP3, in naïve T-cells. It can also trigger an anti-inflammatory transition in macrophages which adds to the immunosuppressive environment(279). The development of a progressively more immunosuppressive environment triggering from TGF β and IL-10 secretion could explain the reason that V-antigen inoculation leads to an inflammatory resistance that continues to grow until it peaks at 48hr and continues beyond 72hr(147).

R.Nakajima, et al. 1995(134) examined the effect of V-antigen on TNF α and IFN γ secretion by utilising V-antigen-/- *Y.pestis* and comparing response with and without inoculation with recombinant V-antigen. As per Chapter 3, they reported that V-antigen induced a strong suppression of TNF α secretion. However, they also reported a strong suppression of IFN γ , in opposition to what was observed in this study (Figure 19B). This, once again, can be explained by the use of human monocytes and the lack of restriction that human monocyte SOCS1 has on the IFN γ pathway unlike other cell lines and murine monocytes(237). This would prevent V-antigen from restricting IFN γ signalling in human monocytes. This also highlights that the use of *in vivo* experiments also likely poses a more accurate view of the total inhibition seen compared to closed *in vitro* systems due to the inhibition to both TGF β (238) and IL-10(277) attributed to IFN γ production, as well as the more diverse cell populations.

These effects were also shown in this project to arise from a central protective epitope within V-antigen, corresponding to aa135-275, which had been previously speculated to contain the active region for V-antigen's immunomodulatory effects. This had been speculated because of the evolutionary conservation of this region(159), the potency of protective antibodies against this region(158), and the importance of immunomodulatory V-antigen in *Yersinia spp* pathogenesis(134). In Chapter 6, previously produced plasmids that encoded peptides corresponding to the central protective epitope (Table 17, Figure 60) were

expressed and tested for changes in both cytokine secretion and gene expression. This included analysis on the induction of TGF β secretion. 6.3 provides a full analysis of the similarities and differences between these but there was sufficient evidence to conclude that the central portion of V-antigen (aa135-275) appeared to create an immunomodulatory effect similar to that of the WT protein. It was therefore theorised that the V-antigen fragments were capable of internalisation and so, this region may also be involved in this mechanism as well. These two effects may therefore be the reason behind the high conservation of this region and the protective nature of antibodies raised to epitopes within it.

7.4: The therapeutic potential of V-antigen

7.4.1: The suppression of MyD88 and the effects within the TLR

signalling pathway

The potential use of V-antigen as a therapeutic for inflammatory conditions is a complicated topic. Originally, the intrigue behind its potential use arose largely due to its then-unknown mechanism of action and the previous evidence that V-antigen protected mice against LPS-induced inflammatory shock(147). However, now that the mechanism of action has, at least in part, been uncovered, there is more evidence to review as to whether V-antigen holds therapeutic potential.

Firstly, the analysis of a wider profile of secreted cytokines provided by this study gives a more expansive understanding of the level of immunosuppression caused by V-antigen. As detailed in 7.3.1 and evidenced within Chapter 3, V-antigen provides a significant inhibition to the secretion of inflammatory cytokines in response to LPS in monocytes. This included, over the scope of 16hr, both proinflammatory cytokines and the anti-inflammatory cytokine, IL-10. IFN γ however had an increased secretion under V-antigen stimulation. This was hypothesized to be due to the use of human monocytes as a model cell line and, as previous studies have shown, does not appear in *in vivo* models and so would not be expected to be present if V-antigen was used as a therapeutic(147).

Secondly, the gene expression data in Chapters 4 and 5 revealed a viral-like inflammatory response which was theorized to be due to inhibition in the MyD88 pathway and a lack of inhibition in the TRIF pathway. Bacterial and fungal PAMPs as well as TLR-interacting DAMPs largely utilise the MyD88 pathway (with the exception of DAMPs that interact with TLR3) and so arguably the inflammatory response triggered through interaction with most TLRs may be reduced in the presence of V-antigen. This study does not, however,

answer whether TLR3 stimuli would escape V-antigen-mediated immunomodulation. Despite being strong inducers of the TRIF-pathway, this pathway still utilises the MyD88 pathway but downstream of MyD88 via TRAF6(280). This route therefore circumvents MyD88 and so, if V-antigen inhibits TLR signalling largely through MyD88 inhibition in monocytes, it remains to be seen whether TLR3 stimuli can still induce NF κ B activation to the same degree in the presence of V-antigen as it can in the absence of it. This distinction could be important in deciding how impactful V-antigen would be as a therapeutic in viral/TLR3-mediated inflammatory disorders such as viral sepsis or cases involving tissue necrosis(281) though likely, as seen in *in vivo* studies and as detailed in 5.4.2.1, 5.3.3, and 7.4.2, the wider anti-inflammatory effects of TGF β would still inhibit inflammation in these cases. The lack of inhibition down the TRIF pathway could also be a positive trait in some inflammatory disorders however as there is evidence that the stimulation of TLR3 or induction of IFN α/β is protective in ulcerative colitis and promotes better tissue function in the ileum in inflammatory bowel disease(282-284). Further investigation into TLR3 stimuli and V-antigen should therefore be conducted.

7.4.2: Endogenous TGF β and its therapeutic potential

Understanding V-antigen's therapeutic potential also requires a fuller understanding of the effects that TGF β induction could have *in vivo*.

TGF β , as outlined in 1.1.4.1, plays a substantial role in the resolution of inflammation. Secreted by resolution phase macrophages, MDSC's, and Treg cells, TGF β orchestrates a reduction in leukocyte responsiveness, promotes pro-resolution phenotypes in leukocytes, and induces tissue repair and fibrosis mechanisms. TGF β is also well-known for inducing tolerance, a similar state to resolution characterised by a reduced responsiveness to proinflammatory stimuli. In the case of proinflammatory stimulation, tolerance can last for up to 48hr after the primary stimulation(285) however tolerance in the gut is sustained indefinitely through TGF β secretion from Th3 cells(286). A form of tolerance has also recently been discovered to be present in healthy *in vivo* inflammation as a post-resolution phase or 'adapted homeostasis' which can last up to a few weeks in some cases(287). This adapted homeostasis sets the tissue microenvironment in a state of reduced responsiveness to reduce the chances of further inflammation and allow for tissue repair to take place. It also has a role in reducing the responsiveness to endogenous 'self' peptides which may still be present as this could further stimulate an immune response and could potentially trigger autoimmunity. These characteristics of TGF β signalling appear promising when determining the therapeutic potential of V-antigen and its mechanism of action as TGF β directs the

resolution of inflammation already and subdues the inflammatory response for a period of time after this resolution too, allowing time for the body to heal.

However, outside of resolution, TGF β is heavily involved in homeostatic processes throughout the body too and has roles in embryo development, cell differentiation, survival, migration, tolerance, and proliferation. TGF β is a highly contextual signalling molecule - different cell types and the presence/absence of other signalling molecules modulate how TGF β affects different tissues. This is because SMADs, the effector TFs of the TGF β signalling pathway, are co-transcriptional activators. They interact with other transcription factors and, via the formation of a heterodimer co-transcription factor complex, they alter the expression of genes. This therefore means that the presence of different transcription factors, activated from other signalling pathways, alter a large number of the genes that get regulated under TGF β stimulation. Its diverse connections and cell-type-dependent effects means it therefore has a wide scope of effects - cytostatic in some cases(288) while promoting growth in others(289), promoting cell survival in some cell types (resting B cells) and apoptosis in others (hepatocytes)(290). Often these effects are regulated by other key developmental/homeostatic pathways like Wnt, Notch, Hedgehog, Jak/STAT, PI3K-Akt, MAPK, and NF κ B. An example of this is active STAT3 which binds to Smad3 to prevent Smad3/4 formation. This prevents the upregulation of genes associated with cell cycle arrest while leaving other aspects of TGF β 's function unaffected(291). It is for this reason that the clinical use of TGF β is remarkably difficult to predict the full effects of. This is especially true in an inflammatory environment as studies have shown that the effects of TGF β can be reduced or altered by proinflammatory cytokines. Depending on the presence of inflammatory cytokines, TGF β can inhibit(292), activate(293), or enhance NF κ B activity, and it can also synergise with TNF α or IL-1 to promote genes not upregulated under solo stimulation(294). This reduces the therapeutic potential of TGF β as the chance of unwanted side effects is high. This remains the case despite *in vivo* mouse studies not reporting any untoward side effects with V-antigen inoculation as a full investigation into the health of the mice has not been undertaken. It is also important to clarify that the healthy lab mice used in these studies only represent acute inflammation or infection and not cases of chronic inflammation, chronic infection, comorbidities, or the dysregulated inflammatory responses of sepsis.

Poorly regulated TGF β can have severe effects *in vivo* and, while it can contribute to pulmonary inflammation and alveolar epithelial cell apoptosis(295) when overexpressed in the lungs, TGF β 's major contributors to disease tend to be linked to its pro-fibrotic effects, its influence in the CNS, and its role in regulating the ECM. For example, Marfan's syndrome is a connective tissue condition caused by a mutation in the fibrillin-1 gene. This mutation

affects the ECM's ability to bind and retain latent TGF β , particularly under mechanical stress, causing higher levels of TGF β release, maturation, and therefore signalling within the tissue(296). This leads to reduced mitosis within interstitial muscle cells and inhibition of the Bone Morphogenic Protein 2 (BMP-2) signalling pathway – a protein key for regulating bone and cartilage production – and this leads to the unusually tall and slender phenotype shown by Marfan's syndrome patients(297). Its ability to promote fibrosis has been linked to fibrotic renal disease, vascular dementia, and systemic sclerosis in cases where regulation becomes lost, and in the CNS, overexpression has been linked to hydrocephaly in both humans and mice(298). While many of these conditions arise due to longer term overexpression of TGF β , it is important to consider that the underlying pathways will still be affected to a degree during shorter term usage and so in cases where patients have risk factors associated with these pathways and disease, the further induction of TGF β may have to be evaluated for safety.

TGF β also has a substantial underlying concern with its induction; the link it has to survival, proliferation, migration, and inhibition of inflammation (5.2.4.1 and 5.3.3) means that TGF β is commonly upregulated in various cancers. It is a highly tumorigenic cytokine(294, 299) and therefore, TGF β has been examined therapeutically largely with the aim to generate anti-TGF β therapies(300) and therefore it's purposeful induction within patients must be considered as to whether it could have any impacts on tumorigenesis. There have already been links drawn between corticosteroid use and increased rates of cancer due to the reduced capability for the immune system to respond to arising cancer cells(301) but these do not additionally promote proliferation and migration like TGF β does.

One study has examined promoting TGF β signalling as a therapeutic and this was achieved via a TGF β -mimic derived from the *Heligmosomoides polygyrus* parasite. The mimic was used to stimulate the differentiation of CD4+ T-cells to FOXP3+ Treg cells as a potential therapy for chronic intestinal diseases like inflammatory bowel disease(302). The study found that the mimic successfully induced a greater number of FOXP3+ Treg cells and that, unlike TGF β , it did not induce the upregulation of pro-fibrotic genes. Therefore, if inducing TGF β is determined to be a viable solution to managing inflammatory disorders, the therapeutic advantage of not inducing fibrosis would make this mimic a much safer therapeutic than endogenous TGF β and therefore would overwrite the potential for V-antigen to be a useful therapeutic.

TGF β therefore presents a potentially useful pathway to trigger as a means of regulating ongoing inflammation however the possibility of side effects via TGF β 's effects on

homeostasis, and its promotion of tumorigenesis and fibrosis, means that more investigation into the effects of its short- and long-term induction is needed.

7.4.3: V-antigen and its fragments as anti-inflammatory therapeutics

The current hypothesis of V-antigen's mechanism of action is that it induces the secretion of TGF β either to stimulate TGF β -mediated immunomodulation or as a byproduct of activating the pathway itself. There has been no evidence provided in this study to determine which of these is true, but when considering the potential for V-antigen as a therapeutic, it becomes an important distinction. Chapter 3, and other previous studies discussed in 3.3.2 and 7.3.2, revealed a lack of potent IL-10 response in the early stages of V-antigen stimulation. In PBMDMs, there were signs of a rapid response (within 1hr) of introduction, however this did not correlate to an IL-10 response. Therefore, the evaluation of V-antigen as a therapeutic relies upon both the source of this initial immunomodulation and the exact mechanism of action of V-antigen. If V-antigen's most substantial immunomodulatory effect is the induction of TGF β secretion, then its use as a therapeutic would be greatly reduced as recombinant TGF β could be supplied with the same efficacy without having to wait additional hours for internalisation and then induction of TGF β secretion. The rapid anti-inflammatory effect seen in TNF α , IL-8, IL-6, and IL-10 in Chapter 3 does however show that V-antigen can have a response that is significantly suppressive within 1hr, and as this does not appear to be caused by IL-10, further investigation into the source of this immunomodulation would provide further insight into the therapeutic potential of the protein. The quick and substantial impact is promising though as most anti-inflammatory treatments are therapeutic and not prophylactic so rapid induction is important. This is supported *in vivo* by *Y.Nedialkov, et al. 1997(147)* who showed that 50 μ g V-antigen injected into mice gave an immediate resistance to LPS-mediated inflammatory shock.

The evidence in Chapter 6 highlights that the immunomodulatory region of V-antigen can be isolated from the full protein. As a virulence protein which has been shown to have other intracellular interactions with host proteins(145), isolating a functional peptide which has the same/similar activity is promising for its potential as a therapeutic. This reduces the chances of side-effects via interactions with other host proteins or infectious pathogens such as in the case of sepsis. The functional peptides also appeared to inhibit IL-1 β to a greater extent than full WT V-antigen. This could be due to a number of reasons such as altered internalisation dynamics, being less of an inflammatory stimulus itself, or the side effect of the dosing discrepancy described in Chapter 6. Investigation into why there appears to be a

more potent immunomodulation in the fragment would shed further light onto whether the peptides have additional advantages over the WT protein as a therapeutic.

It is also worth considering the length of time that V-antigen has been shown to have an immunomodulatory effect for. The natural resolution of inflammation, as described in 7.4.2 can lead to a reduced inflammatory responsiveness for days up to a few weeks and *Y.Nedialkov, et al. 1997(147)* showed that V-antigen can have prominent anti-inflammatory effects *in vivo* up to at least 72hr post inoculation. Non-steroidal anti-inflammatory drugs, which often work through COX1/2 inhibition to inhibit inflammatory signalling molecules like prostaglandins and prostacyclins, have a short half-life of no more than a few hours, whereas steroidal anti-inflammatories, which work by inhibiting the transcription of numerous inflammatory genes, can last from <12hr for shorter-lived drugs like Cortisone up to a biological half-life of 36-54hr for drugs like Dexamethasone and Betamethasone(303). This puts the timing of V-antigen's immunomodulation at the higher end of the window for currently available anti-inflammatory drugs.

However, it is unknown whether TGF β is an ideal therapeutic target, particularly in the case of inflammatory conditions where high levels of secreted cytokines could alter the outcomes of TGF β effectors (7.4.2). This is particularly true in cases of extremely dysregulated inflammation such as in sepsis or other forms of excessive inflammation where TGF β levels have been shown to be negatively correlated to survival(304). The lack of suitability of TGF β as a target is further highlighted by the evidence that TGF β regulation is highly important for the both mother(305) and embryo(306) during pregnancy and so TGF β -inducing therapies would likely not be safe for use in pregnant women either.

In conclusion, V-antigen has clear capabilities as an immunomodulatory protein. However, V-antigen likely does not have much draw as a therapeutic agent. The use of peptides/proteins as therapeutic agents will always generate natural immunity to the treatment over time, meaning that V-antigen has a minimal number of uses per patient. Currently, there are already effective anti-inflammatory drugs on the market and, due to the mechanism of action being centred around TGF β , it is not likely that V-antigen can offer a worthwhile therapeutic advantage over any of these or the mimic described by *C.Johnston, et al. 2017(302)*. The possibility to promote resolution of inflammation rather than just restricting inflammatory signalling/upregulation as steroidal and non-steroidal anti-inflammatory drugs currently do is an interesting concept but as previously mentioned TGF β has the potential for side effects due to its wide range of effects throughout the body and it has already been shown to have a negative effect on prognosis in conditions like sepsis(304). Regardless, this discovery of V-antigen's mechanism of action is still able to

shed an important light on the virulence of *Y.pestis* and give an understanding of why the current literature surrounding V-antigen's immunomodulation are so inconsistent. It also highlights an important question about the early stage of immunomodulation which was seen despite a weak induction of IL-10 therefore there are multiple avenues to continue this research into the future. These are discussed in part in 7.5.

7.5: Future experiments:

While this study has presented promising evidence about the mechanism of action for V-antigen's immunomodulation, there remains the need to further confirm and expand upon these results.

A detailed investigation into the internalisation of V-antigen and its fragments would be important to confirm the timing of the internalisation. Figure 12 shows a single representative image of internalisation at 4hr but further investigation with a tagged control protein like BSA and an extended set of timepoints to show that the uptake into the early endosome was not merely the result of macropinocytosis is needed. This would also confirm that V-antigen internalises beyond the endosome, into the cytoplasm. Examining the internalisation of the V-antigen fragments by Oregon Green conjugation and imaging would also be an ideal future step for the project to take. While there is evidence of the internalisation of these fragments based upon the induction of TGF β maturation and secretion and the transcriptional changes induced by this which correlate closely to WT V-antigen, the conclusive proof via fluorescent imaging would be an important piece of evidence to acquire, especially when aiming to understand the early effects of V-antigen and its fragments.

There is also a clear need to run manual qPCR to determine between the discrepancies in the qPCR gene array plates in Chapters 4 and 5. In 5.2.3, it was highlighted that some of the genes that were present on both plates appeared to show differing levels of expression despite coming from the same RNA sample. Running qPCR outside of the qPCR gene array plates would allow a third value to be gathered from the sample and perhaps identify which of the two values was more accurate to the true level of expression. This could also be performed with some of the more consistent genes too to ensure that they remain consistent and that the variation in some genes is more likely down to an artifact than to inconsistent plates or experimental work. It would also be desirable to repeat the qPCR gene arrays for pV3 and pV6 with new stimulations to determine whether the inhibition of cytokines and induction of TGF β that they both displayed in Chapter 6 also showed similar functional cluster enrichment as the WT, and pV1/pV2. This would be particularly useful for pV6 which

appeared to have a less inhibitory effect on cytokine secretion and so may display a different expression profile to pV1, pV2, and pV3.

It would also be beneficial to test the effect of V-antigen on other TLR stimuli to show how potent the effects of V-antigen are felt on exclusively MyD88 pathway stimuli and exclusively TRIF pathway stimuli. This would confirm whether V-antigen affects only the MyD88 pathway with any substantial modulation. Testing other cell lines could also provide key evidence to show that the monocyte work performed here had an elevated IFN γ response due to the lack of IFN γ signalling pathway suppression by SOCS1 and that it is not an attribute of V-antigen stimulation. Although other papers have not shown that to be the case, our own experimental evidence with the same isolate of recombinant V-antigen would be a more valid test of this to draw conclusions from. It would also be of note to investigate longer stimulations which extend deeper into the secondary immunomodulation effect of V-antigen, such as 24hr, 36hr, and 48hr timepoints to allow it to take a stronger effect on inflammation, and to investigate how V-antigen affects inflammation that has been triggered prior to V-antigen addition by stimulating with LPS before V-antigen.

Further testing on the growth media from the other timepoints of the stimulations would also be beneficial as this would allow the determination of when the increased secretion of TGF β occurs. It would potentially be beneficial to investigate other methods to detect mature TGF β too as the detection limit of 500pg/ml prevented the quantification of TGF β from our LPS-stimulated control and so negatively affected the power of the statistics presented in Figures 58 and 78. It would be important to understand whether the rapid induction of immunomodulation seen in PBMDMs was due to faster TGF β induction or another mechanism. It would also serve as evidence for whether the V-antigen fragments have any altered induction over the WT.

Finally, investigation into the interactome of V-antigen post-internalisation would be very useful in determining how V-antigen induces TGF β secretion. Using antigen-capturing methods and subsequent MS/MS proteomics, it would be possible to identify host proteins that interact with V-antigen and therefore identify key factors and pathways that V-antigen interferes with.

These would solidify the findings and understandings of a detailed *in vitro* study of V-antigen's immunomodulatory effects, paving the way for future *in vivo* studies.

8: Appendix

8.1: Appendix A - recipes

Growth media – Human monocytes/macrophages:

-RPMI 1640 + Glutamax™

-10% (v/v) FCS

-0.02% (v/v) supplementary non-essential amino acids

-1mM oxaloacetate

-0.45mM pyruvate

-0.2U/ml insulin

Miltenyi Buffer:

-5ml 0.5M EDTA

-2.5ml 10% BSA solution

-500ml 1x PBS

-Filter sterilise

Luria broth:

-10g bacteriological peptone

-5g yeast extract

-5g NaCl

-1L ddH₂O

Luria broth agar:

-10g bacteriological peptone

-5g yeast extract

-5g NaCl

-15g agar

-1L ddH₂O

10x PBS:

-100g NaCl

-2.5g KCl

-18g Na₂HPO₄·2H₂O

-2.5g KH₂PO₄

-1L ddH₂O

Phenolchloroform/isoamyl:

-500ml phenol

-480ml chloroform

-20ml isoamyl alcohol

Chloroform:isoamyl alcohol:

-960ml chloroform

-40ml isoamyl alcohol

STET buffer:

-8g sucrose

-500µl Triton X-100

-10ml 500mM EDTA pH8.0

-1ml 1M Tris-HCl pH8.0

-Up to 100ml with ddH₂O

2M sodium acetate:

-16.4g sodium acetate

-Up to 100ml with ddH₂O

-Adjust to pH8.0 with HCl

5x TBE:

-54g Tris base

-27.5g boric acid

-Dissolve in 900ml ddH₂O

-20ml 0.5M EDTA pH8.0

-Up to 1L with ddH₂O

2x sample buffer:

-10ml 0.5M Tris-HCl pH6.8

-8ml 10% SDS

-5g Glycerol

-2ml β-mercaptoethanol

-5mg bromophenol blue

Cleavage buffer:

-1.514g Tris base

-2.19g NaCl

-1mM EDTA

-1mM DTT

-25μl Triton X-100

-Up to 250ml with ddH₂O

-Adjust to pH7.0 with HCl

3M NaCl:

-87.66g NaCl

-500ml 1x PBS

0.5M Tris-HCl pH6.8:

-15.14g Tris base

-250ml ddH₂O

-Adjust to pH6.8 with HCl

1.5M Tris-HCl pH 8.8:

-45.42g Tris base

-250ml ddH₂O

-Adjust to pH8.8 with HCl

SDS-PAGE gel recipes:

Table 25 - SDS-PAGE gel recipes

Reagent	Resolving		Stacking
	10%	14%	4%
ddH ₂ O	4.02ml	2.6ml	6.1ml
0.5M Tris-HCl pH6.8	-	-	2.5ml
1.5M Tris-HCl pH8.8	2.5ml	2.5ml	-
30% acrylamide	3.33ml	4.67ml	1.3ml
10% SDS (w/v)	100µl	100µl	100µl
10% APS (w/v)	50µl	50µl	50µl
TEMED	5µl	10µl	10µl
Total	10ml	10ml	10ml

10x Running buffer:

-144g glycine

-30.2g Tris base

-10g SDS

-1L ddH₂O

1x Transfer buffer:

-4.22g Tris base

-10ml 10% SDS (w/v)

-200ml Propan-2-ol

-Up to 1L with ddH₂O

-Adjust to pH8.3 with acetic acid

Fixing solution:

-10% glacial acetic acid

-50% methanol

-40% ddH₂O

Coomassie blue stain:

-100ml methanol

-20ml acetic acid

-80ml ddH₂O

-0.6g Coomassie blue

Coomassie blue destain:

-100ml ethanol

-100ml acetic acid

-800ml ddH₂O

1M sodium bicarbonate buffer:

-8.4g sodium bicarbonate

-100ml ddH₂O

-Adjust to pH8.0

1.5M hydroxylamine buffer:

-4.95g hydroxylamine

-100ml ddH₂O

-Adjust to pH8.5

4% paraformaldehyde:

-8.0g paraformaldehyde

-100ml ddH₂O

-Heat to 60°C and stir

-Add a few drops of NaOH until it fully dissolves

-100ml 2x PBS

IFA blocking solution:

-0.1g BSA

-0.1g Saponin

-0.1g NaN₃

-500ml 1x PBS

Coupling buffer:

-0.2M NaHCO₃

-0.5M NaCl

-Adjust pH to 8.3

Buffer A:

-0.5M ethanolamine

-0.5M NaCl

-Adjust to pH8.3

Buffer B:

-0.1M acetate

-0.5M NaCl

-Adjust to pH4.0

Elution buffer:

-15mM Triethanolamine

-140mM NaCl

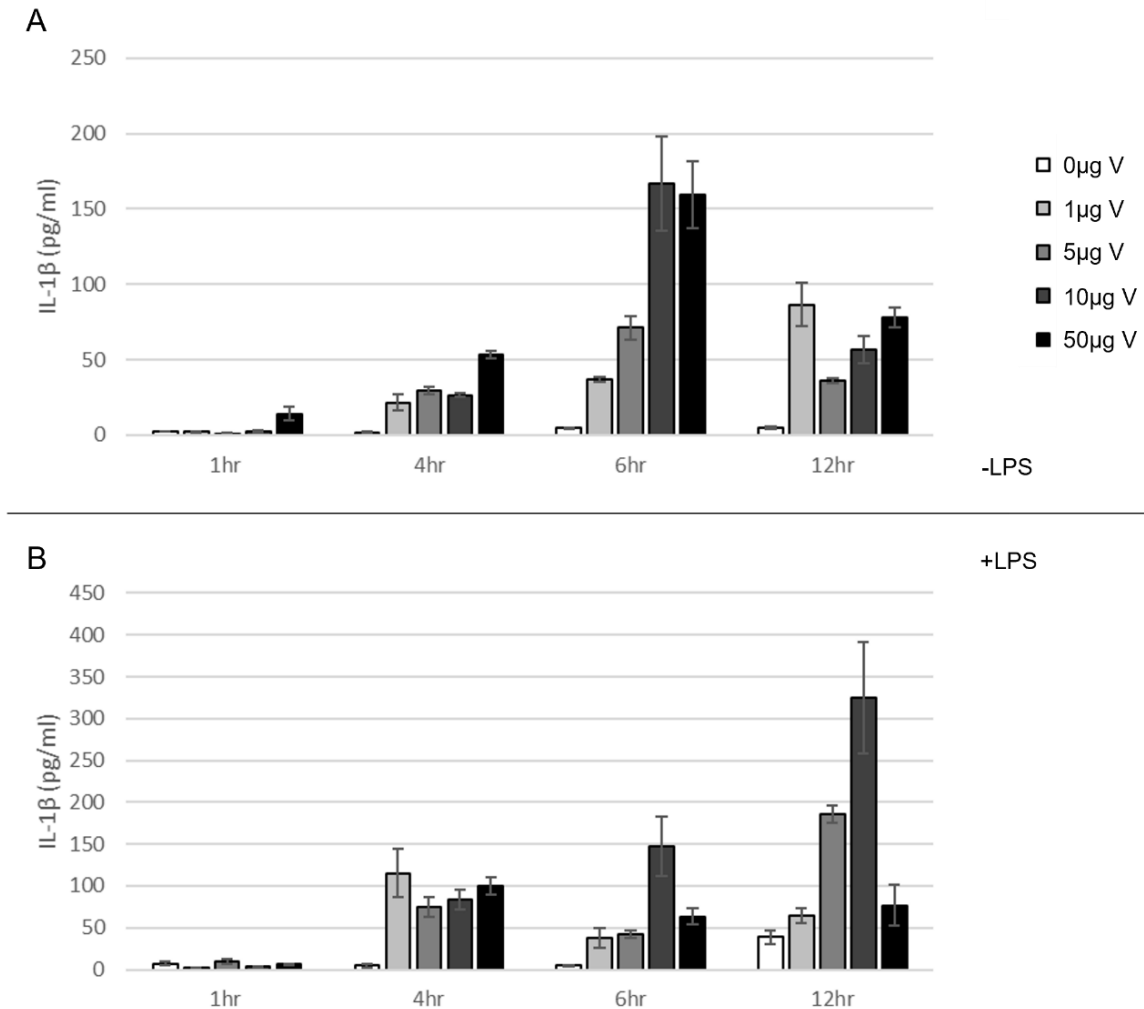
-30mM n-octyl-β-D-glucoside (b-OG)

-Adjust to pH11.5

8.2: Appendix B – Supplementary figures and tables

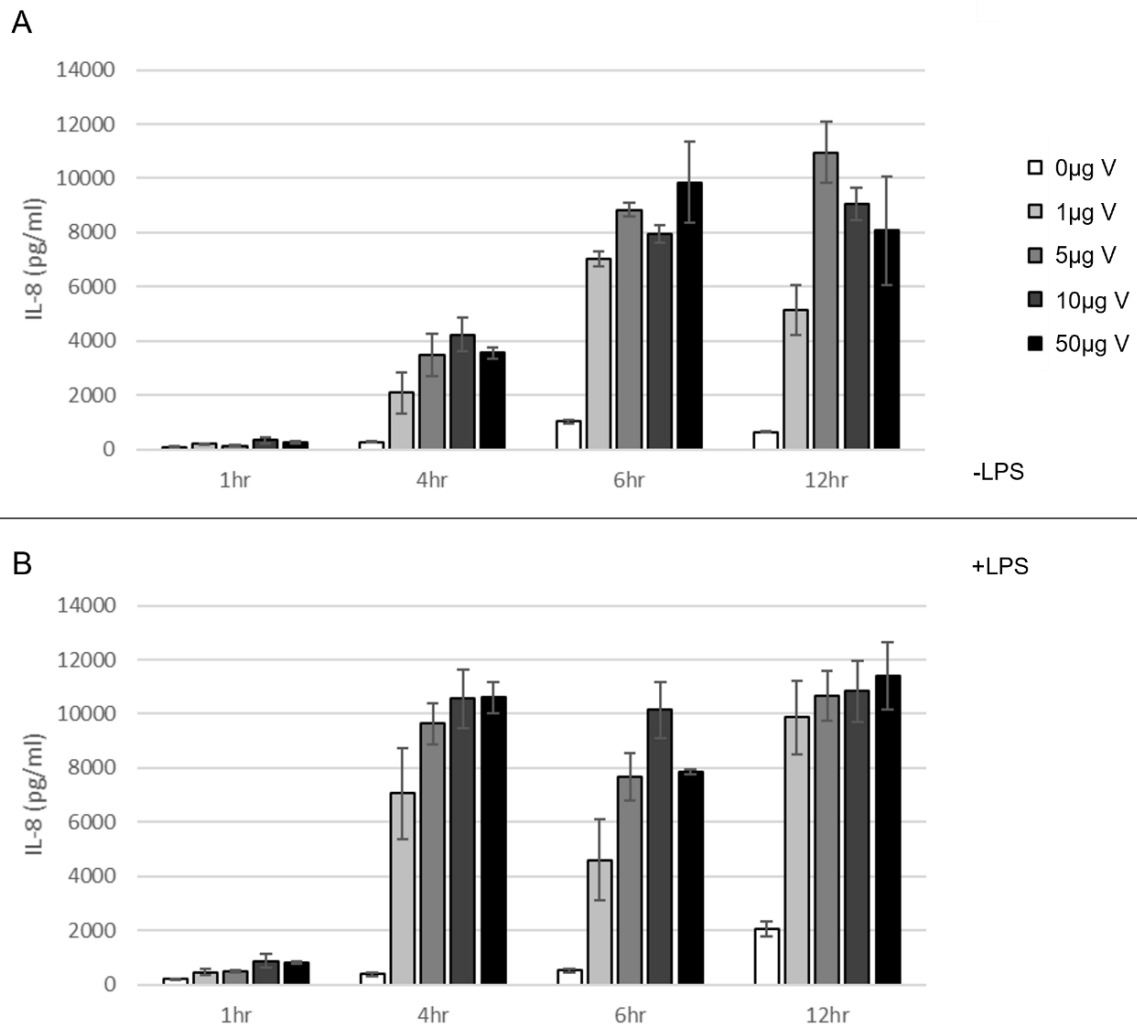
8.2.1: Supplementary figures

Supplementary Figure 1:



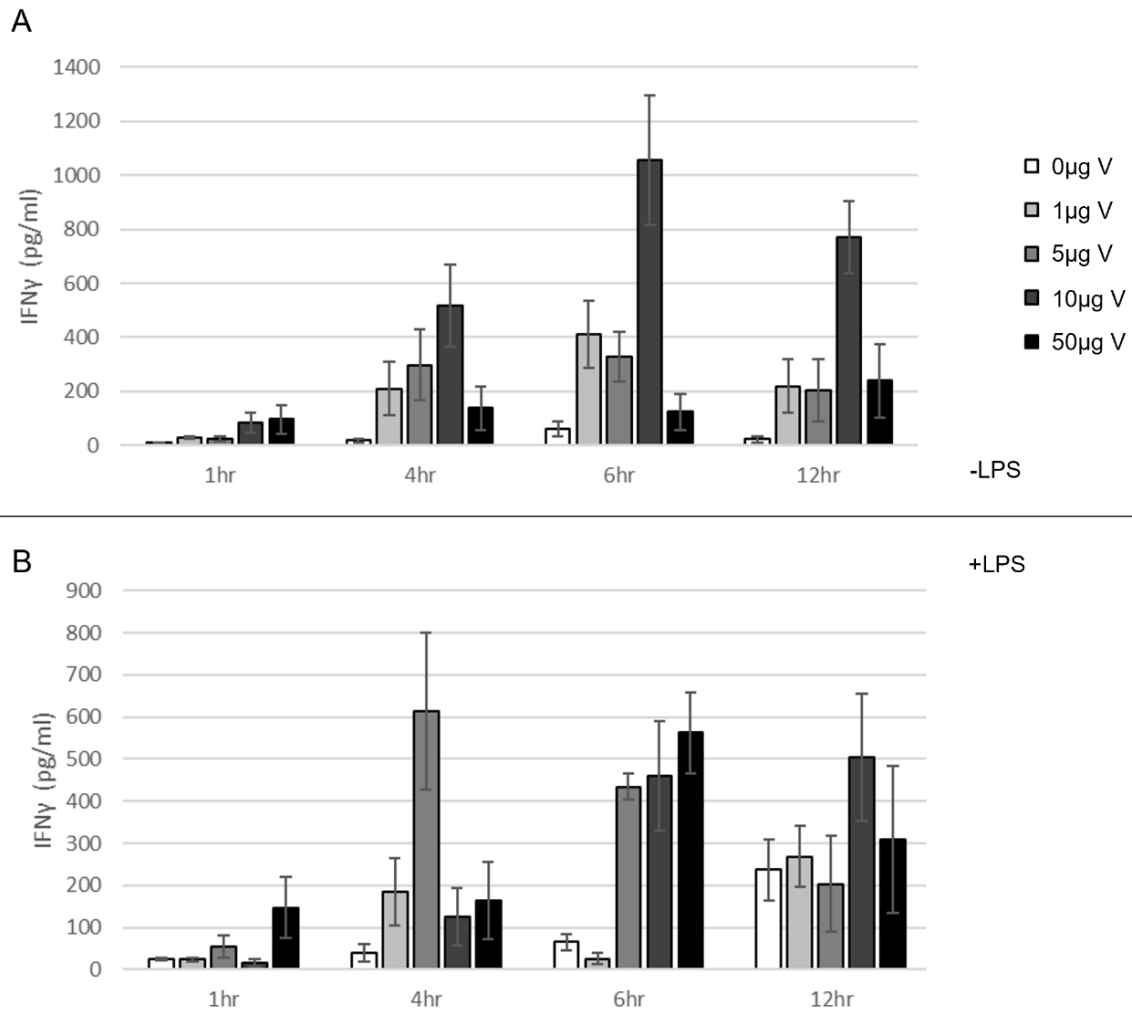
Supplementary Figure 1 - MM6 secreted level of IL-1 β in response to LPS/V-antigen stimulation – Mono-mac 6 (MM6) cells were seeded at a density of 5×10^4 cells/well on 24 well plates and allowed to attach overnight. These were pre-incubated with 0 μ g, 1 μ g, 5 μ g, 10 μ g, or 50 μ g V-antigen for 30min before stimulation with A; 0ng/ml LPS or B; 100ng/ml LPS for 1hr, 4hr, 6hr, and 12hr. The growth media from the cells was harvested and analysed using a 7-plex MSD Multi-spot Assay system kit to determine the level of IL-1 β that had been secreted. The data presented is constructed of 3 technical triplicates

Supplementary Figure 2:



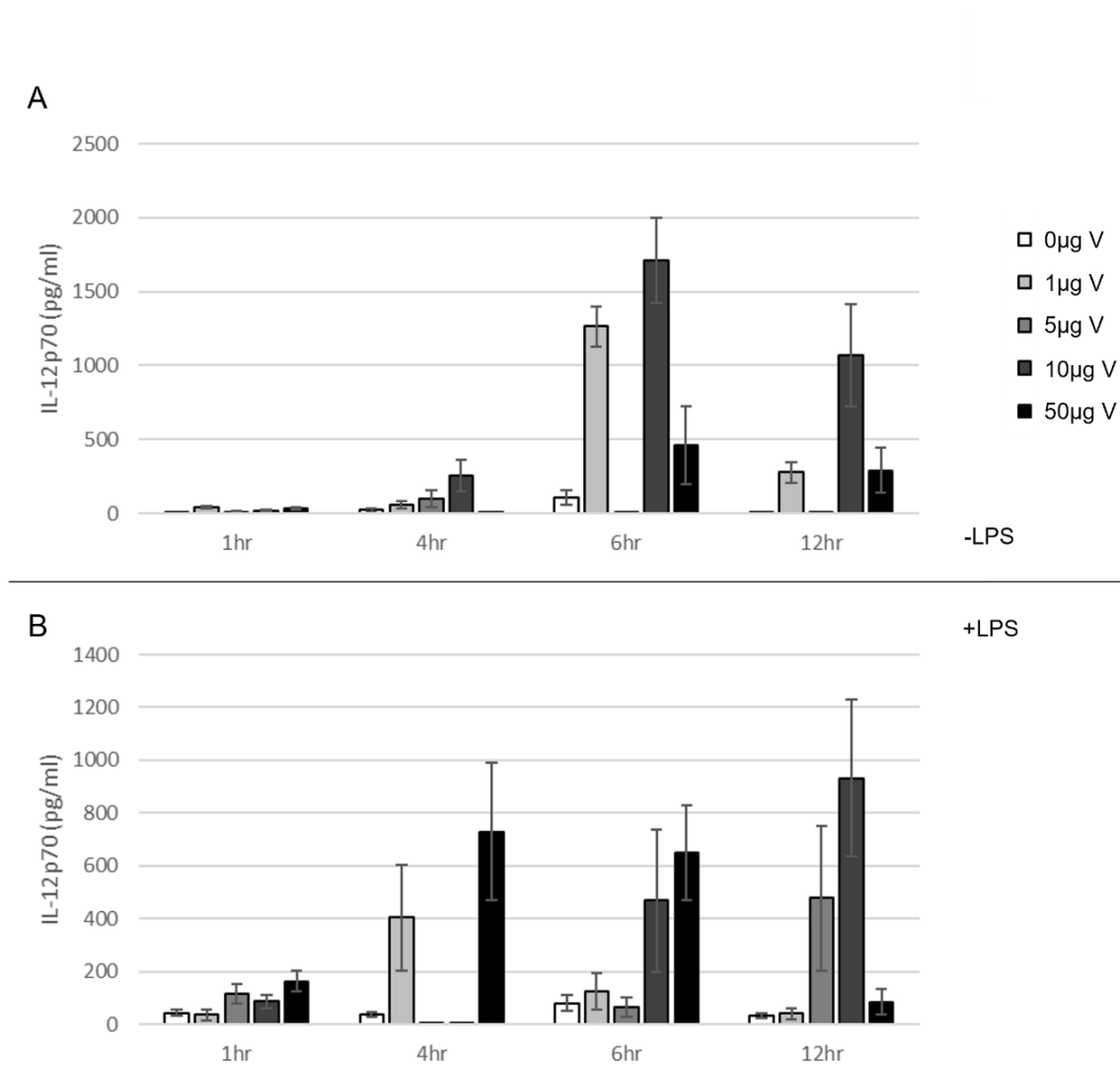
Supplementary Figure 2 - MM6 secreted level of IL-8 in response to LPS/V-antigen stimulation – Mono-mac 6 (MM6) cells were seeded at a density of 5×10^4 cells/well on 24 well plates and allowed to attach overnight. These were pre-incubated with 0µg, 1µg, 5µg, 10µg, or 50µg V-antigen for 30min before stimulation with A; 0ng/ml LPS or B; 100ng/ml LPS for 1hr, 4hr, 6hr, and 12hr. The growth media from the cells was harvested and analysed using a 7-plex MSD Multi-spot Assay system kit to determine the level of IL-8 that had been secreted. The data presented is constructed of 3 technical replicates

Supplementary Figure 3:



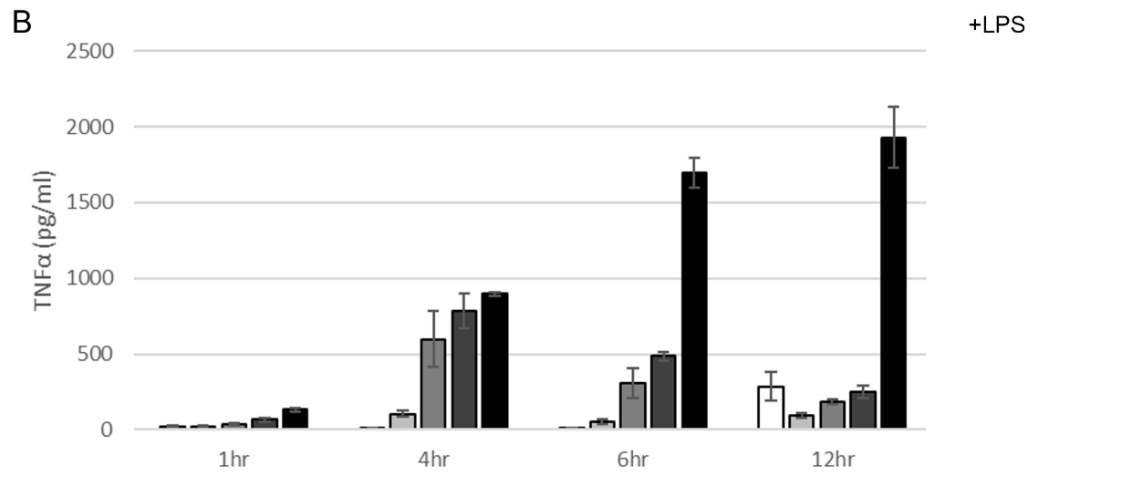
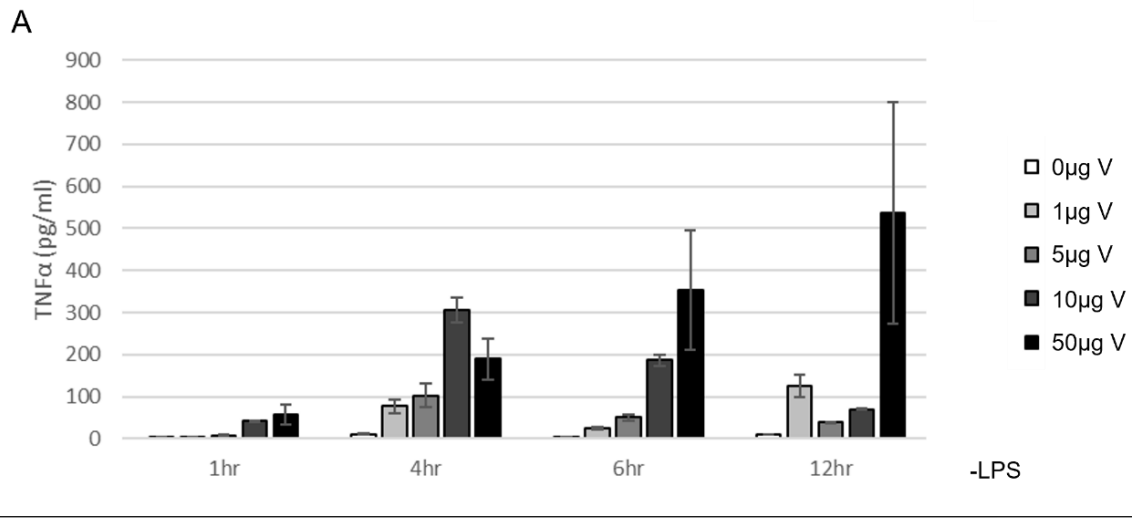
Supplementary Figure 3 - MM6 secreted level of IFN γ in response to LPS/V-antigen stimulation – Mono-mac 6 (MM6) cells were seeded at a density of 5×10^4 cells/well on 24 well plates and allowed to attach overnight. These were pre-incubated with 0µg, 1µg, 5µg, 10µg, or 50µg V-antigen for 30min before stimulation with A; 0ng/ml LPS or B; 100ng/ml LPS for 1hr, 4hr, 6hr, and 12hr. The growth media from the cells was harvested and analysed using a 7-plex MSD Multi-spot Assay system kit to determine the level of IFN γ that had been secreted. The data presented is constructed of 3 technical triplicates

Supplementary Figure 4:



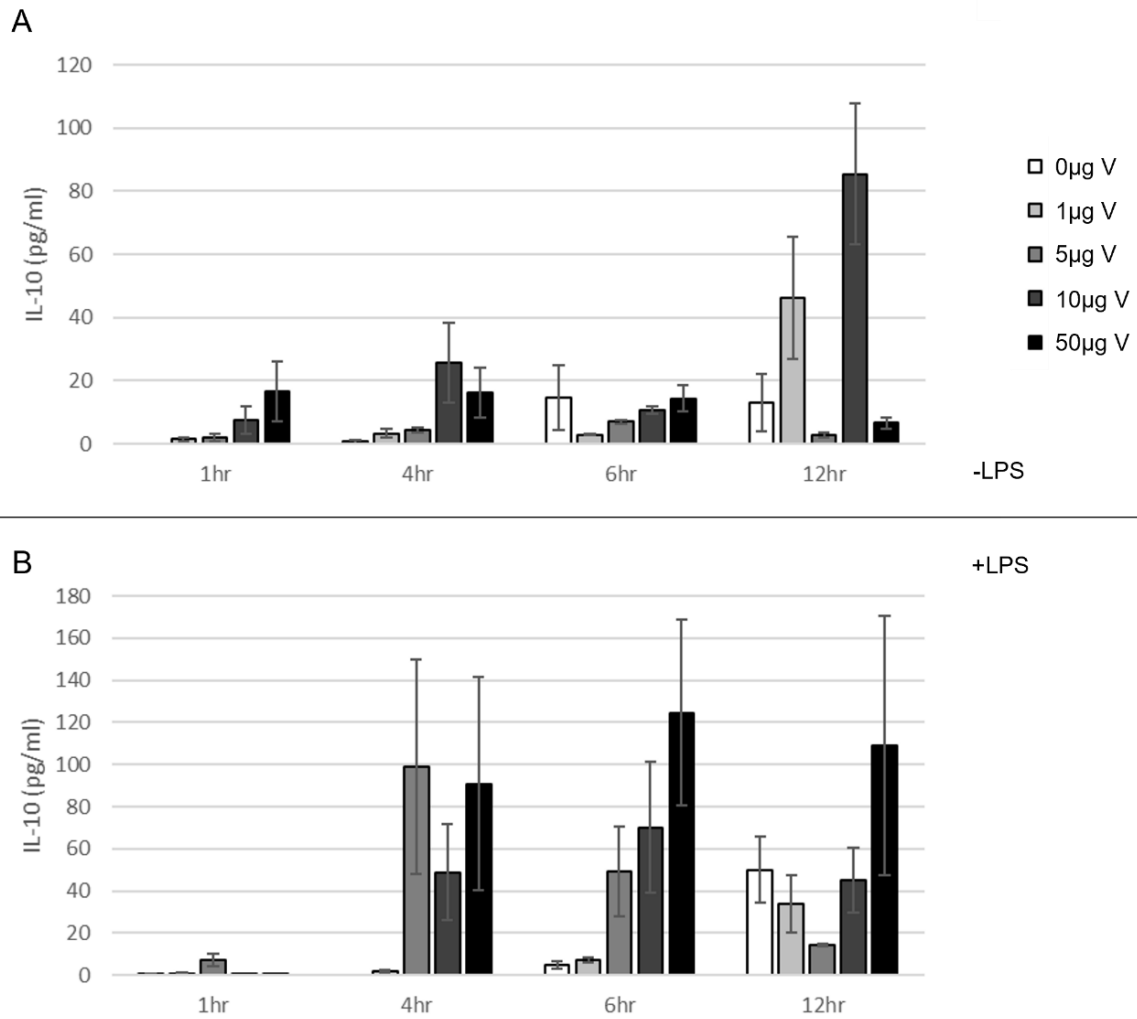
Supplementary Figure 4 - MM6 secreted level of IL-12p70 in response to LPS/V-antigen stimulation – Mono-mac 6 (MM6) cells were seeded at a density of 5×10^4 cells/well on 24 well plates and allowed to attach overnight. These were pre-incubated with 0µg, 1µg, 5µg, 10µg, or 50µg V-antigen for 30min before stimulation with A; 0ng/ml LPS or B; 100ng/ml LPS for 1hr, 4hr, 6hr, and 12hr. The growth media from the cells was harvested and analysed using a 7-plex MSD Multi-spot Assay system kit to determine the level of IL-12p70 that had been secreted. The data presented is constructed of 3 technical triplicates

Supplementary Figure 5:



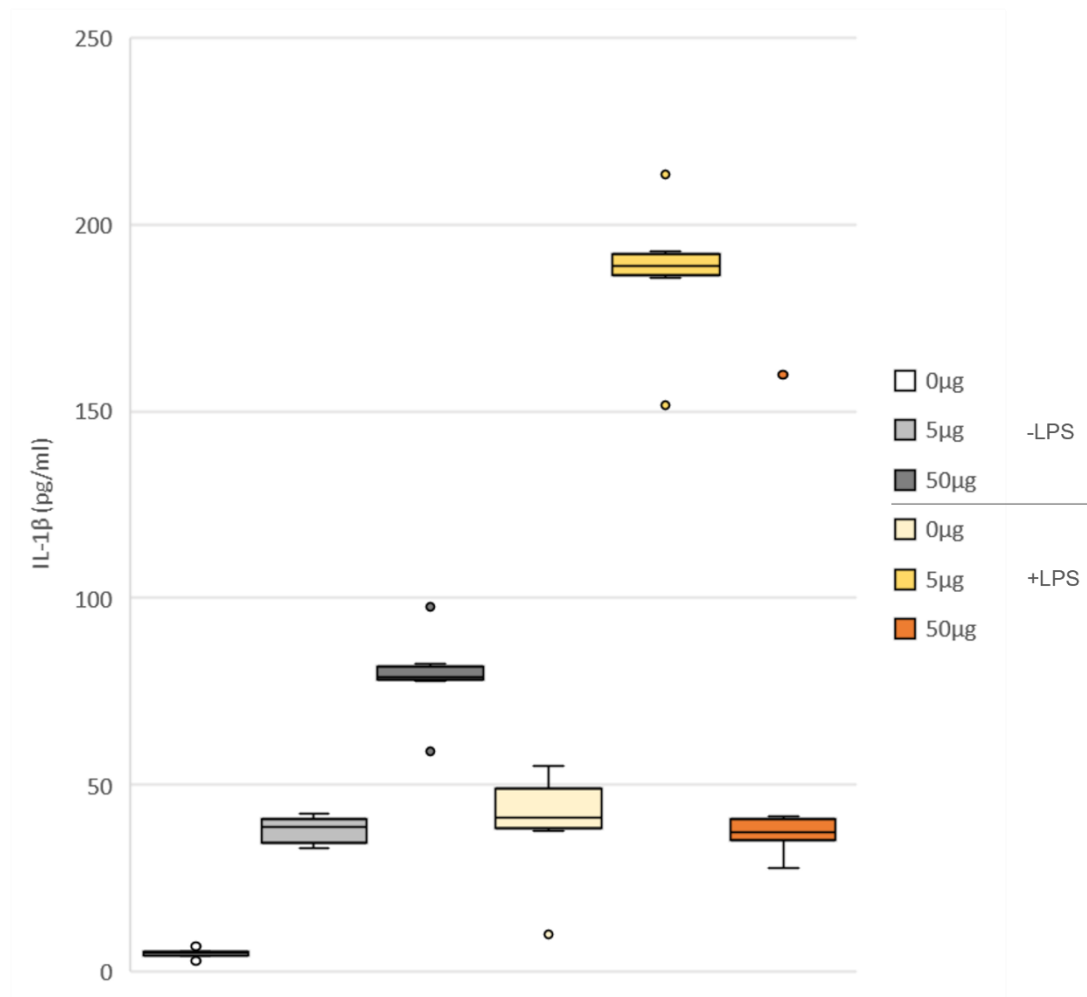
Supplementary Figure 5 - MM6 secreted level of TNFα in response to LPS/V-antigen stimulation – Mono-mac 6 (MM6) cells were seeded at a density of 5×10^4 cells/well on 24 well plates and allowed to attach overnight. These were pre-incubated with 0 μg, 1 μg, 5 μg, 10 μg, or 50 μg V-antigen for 30min before stimulation with A; 0ng/ml LPS or B; 100ng/ml LPS for 1hr, 4hr, 6hr, and 12hr. The growth media from the cells was harvested and analysed using a 7-plex MSD Multi-spot Assay system kit to determine the level of TNFα that had been secreted. The data presented is constructed of 3 technical triplicates

Supplementary Figure 6:



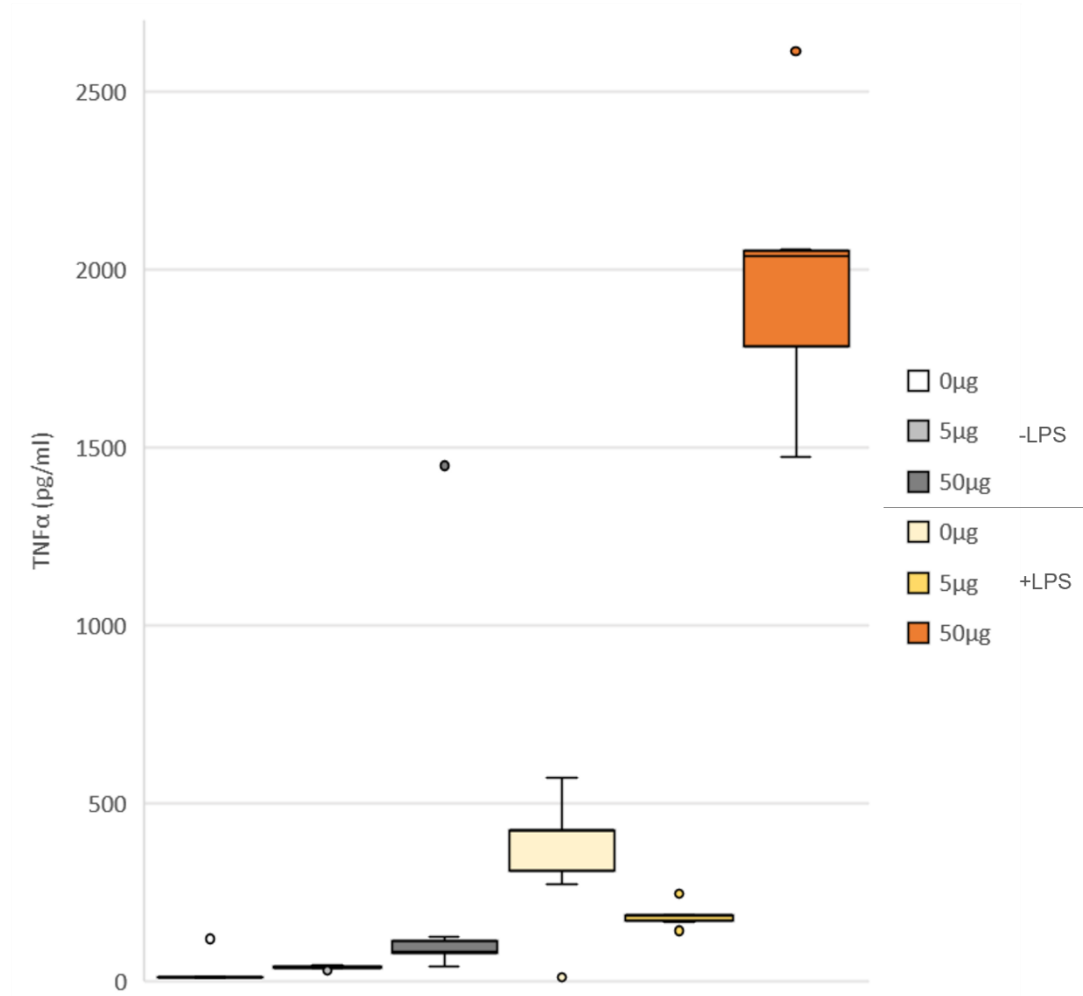
Supplementary Figure 6 - MM6 secreted level of IL-10 in response to LPS/V-antigen stimulation – Mono-mac 6 (MM6) cells were seeded at a density of 5×10^4 cells/well on 24 well plates and allowed to attach overnight. These were pre-incubated with 0µg, 1µg, 5µg, 10µg, or 50µg V-antigen for 30min before stimulation with A; 0ng/ml LPS or B; 100ng/ml LPS for 1hr, 4hr, 6hr, and 12hr. The growth media from the cells was harvested and analysed using a 7-plex MSD Multi-spot Assay system kit to determine the level of IL-10 that had been secreted. The data presented is constructed of 3 technical triplicates

Supplementary Figure 7:



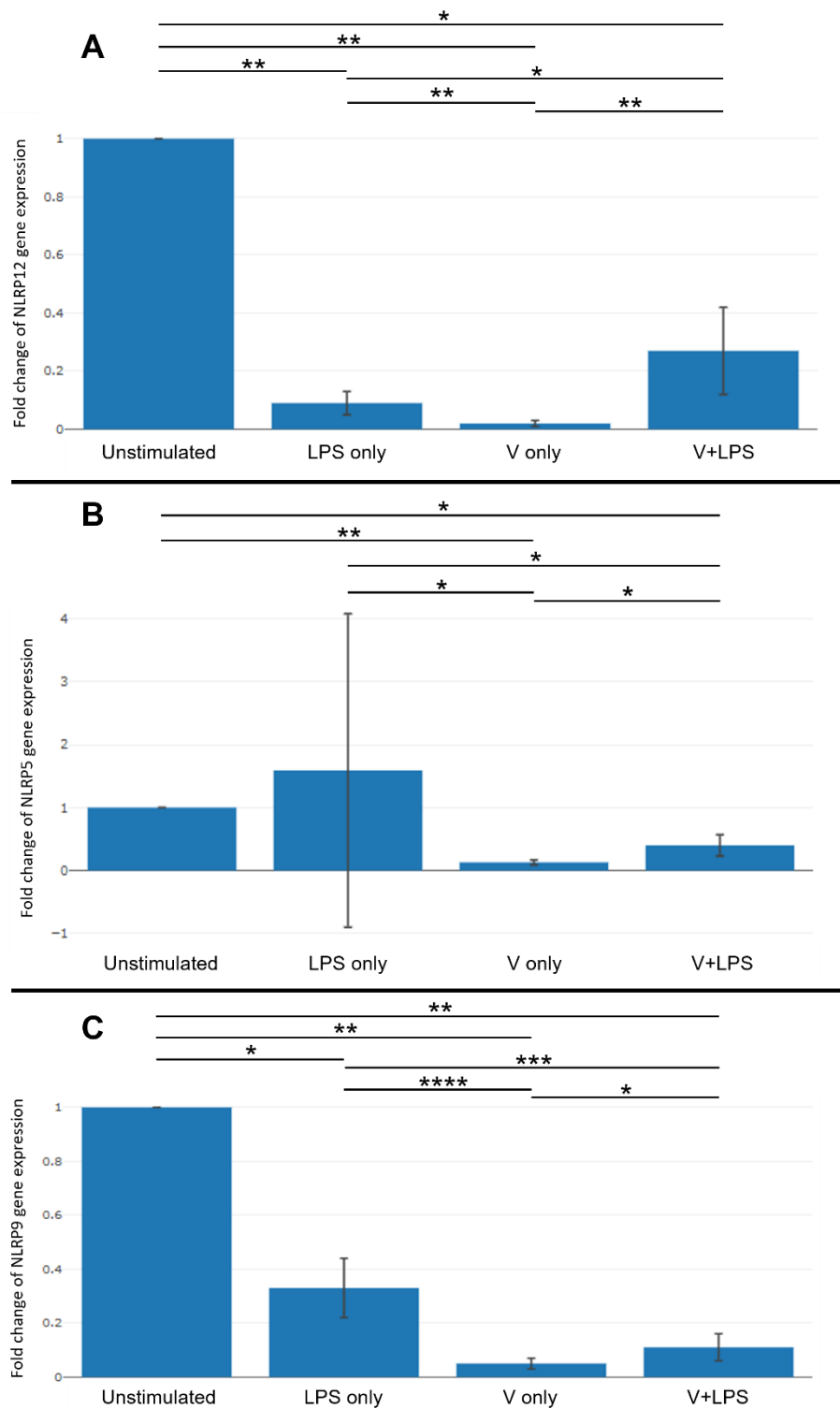
Supplementary Figure 7 - MM6 secreted level of IL-1 β in response to 12hr LPS/V-antigen stimulation – Mono-mac 6 (MM6) cells were seeded at a density of 5×10^4 cells/well on 24 well plates and allowed to attach overnight. These were pre-incubated with 0 μ g, 1 μ g, 5 μ g, 10 μ g, or 50 μ g V-antigen for 30min before stimulation with A; 0ng/ml LPS or B; 100ng/ml LPS for 1hr, 4hr, 6hr, and 12hr. The growth media from the cells was harvested and analysed using a 7-plex MSD Multi-spot Assay system kit to determine the level of IL-1 β that had been secreted. This data was added to a previous dataset (Supplementary Figure 1) for n=2 consisting of 6 technical triplicates. Outliers were presented as datapoints that exceeded 1.5 times the interquartile range from the upper/lower quartile

Supplementary Figure 8:



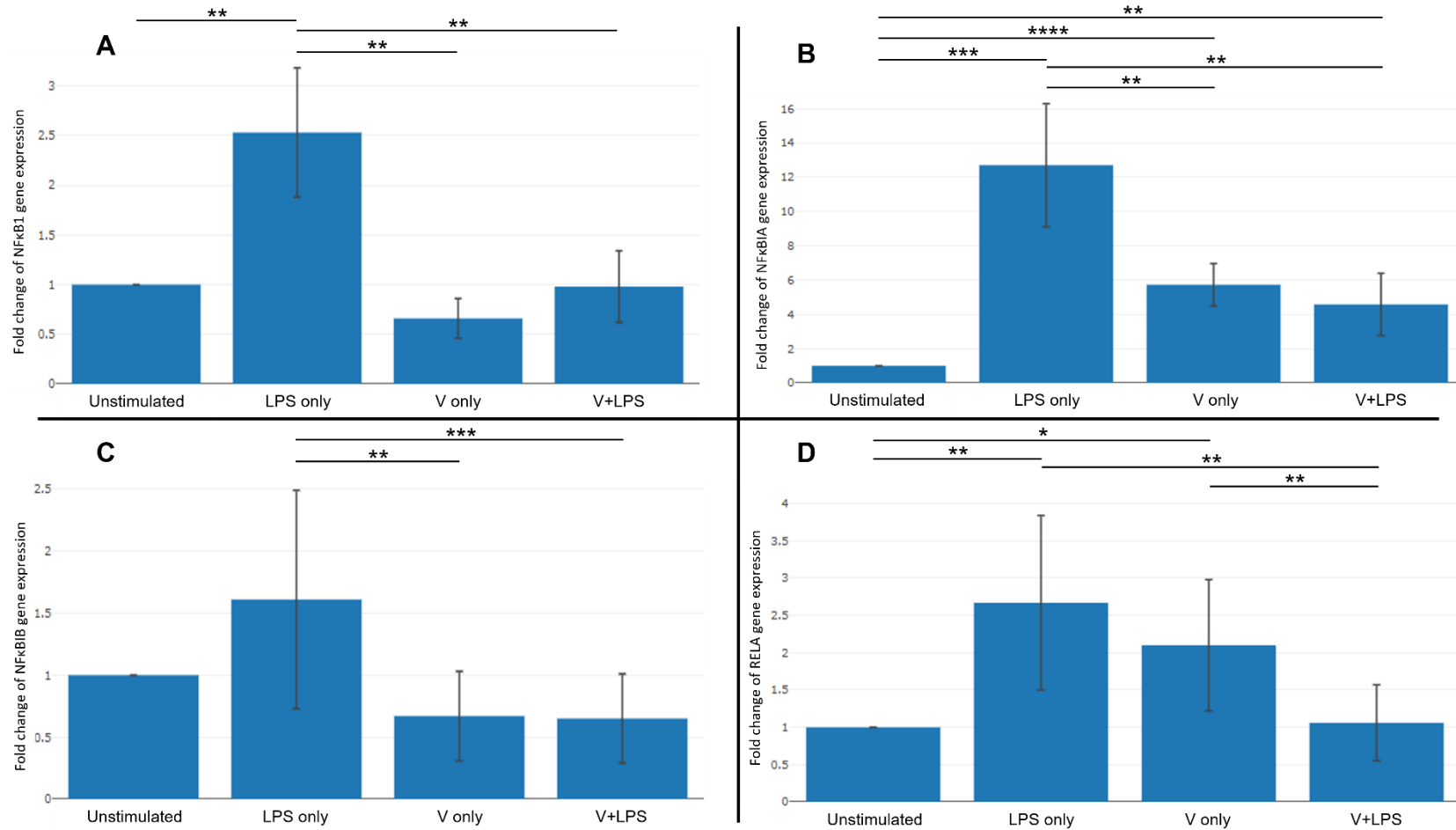
Supplementary Figure 8 - MM6 secreted level of TNFα in response to 12hr LPS/V-antigen stimulation – Mono-mac 6 (MM6) cells were seeded at a density of 5×10^4 cells/well on 24 well plates and allowed to attach overnight. These were pre-incubated with 0µg, 1µg, 5µg, 10µg, or 50µg V-antigen for 30min before stimulation with A; 0ng/ml LPS or B; 100ng/ml LPS for 1hr, 4hr, 6hr, and 12hr. The growth media from the cells was harvested and analysed using a 7-plex MSD Multi-spot Assay system kit to determine the level of TNFα that had been secreted. This data was added to a previous dataset (Supplementary Figure 5) for n=2 consisting of 6 technical triplicates. Outliers were presented as datapoints that exceeded 1.5 times the interquartile range from the upper/lower quartile

Supplementary Figure 9:



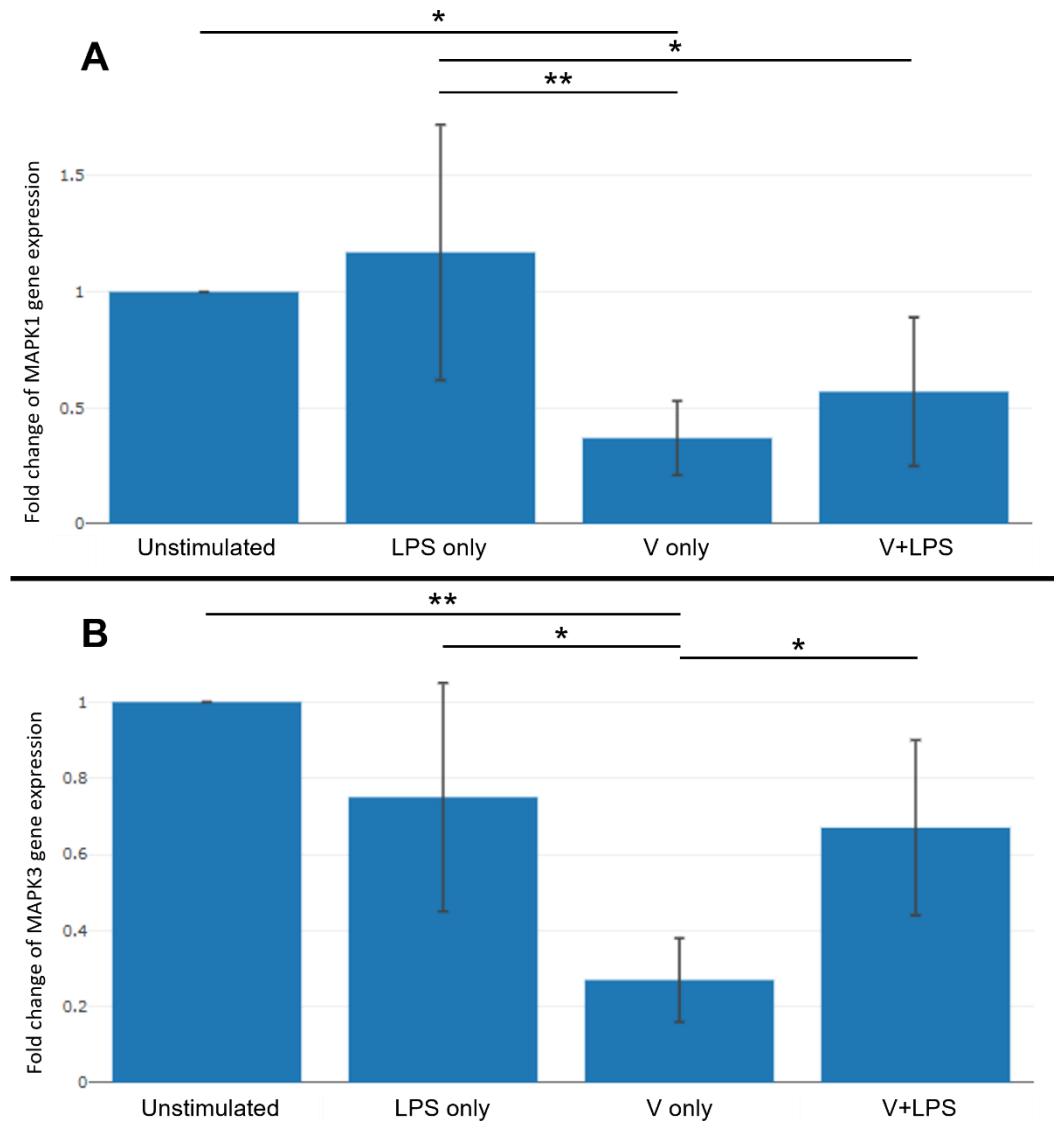
Supplementary Figure 9 - NLRP12, NLRP5, and NLRP9 gene expression under stimulation with combinations of LPS and V-antigen – PBMDMs from 4 separate donors were set up according to the experimental design in Figure 15 with PBMDMs pre-incubated with/without 50 μ g V-antigen and then stimulated with/without 100ng/ml LPS for 16hr. The cells were then lysed, and the RNA was extracted for qPCR analysis using the Qiagen RT² profiler - Human Inflammasome gene array plate. Using the Qiagen Geneglobe analysis software, the average expression of A; NLRP12, B; NLRP5, and C; NLRP9, was evaluated across all four conditions and displayed as a fold-change from the unstimulated control. Data is presented with standard error bars and indicators for statistical significance(* = <0.05, ** = <0.01, *** = <0.001, **** = <0.0001) as determined by Student's T-test adjusted for multiple comparisons post-hoc with a manual Benjamini-Hochberg correction

Supplementary Figure 10:



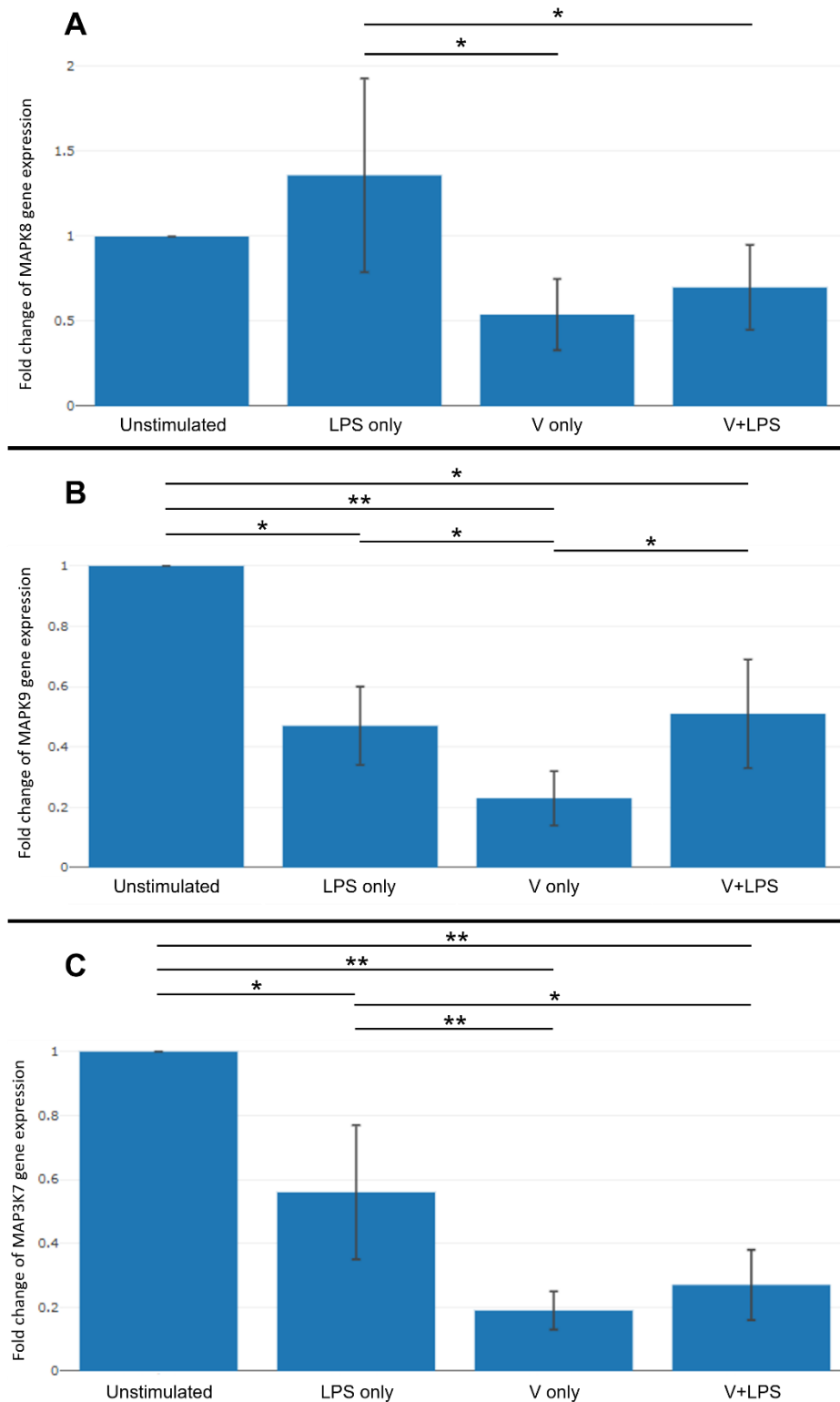
Supplementary Figure 10 - NFKB1, NFKBIA, NFKBIB, and RELA gene expression under stimulation with combinations of LPS and V-antigen – PBMDMs from 4 separate donors were set up according to the experimental design in Figure 15 with PBMDMs pre-incubated with/without 50µg V-antigen and then stimulated with/without 100ng/ml LPS for 16hr. The cells were then lysed, and the RNA was extracted for qPCR analysis using the Qiagen RT² profiler - Human Inflammasome gene array plate. Using the Qiagen Geneglobe analysis software, the average expression of A; NFKB1, B; NFKBIA, C; NFKBIB, and D; RELA was evaluated across all four conditions and displayed as a fold-change from the unstimulated control. Data is presented with standard error bars and indicators for statistical significance(* = <0.05, ** = <0.01, *** = <0.001, **** = <0.0001) as determined by Student's T-test adjusted for multiple comparisons post-hoc with a manual Benjamini-Hochberg correction

Supplementary Figure 11:



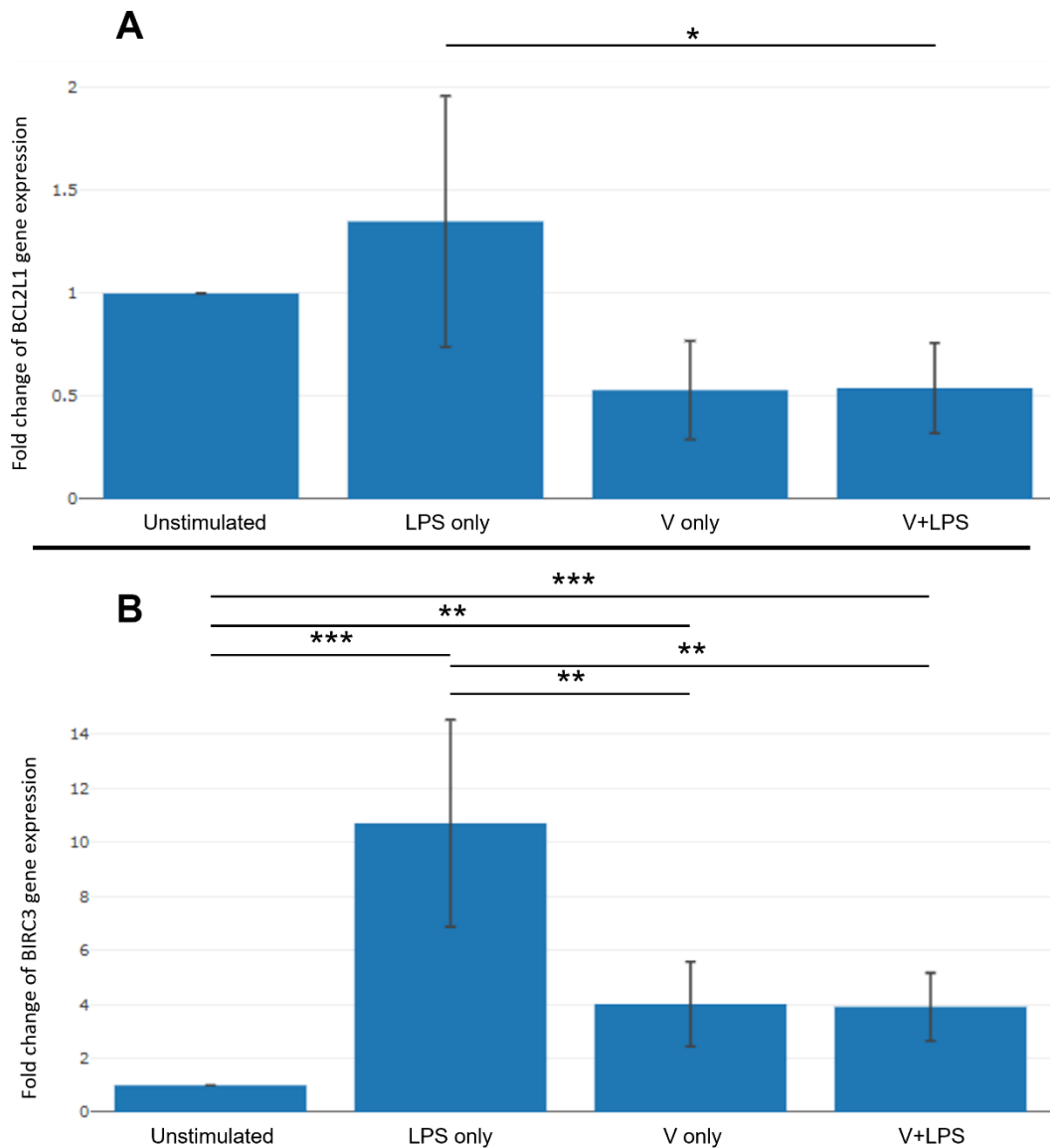
Supplementary Figure 11 - MAPK1 and MAPK3 gene expression under stimulation with combinations of LPS and V-antigen – PBMDMs from 4 separate donors were set up according to the experimental design in Figure 15 with PBMDMs pre-incubated with/without 50 μ g V-antigen and then stimulated with/without 100ng/ml LPS for 16hr. The cells were then lysed, and the RNA was extracted for qPCR analysis using the Qiagen RT² profiler - Human Inflammasome gene array plate. Using the Qiagen Geneglobe analysis software, the average expression of A; MAPK1 and, B; MAPK3 was evaluated across all four conditions and displayed as a fold-change from the unstimulated control. Data is presented with standard error bars and indicators for statistical significance (* = <0.05, ** = <0.01, *** = <0.001, **** = <0.0001) as determined by Student's T-test adjusted for multiple comparisons post-hoc with a manual Benjamini-Hochberg correction

Supplementary Figure 12:



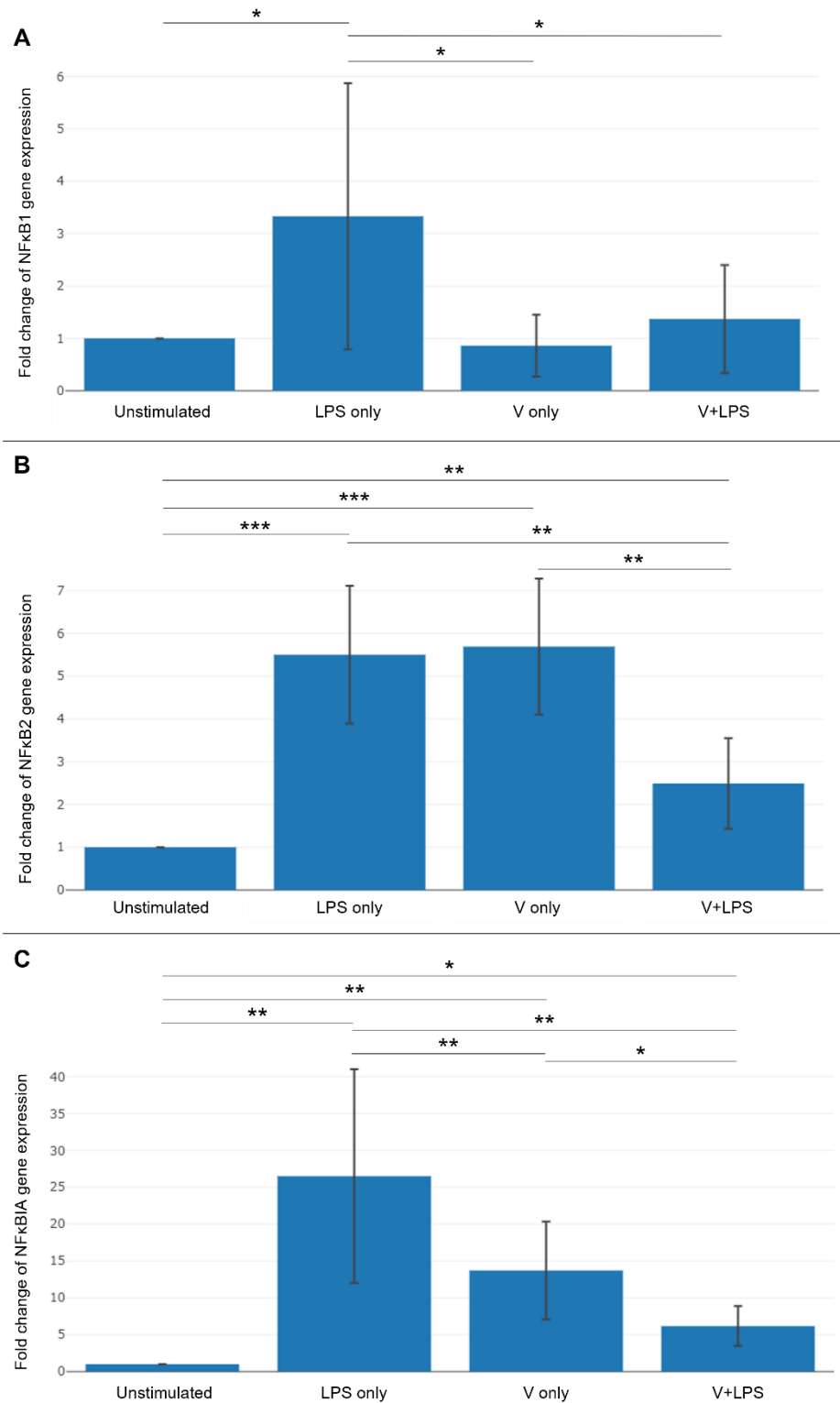
Supplementary Figure 12 - MAPK8, MAPK9, and MAP3K7 gene expression under stimulation with combinations of LPS and V-antigen – PBMDMs from 4 separate donors were set up according to the experimental design in Figure 15 with PBMDMs pre-incubated with/without 50 μ g V-antigen and then stimulated with/without 100ng/ml LPS for 16hr. The cells were then lysed, and the RNA was extracted for qPCR analysis using the Qiagen RT² profiler - Human Inflammasome gene array plate. Using the Qiagen Geneglobe analysis software, the average expression of A; MAPK8, B; MAPK9, and C; MAP3K7 was evaluated across all four conditions and displayed as a fold-change from the unstimulated control. Data is presented with standard error bars and indicators for statistical significance(* = <0.05, ** = <0.01, *** = <0.001, **** = <0.0001) as determined by Student's T-test adjusted for multiple comparisons post-hoc with a manual Benjamini-Hochberg correction

Supplementary Figure 13:



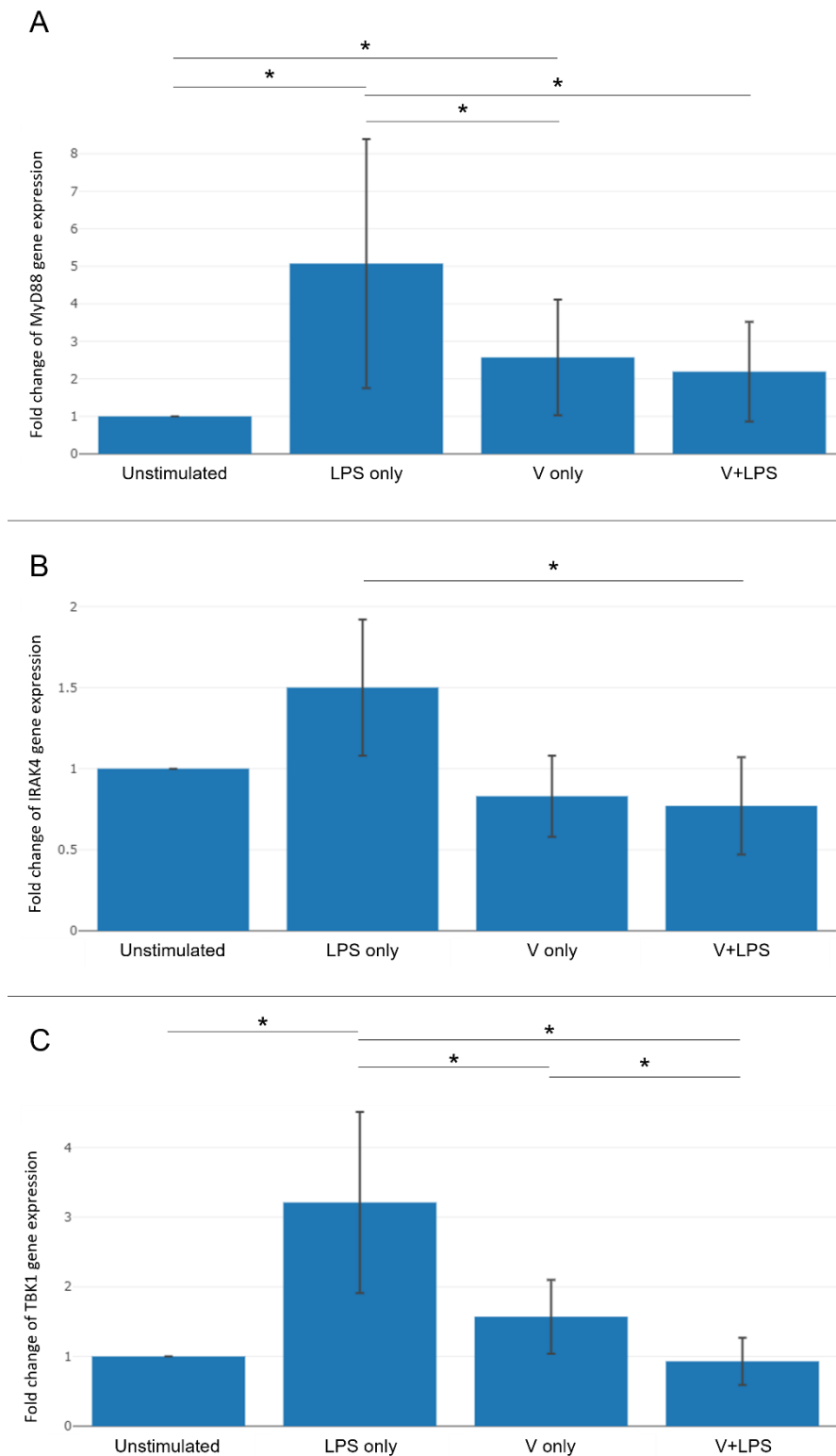
Supplementary Figure 13 - BCL2L1 and BIRC3 gene expression under stimulation with combinations of LPS and V-antigen – PBMDMs from 4 separate donors were set up according to the experimental design in Figure 15 with PBMDMs pre-incubated with/without 50µg V-antigen and then stimulated with/without 100ng/ml LPS for 16hr. The cells were then lysed, and the RNA was extracted for qPCR analysis using the Qiagen RT² profiler - Human Inflammasome gene array plate. Using the Qiagen Geneglobe analysis software, the average expression of A; BCL2L1 and, B; BIRC3 was evaluated across all four conditions and displayed as a fold-change from the unstimulated control. Data is presented with standard error bars and indicators for statistical significance(* = <0.05, ** = <0.01, *** = <0.001, **** = <0.0001) as determined by Student's T-test adjusted for multiple comparisons post-hoc with a manual Benjamini-Hochberg correction

Supplementary Figure 14:



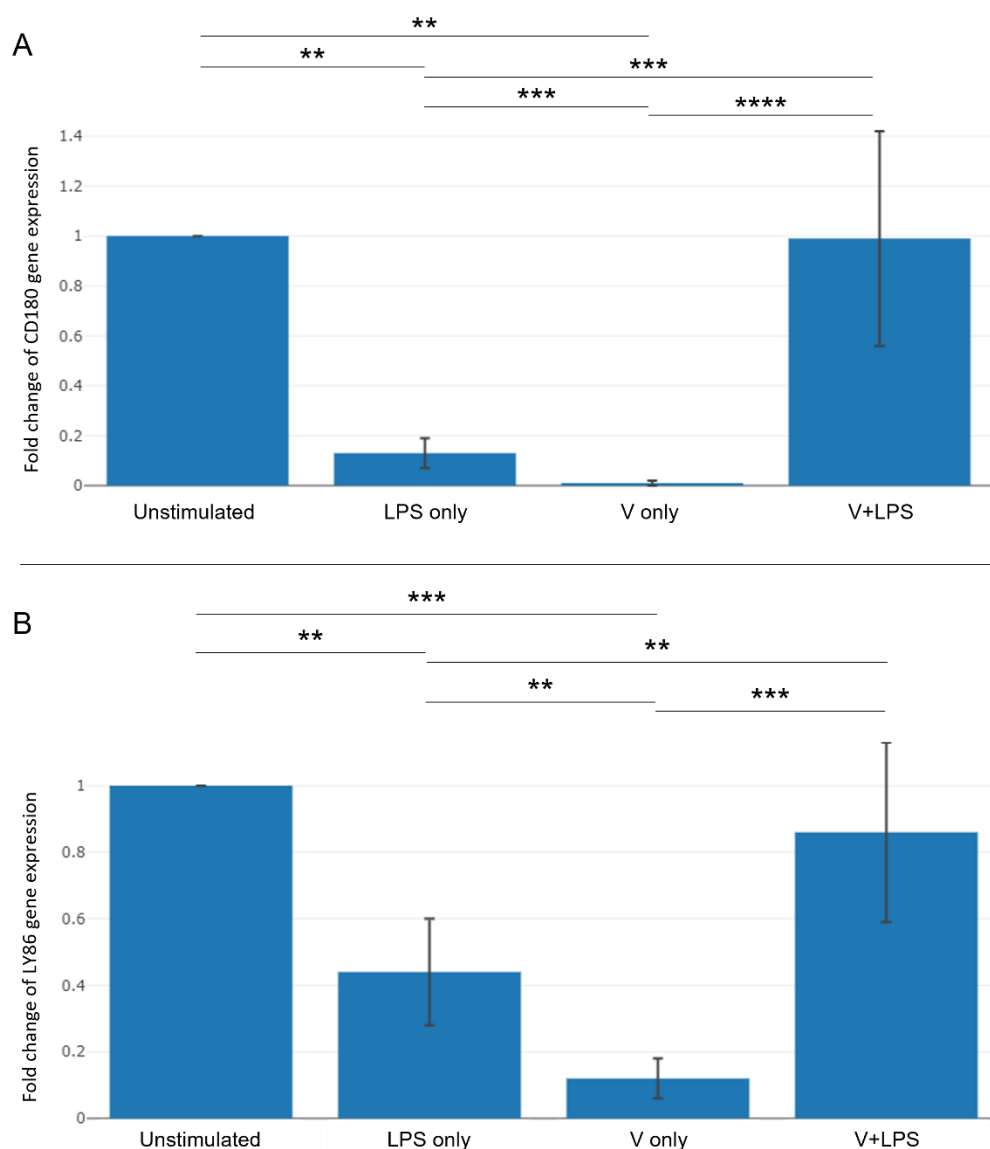
Supplementary Figure 14 - NFKB1, NFKB2, and NFKBIA gene expression under stimulation with combinations of LPS and V-antigen – PBMDMs from 4 separate donors were set up according to the experimental design in Figure 15 with PBMDMs pre-incubated with/without 50µg V-antigen and then stimulated with/without 100ng/ml LPS for 16hr. The cells were then lysed, and the RNA was extracted for qPCR analysis using the Qiagen RT² profiler - Human TLR pathway gene array plate. Using the Qiagen Geneglobe analysis software, the average expression of A; NFKB1, B; NFKB2, and C; NFKBIA, was evaluated across all four conditions and displayed as a fold-change from the unstimulated control. Data is presented with standard error bars and indicators for statistical significance(* = <0.05, ** = <0.01, *** = <0.001, **** = <0.0001) as determined by Student’s T-test adjusted for multiple comparisons post-hoc with a manual Benjamini-Hochberg correction

Supplementary Figure 15:



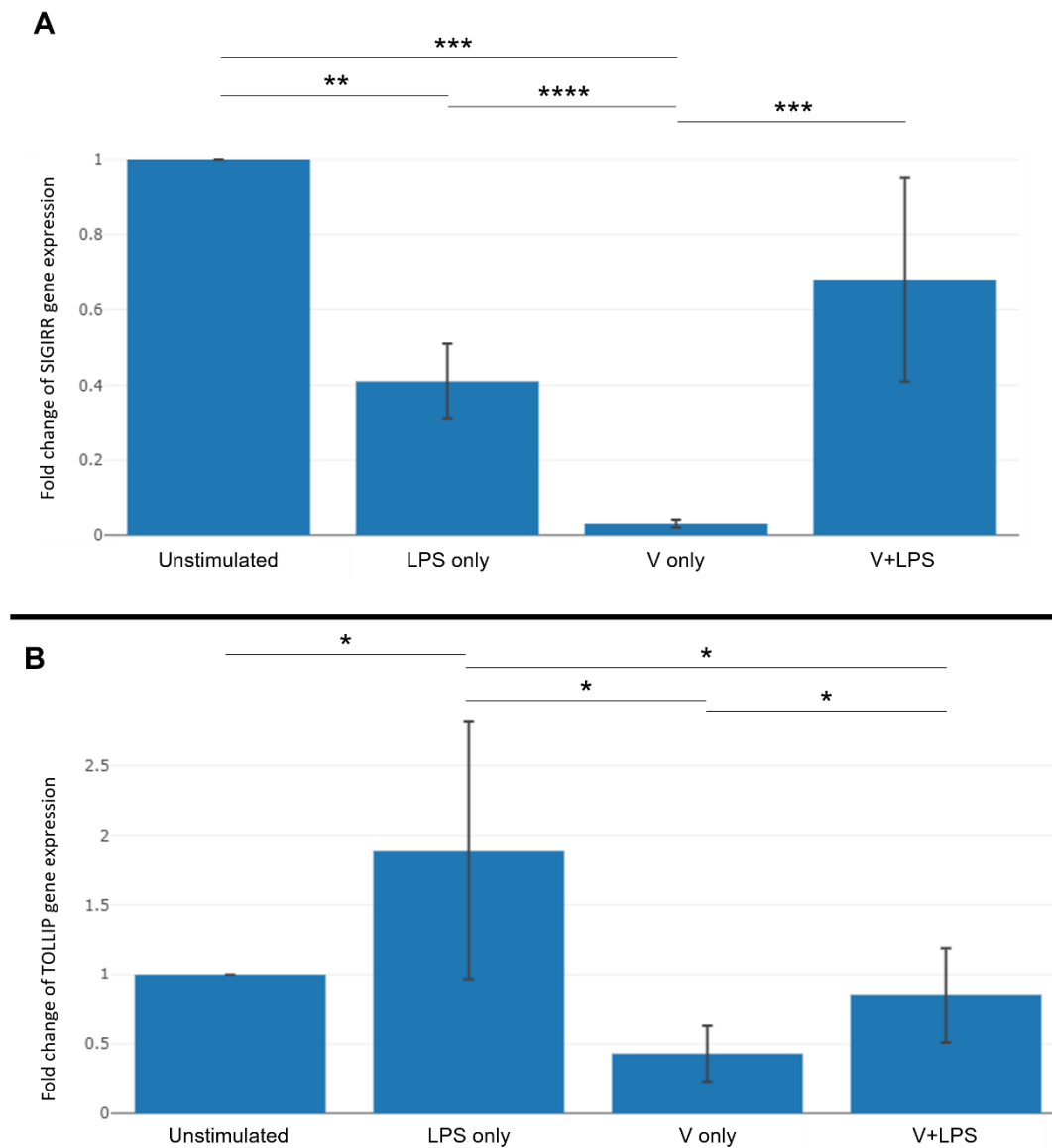
Supplementary Figure 15 - MyD88, IRAK4, and TBK1 gene expression under stimulation with combinations of LPS and V-antigen – PBMDMs from 4 separate donors were set up according to the experimental design in Figure 15 with PBMDMs pre-incubated with/without 50 μ g V-antigen and then stimulated with/without 100ng/ml LPS for 16hr. The cells were then lysed, and the RNA was extracted for qPCR analysis using the Qiagen RT² profiler - Human TLR pathway gene array plate. Using the Qiagen Geneglobe analysis software, the average expression of A; MyD88, B; IRAK4, and C; TBK1, was evaluated across all four conditions and displayed as a fold-change from the unstimulated control. Data is presented with standard error bars and indicators for statistical significance (* = <0.05, ** = <0.01, *** = <0.001, **** = <0.0001) as determined by Student's T-test adjusted for multiple comparisons post-hoc with a manual Benjamini-Hochberg correction

Supplementary Figure 16:



Supplementary Figure 16 - CD180 and LY86 gene expression under stimulation with combinations of LPS and V-antigen – PBMDMs from 4 separate donors were set up according to the experimental design in Figure 15 with PBMDMs pre-incubated with/without 50 μ g V-antigen and then stimulated with/without 100ng/ml LPS for 16hr. The cells were then lysed, and the RNA was extracted for qPCR analysis using the Qiagen RT² profiler - Human TLR pathway gene array plate. Using the Qiagen Geneglobe analysis software, the average expression of A; CD180 and B; LY86 was evaluated across all four conditions and displayed as a fold-change from the unstimulated control. Data is presented with standard error bars and indicators for statistical significance(* = <0.05, ** = <0.01, *** = <0.001, **** = <0.0001) as determined by Student's T-test adjusted for multiple comparisons post-hoc with a manual Benjamini-Hochberg correction

Supplementary Figure 17:



Supplementary Figure 17 - SIGIRR and TOLLIP gene expression under stimulation with combinations of LPS and V-antigen – PBMDMs from 4 separate donors were set up according to the experimental design in Figure 15 with PBMDMs pre-incubated with/without 50 μ g V-antigen and then stimulated with/without 100ng/ml LPS for 16hr. The cells were then lysed, and the RNA was extracted for qPCR analysis using the Qiagen RT² profiler - Human TLR pathway gene array plate. Using the Qiagen Geneglobe analysis software, the average expression of A; SIGIRR and B; TOLLIP was evaluated across all four conditions and displayed as a fold-change from the unstimulated control. Data is presented with standard error bars and indicators for statistical significance(* = <0.05, ** = <0.01, *** = <0.001, **** = <0.0001) as determined by Student's T-test adjusted for multiple comparisons post-hoc with a manual Benjamini-Hochberg correction

8.2.2: Supplementary tables

Supplementary Table 1 - Qiagen RT² qPCR - Inflammasome gene array full results – WT V-antigen

Gene	LPS only			V only			V+LPS		
	Fold regulation	p-value	Comments	Fold regulation	p-value	Comments	Fold regulation	p-value	Comments
AIM2	2.07	0.000647	A	46.72	0.000032	A	9.23	0.000220	A
BCL2	-2.21	0.013928		-3.54	0.003753		-1.30	0.367721	
BCL2L1	1.35	0.261769		-1.89	0.058870		-1.85	0.055240	
BIRC2	-1.25	0.165341		-1.65	0.030715		-2.01	0.007585	
BIRC3	10.71	0.000190		4.01	0.000990		3.91	0.000076	
CARD18	37.84	0.135665	A	-5.11	0.002275		-2.62	0.008152	
CARD6	-1.04	0.677377		-1.93	0.144437		-1.64	0.189301	
CASP1	-2.90	0.057442		-2.05	0.110301		-2.05	0.111473	
CASP5	15.02	0.000210	A	12.86	0.000444	A	7.17	0.000206	A
CASP8	-2.52	0.001110		-3.09	0.000735		-2.61	0.002835	
CCL2	-8.02	0.000000		-7.55	0.000000		-3.33	0.000009	
CCL5	66.28	0.000165		118.58	0.000030		60.93	0.000003	
CCL7	1.06	0.685213		1.53	0.042583		-1.88	0.018999	
CD40LG	1.26	0.312853	B	-1.98	0.031941		1.26	0.345233	B
CFLAR	2.81	0.002635		2.11	0.084335		1.27	0.461920	
CHUK	-1.00	0.875587		-1.62	0.077818		-1.49	0.117073	
CIITA	-11.11	0.000023		-9.94	0.000025		-3.75	0.000188	
CTSB	1.23	0.512572		-2.69	0.022087		-1.23	0.348792	
CXCL1	38.53	0.000129		1.79	0.132350		4.48	0.000934	
CXCL2	43.81	0.000005		3.61	0.011413		9.05	0.000107	
FADD	-1.19	0.133385		-2.90	0.000110		-1.48	0.054662	
HSP90AA1	-2.12	0.005097		-3.03	0.001930		-2.03	0.009688	
HSP90AB1	-1.89	0.058990		-7.48	0.005963		-2.24	0.033254	
HSP90B1	-1.42	0.268063		-6.60	0.018832		-1.75	0.129836	
IFNB1	-2795.43	0.053106	A	-203.59	0.053223	A	-55.77	0.053551	
IFNG	-1.03	0.744728	B	199.04	0.000036	A	380.43	0.000722	A
IKBKB	-2.41	0.080532		-7.09	0.025785		-3.20	0.054136	
IKBKG	1.16	0.378080		-2.23	0.003426		-1.75	0.043359	
IL12A	-2.64	0.359243	B	-1.61	0.365667	B	1.20	0.380753	B
IL12B	4.55	0.000003		17.26	0.001478	A	93.58	0.000633	A
IL18	1.70	0.013909		-1.55	0.014128		-1.69	0.013225	
IL1B	57.00	0.000004		3.99	0.001886		9.16	0.000055	
IL33	-1.23	0.459112	B	-7.75	0.001514	C	-1.50	0.593962	B
IL6	66.14	0.000191	A	11.23	0.000194	A	20.22	0.000310	A
IRAK1	-1.82	0.012843		-2.52	0.002894		-2.08	0.014040	
IRF1	-1.85	0.014642		2.07	0.006143		1.08	0.631153	
IRF2	1.37	0.056557		-1.12	0.789827		-1.00	0.951537	
MAP3K7	-1.78	0.030844		-5.36	0.001270		-3.77	0.002606	
MAPK1	1.17	0.644045		-2.71	0.022545		-1.75	0.109224	
MAPK11	-1.01	0.845929	B	1.47	0.098811	B	-2.33	0.010979	
MAPK12	-1.86	0.009851	A	-10.49	0.000367		-1.17	0.368832	A
MAPK13	-2.12	0.016507		-9.85	0.001572		-1.99	0.021758	
MAPK3	-1.33	0.191531		-3.74	0.001255		-1.50	0.060861	
MAPK8	1.36	0.204735		-1.85	0.035733		-1.43	0.111614	
MAPK9	-2.15	0.008894		-4.32	0.001865		-1.98	0.017674	
MEFV	1.99	0.004227		2.45	0.013994		2.51	0.033946	
MYD88	1.19	0.195645		-1.21	0.076743		-1.03	0.991946	
NAIP	-5.95	0.005503		-34.65	0.002590		-3.76	0.009449	
NFKB1	2.53	0.000803		-1.50	0.037775		-1.02	0.986481	
NFKBIA	12.71	0.000126		5.73	0.000011		4.58	0.004529	
NFKBIB	1.61	0.186272		-1.48	0.212675		-1.54	0.198384	
NLRC4	-1.37	0.274846		-7.40	0.015981		-3.33	0.039623	
NLRC5	-1.90	0.036837		1.56	0.034870		-1.91	0.026131	
NLRP1	-7.14	0.001207		-22.24	0.000679	A	-5.52	0.001513	

NLRP12	-10.86	0.005324		-54.76	0.003728		-3.74	0.015081	
NLRP3	-1.74	0.000960		-9.49	0.000002		-1.84	0.001077	
NLRP4	-5.90	0.001882	C	10.06	0.054954	A	-3.56	0.004094	C
NLRP5	1.59	0.113260	B	-7.75	0.001514	C	-2.50	0.013388	
NLRP6	-3.02	0.034091		-23.42	0.009212		-3.70	0.027278	
NLRP9	-2.99	0.008527		-20.11	0.001679		-9.08	0.002426	
NLRX1	-7.34	0.007400		-35.43	0.004360		-4.50	0.014180	
NOD1	1.23	0.284025		-1.02	0.996532		1.27	0.284756	
NOD2	1.65	0.185148	A	1.39	0.467597	A	1.35	0.535543	A
P2RX7	2.53	0.000232		1.02	0.963497		1.79	0.014468	
PANX1	3.51	0.000292		1.88	0.070953		1.19	0.646219	
PEA15	1.19	0.269310		-3.58	0.000784		-1.76	0.021267	
PSTPIP1	-3.25	0.001476		-15.36	0.000301		-3.62	0.001915	
PTGS2	4.55	0.000074		3.46	0.000108		4.82	0.001109	
PYCARD	-2.53	0.001881		-7.42	0.000170		-2.82	0.001119	
PYDC1	-1.37	0.143863	B	-7.75	0.001514	C	-3.56	0.004094	C
MOK	-1.80	0.007026	A	-4.33	0.000471		-2.61	0.003887	
RELA	2.67	0.002926		2.10	0.008656		1.06	0.959280	
RIPK2	4.62	0.000621		4.04	0.000018		4.54	0.000250	
SUGT1	1.26	0.432069		-1.67	0.093032		-1.02	0.854636	
TAB1	-5.09	0.029976		-13.46	0.018200		-2.86	0.059389	
TAB2	-1.41	0.231959		-2.98	0.029244		-1.48	0.190695	
TIRAP	-1.30	0.194429	A	-3.37	0.002289	A	-1.67	0.028061	A
TNF	1.41	0.076358		1.87	0.007491		1.97	0.044863	
TNFSF11	-2.62	0.008008		-2.48	0.014330		-2.46	0.015685	
TNFSF14	-1.30	0.236393	B	-7.39	0.003405		2.42	0.033647	
TNFSF4	1.16	0.294956	B	-6.03	0.633563	B	1.02	0.855268	B
TRAF6	-2.61	0.030853		-3.48	0.015509		-1.77	0.077035	
TXNIP	-1.36	0.165077		-6.37	0.002824		-2.81	0.010992	
XIAP	1.27	0.517276		-1.81	0.115871		1.08	0.977586	

PBMDMs from 4 separate donors were set up according to the experimental design in Figure 15 with PBMDMs pre-incubated with/without 50µg V-antigen for 30min and then stimulated with/without 100ng/ml LPS for 16hr. The cells were then lysed, and the RNA was extracted for qPCR analysis using the Qiagen RT² profiler - Human Inflammasome gene array plate. Average gene expression for each gene in the three test conditions ('LPS only', 'V only', and 'V+LPS') was compared to gene expression of the same gene in the unstimulated control to determine the change in fold-regulation. A Student's T-test was performed for each comparison via the Qiagen Geneglobe analysis software. The resulting data is presented in the table above alongside any comments about data reliability for that comparison

'Comments' are: A; the gene's average threshold value is high (>30) in one group and low (<30) in the other, B; the gene's average threshold value is >30 in both samples and the p-value for the fold-change is unavailable or high (p>0.05), C; the gene's average threshold value is above the cut-off or undetected in all samples and so is unreliable and cannot be used

Supplementary Table 2 - Qiagen RT² qPCR –TLR pathway gene array full results – WT
V-antigen

Gene	LPS only			V only			V+LPS		
	Fold regulation	p-value	Comments	Fold regulation	p-value	Comments	Fold regulation	p-value	Comments
<i>BTK</i>	-1.10	0.440649		-2.58	0.002455		-1.09	0.644230	
<i>CASP8</i>	1.02	0.855464		-1.86	0.016183		-1.39	0.375354	
<i>CCL2</i>	-3.94	0.000457		-6.79	0.000142		-1.11	0.670238	
<i>CD14</i>	4.21	0.001725		-6.63	0.006145		-1.10	0.721273	
<i>CD180</i>	-7.60	0.002154		-73.50	0.001129		-1.01	0.782702	
<i>CD80</i>	4.01	0.000248		7.64	0.000158		6.48	0.000080	
<i>CD86</i>	1.15	0.535509		-8.94	0.001314		1.05	0.889750	
<i>CHUK</i>	2.25	0.011557		1.08	0.993969		1.93	0.056075	
<i>CLEC4E</i>	66.34	0.000584		38.99	0.000199		18.29	0.000734	
<i>CSF2</i>	52.62	0.000120	A	31.55	0.000025	A	67.73	0.001425	A
<i>CSF3</i>	2512.67	0.000147	A	1210.71	0.000484	A	1435.73	0.000615	A
<i>CXCL10</i>	-2.93	0.006545		1.81	0.016725		2.38	0.007146	
<i>ECSIT</i>	-1.53	0.075755		-12.08	0.000439		-2.28	0.012742	
<i>EIF2AK2</i>	1.37	0.182534		2.35	0.008658		1.25	0.376759	
<i>ELK1</i>	10.25	0.000433		3.16	0.003411		2.58	0.014455	
<i>FADD</i>	1.70	0.029137		-1.92	0.014502		-1.03	0.917041	
<i>FOS</i>	-1.15	0.227884		-10.55	0.000127		-1.25	0.358340	
<i>HMGB1</i>	1.04	0.763409		-2.15	0.001904		-1.01	0.952306	
<i>HRAS</i>	2.02	0.027540		-2.55	0.016612		1.00	0.881132	
<i>HSPA1A</i>	1.03	0.888058		-2.60	0.009019		-1.04	0.720152	
<i>HSPD1</i>	4.05	0.003829		-2.66	0.080264		1.34	0.586327	
<i>IFNA1</i>	-404.53	0.026879	A	-1191.73	0.026852	A	-547.07	0.026869	A
<i>IFNB1</i>	-1133.09	0.038854	A	-217.87	0.038919	A	-134.79	0.038969	A
<i>IFNG</i>	-1.23	0.353446	B	106.31	0.000007	A	223.68	0.000006	A
<i>IKBKB</i>	1.08	0.744281		-2.52	0.008414		-1.69	0.049595	
<i>IL10</i>	60.76	0.000043		10.94	0.008783		13.49	0.001848	
<i>IL12A</i>	-2.14	0.004400		-2.47	0.001886		1.48	0.145317	B
<i>IL1A</i>	16.00	0.000702	A	1.67	0.013251	A	1.22	0.329076	A
<i>IL1B</i>	63.37	0.000019		6.57	0.001958		12.02	0.000059	
<i>IL2</i>	1.94	0.007633		-2.69	0.018487		1031.24	0.060238	A
<i>IL6</i>	55.46	0.001030	A	7.86	0.000495	A	15.21	0.000010	A
<i>CXCL8</i>	45.36	0.000045		33.74	0.000233		72.31	0.000026	
<i>IRAK1</i>	1.58	0.076673		-4.32	0.004244		-1.03	0.990887	
<i>IRAK2</i>	3.96	0.000040		2.15	0.008278		4.15	0.004626	
<i>IRAK4</i>	1.50	0.033919		-1.20	0.271662		-1.30	0.235894	
<i>IRF1</i>	1.31	0.332265		5.20	0.001766		2.46	0.015186	
<i>IRF3</i>	1.24	0.464983		-4.38	0.008314		-2.60	0.031230	
<i>JUN</i>	-1.87	0.000522		-2.94	0.000521		-1.20	0.350868	
<i>LTA</i>	1.80	0.080411	B	-1.24	0.492481	B	2.43	0.039456	
<i>LY86</i>	-2.29	0.003612		-8.37	0.000210		-1.16	0.336225	
<i>LY96</i>	-2.55	0.001966		-7.90	0.000279		-2.16	0.006432	
<i>MAP2K3</i>	2.34	0.001874		-1.49	0.126661		1.40	0.130247	
<i>MAP2K4</i>	1.05	0.728786		-1.97	0.012261		1.17	0.352679	
<i>MAP3K1</i>	1.07	0.777336		-1.61	0.186218		-1.23	0.264746	
<i>MAP3K7</i>	1.70	0.075590		2.06	0.061140		-1.20	0.409499	
<i>MAP4K4</i>	2.12	0.040952		-3.57	0.001171		1.38	0.074928	
<i>MAPK8</i>	2.93	0.002998		4.11	0.040124		14.33	0.045794	
<i>MAPK8IP3</i>	1.15	0.469253		-4.59	0.001330		-2.19	0.008828	
<i>MYD88</i>	5.07	0.003730		2.57	0.019019		2.19	0.047811	
<i>NFKB1</i>	3.33	0.021705		-1.17	0.504355		1.37	0.705550	
<i>NFKB2</i>	5.50	0.000326		5.69	0.000077		2.49	0.008184	
<i>NFKBIA</i>	26.51	0.001242		13.71	0.001336		6.17	0.000660	
<i>NFKBIL1</i>	-1.10	0.522647		-3.44	0.003119		-1.29	0.233665	
<i>NFRKB</i>	2.35	0.044327		-2.29	0.038805		1.02	0.984837	
<i>NR2C2</i>	1.99	0.041281		-1.84	0.025819		-1.16	0.526845	

PELI1	3.48	0.002939		3.36	0.003020		6.29	0.000079	
PPARA	1.38	0.248628		1.49	0.192341		1.39	0.209339	
PRKRA	-87.16	0.628816	A	-2.38	0.006419		-1.56	0.115600	
PTGS2	4.95	0.000360		7.14	0.031830		12.50	0.000510	
REL	1.99	0.042389		-1.35	0.233506		1.38	0.155229	
RELA	3.90	0.003560		3.06	0.004054		3.49	0.006870	
RIPK2	6.58	0.000007		5.30	0.008150		7.06	0.005687	
SARM1	-1.10	0.511471		-2.14	0.011210		-9.83	0.000873	A
SIGIRR	-2.42	0.002350		-32.41	0.000171		-1.47	0.107452	B
TAB1	-1.40	0.103203		-4.98	0.002581		-1.18	0.415424	
TBK1	3.21	0.003767		1.57	0.044310		-1.08	0.683484	
TICAM1	2.04	0.006453		-1.00	0.949271		1.49	0.084173	
TICAM2	1.04	0.941492		-1.62	0.088705		1.24	0.437680	
TIRAP	1.97	0.075120		-2.22	0.054738		1.02	0.977063	
TLR1	1.10	0.538300		-5.06	0.000164		-2.82	0.005261	
TLR10	-1.71	0.085052	B	-11.98	0.001209		-1.61	0.100765	B
TLR2	2.59	0.001669		-2.74	0.153804		-1.04	0.819380	
TLR3	-6.34	0.043871	A	-1.06	0.747337		1.34	0.618462	
TLR4	-1.36	0.144168		-4.41	0.001911		-1.27	0.305528	
TLR5	-2.60	0.010538		-41.69	0.001265	A	-1.07	0.688057	
TLR6	-2.06	0.001455		-8.50	0.000057		-1.64	0.021247	
TLR7	-14.40	0.000347		-18.57	0.000320		-1.80	0.015478	
TLR8	3.02	0.005053		-1.13	0.522691		1.93	0.061395	
TLR9	-2005.39	0.032361	A	-3.05	0.188665		-1260.54	0.032365	A
TNF	1.53	0.059335		2.05	0.014768		4.13	0.008513	
TNFRSF1A	2.10	0.003971		-2.18	0.012995		-1.25	0.684792	
TOLLIP	1.89	0.041407		-2.32	0.017472		-1.17	0.429402	
TRAF6	1.07	0.588091		-1.98	0.004379		-1.09	0.638935	
UBE2N	1.97	0.018004		-1.06	0.885833		-1.06	0.916465	

PBMDMs from 4 separate donors were set up according to the experimental design in Figure 15 with PBMDMs pre-incubated with/without 50µg V-antigen for 30min and then stimulated with/without 100ng/ml LPS for 16hr. The cells were then lysed, and the RNA was extracted for qPCR analysis using the Qiagen RT² profiler - Human TLR pathway gene array plate. Average gene expression for each gene in the three test conditions ('LPS only', 'V only', and 'V+LPS') was compared to gene expression of the same gene in the unstimulated control to determine the change in fold-regulation. A Student's T-test was performed for each comparison via the Qiagen Geneglobe analysis software. The resulting data is presented in the table above alongside any comments about data reliability for that comparison

'Comments' are: A; the gene's average threshold value is high (>30) in one group and low (<30) in the other, B; the gene's average threshold value is >30 in both samples and the p-value for the fold-change is unavailable or high (p>0.05), C; the gene's average threshold value is above the cut-off or undetected in all samples and so is unreliable and cannot be used

Supplementary Table 3 - Qiagen RT² qPCR – TLR pathway gene array full results – pV1/pV2

Gene	LPS only			pV1+LPS			pV2+LPS		
	Fold regulation	p-value	Comments	Fold regulation	p-value	Comments	Fold regulation	p-value	Comments
<i>BTK</i>	1.07	0.997440		-1.57	0.246604		-1.16	0.993100	
<i>CASP8</i>	2.05	0.090118		-1.39	0.344000		-1.12	0.776969	
<i>CCL2</i>	-4.04	0.003888		-7.46	0.002079		-1.35	0.152031	
<i>CD14</i>	3.60	0.000366		-12.88	0.000184		1.04	0.591324	
<i>CD180</i>	-7.25	0.004138		-77.53	0.002405		-1.16	0.497149	
<i>CD80</i>	4.73	0.004045		7.38	0.000062		7.84	0.002021	
<i>CD86</i>	1.57	0.375842		-6.76	0.076764		1.43	0.515875	
<i>CHUK</i>	4.02	0.002140		2.12	0.050681		3.30	0.044045	
<i>CLEC4E</i>	83.05	0.000034		31.53	0.003049		13.71	0.010750	
<i>CSF2</i>	87.06	0.002623	A	36.26	0.000006	A	71.05	0.000503	A
<i>CSF3</i>	3047.46	0.000001	A	1260.50	0.000411	A	1457.30	0.002520	A
<i>CXCL10</i>	-3.04	0.007023		1.36	0.054894		2.33	0.112224	
<i>ECSIT</i>	2.60	0.373929		-8.19	0.000201		-2.77	0.000726	
<i>EIF2AK2</i>	-1.03	0.772076		1.77	0.155040		-1.34	0.359722	
<i>ELK1</i>	13.84	0.003213	A	2.43	0.125025	A	2.49	0.092168	A
<i>FADD</i>	2.28	0.000430		-1.69	0.017358		1.33	0.088822	
<i>FOS</i>	1.20	0.375825		-8.95	0.002633		-1.20	0.378321	
<i>HMGB1</i>	1.05	0.816784		-1.88	0.055052		1.00	0.952261	
<i>HRAS</i>	2.34	0.002856		-2.68	0.024275		-1.07	0.608380	
<i>HSPA1A</i>	1.27	0.020712		-2.70	0.005841		-1.20	0.260488	
<i>HSPD1</i>	5.26	0.016803		-2.98	0.067836		1.46	0.272796	
<i>IFNA1</i>	-3354.59	0.061087	A	-8949.40	0.061060	A	-3059.46	0.061090	A
<i>IFNB1</i>	-5016.87	0.013548	A	-1471.01	0.013569	A	-963.87	0.013585	A
<i>IFNG</i>	1.09	0.511807	B	75.33	0.003243	A	249.56	0.000043	A
<i>IKBKB</i>	1.32	0.095886		-2.24	0.006173		-1.92	0.004806	
<i>IL10</i>	56.29	0.000004		7.78	0.101475		12.55	0.001236	
<i>IL12A</i>	-1.72	0.032744		-2.14	0.027492		1.40	0.126008	B
<i>IL1A</i>	16.25	0.000015	A	1.53	0.028394	A	-1.22	0.853952	A
<i>IL1B</i>	63.18	0.000588		7.51	0.001140		13.00	0.000008	
<i>IL2</i>	2.16	0.045917		-3.12	0.005045		12881.52	0.000469	A
<i>IL6</i>	58.83	0.004094	A	7.78	0.003268	A	11.60	0.000313	A
<i>CXCL8</i>	49.34	0.010380		27.95	0.007307		39.66	0.000065	
<i>IRAK1</i>	1.44	0.423819		-3.45	0.006770		-1.30	0.656943	
<i>IRAK2</i>	3.89	0.000491		1.52	0.176853		3.85	0.000119	
<i>IRAK4</i>	2.39	0.004722		-1.22	0.412756		-1.07	0.735610	
<i>IRF1</i>	2.27	0.021908		8.35	0.001113		3.55	0.009684	
<i>IRF3</i>	1.10	0.637228		-6.99	0.004266		-3.66	0.008805	
<i>JUN</i>	-1.74	0.028707		-3.14	0.014920		-1.14	0.456882	
<i>LTA</i>	2.60	0.012916		-1.04	0.890203	B	2.82	0.085086	B
<i>LY86</i>	-1.86	0.006109		-8.34	0.000035		-1.07	0.836112	
<i>LY96</i>	-1.62	0.137981		-7.63	0.008462		-1.81	0.076440	
<i>MAP2K3</i>	2.58	0.017153		-2.36	0.010252		-1.06	0.735375	
<i>MAP2K4</i>	1.23	0.342285		-2.14	0.037978		-1.28	0.261182	
<i>MAP3K1</i>	1.07	0.743232		-1.76	0.043262		-1.25	0.577460	
<i>MAP3K7</i>	2.06	0.009752		38.50	0.047197		-1.00	0.939726	
<i>MAP4K4</i>	2.16	0.018517		-4.40	0.002226		1.23	0.345798	
<i>MAPK8</i>	5.56	0.008648		71.40	0.002078		234.03	0.001595	
<i>MAPK8IP3</i>	-1.08	0.562838		-4.11	0.001717		-2.05	0.005634	
<i>MYD88</i>	8.85	0.000160		2.77	0.016688		3.29	0.021624	
<i>NFKB1</i>	3.73	0.002028		-1.50	0.277060		1.43	0.383201	
<i>NFKB2</i>	7.50	0.041893		6.79	0.000515		3.25	0.060179	
<i>NFKBIA</i>	43.67	0.000911		16.51	0.024669		8.65	0.001082	
<i>NFKBIL1</i>	1.40	0.441805		-3.23	0.055876		-1.60	0.189895	
<i>NFRKB</i>	2.90	0.005649	A	-2.06	0.140358	A	1.18	0.752230	A
<i>NR2C2</i>	2.32	0.006920		-2.15	0.000092		-1.21	0.215157	

PELI1	5.11	0.003797		3.85	0.001281		7.80	0.013246	
PPARA	1.71	0.226822		1.43	0.489764		1.42	0.503347	
PRKRA	2.81	0.210099		-2.10	0.009946		-2.00	0.012762	
PTGS2	6.31	0.001017		110.00	0.002938		14.50	0.006601	
REL	2.59	0.007446		-1.22	0.812731		2.54	0.011265	
RELA	4.95	0.007063		4.29	0.000003		3.28	0.004568	
RIPK2	7.07	0.000003		3.64	0.186274		5.11	0.014953	
SARM1	1.56	0.022757		-1.77	0.034765		-11.87	0.002200	A
SIGIRR	-1.05	0.642779	B	-23.97	0.000946		1.08	0.673098	B
TAB1	1.39	0.175757		-4.04	0.007138		1.03	0.934217	
TBK1	4.59	0.003941		2.15	0.003212		-1.04	0.825409	
TICAM1	2.19	0.100781		-1.07	0.891491		1.58	0.258785	
TICAM2	1.02	0.918283		-1.87	0.023784		-1.13	0.393515	
TIRAP	2.26	0.002708		-1.76	0.030765		-1.34	0.265533	
TLR1	1.10	0.516851		-4.55	0.001238		-3.34	0.001516	
TLR10	-1.50	0.312925	B	-14.57	0.062756	B	-2.06	0.186713	B
TLR2	4.47	0.028406		5.00	0.064701		1.14	0.411947	
TLR3	-3.81	0.096572	B	-1.02	0.995806	A	1.34	0.631994	A
TLR4	1.01	0.896195		-3.81	0.002655		1.02	0.862882	
TLR5	-1.90	0.046020		-39.64	0.002404	A	-1.23	0.351281	
TLR6	-2.07	0.082060		-9.26	0.017814		-1.88	0.151814	
TLR7	-16.47	0.005102		-18.90	0.004952		-2.15	0.035074	
TLR8	3.97	0.000179		-1.23	0.264786		1.62	0.121742	
TLR9	-28071.09	0.000299	A	-2.25	0.023792		-14230.99	0.000299	A
TNF	1.44	0.102314		1.34	0.099357		3.12	0.043942	
TNFRSF1A	2.07	0.000230		-2.15	0.001564		-1.31	0.395425	
TOLLIP	2.68	0.008100		-2.07	0.001871		1.02	0.810697	
TRAF6	1.07	0.895772		-2.56	0.053192		-1.08	0.825570	
UBE2N	2.55	0.012597		1.24	0.511527		-1.46	0.398729	

PBMDMs from 3 separate donors were set up according to the experimental design in Figure 15 with PBMDMs pre-incubated with/without 50µg V-antigen for 30min and then stimulated with/without 100ng/ml LPS for 16hr. The cells were then lysed, and the RNA was extracted for qPCR analysis using the Qiagen RT² profiler - Human TLR pathway gene array plate. Average gene expression for each gene in the three test conditions ('LPS only', 'pV1+LPS', and 'pV2+LPS') was compared to gene expression of the same gene in the unstimulated control to determine the change in fold-regulation. A Student's T-test was performed for each comparison via the Qiagen Geneglobe analysis software. The resulting data is presented in the table above alongside any comments about data reliability for that comparison

'Comments' are: A; the gene's average threshold value is high (>30) in one group and low (<30) in the other, B; the gene's average threshold value is >30 in both samples and the p-value for the fold-change is unavailable or high (p>0.05), C; the gene's average threshold value is above the cut-off or undetected in all samples and so is unreliable and cannot be used

Supplementary Table 4 - Qiagen RT² profiler gene array – Human TLR pathway full results – pV3/pV6

Gene	LPS only			pV3+LPS			pV6+LPS		
	Fold regulation	p-value	Comments	Fold regulation	p-value	Comments	Fold regulation	p-value	Comments
<i>BTK</i>	-2.62	0.239660	B	-1.91	0.314439	B	-1.47	0.517376	B
<i>CASP8</i>	-1.71	0.314919		-1.51	0.422142		-1.29	0.598822	
<i>CCL2</i>	-1.14	0.802939	B	-1.02	0.736509	B	1.34	0.434618	B
<i>CD14</i>	-2.07	0.026051		-2.03	0.013452		-2.01	0.019549	
<i>CD180</i>	-25.76	0.373565	B	-1.58	0.798699	B	-18.59	0.373669	B
<i>CD80</i>	-21.88	0.365254	B	-2.30	0.931963	B	-15.59	0.366126	B
<i>CD86</i>	-1.68	0.675573	B	-2.12	0.395122	B	-1.78	0.437043	B
<i>CHUK</i>	-1.75	0.430637		-1.77	0.431693		-1.55	0.478649	
<i>CLEC4E</i>	-66.95	0.287288	A	-61.40	0.287446	A	-20.24	0.290800	A
<i>CSF2</i>	2.90	0.190034	A	4.30	0.238386	A	4.89	0.149140	A
<i>CSF3</i>	2.82	0.035691	A	4.37	0.041386	A	6.15	0.009157	A
<i>CXCL10</i>	1.87	0.278901	B	1.86	0.269404	B	3.66	0.188053	B
<i>ECSIT</i>	-1.31	0.484176		-1.39	0.512725		-1.38	0.402447	
<i>EIF2AK2</i>	1.25	0.599003		-1.05	0.937480		1.11	0.633303	
<i>ELK1</i>	-1.19	0.666980		-1.45	0.509882		-1.18	0.673986	
<i>FADD</i>	-1.62	0.522583		-1.81	0.426341		-1.36	0.659598	
<i>FOS</i>	1.18	0.528907		2.21	0.369594		1.28	0.481924	
<i>HMGB1</i>	-1.76	0.281837		-1.78	0.288381		-1.67	0.264182	
<i>HRAS</i>	-1.40	0.505355		-1.62	0.437677		-1.38	0.489712	
<i>HSPA1A</i>	1.03	0.806210		1.17	0.652877		1.13	0.685205	
<i>HSPD1</i>	-1.50	0.428462		-1.86	0.349025		-1.53	0.434748	
<i>IFNA1</i>	-1.58	0.346635	B	-1.15	0.738224	B	1.42	0.412453	B
<i>IFNB1</i>	3.67	0.283378	B	3.32	0.252182	B	5.98	0.171050	B
<i>IFNG</i>	20.73	0.373763	B	-1.09	0.695131	B	1.17	0.922411	C
<i>IKBKB</i>	-1.58	0.544977		-1.75	0.430860		-1.39	0.579278	
<i>IL10</i>	1.35	0.611831	B	13.66	0.367723	B	29.53	0.371827	B
<i>IL12A</i>	1.18	0.934470		1.07	0.989459		1.36	0.754823	
<i>IL1A</i>	2.02	0.398509		2.86	0.337705		2.16	0.392868	
<i>IL1B</i>	1.77	0.601575		1.91	0.555074		2.70	0.353737	
<i>IL2</i>	120.41	0.373901	A	-1.17	0.929668	B	1.35	0.501504	B
<i>IL6</i>	3.06	0.243070		3.09	0.327064		4.76	0.180973	
<i>CXCL8</i>	11.21	0.269904		16.27	0.163681		17.11	0.196848	
<i>IRAK1</i>	-1.37	0.661101		-1.40	0.510907		-1.18	0.728311	
<i>IRAK2</i>	1.68	0.526370		1.53	0.639715		1.96	0.392460	
<i>IRAK4</i>	-1.43	0.483985		-1.36	0.509613		-1.30	0.511475	
<i>IRF1</i>	-1.09	0.965090		-1.07	0.984709		1.19	0.620465	
<i>IRF3</i>	-1.48	0.449075		-1.61	0.382234		-1.38	0.467563	
<i>JUN</i>	1.26	0.971888		1.03	0.649874		1.31	0.933285	
<i>LTA</i>	-2.38	0.294982	B	-2.11	0.438390	B	-1.81	0.302848	B
<i>LY86</i>	-2.25	0.410784	B	-3.56	0.368428	B	-1.94	0.399651	B
<i>LY96</i>	-1.38	0.553780		-1.56	0.493572		-1.23	0.548296	
<i>MAP2K3</i>	-1.26	0.654816		-1.35	0.614195		-1.29	0.576949	
<i>MAP2K4</i>	-1.56	0.250321		-1.48	0.251256		-1.65	0.184275	
<i>MAP3K1</i>	-1.21	0.491904		-1.05	0.917435		-1.22	0.629906	
<i>MAP3K7</i>	-1.51	0.398428		-1.69	0.308373		-1.55	0.306434	
<i>MAP4K4</i>	-1.30	0.624676		-1.49	0.506181		-1.35	0.544667	
<i>MAPK8</i>	-1.52	0.356376		-1.45	0.394876		-1.43	0.351498	
<i>MAPK8IP3</i>	1.23	0.770813		1.45	0.912006		1.52	0.819136	
<i>MYD88</i>	-1.10	0.976155		-1.20	0.685357		1.10	0.708861	
<i>NFKB1</i>	-1.33	0.571766		-1.23	0.678412		-1.30	0.549182	
<i>NFKB2</i>	1.20	0.824041		1.42	0.808923		1.52	0.755243	
<i>NFKBIA</i>	1.64	0.213572		1.53	0.376120		1.91	0.107095	
<i>NFKBIL1</i>	-1.04	0.614283		-1.03	0.687542		1.03	0.775244	
<i>NFRKB</i>	-1.40	0.432434		-1.35	0.477544		-1.31	0.504078	
<i>NR2C2</i>	-1.53	0.474117		-1.53	0.488061		-1.53	0.491594	

PELI1	-1.02	0.649210		1.26	0.572143		-1.07	0.677572	
PPARA	-1.22	0.397450		-1.14	0.560490		-1.19	0.484882	
PRKRA	-1.48	0.402841		-1.65	0.337900		-1.60	0.307955	
PTGS2	1.58	0.438876		3.74	0.380697		2.31	0.428308	
REL	-1.08	0.801754		1.21	0.575930		1.03	0.716712	
RELA	-1.10	0.639862		-1.12	0.698486		-1.16	0.544188	
RIPK2	-1.12	0.602505		-1.36	0.489578		-1.19	0.527804	
SARM1	-1.70	0.519081		-2.05	0.383814		-1.71	0.435257	
SIGIRR	-1.31	0.547404		1.14	0.800767		-1.46	0.571323	
TAB1	-1.51	0.543679		-1.69	0.428219		-1.56	0.458617	
TBK1	-1.47	0.624692		-2.03	0.249709		-1.88	0.308612	
TICAM1	1.24	0.982482		-1.03	0.622001		1.12	0.805178	
TICAM2	-1.20	0.634194		-1.56	0.421214		-1.18	0.594870	
TIRAP	-1.76	0.228597		-1.77	0.178157		-1.76	0.265977	
TLR1	-1.64	0.581804	B	2.56	0.781291	B	-1.03	0.738777	B
TLR10	-1.54	0.474671	B	-1.30	0.908064	B	-1.45	0.508263	B
TLR2	-1.09	0.873346		3.12	0.802551		1.19	0.888915	
TLR3	1.04	0.600161		1.42	0.002579		1.44	0.011885	
TLR4	-1.70	0.799365		-1.86	0.683051		-1.51	0.807736	
TLR5	-2.01	0.686713	B	4.07	0.998088	A	1.08	0.704363	B
TLR6	-1.49	0.351891		-1.56	0.211494		-1.71	0.198735	
TLR7	-1.17	0.607613	B	-1.33	0.481108	B	-1.02	0.671594	B
TLR8	-2.02	0.375996	B	-1.82	0.401452	B	-1.40	0.453624	B
TLR9	2.52	0.369037	B	1.90	0.339876	B	2.01	0.422223	B
TNF	2.86	0.267514	B	5.22	0.251029	A	5.44	0.105811	B
TNFRSF1A	-1.28	0.487462		-1.50	0.250378		-1.38	0.370867	
TOLLIP	-1.33	0.485094		-1.48	0.427080		-1.27	0.546465	
TRAF6	-1.29	0.583017		-1.30	0.574647		-1.27	0.499742	
UBE2N	-1.65	0.405307		-1.69	0.435401		-1.70	0.335995	

PBMDMs from 3 separate donors were set up according to the experimental design in Figure 15 with PBMDMs pre-incubated with/without 50µg V-antigen for 30min and then stimulated with/without 100ng/ml LPS for 16hr. The cells were then lysed, and the RNA was extracted for qPCR analysis using the Qiagen RT² profiler - Human TLR pathway gene array plate. Average gene expression for each gene in the three test conditions ('LPS only', 'pV3+LPS', and 'pV6+LPS') was compared to gene expression of the same gene in the unstimulated control to determine the change in fold-regulation. A Student's T-test was performed for each comparison via the Qiagen Geneglobe analysis software. The resulting data is presented in the table above alongside any comments about data reliability for that comparison

'Comments' are: A; the gene's average threshold value is high (>30) in one group and low (<30) in the other, B; the gene's average threshold value is >30 in both samples and the p-value for the fold-change is unavailable or high (p>0.05), C; the gene's average threshold value is above the cut-off or undetected in all samples and so is unreliable and cannot be used

9: References

1. Man SM, Hopkins LJ, Nugent E, Cox S, Gluck IM, Tourlomousis P, et al. Inflammasome activation causes dual recruitment of NLRC4 and NLRP3 to the same macromolecular complex. *Proc Natl Acad Sci U S A*. 2014;111(20):7403-8.
2. Janeway C. Immunogenicity signals 1, 2, 3... and 0. *Immunol Today*. 1989;10(0):283-6.
3. Matzinger P. Tolerance, Danger, and the Extended Family. *Annu Rev Immunol*. 1994;12:991-1045.
4. O T, S A. Pattern Recognition Receptors and Inflammation. *Cell*. 2010;140(6):805-20.
5. Ermolaeva MA, Michallet MC, Papadopoulou N, Utermohlen O, Kranidioti K, Kollias G, et al. Function of TRADD in tumor necrosis factor receptor 1 signaling and in TRIF-dependent inflammatory responses. *Nat Immunol*. 2008;9(9):1037-46.
6. MC M, E M, MA E, J V, M R, J C, et al. TRADD Protein Is an Essential Component of the RIG-like Helicase Antiviral Pathway. *Immunity*. 2008;28(5):651-61.
7. H K, O T, S S, M Y, M Y, K M, et al. Differential Roles of MDA5 and RIG-I Helicases in the Recognition of RNA Viruses. *Nature*. 2006;441(7089):101-5.
8. KV A, G J, C N-V. Establishment of Dorsal-Ventral Polarity in the Drosophila Embryo: Genetic Studies on the Role of the Toll Gene Product. *Cell*. 1985;42(3):779-89.
9. U H, C C, C G, V S, E M, S T, et al. Human TLR10 Is a Functional Receptor, Expressed by B Cells and Plasmacytoid Dendritic Cells, Which Activates Gene Transcription Through MyD88. *Journal of immunology (Baltimore, Md : 1950)*. 2005;174(5):2942-50.
10. Makkouk A, Abdelnoor AM. The potential use of Toll-like receptor (TLR) agonists and antagonists as prophylactic and/or therapeutic agents. *Immunopharmacol Immunotoxicol*. 2009;31(3):331-8.
11. S F, G E, J B. Mechanisms of Disease: Toll-like Receptors in Cardiovascular Disease. *Nature clinical practice Cardiovascular medicine*. 2007;4(8):444-54.
12. I B, DM S, DR D. The Structural Biology of Toll-like Receptors. *Structure (London, England : 1993)*. 2011;19(4):447-59.
13. Peroval MY, Boyd AC, Young JR, Smith AL. A critical role for MAPK signalling pathways in the transcriptional regulation of toll like receptors. *PLoS One*. 2013;8(2):e51243.
14. Symons A, Beinke S, Ley SC. MAP kinase kinase kinases and innate immunity. *Trends Immunol*. 2006;27(1):40-8.
15. Morrison DK. MAP Kinase Pathways. *Cold Spring Harb Perspect Biol*. 2012;4(11).

16. Kawasaki T, Kawai T. Toll-Like Receptor Signaling Pathways. *Front Immunol.* 2014;5(461).
17. J V, S T, C S, S H, M J, A F, et al. Immune Stimulation Mediated by Autoantigen Binding Sites Within Small Nuclear RNAs Involves Toll-like Receptors 7 and 8. *The Journal of experimental medicine.* 2005;202(11):1575-85.
18. J T, AM A, SY M, B C, K S, H W, et al. Toll-like Receptor 9-dependent Activation by DNA-containing Immune Complexes Is Mediated by HMGB1 and RAGE. *Nature immunology.* 2007;8(5):487-96.
19. SR C, J S, K N, M K, RA F, MJ S. Toll-like Receptor 7 and TLR9 Dictate Autoantibody Specificity and Have Opposing Inflammatory and Regulatory Roles in a Murine Model of Lupus. *Immunity.* 2006;25(3):417-28.
20. GA V, CM L, TM H, BA M, MJ S, A M-R. Activation of Autoreactive B Cells by CpG dsDNA. *Immunity.* 2003;19(6):837-47.
21. MA L-K, M G, D C, L S, K E, YA L, et al. Mutations in the Gene Encoding the 3'-5' DNA Exonuclease TREX1 Are Associated With Systemic Lupus Erythematosus. *Nature genetics.* 2007;39(9):1065-7.
22. PE W, SA D. Models of Inflammation: Adjuvant-Induced Arthritis in the Rat. *Current protocols in pharmacology.* 2001;Chapter 5.
23. KG H, SA J, AL B, M D, CM F, N H, et al. Induction of Experimental Autoimmune Encephalomyelitis With Recombinant Human Myelin Oligodendrocyte Glycoprotein in Incomplete Freund's Adjuvant in Three Non-Human Primate Species. *Journal of neuroimmune pharmacology : the official journal of the Society on NeuroImmune Pharmacology.* 2013;8(5):1251-64.
24. BA C, BR L, S R, M B, C E, AL B, et al. Inflammation and Autoimmunity Caused by a SHP1 Mutation Depend on IL-1, MyD88, and a Microbial Trigger. *Proceedings of the National Academy of Sciences of the United States of America.* 2008;105(39):15028-33.
25. T K, O T, Y T, H K, Y I, T T, et al. TANK Is a Negative Regulator of Toll-like Receptor Signaling and Is Critical for the Prevention of Autoimmune Nephritis. *Nature immunology.* 2009;10(9):965-72.
26. O H, RC A, R T, M W, D P, EE T, et al. The Ubiquitin-Editing Enzyme A20 Restricts Nucleotide-Binding Oligomerization Domain Containing 2-triggered Signals. *Immunity.* 2008;28(3):381-90.

27. Lin E, Freedman JE, Beaulieu LM. Innate immunity and toll-like receptor antagonists: a potential role in the treatment of cardiovascular diseases. *Cardiovasc Ther*. 2009;27(2):117-23.
28. TV A, E O, SC T, J T, SM T, TM W. Toll-like Receptors in Ischemia-Reperfusion Injury. *Shock (Augusta, Ga)*. 2009;32(1):4-16.
29. A P, X H, I S, MY L, C VH, X D, et al. Defective LPS signaling in C3H/HeJ and C57BL/10ScCr mice: mutations in Tlr4 gene. *Science (New York, NY)*. 1998;282(5396).
30. K H, O T, T K, H S, T O, Y T, et al. Cutting edge: Toll-like receptor 4 (TLR4)-deficient mice are hyporesponsive to lipopolysaccharide: evidence for TLR4 as the Lps gene product. *Journal of immunology (Baltimore, Md : 1950)*. 1999;162(7):3749-52.
31. B B, N R. Function and Biogenesis of Lipopolysaccharides. *EcoSal Plus*. 2018;8(1).
32. M G, N M. LPS induction of gene expression in human monocytes. *Cellular signalling*. 2001;13(2):85-94.
33. KA R, MF S, MK S, PB E. Reactive oxygen and nitrogen species differentially regulate Toll-like receptor 4-mediated activation of NF-kappa B and interleukin-8 expression. *Infection and immunity*. 2004;72(4):2123-30.
34. MA L, JE H, M S, MSJ M, CC K, T H, et al. Toll-like Receptor Signaling Rewires Macrophage Metabolism and Promotes Histone Acetylation via ATP-Citrate Lyase. *Immunity*. 2019;51(6):997-1011.
35. J L, M S, B K, H E, M L, JP K. Comparison of bacterial lipopolysaccharide-induced sickness behavior in rodents and humans: Relevance for symptoms of anxiety and depression. *Neuroscience and biobehavioral reviews*. 2020;115(115):15-24.
36. F A, C F, KJ T, JM C, F D. Lipopolysaccharide-induced cytokine cascade and lethality in LT alpha/TNF alpha-deficient mice. *Molecular medicine (Cambridge, Mass)*. 1997;3(12):864-75.
37. K Y, M N, N I. Injection time of interleukin-6 determines fatal outcome in experimental endotoxin shock. *Journal of interferon & cytokine research : the official journal of the International Society for Interferon and Cytokine Research*. 1996;16(12):995-1000.
38. T VB, D D, P B, B V, A G, B D, et al. Simultaneous targeting of IL-1 and IL-18 is required for protection against inflammatory and septic shock. *American journal of respiratory and critical care medicine*. 2014;189(3):282-91.
39. Parmely MJ, Hao S-Y, Morrison DC, Pace JL. Role of macrophage-derived nitric oxide in endotoxin lethality in mice. *Journal of Endotoxin Research*. 1995;2(1):45-52.

40. X Y, X C, Y T, X Q, Y W, H K, et al. Bacterial Endotoxin Activates the Coagulation Cascade through Gasdermin D-Dependent Phosphatidylserine Exposure. *Immunity*. 2019;51(6):983-96.
41. M H, T M, S A, S M. Interleukin 10 protects mice from lethal endotoxemia. *The Journal of experimental medicine*. 1993;177(4):1205-8.
42. S C, HS W, SF L, SE C, D R. Acute inflammatory response to endotoxin in mice and humans. *Clinical and diagnostic laboratory immunology*. 2005;12(1):60-7.
43. T T, R vG, P P, L K. Monocyte Subsets Are Differentially Lost from the Circulation during Acute Inflammation Induced by Human Experimental Endotoxemia. *Journal of innate immunity*. 2017;9(5):464-74.
44. C S, T J, S M-F, TM H, NV S, L L, et al. Bone marrow mesenchymal stem and progenitor cells induce monocyte emigration in response to circulating toll-like receptor ligands. *Immunity*. 2011;34(4):590-601.
45. M B, G M, R P, I V, V T, G O, et al. Prevalence and clinical significance of early high Endotoxin Activity in septic shock: An observational study. *Journal of critical care*. 2017;41:124-9.
46. Singer M, Deutschman CS, Seymour CW, Shankar-Hari M, Annane D, Bauer M, et al. The Third International Consensus Definitions for Sepsis and Septic Shock (Sepsis-3). *JAMA*. 2016;315(8):801-10.
47. Mayr FB, Yende S, Angus DC. Epidemiology of severe sepsis. *Virulence*. 2014;5(1):4-11.
48. LA vV, BP S, MA W, AJ H, PM KK, M F, et al. Comparative Analysis of the Host Response to Community-acquired and Hospital-acquired Pneumonia in Critically Ill Patients. *American journal of respiratory and critical care medicine*. 2016;194(11):1366-74.
49. KL B, EE D, J R, P H, AC G, P H, et al. Shared and Distinct Aspects of the Sepsis Transcriptomic Response to Fecal Peritonitis and Pneumonia. *American journal of respiratory and critical care medicine*. 2017;196(3):328-39.
50. Osuchowski MF, Welch K, Siddiqui J, Remick DG. Circulating cytokine/inhibitor profiles reshape the understanding of the SIRS/CARS continuum in sepsis and predict mortality. *J Immunol*. 2006;177(3):1967-74.
51. A O, SM S, SK T, C O, A A, JP P, et al. Plasma Cytokine Measurements Augment Prognostic Scores as Indicators of Outcome in Patients With Severe Sepsis. *Shock*. 2005;23(6):488-93.

52. RS H, KW T, PE S, IE K. Endothelial Cell Apoptosis in Sepsis. *Critical care medicine*. 2002;30(5 Suppl):225-8.
53. R G, Y W, AW M, RJ Q, PN C. Acute renal failure in endotoxemia is dependent on caspase activation. *Journal of the American Society of Nephrology : JASN*. 2004;15(12):3093-102.
54. G D, I D-S, P T, J P. Innate immune functions of immature neutrophils in patients with sepsis and severe systemic inflammatory response syndrome. *Critical care medicine*. 2013;41(3):820-32.
55. SR C, AC M, SA T, B M, Z G, MM K, et al. Platelet TLR4 activates neutrophil extracellular traps to ensnare bacteria in septic blood. *Nature medicine*. 2007;13(4):463-9.
56. E vG, J T, LSP H, K W, L K, N V. Immature Neutrophils Released in Acute Inflammation Exhibit Efficient Migration despite Incomplete Segmentation of the Nucleus. *Journal of immunology (Baltimore, Md : 1950)*. 2019;202(1):201-17.
57. MJ S, S S, EB C, RC L, J N, J B, et al. Transcriptomic Analyses of Murine Resolution-Phase Macrophages. *Blood*. 2011;118(26):192-208.
58. F Z, H W, X W, G J, H L, G Z, et al. TGF- β induces M2-like macrophage polarization via SNAIL-mediated suppression of a pro-inflammatory phenotype. *Oncotarget*. 2016;7(32):52294-306.
59. S S-Z, N G, S A, R R, CN S, A A. Saturated-efferocytosis Generates Pro-Resolving CD11b Low Macrophages: Modulation by Resolvins and Glucocorticoids. *European journal of immunology*. 2011;41(2):366-79.
60. VA F, DL B, A K, PW F, JY W, PM H. Macrophages That Have Ingested Apoptotic Cells in Vitro Inhibit Proinflammatory Cytokine Production Through Autocrine/Paracrine Mechanisms Involving TGF-beta, PGE2, and PAF. *The Journal of clinical investigation*. 1998;101(4):890-8.
61. ND S, T dB, KV W, SA J, K vM, A G, et al. Human Anti-Inflammatory Macrophages Induce Foxp3+ GITR+ CD25+ Regulatory T Cells, Which Suppress via Membrane-Bound TGFbeta-1. *Journal of immunology (Baltimore, Md : 1950)*. 2008;181(3):2220-6.
62. RA D, JH C, CL B, A D, AE S, CM O. Macrophage-specific Metalloelastase (MMP-12) Truncates and Inactivates ELR+ CXC Chemokines and Generates CCL2, -7, -8, and -13 Antagonists: Potential Role of the Macrophage in Terminating Polymorphonuclear Leukocyte Influx. *Blood*. 2008;112(8):3455-64.

63. GA M, JH G, EM T, CA M, I C-L, CM O. Inflammation Dampened by Gelatinase A Cleavage of Monocyte Chemoattractant protein-3. *Science (New York, NY)*. 2000;289(5482):1202-6.
64. A M, R B, M L. Tuning Inflammation and Immunity by Chemokine Sequestration: Decoys and More. *Nature reviews Immunology*. 2006;6(12):907-18.
65. L G, AM P, BA A, MA S, J M. The Human Duffy Antigen Binds Selected Inflammatory but Not Homeostatic Chemokines. *Biochemical and biophysical research communications*. 2004;321(2):306-12.
66. A A, G F, YP S, A K, TE VD, AD L, et al. Apoptotic Neutrophils and T Cells Sequester Chemokines During Immune Response Resolution Through Modulation of CCR5 Expression. *Nature immunology*. 2006;7(11):1209-16.
67. G DA, G F, G B, P T, A D, A V, et al. Uncoupling of Inflammatory Chemokine Receptors by IL-10: Generation of Functional Decoys. *Nature immunology*. 2000;1(5):387-91.
68. Yates CC, Rodrigues M, Nuschke A, Johnson ZI, Whaley D, Stolz D, et al. Multipotent stromal cells/mesenchymal stem cells and fibroblasts combine to minimize skin hypertrophic scarring. *Stem Cell Research & Therapy*. 2017;8(1):1-13.
69. DA R, D M, MJ B, Z W. Wound Macrophages Express TGF- α and Other Growth Factors in Vivo: Analysis by mRNA Phenotyping. *Science (New York, NY)*. 1988;241(4866):708-12.
70. TJ C, G C, L Z, X A, P C, P M, et al. Specific Recruitment of Regulatory T Cells in Ovarian Carcinoma Fosters Immune Privilege and Predicts Reduced Survival. *Nature medicine*. 2004;10(9):942-9.
71. Penn JW, Grobbelaar AO, Rolfe KJ. The role of the TGF- β family in wound healing, burns and scarring: a review. *Int J Burns Trauma*. 2012;2(1):18-28.
72. K A, S J, N A, A K, M L, W M, et al. Mfge8 Diminishes the Severity of Tissue Fibrosis in Mice by Binding and Targeting Collagen for Uptake by Macrophages. *The Journal of clinical investigation*. 2009;119(12):3713-22.
73. DR K, TK H, H S, BJ H, Z W, MJ B. Oxygen Tension Regulates the Expression of Angiogenesis Factor by Macrophages. *Science*. 1983;221(4617):1283-5.
74. Marik PE. Glucocorticoids in sepsis: dissecting facts from fiction. *Crit Care*. 2011;15(3):158.
75. PC M, KJ D, PQ E, C N. The Effects of Steroids During Sepsis Depend on Dose and Severity of Illness: An Updated Meta-Analysis. *Clinical microbiology and infection : the*

official publication of the European Society of Clinical Microbiology and Infectious Diseases. 2009;15(4):308-18.

76. TW R, AP W, GR B, JL V, DC A, N A, et al. A randomized, double-blind, placebo-controlled trial of TAK-242 for the treatment of severe sepsis. *Critical care medicine*. 2010;38(8):1685-94.

77. A B, S S, X C, C N, PQ E. Eritoran tetrasodium (E5564) treatment for sepsis: review of preclinical and clinical studies. *Expert opinion on drug metabolism & toxicology*. 2011;7(4):479-94.

78. KPH M, IR G, JCF Q, MA C, PENS V, P M. Polymyxin B clinical outcomes: A prospective study of patients undergoing intravenous treatment. *Journal of clinical pharmacy and therapeutics*. 2019;44(3):415-9.

79. X Z, D Y, X L, N W, B L, H C, et al. Identification of a new anti-LPS agent, geniposide, from *Gardenia jasminoides* Ellis, and its ability of direct binding and neutralization of lipopolysaccharide in vitro and in vivo. *International immunopharmacology*. 2010;10(10):1209-19.

80. B S, RS M, R K, AW V. Hepatic uptake and deacylation of the LPS in bloodborne LPS-lipoprotein complexes. *Innate immunity*. 2012;18(6):825-33.

81. M B, A W, G M, F B, S W, N W, et al. Efficacy and Safety of Vilobelimab (IFX-1), a Novel Monoclonal Anti-C5a Antibody, in Patients With Early Severe Sepsis or Septic Shock-A Randomized, Placebo-Controlled, Double-Blind, Multicenter, Phase IIa Trial (SCIENS Study). *Critical care explorations*. 2021;3(11).

82. A K, R G, F K, M K, V A, A T-E. Therapeutic effects of curcumin on sepsis and mechanisms of action: A systematic review of preclinical studies. *Phytotherapy research : PTR*. 2019;33(11):2798-820.

83. SM O, CJ F, JF D, JL V, R B, SF L, et al. Confirmatory interleukin-1 Receptor Antagonist Trial in Severe Sepsis: A Phase III, Randomized, Double-Blind, Placebo-Controlled, Multicenter Trial. The Interleukin-1 Receptor Antagonist Sepsis Investigator Group. *Critical care medicine*. 1997;25(7):1115-1124.

84. CJ F, GJ S, SM O, JP P, RC B, G E, et al. Initial Evaluation of Human Recombinant interleukin-1 Receptor Antagonist in the Treatment of Sepsis Syndrome: A Randomized, Open-Label, Placebo-Controlled Multicenter Trial. *Critical care medicine*. 1994;22(1):12-21.

85. CJ F, JF D, SM O, JP P, RA B, GJ S, et al. Recombinant Human Interleukin 1 Receptor Antagonist in the Treatment of Patients With Sepsis Syndrome. Results From a

Randomized, Double-Blind, Placebo-Controlled Trial. Phase III rhIL-1ra Sepsis Syndrome Study Group. *JAMA*. 1994;271(23):1836-43.

86. K R, C W-L, F G, M K, S W, D T, et al. Assessment of the Safety and Efficacy of the Monoclonal Anti-Tumor Necrosis Factor Antibody-Fragment, MAK 195F, in Patients With Sepsis and Septic Shock: A Multicenter, Randomized, Placebo-Controlled, Dose-Ranging Study. *Critical care medicine*. 1996;24(5):733-42.

87. JF D, JL V, C R, P L, C M, L F, et al. CDP571, a Humanized Antibody to Human Tumor Necrosis Factor-Alpha: Safety, Pharmacokinetics, Immune Response, and Influence of the Antibody on Cytokine Concentrations in Patients With Septic Shock. CPD571 Sepsis Study Group. *Critical care medicine*. 1995;23(9):1461-9.

88. E A, A A, G G, S T, G SP, R W, et al. Double-blind Randomised Controlled Trial of Monoclonal Antibody to Human Tumour Necrosis Factor in Treatment of Septic Shock. NORASEPT II Study Group. *Lancet*. 1998;351(9107):929-33.

89. MA C, LD P, AB C, SJ S, AA H, R G, et al. Effect of a Chimeric Antibody to Tumor Necrosis Factor-Alpha on Cytokine and Physiologic Responses in Patients With Severe Sepsis--A Randomized, Clinical Trial. *Critical care medicine*. 1998;26(10):1650-9.

90. E A, R W, H S, TM P, S N, H L, et al. Efficacy and Safety of Monoclonal Antibody to Human Tumor Necrosis Factor Alpha in Patients With Sepsis Syndrome. A Randomized, Controlled, Double-Blind, Multicenter Clinical Trial. TNF-alpha MAb Sepsis Study Group. *JAMA*. 1995;273(12):934-41.

91. CJ F, SM O, JF D, S S, JL Z, P N, et al. Influence of an Anti-Tumor Necrosis Factor Monoclonal Antibody on Cytokine Levels in Patients With Sepsis. The CB0006 Sepsis Syndrome Study Group. *Critical care medicine*. 1993;21(3):318-27.

92. J C, J C. INTERSEPT: An International, Multicenter, Placebo-Controlled Trial of Monoclonal Antibody to Human Tumor Necrosis Factor-Alpha in Patients With Sepsis. International Sepsis Trial Study Group. *Critical care medicine*. 1996;24(9):1431-40.

93. CJ F, JM A, SM O, SF L, RA B, JC S, et al. Treatment of Septic Shock With the Tumor Necrosis Factor receptor:Fc Fusion Protein. The Soluble TNF Receptor Sepsis Study Group. *The New England journal of medicine*. 1996;334(26):1697-702.

94. Lv S, Han M, Yi R, Kwon S, Dai C, Wang R. Anti-TNF-alpha therapy for patients with sepsis: a systematic meta-analysis. *Int J Clin Pract*. 2014;68(4):520-8.

95. DG R, DR C, SJ E, DE N, P N, JA N, et al. Combination Immunotherapy With Soluble Tumor Necrosis Factor Receptors Plus Interleukin 1 Receptor Antagonist Decreases Sepsis Mortality. *Critical care medicine*. 2001;29(3):473-81.
96. WJ K, RC B, D K, WD D, SN K, H W, et al. Interferon gamma-1b in the Treatment of Compensatory Anti-Inflammatory Response Syndrome. A New Approach: Proof of Principle. *Archives of internal medicine*. 1997;157(4):389-93.
97. TE T-K, W C, ED M, C L, ER S. Enhancement of Dendritic Cell Production by Fms-Like Tyrosine kinase-3 Ligand Increases the Resistance of Mice to a Burn Wound Infection. *Journal of immunology (Baltimore, Md : 1950)*. 2005;174(1):404-10.
98. RS H, KW T, PE S, KC C, JP C, TG B, et al. Prevention of Lymphocyte Cell Death in Sepsis Improves Survival in Mice. *Proceedings of the National Academy of Sciences of the United States of America*. 1999;96(25):14541-6.
99. ST OS, JA L, AF H, DH C, JA M, ML R. Major Injury Leads to Predominance of the T helper-2 Lymphocyte Phenotype and Diminished interleukin-12 Production Associated With Decreased Resistance to Infection. *Annals of surgery*. 1995;222(4):490-2.
100. WD D, F R, U S, D K, K A, P R, et al. Monocyte Deactivation in Septic Patients: Restoration by IFN-gamma Treatment. *Nature medicine*. 1997;3(6):678-81.
101. J L, M K, RM K, F P, LA J, JG vdH, et al. Reversal of Immunoparalysis in Humans in Vivo: A Double-Blind, Placebo-Controlled, Randomized Pilot Study. *American journal of respiratory and critical care medicine*. 2012;186(9):838-45.
102. R K, A K, O A, M O, V K, D R, et al. Use of IFN γ /IL10 Ratio for Stratification of Hydrocortisone Therapy in Patients With Septic Shock. *Frontiers in immunology*. 2021;12.
103. A P, E P, Z R, S P, D A. Vasopressin for Treatment of Vasodilatory Shock: An ESICM Systematic Review and Meta-Analysis. *Intensive care medicine*. 2012;38(1):9-19.
104. P A, F M, JF H, F G, B M, N A, et al. High Versus Low Blood-Pressure Target in Patients With Septic Shock. *The New England journal of medicine*. 2014;370(17):1583-93.
105. GR B, JL V, PF L, SP L, JF D, A L-R, et al. Efficacy and safety of recombinant human activated protein C for severe sepsis. *The New England journal of medicine*. 2001;344(10):699-709.
106. AJ M-C, I S, D L, AF C. Human recombinant activated protein C for severe sepsis. *The Cochrane database of systematic reviews*. 2011(4).

107. CE D, O D, G MF, AS LG, C S, J P-C. Yersinia Pestis and Plague: An Updated View on Evolution, Virulence Determinants, Immune Subversion, Vaccination, and Diagnostics. *Genes and immunity*. 2019;20(5):357-70.
108. RJ E, JM P, CL H, D W, CE L, PS M, et al. Persistence of Yersinia Pestis in Soil Under Natural Conditions. *Emerging infectious diseases*. 2008;14(6):941-3.
109. R R, V A, B N, B R, J P, QA TB, et al. Epidemiological Characteristics of an Urban Plague Epidemic in Madagascar, August-November, 2017: An Outbreak Report. *The Lancet Infectious diseases*. 2019;19(5):537-45.
110. KA B, CB G, TL J, JA M, RJ E. Infection Prevalence, Bacterial Loads, and Transmission Efficiency in *Oropsylla Montana* (Siphonaptera: Ceratophyllidae) One Day After Exposure to Varying Concentrations of Yersinia Pestis in Blood. *Journal of medical entomology*. 2016;53(3):674-80.
111. Y F, M F, A T, A M, D G, G H, et al. The Search for Early Markers of Plague: Evidence for Accumulation of Soluble Yersinia Pestis LcrV in Bubonic and Pneumonic Mouse Models of Disease. *FEMS immunology and medical microbiology*. 2010;59(2):197-206.
112. Pujol C, Klein KA, Romanov GA, Palmer LE, Ciota C, Zhao Z, et al. Yersinia pestis Can Reside in Autophagosomes and Avoid Xenophagy in Murine Macrophages by Preventing Vacuole Acidification. *Infect Immun*. 2009;77(6):2251-61.
113. V S, RD P, NM S, KR E, EA M, WE G. Yersinia Pestis Activates Both IL-1 β and IL-1 Receptor Antagonist to Modulate Lung Inflammation During Pneumonic Plague. *PLoS pathogens*. 2015;11(3).
114. AM C, SS B, PH D. YopH Inhibits Early Pro-Inflammatory Cytokine Responses During Plague Pneumonia. *BMC immunology*. 2010;11(1).
115. Zwack EE, Snyder AG, Wynosky-Dolfi MA, Ruthel G, Philip NH, Marketon MM, et al. Inflammasome activation in response to the Yersinia type III secretion system requires hyperinjection of translocon proteins YopB and YopD. *MBio*. 2015;6(1):e02095-14.
116. EJ K, DA C, AM K, SC S. The Plague Virulence Protein YopM Targets the Innate Immune Response by Causing a Global Depletion of NK Cells. *Infection and immunity*. 2004;72(8):4589-602.
117. LaRock CN, Cookson BT. The Yersinia virulence effector YopM binds caspase-1 to arrest inflammasome assembly and processing. *Cell Host Microbe*. 2012;12(6):799-805.

118. SP G, EL H, RM R-B, WA P. Role of YopH in the Suppression of Tyrosine Phosphorylation and Respiratory Burst Activity in Murine Macrophages Infected With *Yersinia Enterocolitica*. *Journal of leukocyte biology*. 1995;57(6):972-7.
119. S B, S R, L T, JB D, A A, B B, et al. *Yersinia* Phosphatase Induces Mitochondrially Dependent Apoptosis of T Cells. *The Journal of biological chemistry*. 2005;280(11):10388-94.
120. M A, J H. Modulation of Rho GTPases and the Actin Cytoskeleton by *Yersinia* Outer Proteins (Yops). *International journal of medical microbiology : IJMM*. 2001;291(4):269-74.
121. A B, GR C. Role of YopP in Suppression of Tumor Necrosis Factor Alpha Release by Macrophages During *Yersinia* Infection. *Infection and immunity*. 1998;66(5):1878-84.
122. K T, G G, T S, K R, R H, J H, et al. *Yersinia* Outer Protein P Inhibits CD8 T Cell Priming in the Mouse Infection Model. *Journal of immunology (Baltimore, Md : 1950)*. 2005;174(7):4244-51.
123. E B, S M, J L, R G, N S, C S, et al. Gene Expression Patterns of Epithelial Cells Modulated by Pathogenicity Factors of *Yersinia Enterocolitica*. *Cellular microbiology*. 2004;6(2):129-41.
124. A Z, S C, E M, Y F, A T, R B, et al. Interaction of *Yersinia Pestis* With Macrophages: Limitations in YopJ-dependent Apoptosis. *Infection and immunity*. 2006;74(6):3239-50.
125. Mukherjee S, Orth K. In Vitro Signaling by MAPK and NF κ B Pathways Inhibited by *Yersinia* YopJ. *Methods Enzymol*. 2008;438:343-53.
126. P S, G D, A VDB, P V, GR C, R B. Targeting Rac1 by the *Yersinia* Effector Protein YopE Inhibits caspase-1-mediated Maturation and Release of interleukin-1beta. *The Journal of biological chemistry*. 2004;279(24):25134-42.
127. MV T, GR K, J H, YA K, AP A, VL M. Tetraacylated Lipopolysaccharide of *Yersinia Pestis* Can Inhibit Multiple Toll-like Receptor-Mediated Signaling Pathways in Human Dendritic Cells. *The Journal of infectious diseases*. 2009;200(11):1694-702.
128. JJ T, SC P, ES K. Ail Provides Multiple Mechanisms of Serum Resistance to *Yersinia Pestis*. *Molecular microbiology*. 2019;111(1):82-95.
129. TW B, GA B. The Basis of Virulence in *Pasteurella Pestis*: Comparative Behaviour of Virulent and Avirulent Strains in Vivo. *British journal of experimental pathology*. 1954;35(2):134-43.
130. Schmidt A, Rollinghoff M, Beuscher HU. Suppression of TNF by V antigen of *Yersinia* spp. involves activated T cells. *Eur J Immunol*. 1999;29(4):1149-57.

131. Derewenda U, Mateja A, Devedjiev Y, Routzahn KM, Evdokimov AG, Derewenda ZS, et al. The structure of *Yersinia pestis* V-antigen, an essential virulence factor and mediator of immunity against plague. *Structure*. 2004;12(2):301-6.
132. Pouliot K, Pan N, Wang S, Lu S, Lien E, Goguen JD. Evaluation of the role of LcrV-Toll-like receptor 2-mediated immunomodulation in the virulence of *Yersinia pestis*. *Infect Immun*. 2007;75(7):3571-80.
133. Verma SK, Batra L, Tuteja U. A Recombinant Trivalent Fusion Protein F1-LcrV-HSP70(II) Augments Humoral and Cellular Immune Responses and Imparts Full Protection against *Yersinia pestis*. *Front Microbiol*. 2016;7:1053.
134. Nakajima R, Motin VL, Brubaker RR. Suppression of cytokines in mice by protein A-V antigen fusion peptide and restoration of synthesis by active immunization. *Infect Immun*. 1995;63(8):3021-9.
135. Fields KA, Straley SC. LcrV of *Yersinia pestis* enters infected eukaryotic cells by a virulence plasmid-independent mechanism. *Infect Immun*. 1999;67(9):4801-13.
136. ML N, KA F, SC S. The V Antigen of *Yersinia Pestis* Regulates Yop Vectorial Targeting as Well as Yop Secretion Through Effects on YopB and LcrG. *Journal of bacteriology*. 1998;180(13):3410-20.
137. ML N, AW W, E S, SC S. *Yersinia Pestis* LcrV Forms a Stable Complex With LcrG and May Have a Secretion-Related Regulatory Role in the low-Ca²⁺ Response. *Journal of bacteriology*. 1997;179(4):1307-16.
138. Pettersson J, Holmstrom A, Hill J, Leary S, Frithz-Lindsten E, von Euler-Matell A, et al. The V-antigen of *Yersinia* is surface exposed before target cell contact and involved in virulence protein translocation. *Mol Microbiol*. 1999;32(5):961-76.
139. Ekestubbe S, Bröms JE, Edgren T, Fällman M, Francis MS, Forsberg Å. The Amino-Terminal Part of the Needle-Tip Translocator LcrV of *Yersinia pseudotuberculosis* Is Required for Early Targeting of YopH and In vivo Virulence. *Front Cell Infect Microbiol*. 2016;6(175).
140. PC L, CM S, AG S, A R. Control of Effector Export by the *Pseudomonas Aeruginosa* Type III Secretion Proteins PcrG and PcrV. *Molecular microbiology*. 2010;75(4):924-41.
141. L S, A M, Y C, L B, A B, A A. Functional Insights Into the *Shigella* Type III Needle Tip IpaD in Secretion Control and Cell Contact. *Molecular microbiology*. 2013;88(2):268-82.
142. Fields KA, Nilles ML, Cowan C, Straley SC. Virulence role of V antigen of *Yersinia pestis* at the bacterial surface. *Infect Immun*. 1999;67(10):5395-408.

143. VL M, SM K, RR B. Suppression of Mouse Skin Allograft Rejection by Protein A-Yersinia V Antigen Fusion Peptide. *Transplantation*. 1997;63(7):1040-2.
144. Abramov VM, Kosarev IV, Motin VL, Khlebnikov VS, Vasilenko RN, Sakulin VK, et al. Binding of LcrV protein from *Yersinia pestis* to human T-cells induces apoptosis, which is completely blocked by specific antibodies. *Int J Biol Macromol*. 2019;122:1062-70.
145. Mitchell A, Tam C, Elli D, Charlton T, Osei-Owusu P, Fazlollahi F, et al. Glutathionylation of *Yersinia pestis* LcrV and Its Effects on Plague Pathogenesis. *MBio*. 2017;8(3).
146. Mosser DM, Zhang X. Interleukin-10: new perspectives on an old cytokine. *Immunol Rev*. 2008;226:205-18.
147. Nedialkov YA, Motin VL, Brubaker RR. Resistance to lipopolysaccharide mediated by the *Yersinia pestis* V antigen-polyhistidine fusion peptide: amplification of interleukin-10. *Infect Immun*. 1997;65(4):1196-203.
148. Sing A, Roggenkamp A, Geiger AM, Heesemann J. *Yersinia enterocolitica* evasion of the host innate immune response by V antigen-induced IL-10 production of macrophages is abrogated in IL-10-deficient mice. *J Immunol*. 2002;168(3):1315-21.
149. Sing A, Rost D, Tvardovskaia N, Roggenkamp A, Wiedemann A, Kirschning CJ, et al. *Yersinia* V-antigen exploits toll-like receptor 2 and CD14 for interleukin 10-mediated immunosuppression. *J Exp Med*. 2002;196(8):1017-24.
150. Sing A, Reithmeier-Rost D, Granfors K, Hill J, Roggenkamp A, Heesemann J. A hypervariable N-terminal region of *Yersinia* LcrV determines Toll-like receptor 2-mediated IL-10 induction and mouse virulence. *Proc Natl Acad Sci U S A*. 2005;102(44):16049-54.
151. DePaolo RW, Tang F, Kim IY, Han M, Levin N, Ciletti N, et al. TLR6 drives differentiation of tolerogenic DC and contributes to LcrV-mediated plague pathogenesis. *Cell Host Microbe*. 2008;4(4):350-61.
152. Abramov VM, Khlebnikov VS, Vasiliev AM, Kosarev IV, Vasilenko RN, Kulikova NL, et al. Attachment of LcrV from *Yersinia pestis* at dual binding sites to human TLR-2 and human IFN-gamma receptor. *J Proteome Res*. 2007;6(6):2222-31.
153. Sun W, Curtiss R, 3rd. Amino acid substitutions in LcrV at putative sites of interaction with Toll-like receptor 2 do not affect the virulence of *Yersinia pestis*. *Microb Pathog*. 2012;53(5-6):198-206.

154. Liu H, Ma Y, Pagliari LJ, Perlman H, Yu C, Lin A, et al. TNF-alpha-induced apoptosis of macrophages following inhibition of NF-kappa B: a central role for disruption of mitochondria. *J Immunol.* 2004;172(3):1907-15.
155. Erl W, Weber C, Wardemann C, Weber PC. Adhesion properties of Mono Mac 6, a monocytic cell line with characteristics of mature human monocytes. *Atherosclerosis.* 1995;113(1):99-107.
156. M A, AE G, R H, K N, L H. Human cell lines U-937, THP-1 and Mono Mac 6 represent relatively immature cells of the monocyte-macrophage cell lineage. *Leukemia.* 1994;8(9).
157. P N, JM B, A K, H K. Cytokine production of the human monocytic cell line Mono Mac 6 in comparison to mature monocytes in peripheral blood mononuclear cells. *Immunobiology.* 1993;188(3).
158. Vernazza C, Lingard B, Flick-Smith HC, Baillie LW, Hill J, Atkins HS. Small protective fragments of the *Yersinia pestis* V antigen. *Vaccine.* 2009;27(21):2775-80.
159. Hill J, Leary SE, Griffin KF, Williamson ED, Titball RW. Regions of *Yersinia pestis* V antigen that contribute to protection against plague identified by passive and active immunization. *Infect Immun.* 1997;65(11):4476-82.
160. Carr S, Miller J, Leary SE, Bennett AM, Ho A, Williamson ED. Expression of a recombinant form of the V antigen of *Yersinia pestis*, using three different expression systems. *Vaccine.* 1999;18(1-2):153-9.
161. Sagulenko V, Thygesen SJ, Sester DP, Idris A, Cridland JA, Vajjhala PR, et al. AIM2 and NLRP3 inflammasomes activate both apoptotic and pyroptotic death pathways via ASC. *Cell Death Differ.* 2013;20(9):1149-60.
162. Stevenson FT, Torrano F, Locksley RM, Lovett DH. Interleukin 1: the patterns of translation and intracellular distribution support alternative secretory mechanisms. *J Cell Physiol.* 1992;152(2):223-31.
163. Auron PE, Webb AC, Rosenwasser LJ, Mucci SF, Rich A, Wolff SM, et al. Nucleotide sequence of human monocyte interleukin 1 precursor cDNA. *Proc Natl Acad Sci U S A.* 1984;81(24):7907-11.
164. Andrei C, Dazzi C, Lotti L, Torrisi MR, Chimini G, Rubartelli A. The secretory route of the leaderless protein interleukin 1beta involves exocytosis of endolysosome-related vesicles. *Mol Biol Cell.* 1999;10(5):1463-75.

165. Rubartelli A, Cozzolino F, Talio M, Sitia R. A novel secretory pathway for interleukin-1 beta, a protein lacking a signal sequence. *Embo j.* 1990;9(5):1503-10.
166. Harris J, Hartman M, Roche C, Zeng SG, O'Shea A, Sharp FA, et al. Autophagy controls IL-1beta secretion by targeting pro-IL-1beta for degradation. *J Biol Chem.* 2011;286(11):9587-97.
167. MacKenzie A, Wilson HL, Kiss-Toth E, Dower SK, North RA, Surprenant A. Rapid secretion of interleukin-1beta by microvesicle shedding. *Immunity.* 2001;15(5):825-35.
168. Qu Y, Franchi L, Nunez G, Dubyak GR. Nonclassical IL-1 beta secretion stimulated by P2X7 receptors is dependent on inflammasome activation and correlated with exosome release in murine macrophages. *J Immunol.* 2007;179(3):1913-25.
169. Lindemann S, Tolley ND, Dixon DA, McIntyre TM, Prescott SM, Zimmerman GA, et al. Activated platelets mediate inflammatory signaling by regulated interleukin 1beta synthesis. *J Cell Biol.* 2001;154(3):485-90.
170. Pizzirani C, Ferrari D, Chiozzi P, Adinolfi E, Sandona D, Savaglio E, et al. Stimulation of P2 receptors causes release of IL-1beta-loaded microvesicles from human dendritic cells. *Blood.* 2007;109(9):3856-64.
171. Qu Y, Ramachandra L, Mohr S, Franchi L, Harding CV, Nunez G, et al. P2X7 receptor-stimulated secretion of MHC class II-containing exosomes requires the ASC/NLRP3 inflammasome but is independent of caspase-1. *J Immunol.* 2009;182(8):5052-62.
172. Fink SL, Cookson BT. Caspase-1-dependent pore formation during pyroptosis leads to osmotic lysis of infected host macrophages. *Cell Microbiol.* 2006;8(11):1812-25.
173. Hogquist KA, Nett MA, Unanue ER, Chaplin DD. Interleukin 1 is processed and released during apoptosis. *Proc Natl Acad Sci U S A.* 1991;88(19):8485-9.
174. Joosten LA, Netea MG, Fantuzzi G, Koenders MI, Helsen MM, Sparrer H, et al. Inflammatory arthritis in caspase 1 gene-deficient mice: contribution of proteinase 3 to caspase 1-independent production of bioactive interleukin-1beta. *Arthritis Rheum.* 2009;60(12):3651-62.
175. Evavold CL, Ruan J, Tan Y, Xia S, Wu H, Kagan JC. The Pore-Forming Protein Gasdermin D Regulates Interleukin-1 Secretion from Living Macrophages. *Immunity.* 2018;48(1):35-44.e6.

176. Marty V, Medina C, Combe C, Parnet P, Amedee T. ATP binding cassette transporter ABC1 is required for the release of interleukin-1beta by P2X7-stimulated and lipopolysaccharide-primed mouse Schwann cells. *Glia*. 2005;49(4):511-9.
177. Zhou X, Engel T, Goepfert C, Erren M, Assmann G, von Eckardstein A. The ATP binding cassette transporter A1 contributes to the secretion of interleukin 1beta from macrophages but not from monocytes. *Biochem Biophys Res Commun*. 2002;291(3):598-604.
178. Landolfo S, Gariglio M, Gribaudo G, Lembo D. The Irfi 200 genes: an emerging family of IFN-inducible genes. *Biochimie*. 1998;80(8-9):721-8.
179. Hornung V, Ablasser A, Charrel-Dennis M, Bauernfeind F, Horvath G, Caffrey DR, et al. AIM2 recognizes cytosolic dsDNA and forms a caspase-1-activating inflammasome with ASC. *Nature*. 2009;458(7237):514-8.
180. Mariathasan S, Weiss DS, Newton K, McBride J, O'Rourke K, Roose-Girma M, et al. Cryopyrin activates the inflammasome in response to toxins and ATP. *Nature*. 2006;440(7081):228-32.
181. Zhou R, Yazdi AS, Menu P, Tschopp J. A role for mitochondria in NLRP3 inflammasome activation. *Nature*. 2011;469(7329):221-5.
182. Munoz-Planillo R, Kuffa P, Martinez-Colon G, Smith BL, Rajendiran TM, Nunez G. K(+) efflux is the common trigger of NLRP3 inflammasome activation by bacterial toxins and particulate matter. *Immunity*. 2013;38(6):1142-53.
183. Kinnunen K, Piippo N, Loukovaara S, Hytti M, Kaarniranta K, Kauppinen A. Lysosomal destabilization activates the NLRP3 inflammasome in human umbilical vein endothelial cells (HUVECs). *J Cell Commun Signal*. 2017;11(3):275-9.
184. Yang CS, Kim JJ, Kim TS, Lee PY, Kim SY, Lee HM, et al. Small heterodimer partner interacts with NLRP3 and negatively regulates activation of the NLRP3 inflammasome. *Nat Commun*. 2015;6:6115.
185. Subramanian N, Natarajan K, Clatworthy MR, Wang Z, Germain RN. The adaptor MAVS promotes NLRP3 mitochondrial localization and inflammasome activation. *Cell*. 2013;153(2):348-61.
186. Hu Y, Mao K, Zeng Y, Chen S, Tao Z, Yang C, et al. Tripartite-motif protein 30 negatively regulates NLRP3 inflammasome activation by modulating reactive oxygen species production. *J Immunol*. 2010;185(12):7699-705.

187. Hernandez-Cuellar E, Tsuchiya K, Hara H, Fang R, Sakai S, Kawamura I, et al. Cutting edge: nitric oxide inhibits the NLRP3 inflammasome. *J Immunol*. 2012;189(11):5113-7.
188. Huai W, Zhao R, Song H, Zhao J, Zhang L, Gao C, et al. Aryl hydrocarbon receptor negatively regulates NLRP3 inflammasome activity by inhibiting NLRP3 transcription. *Nat Commun*. 2014;5:4738.
189. Saitoh T, Fujita N, Jang MH, Uematsu S, Yang BG, Satoh T, et al. Loss of the autophagy protein Atg16L1 enhances endotoxin-induced IL-1 β production. *Nature*. 2008;456(7219):264-8.
190. Bertinaria M, Gastaldi S, Marini E, Giorgis M. Development of covalent NLRP3 inflammasome inhibitors: Chemistry and biological activity. *Arch Biochem Biophys*. 2019;670:116-39.
191. Sorbara MT, Girardin SE. Mitochondrial ROS fuel the inflammasome. *Cell Res*. 2011;21(4):558-60.
192. Gaidt MM, Ebert TS, Chauhan D, Schmidt T, Schmid-Burgk JL, Rapino F, et al. Human Monocytes Engage an Alternative Inflammasome Pathway. *Immunity*. 2016;44(4):833-46.
193. S G-P, RG C, C N, EC H, E P-M, EK R, et al. Malonylation of GAPDH is an inflammatory signal in macrophages. *Nature communications*. 2019;10(1).
194. Piehler AP, Grimholt RM, Ovstebo R, Berg JP. Gene expression results in lipopolysaccharide-stimulated monocytes depend significantly on the choice of reference genes. *BMC Immunol*. 2010;11:21.
195. P G, B L, RK SM, M L, TL G, TD K. Chronic TLR Stimulation Controls NLRP3 Inflammasome Activation through IL-10 Mediated Regulation of NLRP3 Expression and Caspase-8 Activation. *Scientific reports*. 2015;5.
196. Q F, P L, PC L, N A. Caspase-1zeta, a new splice variant of the caspase-1 gene. *Genomics*. 2004;84(3):587-91.
197. Brubaker RR. Interleukin-10 and Inhibition of Innate Immunity to Yersiniae: Roles of Yops and LcrV (V Antigen). *Infect Immun*. 2003;71(7):3673-81.
198. H K, P G, R D, M B, C S, K M, et al. Interleukin-12-induced interferon-gamma production by human peripheral blood T cells is regulated by mammalian target of rapamycin (mTOR). *The Journal of biological chemistry*. 2005;280(2):1037-43.

199. KE T, CL G, RD N, EN F, SN V. Contribution of interferon-beta to the murine macrophage response to the toll-like receptor 4 agonist, lipopolysaccharide. *The Journal of biological chemistry*. 2006;281(41):31119-30.
200. D A-B, CM U, P G, M S, M L, C B, et al. A functional screen reveals an extensive layer of transcriptional and splicing control underlying RAS/MAPK signaling in *Drosophila*. *PLoS biology*. 2014;12(3).
201. VM RR, J R, N N, NM P, IJ S, BM Y, et al. Broad detection of bacterial type III secretion system and flagellin proteins by the human NAIP/NLRC4 inflammasome. *Proceedings of the National Academy of Sciences of the United States of America*. 2017;114(50):13242-7.
202. S S, S G, V R, K B, TK K, G S. Caspase-1 activator Ipaf is a p53-inducible gene involved in apoptosis. *Oncogene*. 2005;24(4):627-36.
203. AS A, SM A, BS L, N D, KT H, A Q, et al. Type 1 interferon-dependent repression of NLRC4 and iPLA2 licenses down-regulation of *Salmonella* flagellin inside macrophages. *Proceedings of the National Academy of Sciences of the United States of America*. 2020;117(47).
204. MH Z, SM M, P V, M L, TD K. *Salmonella* exploits NLRP12-dependent innate immune signaling to suppress host defenses during infection. *Proceedings of the National Academy of Sciences of the United States of America*. 2014;111(1):385-90.
205. S N, N W, A N, RJ M-T, C C, A C-M, et al. Proteasomal degradation of NOD2 by NLRP12 in monocytes promotes bacterial tolerance and colonization by enteropathogens. *Nature communications*. 2018;9(1).
206. Chow JC, Young DW, Golenbock DT, Christ WJ, Gusovsky F. Toll-like receptor-4 mediates lipopolysaccharide-induced signal transduction. *J Biol Chem*. 1999;274(16):10689-92.
207. Kurt-Jones EA, Popova L, Kwinn L, Haynes LM, Jones LP, Tripp RA, et al. Pattern recognition receptors TLR4 and CD14 mediate response to respiratory syncytial virus. *Nat Immunol*. 2000;1(5):398-401.
208. Rassa JC, Meyers JL, Zhang Y, Kudravalli R, Ross SR. Murine retroviruses activate B cells via interaction with toll-like receptor 4. *Proc Natl Acad Sci U S A*. 2002;99(4):2281-6.

209. Modhiran N, Watterson D, Blumenthal A, Baxter AG, Young PR, Stacey KJ. Dengue virus NS1 protein activates immune cells via TLR4 but not TLR2 or TLR6. *Immunol Cell Biol.* 2017;95(5):491-5.
210. Lu YC, Yeh WC, Ohashi PS. LPS/TLR4 signal transduction pathway. *Cytokine.* 2008;42(2):145-51.
211. Zanoni I, Ostuni R, Marek LR, Barresi S, Barbalat R, Barton GM, et al. CD14 controls the LPS-induced endocytosis of Toll-like receptor 4. *Cell.* 2011;147(4):868-80.
212. Saitoh S, Akashi S, Yamada T, Tanimura N, Matsumoto F, Fukase K, et al. Ligand-dependent Toll-like receptor 4 (TLR4)-oligomerization is directly linked with TLR4-signaling. *J Endotoxin Res.* 2004;10(4):257-60.
213. Kawai T, Takeuchi O, Fujita T, Inoue J, Muhlradt PF, Sato S, et al. Lipopolysaccharide stimulates the MyD88-independent pathway and results in activation of IFN-regulatory factor 3 and the expression of a subset of lipopolysaccharide-inducible genes. *J Immunol.* 2001;167(10):5887-94.
214. Fitzgerald KA, Palsson-McDermott EM, Bowie AG, Jefferies CA, Mansell AS, Brady G, et al. Mal (MyD88-adaptor-like) is required for Toll-like receptor-4 signal transduction. *Nature.* 2001;413(6851):78-83.
215. Scherle PA, Jones EA, Favata MF, Daulerio AJ, Covington MB, Nurnberg SA, et al. Inhibition of MAP kinase kinase prevents cytokine and prostaglandin E2 production in lipopolysaccharide-stimulated monocytes. *J Immunol.* 1998;161(10):5681-6.
216. Geppert TD, Whitehurst CE, Thompson P, Beutler B. Lipopolysaccharide signals activation of tumor necrosis factor biosynthesis through the ras/raf-1/MEK/MAPK pathway. *Mol Med.* 1994;1(1):93-103.
217. Lim W, Gee K, Mishra S, Kumar A. Regulation of B7.1 costimulatory molecule is mediated by the IFN regulatory factor-7 through the activation of JNK in lipopolysaccharide-stimulated human monocytic cells. *J Immunol.* 2005;175(9):5690-700.
218. Anand RJ, Kohler JW, Cavallo JA, Li J, Dubowski T, Hackam DJ. Toll-like receptor 4 plays a role in macrophage phagocytosis during peritoneal sepsis. *J Pediatr Surg.* 2007;42(6):927-32; discussion 33.
219. Ryan KA, Smith MF, Sanders MK, Ernst PB. Reactive Oxygen and Nitrogen Species Differentially Regulate Toll-Like Receptor 4-Mediated Activation of NF- κ B and Interleukin-8 Expression. *Infect Immun.* 722004. p. 2123-30.

220. De Filippo K, Henderson RB, Laschinger M, Hogg N. Neutrophil chemokines KC and macrophage-inflammatory protein-2 are newly synthesized by tissue macrophages using distinct TLR signaling pathways. *J Immunol.* 2008;180(6):4308-15.
221. Grobner S, Lukowski R, Autenrieth IB, Ruth P. Lipopolysaccharide induces cell volume increase and migration of dendritic cells. *Microbiol Immunol.* 2014;58(1):61-7.
222. Vizcaino C, Mansilla S, Portugal J. Sp1 transcription factor: A long-standing target in cancer chemotherapy. *Pharmacol Ther.* 2015;152:111-24.
223. Scott ML, Fujita T, Liou HC, Nolan GP, Baltimore D. The p65 subunit of NF-kappa B regulates I kappa B by two distinct mechanisms. *Genes Dev.* 1993;7(7a):1266-76.
224. Wang J, Basagoudanavar SH, Wang X, Hopewell E, Albrecht R, García-Sastre A, et al. NF- κ B RelA subunit is crucial for early IFN- β expression and resistance to RNA virus replication. *J Immunol.* 2010;185(3):1720-9.
225. Cusson-Hermance N, Khurana S, Lee TH, Fitzgerald KA, Kelliher MA. Rip1 mediates the Trif-dependent toll-like receptor 3- and 4-induced NF- κ B activation but does not contribute to interferon regulatory factor 3 activation. *J Biol Chem.* 2005;280(44):36560-6.
226. Takahashi K, Kawai T, Kumar H, Sato S, Yonehara S, Akira S. Roles of caspase-8 and caspase-10 in innate immune responses to double-stranded RNA. *J Immunol.* 2006;176(8):4520-4.
227. Sakaguchi S, Negishi H, Asagiri M, Nakajima C, Mizutani T, Takaoka A, et al. Essential role of IRF-3 in lipopolysaccharide-induced interferon-beta gene expression and endotoxin shock. *Biochem Biophys Res Commun.* 2003;306(4):860-6.
228. Grandvaux N, Gaboriau F, Harris J, tenOever BR, Lin R, Hiscott J. Regulation of arginase II by interferon regulatory factor 3 and the involvement of polyamines in the antiviral response. *Febs j.* 2005;272(12):3120-31.
229. Genin P, Morin P, Civas A. Impairment of interferon-induced IRF-7 gene expression due to inhibition of ISGF3 formation by trichostatin A. *J Virol.* 2003;77(12):7113-9.
230. Honda K, Yanai H, Negishi H, Asagiri M, Sato M, Mizutani T, et al. IRF-7 is the master regulator of type-I interferon-dependent immune responses. *Nature.* 2005;434(7034):772-7.
231. Honda K, Ohba Y, Yanai H, Negishi H, Mizutani T, Takaoka A, et al. Spatiotemporal regulation of MyD88-IRF-7 signalling for robust type-I interferon induction. *Nature.* 2005;434(7036):1035-40.

232. Balkhi MY, Fitzgerald KA, Pitha PM. Functional Regulation of MyD88-Activated Interferon Regulatory Factor 5 by K63-Linked Polyubiquitination ∇ . *Mol Cell Biol*. 2008;28(24):7296-308.
233. Wei J, Tang D, Lu C, Yang J, Lu Y, Wang Y, et al. Irf5 deficiency in myeloid cells prevents necrotizing enterocolitis by inhibiting M1 macrophage polarization. *Mucosal Immunol*. 2019;12(4):888-96.
234. M C, W J, SC S. Peli1 facilitates TRIF-dependent Toll-like receptor signaling and proinflammatory cytokine production. *Nature immunology*. 2009;10(10):1089-95.
235. Komai T, Inoue M, Okamura T, Morita K, Iwasaki Y, Sumitomo S, et al. Transforming Growth Factor-beta and Interleukin-10 Synergistically Regulate Humoral Immunity via Modulating Metabolic Signals. *Front Immunol*. 2018;9:1364.
236. Naiki Y, Michelsen KS, Zhang W, Chen S, Doherty TM, Arditi M. Transforming growth factor-beta differentially inhibits MyD88-dependent, but not TRAM- and TRIF-dependent, lipopolysaccharide-induced TLR4 signaling. *J Biol Chem*. 2005;280(7):5491-5.
237. Zhang YE. Non-Smad pathways in TGF- β signaling. *Cell Res*. 2009;19(1):128-39.
238. Ishida Y, Kondo T, Takayasu T, Iwakura Y, Mukaida N. The essential involvement of cross-talk between IFN-gamma and TGF-beta in the skin wound-healing process. *J Immunol*. 2004;172(3):1848-55.
239. Atfi A, Djelloul S, Chastre E, Davis R, Gespach C. Evidence for a role of Rho-like GTPases and stress-activated protein kinase/c-Jun N-terminal kinase (SAPK/JNK) in transforming growth factor beta-mediated signaling. *J Biol Chem*. 1997;272(3):1429-32.
240. Hocevar BA, Brown TL, Howe PH. TGF-beta induces fibronectin synthesis through a c-Jun N-terminal kinase-dependent, Smad4-independent pathway. *Embo j*. 1999;18(5):1345-56.
241. G H, RH M, G C, R C, C B, JK H. Transforming growth factor-beta 1 lowers the CD14 content of monocytes. *The Journal of surgical research*. 1994;57(5):574-8.
242. Sly LM, Rauh MJ, Kalesnikoff J, Song CH, Krystal G. LPS-induced upregulation of SHIP is essential for endotoxin tolerance. *Immunity*. 2004;21(2):227-39.
243. Nguyen KB, Watford WT, Salomon R, Hofmann SR, Pien GC, Morinobu A, et al. Critical role for STAT4 activation by type 1 interferons in the interferon-gamma response to viral infection. *Science*. 2002;297(5589):2063-6.

244. Vila-del Sol V, Punzon C, Fresno M. IFN-gamma-induced TNF-alpha expression is regulated by interferon regulatory factors 1 and 8 in mouse macrophages. *J Immunol.* 2008;181(7):4461-70.
245. Thiefes A, Wolf A, Doerrie A, Grassl GA, Matsumoto K, Autenrieth I, et al. The *Yersinia enterocolitica* effector YopP inhibits host cell signalling by inactivating the protein kinase TAK1 in the IL-1 signalling pathway. *EMBO Rep.* 2006;7(8):838-44.
246. Mukherjee S, Keitany G, Li Y, Wang Y, Ball HL, Goldsmith EJ, et al. *Yersinia* YopJ acetylates and inhibits kinase activation by blocking phosphorylation. *Science.* 2006;312(5777):1211-4.
247. Mittal R, Peak-Chew SY, McMahon HT. Acetylation of MEK2 and I kappa B kinase (IKK) activation loop residues by YopJ inhibits signaling. *Proc Natl Acad Sci U S A.* 2006;103(49):18574-9.
248. Rana RR, Simpson P, Zhang M, Jennions M, Ukegbu C, Spear AM, et al. *Yersinia pestis* TIR-domain protein forms dimers that interact with the human adaptor protein MyD88. *Microb Pathog.* 2011;51(3):89-95.
249. Kim DW, Lenzen G, Page AL, Legrain P, Sansonetti PJ, Parsot C. The *Shigella flexneri* effector OspG interferes with innate immune responses by targeting ubiquitin-conjugating enzymes. *Proc Natl Acad Sci U S A.* 2005;102(39):14046-51.
250. Jones RM, Wu H, Wentworth C, Luo L, Collier-Hyams L, Neish AS. *Salmonella* AvrA Coordinates Suppression of Host Immune and Apoptotic Defenses via JNK Pathway Blockade. *Cell Host Microbe.* 2008;3(4):233-44.
251. Yen H, Ooka T, Iguchi A, Hayashi T, Sugimoto N, Tobe T. NleC, a type III secretion protease, compromises NF-kappaB activation by targeting p65/RelA. *PLoS Pathog.* 2010;6(12):e1001231.
252. Lad SP, Yang G, Scott DA, Wang G, Nair P, Mathison J, et al. Chlamydial CT441 is a PDZ domain-containing tail-specific protease that interferes with the NF-kappaB pathway of immune response. *J Bacteriol.* 2007;189(18):6619-25.
253. Imai K, Takeshita A, Hanazawa S. Transforming Growth Factor- β Inhibits Lipopolysaccharide-Stimulated Expression of Inflammatory Cytokines in Mouse Macrophages through Downregulation of Activation Protein 1 and CD14 Receptor Expression. *Infect Immun.* 682000. p. 2418-23.

254. Wang B, Dileepan T, Briscoe S, Hyland KA, Kang J, Khoruts A, et al. Induction of TGF- β 1 and TGF- β 1–dependent predominant Th17 differentiation by group A streptococcal infection. *Proc Natl Acad Sci U S A*. 2010;107(13):5937-42.
255. Huss DJ, Winger RC, Peng H, Yang Y, Racke MK, Lovett-Racke AE. TGF-beta enhances effector Th1 cell activation but promotes self-regulation via IL-10. *J Immunol*. 2010;184(10):5628-36.
256. Kapitein B, Tiemessen MM, Liu WM, van Ieperen-van Dijk AG, Hoekstra MO, van Hoffen E, et al. The interleukin-10 inducing effect of transforming growth factor- β on human naive CD4+ T cells from cord blood is restricted to the TH1 subset. *Clin Exp Immunol*. 2007;147(2):352-8.
257. Fuss IJ, Boirivant M, Lacy B, Strober W. The interrelated roles of TGF-beta and IL-10 in the regulation of experimental colitis. *J Immunol*. 2002;168(2):900-8.
258. Huber S, Schramm C, Lehr HA, Mann A, Schmitt S, Becker C, et al. Cutting edge: TGF-beta signaling is required for the in vivo expansion and immunosuppressive capacity of regulatory CD4+CD25+ T cells. *J Immunol*. 2004;173(11):6526-31.
259. Sawa T, Katoh H, Yasumoto H. V-antigen homologs in pathogenic gram-negative bacteria. *Microbiol Immunol*. 2014;58(5):267-85.
260. Anisimov AP, Dentovskaya SV, Panfertsev EA, Svetoch TE, Kopylov P, Segelke BW, et al. Amino acid and structural variability of *Yersinia pestis* LcrV protein. *Infect Genet Evol*. 2010;10(1):137-45.
261. A H, J O, P C, E M, R N, J P, et al. LcrV is a channel size-determining component of the Yop effector translocon of *Yersinia*. *Molecular microbiology*. 2001;39(3):620-32.
262. Hamad MA, Nilles ML. Structure-function analysis of the C-terminal domain of LcrV from *Yersinia pestis*. *J Bacteriol*. 2007;189(18):6734-9.
263. E S, SC S. Differential effects of deletions in LcrV on secretion of V antigen, regulation of the low-Ca²⁺ response, and virulence of *Yersinia pestis*. *Journal of bacteriology*. 1995;177(9):2530-42.
264. Li B, Yang R. Interaction between *Yersinia pestis* and the Host Immune System ∇ . *Infect Immun*. 2008;76(5):1804-11.
265. AA K, JP B, G G, DN R. Identifying B and T cell epitopes and studying humoral, mucosal and cellular immune responses of peptides derived from V antigen of *Yersinia pestis*. *Vaccine*. 2008;26(3):316-32.

266. Sakinc T, Kleine B, Michalski N, Kaase M, Gatermann SG. SdrI of *Staphylococcus saprophyticus* is a multifunctional protein: localization of the fibronectin-binding site. *FEMS Microbiol Lett.* 2009;301(1):28-34.
267. N K, U G, S P, JN A. Manipulation of costimulatory molecules by intracellular pathogens: veni, vidi, vici!! *PLoS pathogens.* 2012;8(6).
268. S D, A T, SF A, R M, DT G, A V, et al. Inhibition of TLR-4/MD-2 signaling by RP105/MD-1. *Journal of endotoxin research.* 2005;11(6):363-8.
269. Fang L, Chang HM, Cheng JC, Leung PC, Sun YP. TGF-beta1 induces COX-2 expression and PGE2 production in human granulosa cells through Smad signaling pathways. *J Clin Endocrinol Metab.* 2014;99(7):E1217-26.
270. Chentouh R, Fitting C, Cavaillon JM. Specific features of human monocytes activation by monophosphoryl lipid A. *Sci Rep.* 82018.
271. Depaolo RW, Tang F, Kim I, Han M, Levin N, Ciletti N, et al. Toll-like receptor 6 drives differentiation of tolerogenic dendritic cells and contributes to LcrV-mediated plague pathogenesis. *Cell Host Microbe.* 2008;4(4):350-61.
272. TS K, L B, I G, N R, A S, ER H, et al. Human Monocyte Subsets and Phenotypes in Major Chronic Inflammatory Diseases. *Frontiers in immunology.* 2019;10.
273. AK R, Y L, Q D, F Y. Monocytes in rheumatoid arthritis: Circulating precursors of macrophages and osteoclasts and, their heterogeneity and plasticity role in RA pathogenesis. *International immunopharmacology.* 2018;65.
274. S K, T K, J H, A N, A L. Investigating the role of proinflammatory CD16+ monocytes in the pathogenesis of inflammatory bowel disease. *Clinical and experimental immunology.* 2010;161(2):332-41.
275. Ziegler-Heitbrock HW, Thiel E, Futterer A, Herzog V, Wirtz A, Riethmuller G. Establishment of a human cell line (Mono Mac 6) with characteristics of mature monocytes. *Int J Cancer.* 1988;41(3):456-61.
276. H D, N V, F S, S G, PJ M, JJ R, et al. Suppressor of cytokine signaling-1 is an IL-4-inducible gene in macrophages and feedback inhibits IL-4 signaling. *Genes and immunity.* 2007;8(1):21-7.
277. Chomarat P, Risoan MC, Banchereau J, Miossec P. Interferon gamma inhibits interleukin 10 production by monocytes. *J Exp Med.* 1993;177(2):523-7.

278. Y A, C M, S A, M SC, N F. The induction of IL-10 by zymosan in dendritic cells depends on CREB activation by the coactivators CREB-binding protein and TORC2 and autocrine PGE2. *Journal of immunology (Baltimore, Md : 1950)*. 2009;183(2):1471-9.
279. D G, W S, SJ Y, H C, J G, N H. TGF β signaling plays a critical role in promoting alternative macrophage activation. *BMC immunology*. 2012;13.
280. Moynagh PN. TLR signalling and activation of IRFs: revisiting old friends from the NF-kappaB pathway. *Trends Immunol*. 2005;26(9):469-76.
281. KA C, M I, H W, MA S, PM L, NW L, et al. TLR3 is an endogenous sensor of tissue necrosis during acute inflammatory events. *The Journal of experimental medicine*. 2008;205(11).
282. JY Y, MS K, E K, JH C, YS L, Y K, et al. Enteric Viruses Ameliorate Gut Inflammation via Toll-like Receptor 3 and Toll-like Receptor 7-Mediated Interferon- β Production. *Immunity*. 2016;44(4).
283. SK S, KS B, K A, Q L, CW H, S A, et al. Toll-like receptor-7 ligand Imiquimod induces type I interferon and antimicrobial peptides to ameliorate dextran sodium sulfate-induced acute colitis. *Inflammatory bowel diseases*. 2012;18(5).
284. PJ M, RL H, Z Y, C Y, C G, J F, et al. Suppression of inflammation in ulcerative colitis by interferon- β -1a is accompanied by inhibition of IL-13 production. *Gut*. 2011;60(4).
285. MA F, C G. Induction of tolerance to lipopolysaccharide (LPS)-D-galactosamine lethality by pretreatment with LPS is mediated by macrophages. *Infection and immunity*. 1988;56(5):1352-7.
286. AM F, HL W. Oral tolerance and TGF-beta-producing cells. *Inflammation & allergy drug targets*. 2006;5(3).
287. J N, MP M, AC K, A N, GG M, M A, et al. Inflammatory Resolution Triggers a Prolonged Phase of Immune Suppression through COX-1/mPGES-1-Derived Prostaglandin E 2. *Cell reports*. 2017;20(13):3162-75.
288. P R, T K. The intracellular form of notch blocks transforming growth factor beta-mediated growth arrest in Mv1Lu epithelial cells. *Molecular and cellular biology*. 2003;23(18):6694-701.
289. S L, A D, A C, L W, TC W. The murine gastrin promoter is synergistically activated by transforming growth factor-beta/Smad and Wnt signaling pathways. *The Journal of biological chemistry*. 2004;279(41):42492-9502.

290. AR C, Y C, EA T, CM T, TC K, K L. Akt interacts directly with Smad3 to regulate the sensitivity to TGF-beta induced apoptosis. *Nature cell biology*. 2004;6(4):366-72.
291. G W, Y Y, C S, T L, T L, L Z, et al. STAT3 selectively interacts with Smad3 to antagonize TGF- β signalling. *Oncogene*. 2016;35(33):4388-98.
292. G M, J M, I M, P V, R B, M F, et al. A failure of transforming growth factor-beta1 negative regulation maintains sustained NF-kappaB activation in gut inflammation. *The Journal of biological chemistry*. 2004;279(6):3925-32.
293. T L-R, E C, JL R, R B, F V. Interaction and functional cooperation of NF-kappa B with Smads. Transcriptional regulation of the junB promoter. *The Journal of biological chemistry*. 2000;275(37):28937-46.
294. A K, L V, DJ K, Y F, J U, A M. Cooperation between SMAD and NF-kappaB in growth factor regulated type VII collagen gene expression. *Oncogene*. 1999;18(10):1837-44.
295. N H, K K, I I, M Y, N N, M F, et al. TGF-beta 1 as an enhancer of Fas-mediated apoptosis of lung epithelial cells. *Journal of immunology (Baltimore, Md : 1950)*. 2002;168(12).
296. K B, B Á, B S, F T, ZB N, M P, et al. The role of transforming growth factor-beta in Marfan syndrome. *Cardiology journal*. 2013;20(3).
297. N Q, S L, A R, MT L. Exogenous activation of BMP-2 signaling overcomes TGF β -mediated inhibition of osteogenesis in Marfan embryonic stem cells and Marfan patient-specific induced pluripotent stem cells. *Stem cells (Dayton, Ohio)*. 2012;30(12).
298. A W, S C, I P. Transforming growth factor-beta1: a possible signal molecule for posthemorrhagic hydrocephalus? *Pediatric research*. 1999;46(5).
299. Y L, H L, C M, J L, S N, A K, et al. Transforming growth factor- β (TGF- β)-mediated connective tissue growth factor (CTGF) expression in hepatic stellate cells requires Stat3 signaling activation. *The Journal of biological chemistry*. 2013;288(42):30708-19.
300. CY H, CL C, TH H, JJ C, PF L, CL C. Recent progress in TGF- β inhibitors for cancer therapy. *Biomedicine & pharmacotherapy = Biomedecine & pharmacotherapie*. 2021;134.
301. JR T, LM F, B C, DJ L, AE B, ST M. Systemic glucocorticoid use and early-onset basal cell carcinoma. *Annals of epidemiology*. 2014;24(8).
302. CJC J, DJ S, RB K, MPJ W, Y H, KJ F, et al. A structurally distinct TGF- β mimic from an intestinal helminth parasite potently induces regulatory T cells. *Nature communications*. 2017;8(1).

303. Yasir M, Goyal A, Sonthalia S. Corticosteroid Adverse Effects [Text]. FL, US: StatPearls Publishing; 2021. Available from: <https://www.ncbi.nlm.nih.gov/pubmed/>.
304. JS B, W L, JO N, JE K, SW K, IS K. Transforming growth factor β -induced protein promotes severe vascular inflammatory responses. *American journal of respiratory and critical care medicine*. 2014;189(7):779-86.
305. M S, NC O, J A, JC K. Changes in maternal serum transforming growth factor beta-1 during pregnancy: a cross-sectional study. *BioMed research international*. 2013;2013(2013).
306. MY W, CS H. Tgf-beta superfamily signaling in embryonic development and homeostasis. *Developmental cell*. 2009;16(3):329-43.